

# **Synthesis and Structure-property Evaluation of Novel Cellulosic Polymers as Amorphous Solid Dispersion Matrices for Enhanced Oral Drug Delivery**

**Haoyu Liu**

Dissertation submitted to the faculty of the Virginia Polytechnic Institute and State University in  
partial fulfillment of the requirements for the degree of

Doctor of Philosophy

In

Macromolecular Science and Engineering

Kevin J. Edgar, Chair

Richey M. Davis

Maren Roman

Lynne S. Taylor

S. Richard Turner

December 2, 2013

Blacksburg, VA

Keywords: cellulose  $\omega$ -carboxyesters, amorphous solid dispersion, amphiphilicity, structure-property relationship, oral drug delivery

**Copyright © 2013 by Haoyu Liu**

# **Synthesis and Structure-property Evaluation of Novel Cellulosic Polymers as Amorphous Solid Dispersion Matrices for Enhanced Oral Drug Delivery**

**Haoyu Liu**

## **ABSTRACT**

The use of amorphous solid dispersions (ASDs) is an effective and increasingly widely adopted approach for solubility and bioavailability enhancement of hydrophobic drugs. Cellulose derivatives have strong potential as ASD polymers. We demonstrate herein design, synthesis and structure-property relationship characterization of a new series of organo-soluble cellulose  $\omega$ -carboxyalkanoates for ASDs, by two different synthetic approaches.

These carboxyl-containing cellulose mixed-esters possessed relatively high  $T_g$  values with sufficient  $\Delta T$  versus ambient temperature, useful to prevent drug mobility and crystallization during storage or transport. Screening experiments were utilized to study the impact of ASD polymers including our new family of cellulose  $\omega$ -carboxyesters on both nucleation induction time and crystal growth rate of three poorly soluble model drugs from supersaturated solutions. Attributed to relatively rigid structures and bulky substituent groups, cellulose derivatives were more significant crystallization inhibitors compared to the synthetic polymers. The effective cellulose  $\omega$ -carboxyesters were identified as possessing a similar hydrophobicity to the drug molecule and high number of ionization groups. Among them, cellulose acetate suberate prepared by us was an extraordinary solution crystal growth inhibitor for ritonavir and its formulated solid dispersions provided a substantial 15-fold enhancement of apparent solution concentration vs. the equilibrium solubility of the crystalline drug. To offset the issue of slow drug release from some

cellulose  $\omega$ -carboxyester-based formulations, a new class of amphiphilic cellulosic polymers with hydrophilic oligo(ethylene oxide)-containing side chains was developed via versatile synthetic pathways, and the evaluation of these materials alone or by pairwise polymer blends will be performed as ASD matrices for the enhancement of drug solubility and stability.

## **ACKNOWLEDGEMENTS**

First of all, I would like to thank my beloved parents and grandparents, they have been always standing by my side, bearing my bad temper through difficult times and giving me heart-warming support and suggestions, even though I am far away and unable to take care of them for the past four years.

I would like to thank Dr. Judy Riffle, the director of our Macromolecular Science & Engineering program. I was applying for graduate schools from China back in 2009 and never met her personally. Just after knowing my background through email, she was very kind to introduce me to my advisor Dr. Kevin Edgar. That was how I could talk with him and luckily receive the offer, and truly, joining our polysaccharide research group was the best and most correct decision that I have made. I sincerely thank Dr. Edgar for allowing me to study under his guidance for my Ph.D. He is extremely knowledgeable in the fields including polysaccharides, organic chemistry and drug delivery. His knowledge and experience are the major reasons that I could complete a productive work over these four years. His influence on me is much beyond this. I was very confused about blending into the new learning environment when I began graduate study in a different country, greatly thanks to Dr. Edgar's patience and continuous guidance, I started to learn how to learn, make discoveries on my own and interact with other scientists happily and productively.

I am also deeply grateful to Dr. Lynne Taylor, Dr. Maren Roman, Dr. Richard Turner and Dr. Richey Davis for serving on my graduate committee, providing invaluable resources during my study, and reviewing my dissertation.

The next acknowledgement should be delivered to Dr. Nilanjana Kar, who taught me the basic knowledge and techniques in the field of cellulose chemistry when I started to work in the lab. I learned from her that punctiliousness is very important when working on projects, the experience working with her only lasted for less than a quarter but it really shaped me as a real, serious scientific researcher. The same thanks should go to all my collaborators, especially Dr. Grace Ilevbare who is now working at Merck as a senior scientist. She is the best collaborator I could expect, her knowledge, insight and great personality led me to get familiar with, and eventually love the pharmaceutical field.

I would like to thank staff from Departments of Sustainable Biomaterials and Chemistry, Macromolecules and Interfaces Institute for all of their help, especially Ms. Debbie Garnand, Ms. Tammy Jo Hiner and Ms. Cyndy Graham for academic and research service, Dr. Hugo Azumendi and Mr. Geno Iannaccone for NMR service, Mr. Rick Caudill for XRD service and repairing lab equipment.

I would also like to thank all of my lovely labmates, Dr. Carter Fox, Dr. Bin Li, Dr. Daiqiang Xu, Dr. Sidd Pawar, Dr. Junia Pereira, Joyann Marks, Xueyan Zheng, Ruoran Zhang, Thomas Simerly, Xiangtao Meng and Cigdem Arca. Thanks also go to all students, postdoctoral associates and professors who I have worked with and learned from in Macromolecular Science and Engineering program and the Departments of Sustainable Biomaterials and Chemistry. Please forgive me not mentioning all the names, I am very grateful and proud of being a part of Virginia Tech community in our beautiful town, Blacksburg.

# **TABLE OF CONTENTS**

ABSTRACT.....	ii
ACKNOWLEDGEMENTS.....	iv
TABLE OF CONTENTS.....	vi
LIST OF FIGURES.....	x
LIST OF SCHEMES.....	xiv
LIST OF TABLES.....	xv
<b>CHAPTER 1 INTRODUCTION.....</b>	<b>1</b>
References.....	3
<b>CHAPTER 2 LITERATURE REVIEW.....</b>	<b>4</b>
2.1 Introduction – Cellulose and Cellulose esters: Their Properties and Applications.....	4
2.2 Importance of Novel Drug Delivery Systems.....	7
2.3 Approaches to Enhance Dissolution of Poorly Soluble Drugs.....	8
2.3.1 Cyclodextrin-drug complexation.....	9
2.3.2 Nanosizing: Nanoparticles with large surface area.....	12
2.3.3 Lipid-based delivery.....	14
2.3.4 Micellar solubilization – The use of artificial surfactants as excipients.....	16
2.3.5 Amorphous solid dispersions.....	18
2.4 Polymer Matrices for Amorphous Dispersion Formulations.....	20
2.4.1 Synthetic polymers.....	21
2.4.2 Conventional pH-independent cellulose esters and ethers.....	24
2.4.3 pH-dependent cellulose derivatives.....	27
2.5 Concluding Remarks.....	38
2.6 References.....	39
<b>CHAPTER 3 PIONEERING STUDIES ON SYNTHESIS OF CELLULOSE ADIPATE DERIVATIVES.....</b>	<b>46</b>
3.1 Abstract.....	46
3.2 Introduction.....	46
3.3 Experimental Section.....	49

3.3.1 Materials .....	49
3.3.2 Measurements .....	50
3.3.3 Reaction of cellulose in DMAc/LiCl solution with adipic anhydride .....	51
3.3.4 Synthesis of benzyl-protected cellulose adipate mixed esters .....	51
3.3.5 Deprotection of benzyl cellulose adipate esters.....	54
3.4 Results and Discussion.....	55
3.4.1 Direct synthesis using adipic anhydride and crosslinking problem.....	55
3.4.2 Two-step synthesis using monobenzyl ester mono acid chloride .....	59
3.5 Conclusions .....	65
3.6 Supplementary Material .....	66
3.7 Acknowledgements .....	67
3.8 References .....	67
<b>CHAPTER 4 DIRECT SYNTHESIS OF CELLULOSE ADIPATE DERIVATIVES USING ADIPIC ANHYDRIDE .....</b>	<b>71</b>
4.1 Abstract.....	71
4.2 Introduction .....	71
4.3 Experimental Section .....	74
4.3.1 Materials .....	74
4.3.2 Characterization .....	75
4.3.3 Synthesis of cellulose adipates esters .....	76
4.4 Results and Discussion.....	78
4.4.1 Crosslinking issue and mechanistic understanding.....	78
4.4.2 Synthesis of organo-soluble cellulose adipate esters .....	82
4.4.3. Property evaluation of cellulose adipate esters.....	91
4.5 Conclusion.....	93
4.6 Supplementary Material .....	94
4.7 Acknowledgements .....	96
4.8 References .....	96
<b>CHAPTER 5 SYNTHESIS AND STRUCTURE-PROPERTY EVALUATION OF CELLULOSE <math>\Omega</math>-CARBOXYESTERS FOR AMORPHOUS SOLID DISPERSIONS .....</b>	<b>99</b>
5.1 Abstract.....	99
5.2 Introduction .....	100
5.3 Experimental Section .....	102

5.3.1 Materials .....	102
5.3.2 Measurements .....	103
5.3.3 Methods.....	104
5.4 Results and Discussion.....	110
5.4.1 Synthesis and characterization of cellulose $\omega$ -carboxyalkanoates.....	110
5.4.2 Regioselectivity.....	115
5.4.3 Effect of newly synthesized polymers on solution crystal growth inhibition of ritonavir.....	117
5.4.4 ASDs of ritonavir in cellulose $\omega$ -carboxyalkanoate matrices .....	120
5.5 Conclusions .....	122
5.6 Supplementary Material .....	122
5.7 Acknowledgements .....	124
5.8 References .....	125
<b>CHAPTER 6 IMPACT OF CHEMICALLY DIVERSE POLYMERS ON CRYSTALLIZATION OF LIPOPHILIC DRUG COMPOUNDS FROM SUPERSATURATED SOLUTION .....</b>	<b>127</b>
6.1 Abstract.....	127
6.2 Introduction .....	128
6.3 Experimental Section .....	130
6.3.1 Materials .....	130
6.3.2 Methods.....	133
6.4 Results .....	136
6.4.1 Physicochemical properties of model drug compounds .....	136
6.4.2 Impact of polymers on nucleation inhibition of the model compounds .....	139
6.4.3 Impact of polymers on crystal growth inhibition of the model drug compounds.....	144
6.5 Discussion .....	147
6.5.1 Impact of polymers on nucleation-induction times .....	147
6.5.2 Impact of polymers on crystal growth rate .....	149
6.6 Conclusion.....	151
6.7 References .....	151
<b>CHAPTER 7 AMPHIPHILIC CELLULOSE ESTERS FOR ORAL DRUG DELIVERY.....</b>	<b>154</b>
7.1 Abstract.....	154



7.2 Introduction .....	154
7.3 Experimental Section .....	157
7.3.1 Materials .....	157
7.3.2 Analytical measurements .....	158
7.3.3 Methods.....	159
7.4 Results and Discussion.....	162
7.4.1 General description and comparison of different esterification approaches.....	162
7.4.2 Degree of substitution (DS) determination.....	163
7.3.3 Investigation on physiochemical properties.....	169
7.3.4 pH-Sensitive materials derived from cellulose trioxadecanoate.....	173
7.5 Conclusion.....	175
7.6 Supplementary Material .....	176
7.7 Acknowledgement .....	178
7.8 References .....	178
<b>CHAPTER 8 SUMMARY AND FUTURE WORK.....</b>	<b>182</b>
8.1 Direct Synthesis of Cellulose Adipate Derivatives .....	182
8.2 Two-step Synthesis of Cellulose $\omega$ -Carboxyesters (adipates/ suberates/sebacates) by Protecting Group. ....	183
8.3 Mechanistic Understanding of Polymer Impact on Drug Solubilization and Stabilization.....	184
8.4 Further Development of Cellulose-based Polymers: Cellulose Trioxadecanoate .....	184
8.5 Proposed Future Work.....	185

## **LIST OF FIGURES**

<b>Figure 2.1</b> Extensive inter- and intra-hydrogen bonding of cellulose.....	5
<b>Figure 2.2</b> Heterogeneous synthesis of cellulose acetate propionate.....	7
<b>Figure 2.3</b> Synthesis of hydropropyl- $\beta$ -cyclodextrin (HPCD) and sulfobutyl- $\beta$ -cyclodextrin (SBCD) .....	10
<b>Figure 2.4</b> Lipid digestion models for <i>in vitro</i> assessment of lipid-based formulations, reprinted from Dahan, A.; Hoffman, A. <i>J Control Release</i> <b>2008</b> , 129, (1), 1-10. Used with permission of Elsevier, 2008. ....	16
<b>Figure 2.5</b> Spray-drying process and the image of a Mini Spray Dryer B-290, reprinted from Chavarri, M.; Maranon, I.; Villaran, M. C. <i>Probiotics</i> <b>2012</b> , 501-540. Used with open access from InTech, 2012. ....	20
<b>Figure 2.6</b> Two-step preparation of CMCAB with DS of carboxymethyl 0.33.....	29
<b>Figure 2.7</b> Ibuprofen release with physical blends of CMCAB and microcrystalline cellulose (MC), reprinted from Posey-Dowty, J. D.; Watterson, T. L.; Wilson, A. K.; Edgar, K. J.; Shelton, M. C.; Lingerfelt, L. R. <i>Cellulose</i> <b>2007</b> , 14, (1), 73-83. Used with permission of Springer, 2006.....	30
<b>Figure 2.8</b> Comparison of Fexofenadine HCl release from a compression tablet of a physical blend of CMCAB/drug with capsule containing amorphous formulation, reprinted from Shelton, M. C.; Posey-Dowty, J. D.; Lingerfelt, L. R.; Kirk, S. K.; Klein, S.; Edgar, K. J. <i>Polysaccharide Materials: Performance by Design</i> <b>2009</b> . Used with permission of American Chemical Society, 2010.....	31
<b>Figure 2.9</b> CMCAB crosslink mechanisms of (1) acid-catalyzed crosslink (2) multivalent ions crosslink .....	32
<b>Figure 2.10</b> Mechanism of cellulose dissolution in DMAc/ LiCl by Gray et al (1995) .....	33
<b>Figure 2.11</b> Industrial preparation of CAB-SU160 starting from CAB-553-0.4.....	35
<b>Figure 2.12</b> Chemical structure of HPMCAS .....	36
<b>Figure 2.13</b> Proposed CAB-Su Hydrolysis Mechanism .....	38
<b>Figure 3.1</b> CP/MAS <sup>13</sup> C NMR spectrum of cross-linked cellulose adipate .....	57
<b>Figure 3.2</b> IR spectrum of cross-linked cellulose adipate .....	57
<b>Figure 3.3</b> <sup>1</sup> H NMR spectrum of benzyl cellulose acetate adipate propionate in CDCl <sub>3</sub> .....	61

<b>Figure 3.4</b> $^1\text{H}$ NMR spectrum of cellulose acetate adipate propionate in $\text{CDCl}_3$ .....	62
<b>Figure 3.5</b> $^{13}\text{C}$ NMR spectrum of cellulose acetate adipate propionate in $\text{DMSO}-d_6$ .....	62
<b>Figure 3.6</b> DSC curves of cellulose adipate derivatives at heating rate $10\text{ }^\circ\text{C}/\text{min}$ (2nd heat)...	64
<b>Figure S3.1</b> $^1\text{H}$ NMR spectrum of monobenzyl adipate .....	66
<b>Figure S3.2</b> $^1\text{H}$ NMR spectrum of monobenzyl adipoyl chloride.....	67
<b>Figure 4.1</b> CP/MAS $^{13}\text{C}$ NMR spectrum of cross-linked CAAdP.....	80
<b>Figure 4.2</b> CAAdP DS(Ad) vs. reaction time under different reaction conditions .....	84
<b>Figure 4.3</b> $^1\text{H}$ NMR spectrum of CAAdP (Sample 7, Table 4.1) in $\text{DMSO}-d_6$ .....	85
<b>Figure 4.4</b> $^{13}\text{C}$ NMR spectrum of CAAdP (Sample 7, Table 4.1) in $\text{DMSO}-d_6$ .....	86
<b>Figure 4.5</b> FT-IR spectra of starting material CAP-504-2 (spectrum a), and two lab-synthesized CAAdP samples with lower (spectrum b, sample 2) or higher DSAd (spectrum c, sample 7) ...	86
<b>Figure 4.6</b> $^1\text{H}$ NMR spectrum of CA-398-30 adipate (Sample 17, Table 4.3) in $\text{DMSO}-d_6$ .....	89
<b>Figure 4.7</b> DSC thermograms (2nd heating scan) of cellulose adipate mixed esters.....	92
<b>Figure S4.1</b> $^1\text{H}$ NMR spectrum of pure adipic anhydride.....	94
<b>Figure S4.2</b> $^1\text{H}$ NMR of CAAdP (Sample 3, Table 4.1) before the hot water wash step .....	95
<b>Figure S4.3</b> $^1\text{H}$ NMR spectrum of CAAdP (Sample 3, Table 4.1) in acetone- $d_6$ .....	95
<b>Figure 5.1</b> $^1\text{H}$ NMR of benzyl CAP-504-0.2 sebacate (DS Se = 0.24) in $\text{CDCl}_3$ .....	113
<b>Figure 5.2</b> $^1\text{H}$ NMR (2a) and $^{13}\text{C}$ NMR (2b) of CAP-504-0.2 sebacate (DS Se 0.24) in $\text{DMSO}-d_6$ .....	114
<b>Figure 5.3</b> $^{13}\text{C}$ NMR of fully-substituted cellulose acetate sebacate (DS Se 0.55) in $\text{DMSO}-d_6$ .....	116
<b>Figure 5.4</b> Crystal growth rate ratio of ritonavir at an initial ritonavir concentration of $10\text{ }\mu\text{g}/\text{mL}$ . The data is arranged in order of hydrophobicity: least hydrophobic to most hydrophobic (left to right). Crystal growth rate experiments were performed in triplicate. Each column is an average of the effectiveness ratio and error bars indicate one standard deviation. The y-axis is a ratio of the growth rate of ritonavir in the absence of polymer to growth rate of ritonavir in the presence of polymer ( $5\text{ }\mu\text{g}/\text{mL}$ ). Polymers with a ratio $> 1$ are considered effective crystal growth inhibitors. With the exception of CA 320S Sub and CA 320S Seb, the effectiveness growth ratios for all cellulose $\omega$ -carboxyalkanoates were previously reported.....	119
<b>Figure 5.5</b> PXRD pattern of ritonavir crystalline powder and amorphous solid dispersions prepared by co-precipitation with cellulose $\omega$ -carboxyalkanoates .....	121

<b>Figure 5.6</b> Ritonavir in vitro release from cellulose $\omega$ -carboxyesters-based amorphous solid dispersions, prepared by co-precipitation .....	121
<b>Figure S5.1</b> $^1\text{H}$ NMR of monobenzyl sebacoyl chloride in $\text{CDCl}_3$ .....	123
<b>Figure S5.2</b> $^1\text{H}$ NMR of fully-substituted benzyl cellulose acetate sebacate (DS Se = 1.95) in $\text{CDCl}_3$ .....	123
<b>Figure S5.3</b> DSC thermograms of ritonavir (A; left) and amorphous solid dispersions in cellulose $\omega$ -carboxyalkanoates (B; right).....	124
<b>Figure 6.1</b> Molecular structures of (a) ritonavir, (b) efavirenz and, (c) celecoxib.....	131
<b>Figure 6.2</b> Molecular structure of the novel synthesized cellulose derivatives and the substituent groups. These cellulose derivatives are not regioselectively substituted. The abbreviations are presented in Table 6.1. ....	131
<b>Figure 6.3</b> Representative plots of extinction (which characterizes turbidity) with time from desupersaturation experiments for celecoxib (a & b), efavirenz (c & d) and ritonavir (e & f), in the absence and presence of the most effective polymers for each of the model compounds...	140
<b>Figure 6.4</b> Induction times for ritonavir, from unseeded desupersaturation experiments, in the absence and presence of polymers (n = 3). An initial concentration corresponding of 20 $\mu\text{g}/\text{mL}$ ritonavir and the polymer concentration was 5 $\mu\text{g}/\text{mL}$ . ....	141
<b>Figure 6.5</b> Rate of desupersaturation of ritonavir with seed crystals in the absence and presence of polymer at an initial concentration of 10 $\mu\text{g}/\text{mL}$ ritonavir. All experiments were performed in triplicate and errors indicate one standard deviation .....	144
<b>Figure 6.6</b> Crystal growth rate ratio of ritonavir at an initial concentration of 10 $\mu\text{g}/\text{mL}$ . The data is arranged in order of hydrophobicity: least hydrophobic to most hydrophobic (left to right). Crystal growth rate experiments were performed in triplicate. Each column is an average of the effectiveness ratio of the polymers (5 $\mu\text{g}/\text{mL}$ ) and error bars indicate one standard deviation.....	145
<b>Figure 7.1</b> Representative $^1\text{H}$ NMR of cellulose trioxadecanoate (a) and cellulose trioxadecanoate propionate after peracylation (b) .....	164
<b>Figure 7.2</b> ATR spectra of cellulose trioxadecanoate (B2, via CDI activation 1-3-3), before and after saponification at 25 $^\circ\text{C}$ and 50 $^\circ\text{C}$ for 24 h.....	166
<b>Figure 7.3</b> Potentiometric titration and its derivative curve of cellulose trioxadecanoate (B1, via CDI activation 1-1-1) after saponification at 25 $^\circ\text{C}$ for 24 h .....	167

<b>Figure 7.4</b> DSC thermograms of C1, C3 and C4 and modulated DSC thermogram of C2 .....	171
<b>Figure 7.5</b> <sup>1</sup> H NMR of cellulose trioxadecanoate phthalate/succinate/adipate, derived from cellulose trioxadecanoate A1 .....	175
<b>Figure S7.1</b> <sup>13</sup> C NMR of cellulose trioxadecanoate C1 in D <sub>2</sub> O at 70 °C (DS 0.48 via TosCl activation) .....	176
<b>Figure S7.2</b> <sup>1</sup> H NMR of cellulose trioxadecanoate propionate C4 in CDCl <sub>3</sub> (DS 2.02 via TosCl activation, derived from C2) .....	177
<b>Figure S7.3</b> Potentiometric (square dots) and conductometric (diamond dots) measurements of cellulose trioxadecanoate (C1, TosCl activation) after complete saponification. The inflection point for pH measurements is at 15.5 mL and the inflexion point for conductivity measurements is at 15.6 mL .....	177
<b>Figure S7.4</b> Graphical solution for the DS determination from the carbon and hydrogen contents (C and H). Carbon and hydrogen iso-content lines were shown for the analysis of cellulose trioxadecanoate propionates .....	178
<b>Figure 8.1</b> Direct preparation of cellulose adipate esters using adipic anhydride .....	182
<b>Figure 8.2</b> Synthetic route of cellulose adipate/suberate/sebacate mixed esters.....	183

## LIST OF SCHEMES

<b>Scheme 3.1</b> Predicted hydrolytic stability of cellulose adipate esters.....	49
<b>Scheme 3.2</b> Reaction of cellulose with adipic anhydride.....	56
<b>Scheme 3.3</b> Reaction of cellulose with poly(adipic anhydride).....	58
<b>Scheme 3.4</b> Monobenzyl adipoyl chloride synthesis .....	59
<b>Scheme 3.5</b> Synthesis of cellulose adipates via acid chloride.....	60
<b>Scheme 4.1</b> Proposed crosslinking mechanism.....	79
<b>Scheme 4.2</b> Reaction of CAP with freshly prepared adipic anhydride .....	80
<b>Scheme 4.3</b> Alternative proposed crosslinking mechanism .....	81
<b>Scheme 4.4</b> Reactions of cellulose esters with freshly prepared adipic anhydride .....	82
<b>Scheme 5.1</b> General two-step synthetic method for $\omega$ -carboxyalkanoate derivatives of cellulose .....	106

## LIST OF TABLES

<b>Table 2.1</b> Properties of cellulose esters used in pharmaceutical formulation, reprinted from Edgar, K. J. <i>Cellulose</i> <b>2007</b> , 14, (1), 49-64. Used with permission of Springer, 2006. ....	25
<b>Table 2.2</b> Degree of substitution of HPMCAS .....	36
<b>Table 3.1</b> Synthesis of cellulose adipate under different conditions using adipic anhydride .....	56
<b>Table 3.2</b> Synthesis of benzyl cellulose adipate derivatives using monobenzyl adipoyl chloride (MAC).....	60
<b>Table 3.3</b> Properties of starting materials and deprotected cellulose ester adipates .....	65
<b>Table 4.1</b> Synthesis of CAP-504-0.2 adipates and full DS information .....	83
<b>Table 4.2</b> Synthesis of CAB-553-0.4 adipates and full DS information.....	87
<b>Table 4.3</b> Synthesis of CA adipates and full DS information .....	89
<b>Table 4.4</b> Solubility of starting cellulose esters and cellulose adipate esters.....	91
<b>Table 4.5</b> Properties of starting materials and cellulose adipate mixed esters.....	93
<b>Table 5.1</b> Cellulose suberate/sebacate mixed-ester syntheses, DS values and properties .....	112
<b>Table 5.2</b> DS and SP values for cellulose derivatives and their ranking .....	118
<b>Table S5.1</b> Partial degree of substitution values of benzyl cellulose $\omega$ -carboxyesters .....	124
<b>Table 6.1</b> Polymers additives and abbreviations used in this study .....	132
<b>Table 6.2</b> Physicochemical properties of the model compounds .....	137
<b>Table 6.3</b> Solubility parameter (SP) values of the polymers investigated; summary and comparison of the effect of polymers on the drug molecules.....	143
<b>Table 6.4</b> Comparison of the SP values of the model compounds and average SP value of the effective polymers.....	148
<b>Table 7.1</b> Reaction conditions and the degree of substitution (DS) determined by 3 analytical methods.....	169
<b>Table 7.2</b> Physicochemical properties of cellulose trioxdecanoates and perpropionylated products.....	172
<b>Table 7.3</b> Solubility range of cellulose trioxadecanoates.....	173

# CHAPTER 1 INTRODUCTION

My doctoral research pursues design and development of novel oral drug-delivery systems based on cellulosic polymers for drug solubility and bioavailability enhancement. Due to ease of use and convenience, oral drug administration is strongly preferred by patients leading to high compliance with dosage regimes. However, efficient drug absorption is often difficult to achieve because of poor aqueous solubility of the existing and new drugs (estimated as high as 40–70%). That is because drugs are generally produced as crystalline solids to provide high purity, as well as physical and chemical stability. The poor solubility of drugs can also be attributed to the presence of hydrophobic groups and strong interactions in the crystal lattice. Formulation of drugs as amorphous solid dispersions (ASD) in polymer matrices is one of the fastest growing techniques to solve the low solubility problem.<sup>1</sup> When entrapped in a high energy, metastable amorphous form, drug molecules do not have to overcome the heat of fusion to dissolve. The incorporation of a polymer in which the drug is miscible forms a molecular dispersion and disrupts the crystal lattice of the drug, which increases the drug dissolution rate and extent, and thus enhances the oral bioavailability of drugs where solubility is the limiting factor (BCS Class II).<sup>2</sup> The disadvantage of using amorphous drugs is that they are inherently unstable towards transformation back to more stable crystalline state, thereby negating the solubility enhancement. Carefully chosen matrix polymers also have been recognized for improving amorphous drug stability against re-crystallization during storage and delivery to the body.<sup>3</sup> Moreover, many drugs degrade in gastric juices ( $\text{pH} \leq 2$ ), or exhibit an irritant effect on the stomach. Therefore, a highly effective delivery system has to protect them from strong acid and digestive enzymes in stomach, enhance dissolution in the aqueous environment of the small intestine, inhibit drug solutes from precipitating out of the fluid and finally allow to permeate the gastrointestinal epithelium to reach the bloodstream in sufficient concentration for diffusion efficacy.

Currently, cellulosic polymers are widely used as ASD matrix polymers, because they are based on dietary and endogenous components, generally possess high  $T_g$ s to prevent drug migration and re-crystallization, and because we have the ability to tailor cellulose derivative



structure to achieve miscible blends with drugs.<sup>4, 5</sup> Amphiphilic cellulose mixed ethers/esters are designed, which contain pendent CO<sub>2</sub>H groups to provide a pH-trigger for swelling and drug release. These polar groups also provide energetically favorable specific H-bonding interactions with the drug molecule. Unfortunately, there are a limited number of methods available for the synthesis and manufacture of carboxyl-containing polysaccharides, and the existing candidates (carboxymethyl cellulose acetate butyrate, hydroxypropyl methylcellulose acetate succinate, cellulose acetate phthalate) have distinctive disadvantages described in previous literature reports and industrial practice.<sup>6</sup>

Therefore, this thesis presents the first study on the synthesis of cellulose  $\omega$ -carboxyalkanoates, preparation of a diverse range of these polymers, and the determination of their structure-property relationships, including organic solubility and thermal profiles that are pertinent to amorphous dispersion formulations. I describe our collaboration with pharmaceutical scientists to yield new insights into the mechanisms of inhibiting drug crystallization in solution by the presence of cellulosic polymers.

**Chapter 3** discusses attempts to circumvent a crosslinking issue present in the direct synthesis of cellulose adipate esters and a pioneering synthesis route to achieve those cellulosic polymers will be presented.

**Chapter 4** then presents development of a direct synthesis method for and characterization of organo-soluble cellulose alkanoate adipates.

**Chapter 5** further explores the synthesis and structure-property evaluation of a family of cellulose  $\omega$ -carboxyesters and the formulation of amorphous solid dispersions with the poorly water-soluble drug ritonavir.

**Chapter 6** covers our collaborative work on the influence of those cellulose  $\omega$ -carboxyesters on lipophilic drugs stability in solution, demonstrating that some of our novel cellulose derivatives substantially outperform existing polymeric carriers in inhibiting drug re-crystallization.

**Chapter 7** describes versatile approaches to a novel non-ionic, water-soluble cellulose esters as precursors for preparation of amphiphilic cellulosic polymers, to address the slow drug release from cellulose  $\omega$ -carboxyester matrices.

**Chapter 8** summarizes the research results for each chapter in this dissertation and suggests a

course for future experiments.

## References

1. Newman, A.; Knipp, G.; Zografi, G., Assessing the performance of amorphous solid dispersions. *J. Pharm. Sci.* **2012**, 101, (4), 1355-1377.
2. Rumondor, A. C.; Ivanisevic, I.; Bates, S.; Alonzo, D. E.; Taylor, L. S., Evaluation of Drug-Polymer Miscibility in Amorphous Solid Dispersion Systems. *Pharm Res* **2009**, 26, (11), 2523-2534.
3. Alonzo, D. E.; Raina, S.; Zhou, D.; Gao, Y.; Zhang, G. G. Z.; Taylor, L. S., Characterizing the Impact of Hydroxypropylmethyl Cellulose on the Growth and Nucleation Kinetics of Felodipine from Supersaturated Solutions. *Cryst. Growth Des.* **2012**, 12, (3), 1538-1547.
4. Tanno, F.; Nishiyama, Y.; Kokubo, H.; Obara, S., Evaluation of Hypromellose Acetate Succinate (HPMCAS) as a Carrier in Solid Dispersions. *Drug Dev. Ind. Pharm.* **2004**, 30, (1), 9-17.
5. Shelton, M. C.; Posey-Dowty, J. D.; Lingerfelt, L. R.; Kirk, S. K.; Klein, S.; Edgar, K. J., Enhanced dissolution of poorly soluble drugs from solid dispersions in carboxymethylcellulose acetate butyrate matrices. In *Polysaccharide Materials: Performance by Design*, Edgar, K. J.; Heinze, T.; Liebert, T., Eds. American Chemical Society: Washington, D.C., 2009.
6. Kar, N.; Liu, H.; Edgar, K. J., Synthesis of Cellulose Adipate Derivatives. *Biomacromolecules* **2011**, 12, (4), 1106-1115.

## Chapter 2 Literature Review

### 2.1 Introduction – Cellulose and Cellulose esters: Their Properties and Applications

Cellulose is one of the most common and widely-used polysaccharides, produced by plants, sea organisms such as Tunicin from the *Tunicat* class<sup>1, 2</sup> and microorganisms like *Gluconacetobacter xylinus*<sup>3</sup> in huge amounts. In general, cellulose is a highly abundant natural biopolymer (DP ranging from 1,000 to 15,000) with a very uniform molecular composition. The structure of cellulose consists of a linear chain of repeated  $\beta$ -D-(1 $\rightarrow$ 4) linked anhydroglucose units (AGU)  $(C_6H_{10}O_5)_n$  without any branching or substituents. Due to its natural abundance, along with the fact that properties are adjustable through selective chemical conversions of its hydroxyl groups, cellulose and its derivatives are the most commercially attractive polysaccharides for a wide range of applications. Thus, a huge quantity of the feedstock is produced annually.

While cellulose is mainly used in paper-making, and green energy areas by the conversion of cellulose from energy crops into biofuels such as cellulosic ethanol as an alternative fuel source,<sup>4</sup> it is also one of the most important pharmaceutical excipients in the modern drug delivery enterprise. This application shows great potential given the fact that orally administered cellulose has little toxic effect upon the human body. Cellulose can hardly be absorbed or degraded but passes through the gastrointestinal (GI) tract undisturbed. By direct compression, microcrystalline cellulose (MCC, DP  $\approx$  280) is primarily known to generate hard drug tablets with excellent compressibility.<sup>5</sup> As a result, MCC is frequently used as a tablet and capsule diluent in oral dosage forms.

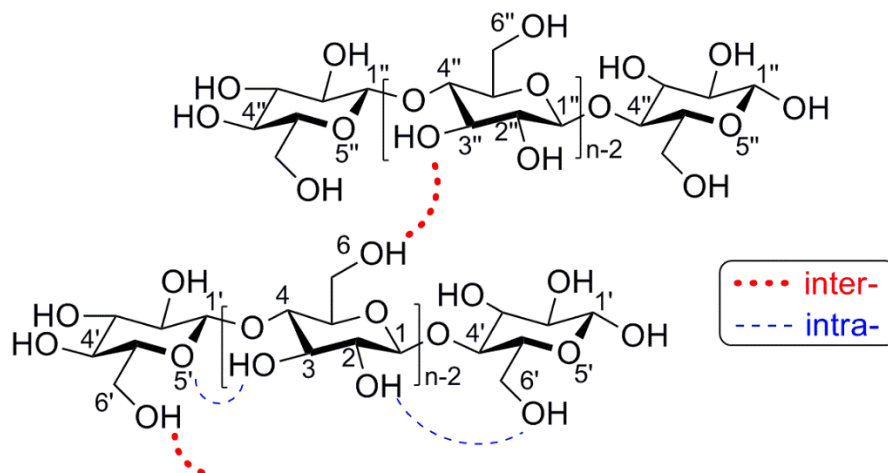


**Figure 2.1** Extensive inter- and intra-hydrogen bonding of cellulose<sup>6</sup>

However, some major drawbacks limit the application of cellulose. The uniform molecular structure combined with three hydroxyls per anhydroglucose unit (AGU) result in extensive intra- and inter-hydrogen bonding and high crystallinity depending on source. To specify, the major intra-molecular types occur at  $O_3\text{-H}\cdots O_5'$  and  $O_2\text{-H}\cdots O_6'$ , where  $O_5'$  and  $O_6'$  originate from an adjacent repeating AGU. And the major inter-molecular H-bonds are identified as interactions between  $O_6\text{-H}\cdots O_3''$  along the  $y$  axis (**Fig. 2.1**).<sup>6</sup> Due to this high crystallinity and lattice energy, cellulose is insoluble in almost all common organic and inorganic solvents. To disrupt crystallinity and render good aqueous/organic solubility for further processing, derivatization of cellulose is required. However, industrial chemical preparations of cellulose esters mostly employ heterogeneous synthesis procedures by reacting cellulose suspension in organic solvent systems to a triester, followed by hydrolysis back to the desired degree of substitution (DS). Through this pathway, the hydrolysis and back-esterification take place simultaneously and therefore the functionalization pattern is random and uncontrolled. In addition, cellulose degrades before melting, which makes melt processing impossible. Furthermore, the cellulose chain is sensitive to strong acids, which causes random breakage of glycosidic bonds in AGU chains and the formation of terminal aldo-pyranose units.<sup>7</sup> This random cleavage suggests that the cationic reaction reduces chain length and thus molecular weight very rapidly. Cellulose is more stable in alkaline media but under severe conditions of temperature or time, cellulose degradation (called alkaline peeling) still can be quite significant.<sup>8</sup>

Accordingly, cellulose is modified to create processable derivatives with enhanced or other specifically required properties. Cellulose esters are the focus of this review, and they have been substantially studied and explored over nearly a century. To alter the properties for various applications, the esterification of cellulose affords cellulose esters with hydrophilic or hydrophobic, non-ionic or charged substituents.

Cellulose organic esters such as cellulose acetates and cellulose propionates are of great practical importance because they are environmentally friendly, stable, non-toxic, and the renewable-based esters exhibit a large range of expanded properties compared to the parent cellulose, which meet specific requirements for a variety of applications. Physical and chemical characteristics can be controlled by tuning polymer chemical structure including the degree of substitution (DS) and type of acyl substituent, and average substitution patterns within the AGU. Cellulose triacetate (CTA, DS  $\approx$  2.9) is prepared in acetic acid suspension with acetic anhydride in the presence of sulfuric acid catalyst<sup>9</sup>. Commercial CTA immediately replaced the use of cellulose nitrate for photographic/movie film applications due to its non-toxic and UV/thermo-stable nature. Organic soluble CTA can be cast to make optically clear films. CTA is also considered superior to unmodified cellulose, due to the fact that it shows low haze and birefringence, together with high modulus and water permeability.

Given the structural regularity, CTA partially crystallizes which leads to limited solubility and miscibility. To resolve the problem, CTA can be back-hydrolyzed to cellulose diacetate (CDA, DS  $\approx$  2.5) or other cellulose acetates with even lower DS.<sup>10, 11</sup> Derived cellulose acetate is a complex copolymer, composed of random sequence of 8 possible monosaccharide units which completely destroys the crystallinity. Consequently, CDA shows much better solubility than CTA, it could be soluble even in polar aprotic solvents such as acetone and THF. Attributes of CDA including high tensile strength, low elongation and low tear initiation resistance, meet the needs of adhesive tape applications.

Furthermore, esters of cellulose with mixed acetic, propionic, and butyric acids can be readily prepared (e.g. cellulose acetate propionate, CAP, **Fig. 2.2**) in industrial heterogeneous production, with good control over substituent type, DS, and to some extent, molecular weight.

During the synthesis process of CAP, no acetic anhydride is used, but the product contains a small amount of acetate groups. This is due to the acid-catalyzed reaction of acids and anhydrides which generates acetic anhydride *in situ*. By tailoring properties like solubility, glass transition temperature, compatibility and optical properties, researchers have created applications in fields ranging from car paint to flat panel displays.<sup>12</sup>

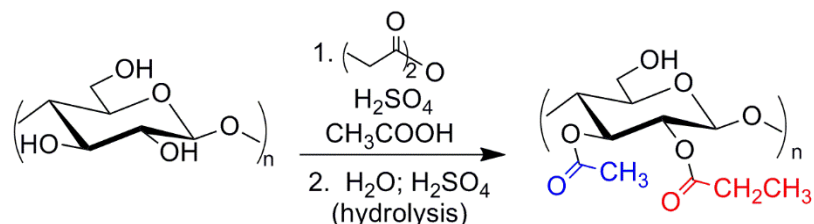


**Figure 2.2** Heterogeneous synthesis of cellulose acetate propionate

## 2.2 Importance of Novel Drug Delivery Systems

The particular interest of our research group is the creation of novel drug delivery systems based on polysaccharide derivatives for lipophilic drug solubilization, stabilization and bioavailability enhancement. Oral drug delivery is preferred in part because it allows precise administered dose and high patient compliance. Due to its large surface area and close-to-neutral pH, the small intestine is the primary absorptive organ for drugs in the human body. Although stomach-specific drug delivery is desired in some cases (for example, floating beads containing clarithromycin were designed to be delivered to the stomach site against *Helicobacter pylori*<sup>13</sup>), many drugs suffer from severe degradation in gastric juice where the surrounding pH is on the order of 2 or less. Meanwhile, some unprotected irritant drugs, such as aspirin, can cause severe stomach discomfort. Thus, for these drugs to be effective, the delivery system has to protect them from strong acid and digestive enzymes in stomach, dissolve in the aqueous environment of the small intestine and finally allow the drug to permeate the gastrointestinal epithelium to diffuse into the bloodstream in sufficient concentration for efficacy. Other factors such as fed vs. fasted state and gut motility also have significant impact on oral drug delivery. To have a successful medication, developers have to control features like solubility, permeability, metabolism and efflux transport of the pharmaceutical actives by various formulation techniques.

However, in oral drug delivery efficient drug absorption is often difficult to achieve because of poor aqueous solubility of drugs. Drugs are generally produced as crystalline solids to provide high levels of purity, as well as physical and chemical stability. The Biopharmaceutics Classification System (BCS) is the international standard used to differentiate the drugs on the basis of their solubility and permeability. A high proportion of new and existing drugs and drug candidates, estimated as high as 40–70%, are classified into Class II (high permeability, low solubility) and Class IV (low permeability, low solubility).<sup>14</sup> The poor aqueous solubility and oral bioavailability of certain drugs can be attributed to the presence of hydrophobic groups and to strong interactions in the crystal lattice. It has also been identified that the formation of a thermodynamically stable crystalline phase of the active during storage further reduced the solubility.<sup>15</sup> A commonly used approach for enhancing solubility in aqueous solution is to convert drugs into their salt forms.<sup>16</sup> However, salt formation may not be feasible due to the nature of the drug. In many other cases, ionized drugs may be less stable *in vivo* and the salt forms do not always serve the purpose of enhancing solubility and bioavailability. Moreover, back-conversion to the original free acid or base forms may also take place during the dissolution in reactive media.<sup>16</sup> As a result, selection of salt forms of drugs that could survive stabilization and solubility tests is still a trial and error process. Based on those facts, scientists have to explore other more effective and reliable alternatives.

### **2.3 Approaches to Enhance Dissolution of Poorly Soluble Drugs**

Other than conversion to salt form, there are several existing methods of overcoming aqueous solubility limitations to achieve effective oral drug delivery. Moreover, some approaches have been also reported to aid in targeted-organ drug release, or zero-order release over a long period of time. Zero-order kinetics may in many cases be ideal for effective drug delivery, wherein the release rate is independent of time, and plasma concentration of drugs remains constant throughout the delivery period. These useful properties help to achieve enhanced patient convenience and compliance with lower dosage and frequency of medication, and in the case of drugs with narrow therapeutic indices may significantly reduce side effects. In the following sections, several widely-adopted approaches are introduced.

### 2.3.1 Cyclodextrin-drug complexation

Cyclodextrins (CDs) are presented as an effective delivery vehicle to achieve better drug solubility.<sup>17</sup> It has been discovered that starch (mostly amylose) can be converted enzymatically to form these cyclic oligomers of  $\alpha$ -(1 $\rightarrow$ 4) linked glucose. From topological view, CDs form a torus that has a hydrophobic interior and a hydrophilic exterior.<sup>18</sup> This structure allows CDs to host hydrophobic guest drug actives (usually the host to guest ratio is 1:1) and form inclusion complexes, which can still be soluble in water due to the hydrophilic edges of the torus. As a result, CDs are widely used in pharmaceutical formulations to improve solubility of lipophilic drugs,<sup>19</sup> thus achieving high drug bioavailability. The methodology of drug/CD formulation often involves addition of the drug to an aqueous solution of CD where it is solubilized as the CD complex. Then the solid complex can be isolated from the solution by methods of co-precipitation, freeze-drying, or spray-drying. Compared with solution phase, the solid complex is more stable against microbial growth. And it can be easily reconstituted to solution form by adding water or saline for intravenous administration. The major product of enzymatic synthesis from starch is  $\beta$ -CD, which has the best binding affinity with hydrophobic solutes and is the most widely-used CD for preparation of complexes with organic molecules. However, compared with other cyclodextrins, a strong interaction “belt” is formed by intramolecular hydrogen bonds between the C-2-OH group of one glucopyranoside unit with the C-3-OH group of the adjacent glucopyranose unit in  $\beta$ -CD, which results in a rather rigid structure.<sup>18</sup> Therefore,  $\beta$ -CD has the poorest solubility in water (1.85 g/100 mL, 25°C), and this directly impacts the complex solubility. Furthermore, it was reported that the injected  $\beta$ -CD in plasma is excreted through the kidney, where it can precipitate upon concentration in the microtubules as small crystals. The crystals cause microtubule necrosis, making kidney unable to concentrate urine due to premature tissue death. Due to these disadvantages, the use in IV application was restricted or prohibited and  $\beta$ -CD is only used in oral formulations in certain areas of the world.

To overcome the inherent low water solubility of  $\beta$ -CD and eliminate toxicity concerns, chemical modifications with functional groups were applied. Enhanced solubility is achieved by etherification through disruption of the regular crystalline CD structure and the addition of hydrophilic substituents. Important commercial examples include 2-hydropropyl- $\beta$ -cyclodextrin



(HPCD) and sulfobutyl- $\beta$ -cyclodextrin (SBCD) (**Fig. 2.3**).

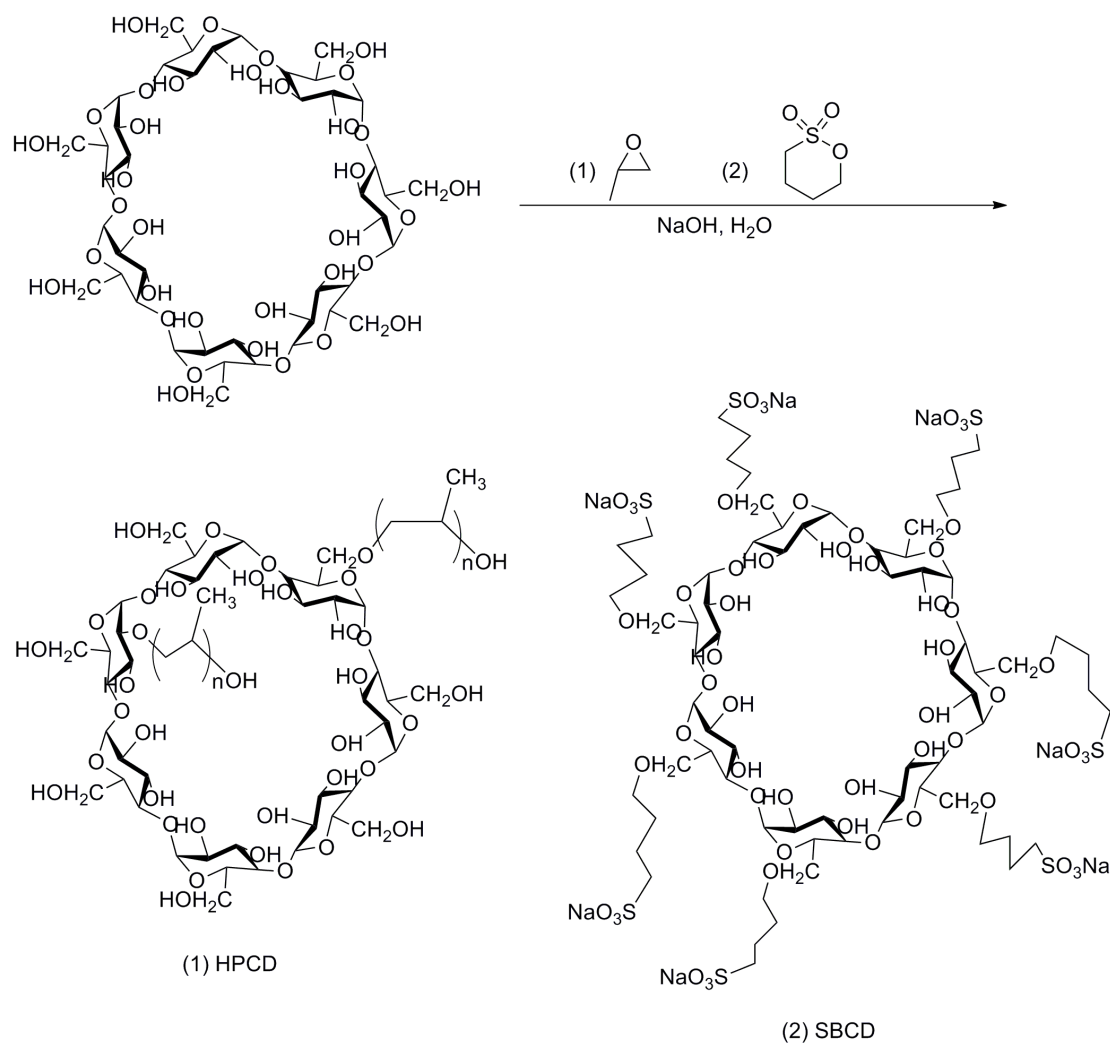


**Figure 2.3** Synthesis of hydropropyl- $\beta$ -cyclodextrin (HPCD) and sulfobutyl- $\beta$ -cyclodextrin (SBCD)

As described previously, in certain cases salt formation could not provide adequate drug solubility (e.g. the mesylate salt of ziprasodone (ZM) only has an aqueous solubility of 0.89 mg/mL at pH 2.7). It was reasoned that the salt form could not be fully dissociated to its soluble ionic product in a physiologically acceptable aqueous solution. Thus, a strategy that combines SBCD with a salt form of drug was developed and solved the problem. Kim et al. prepared an 1:1 stoichiometric inclusion complex of the mesylate salt of ZM with SBCD, which increased the target concentration in aqueous solution to 44.0 mg/mL.<sup>20</sup> However, it was not suggested that ZM

became fully dissociated in the complexation system, instead, the drug ion pair was even more favorable because the hydrophobic nature of cyclodextrin cavity makes it interact strongly with uncharged molecules.<sup>21</sup> Using similar combination method of ionization and SBCD complexation, the aqueous solubility of kynostatin, a tripeptide HIV protease inhibitor, was able to increase substantially from the equilibrium solubility (4  $\mu\text{g/mL}$ ). Optimal results (5-50  $\text{mg/mL}$ ) were obtained with high concentrations of SBCD (50 wt%) at low pH (pH = 3.0).<sup>21</sup>

HPCD is also an excellent candidate for drug solubility enhancement. Its low cytotoxicity, minor organ irritation and weak haemolytic activity<sup>22</sup> allow the application in pharmaceutical areas. In the 1990s researchers developed a combined approach of pH adjustment with CD complexation for thiazolobenzimidazole solubilization.<sup>23</sup> This anti-AIDS drug has a single ionizable group with  $pK_a$  3.55. However, in the physiologically acceptable range (pH > 2), the  $pK_a$  is too low to achieve adequate solubility enhancement by salt formulation. Through formation of a protonated complex with HPCD, solubility was enhanced by 3 orders of magnitude vs. when only ionization method was applied. It was further identified that the formation of stable a HPCD-rutin complex led to inhibition of the chemical or enzymatic anti-oxidant hydrolysis, and enhanced gastrointestinal stability in an *in vivo* absorption study.<sup>24</sup> Boudad et al. also described a combined method of HPCD complexation and poly(alkylcyanoacrylate) nanoparticle incorporation with saquinavir, a HIV protease inhibitor.<sup>25</sup> It not only led to the result that the apparent solubility of saquinavir was increased 400-fold at pH 7.0, but also achieved a 20-fold increase in saquinavir loading compared to nanoparticles prepared in the absence of modified cyclodextrins.

Later, Buchanan *et al.* discovered that a modified CD, hydroxybutenyl- $\beta$ -cyclodextrin (HBenBCD) is highly soluble in water and organic solvents and it forms complexes with a broad range of drugs.<sup>26</sup> HBenBCD was prepared by reacting parent CDs with 3,4-epoxy-1-butene in the presence of KOH at elevated temperature. Low molecular weight by-products after the reaction could be easily removed by nanofiltration. From the MALDI-TOF-MS analysis, HBenBCD was shown to have a random substitution pattern which impeded crystallization and promoted high, rapid water solubility (> 500  $\text{mg/mL}$ ) and organic solubility (> 400  $\text{mg/mL}$  in polyethylene glycol).

The use of HBenBCD for enhancing *in vitro* solubility and *in vivo* bioavailability of drugs

was studied systematically. For instance, Buchanan et al. examined oral administration of tamoxifen-HBenBCD formulations.<sup>27-29</sup> In solubility and dissolution studies, the results showed that these formulations provided a 10-14-fold increase in bioavailability relative to that of tamoxifen base alone, and eliminated the need for conversion to the nitrate salt of the drug to enable higher solubility and efficacy. Similarly, the solid powder complexes of HBenBCD (10 wt%) with saquinavir, which has poor aqueous solubility ( $207 \pm 5 \mu\text{g/mL}$  in base form and  $2.1 \pm 0.3 \text{ mg/mL}$  in mesylate form), were discovered to enhance the equilibrium solubility by 26 and 6 fold, respectively. The dissolution profiles showed that the complexes have a rapid and stable dissolution rate in the pH range of 1.2-6.8.<sup>30</sup> From the pharmacokinetic perspective, 3 important parameters, area under the plasma concentration–time curves (AUC), maximum plasma drug concentrations ( $C_{\text{max}}$ ) and time to reach  $C_{\text{max}}$  ( $T_{\text{max}}$ ) were studied.<sup>31</sup> The determined oral bioavailability (F) in rats after dosing with saquinavir mesylate capsules is only  $2.0 \pm 0.7 \%$ , and interestingly, a nearly 9-fold increased oral bioavailability was observed in this animal model when dosed with saquinavir base-HBenBCD capsules. In conclusion, the series of studies proved that HBenBCD is a significantly valuable vehicle in drug delivery systems, especially for IV drug formulations, and helped to increase drug oral bioavailability. However, the use of modified CD complexation is still limited due to the potential of poor patient compliance, resulting from bitter taste of CD itself, stomach pain, diarrhea,<sup>32</sup> together with the issue that only drugs with the right size, geometry and intrinsic solubility properties can benefit from CD complexation.<sup>33</sup>

### **2.3.2 Nanosizing: Nanoparticles with large surface area**

The increase in surface area with reduction of particle size enables drugs to be dissolved more efficiently and effectively. In this approach, poorly-soluble drugs are formulated as nanometer-sized drug particles for better bioavailability.<sup>34</sup> This method is prevalently called nanosizing, wherein a pulverized nanoparticle commonly is defined as having a size between several nanometers and  $1 \mu\text{m}$ . A co-grinding method of poorly-soluble drug with polymeric stabilizer and surfactant is used most often to produce such nanoparticles.<sup>35</sup> The use of polymeric stabilizers such as the celluloses, polysorbates, or polyvinylpyrrolidones (PVP) is intended to inhibit hydrophobic aggregation among drug nanocrystals by their strong absorption to the particle surface. The amount of stabilizer added is crucial during formulation because agglomeration or

Ostwald ripening would occur respectively in the case of too low or too high weight ratio of drug to stabilizer.

Itoh et al. have demonstrated a dry co-grinding method of poorly water-soluble drugs with PVP and sodium dodecyl sulfate (SDS) by the means of a vibrational rod mill.<sup>36</sup> The negative charge of SDS created electrostatic repulsion, thus, the addition of SDS provided the nanoparticles with good stability in aqueous dispersions. However, as long as the drug is not sensitive to hydrolysis, generally the dry co-grinding method is less effective than wet methods in the aspect of reducing particle size. Liversidge et al. reported the use of wet milling, named as NanoCrystal<sup>®</sup> Technology, to formulate nano-sized drug crystals.<sup>35</sup> Micron-sized drug crystals underwent a media milling process and were fractured in a water-based dispersion into a homogeneous nanoparticle dispersion with mean diameters less than 200 nm. Highly crosslinked polystyrene resin was frequently used as the milling medium and the entire process could be completed within 60 min. Takatsuka et al. further reduced the time of wet milling process to 5 min using a rotation/revolution mixer and zirconia balls.<sup>37</sup> The original bulk of drugs were dispersed in aqueous methylcellulose (stabilizer) solution and then pulverized. Freeze-dried phenytoin nanoparticles were created with mean diameter of 129 nm, which was  $\sim 1/10$  the diameter of the original drug. However the pulverized nanoparticles retained their crystallinity which could grow and aggregate over time during storage.

Nanoprecipitation is an easy and efficient method for the small-scale production of nanoparticles in the laboratory. Two different techniques were used in many studies: dialysis and dropping techniques. Membrane-dialysis of the compound dissolved in a solvent against a non-solvent yields regular nanospheres, whereas the precipitation in a nonsolvent by dropwise addition affords nanoscale bean-shaped particles.<sup>38</sup> Recently, flash nanoprecipitation was introduced by Prud'homme et al., in which the multi-inlet vortex mixer (MIVM) was used to rapidly mix two or more streams, usually a amphiphilic polymer solution with an anti-solvent, to create high and uniform supersaturation.<sup>39</sup> The amphiphilic polymer was absorbed uniformly onto nanoparticle surfaces and this slowed down nanoparticle nucleation. As a result, this method ideally resulted in production of nanospheres with narrow size distribution.

In conclusion, using nanosizing methodology, the formation of near-spherical-shaped nanoparticles reduced in average diameter from 10 microns to 200 nm, leading to an increase in surface area by nearly 50 fold.<sup>35</sup> The significant particle size reduction has made a positive impact on faster absorption and enhanced bioavailability based on the *in vivo* study. However the drawback of this technology is, without a suitable dissolution method, the formation of aggregates due to the high surface energy of nanoparticles, along with associated wetting and floating problems made the dissolution rate similar or even lower than unprocessed crystalline form.<sup>40</sup> Additionally, easy contamination from the grinding medium is the other issue with those high-surface nanoparticles prepared by the grinding method.

### **2.3.3 Lipid-based delivery**

Utilization of lipid based drug delivery systems is another major approach to overcome the poor solubility of lipophilic drugs. It has long been realized that oral bioavailability can be enhanced when a drug is co-administered with a meal rich in fat. From the standpoint of drug delivery, the presentation of poorly water soluble drug as a solubilized formulation, avoiding solid-state limitation, is the primary mechanism for lipid-based enhanced delivery.<sup>41</sup> By selecting the optimum lipid vehicle and form, it is possible to minimize or even eliminate crystallization of the drug in the GI tract. As a result, the lipid component can be non-digestible, including mineral oil, sucrose polyesters, or digestible ones including triglycerides (TG), diglycerides (DG), phospholipids (PL), fatty acids (FA), cholesterol and other synthetic derivatives. Moreover, lipid-based delivery systems can be formulated as solutions, suspensions, emulsions, microemulsions, or self-emulsifying drug delivery systems.<sup>42</sup>

Traditional formulations of lipophilic drugs in lipid-based systems are simple and maneuverable. Drugs are dissolved or suspended in either a single lipid or a blend of lipids, or incorporated into the oil phase of oil-in-water emulsions.<sup>43</sup> The chemical nature of the lipid used greatly impacts the oral bioavailability of drugs after formulation. The important factors include fatty acid chain length, the degree of unsaturation and the lipid class (TG, DG, PL or FA). For instance, towards highly lipophilic drugs such as cyclosporine<sup>44</sup> and halofantrine,<sup>45</sup> a long chain triglyceride solution formulation showed increased solubilization capacity, as well as more

effective lymphatic drug transport when compared with medium chain triglycerides solutions.

As technology develops, self-emulsifying drug delivery systems (SEDDS) have been increasingly employed in oral administration. To spontaneously emulsify and form oil-in water emulsions or microemulsions in GI tract, isotropic mixtures of natural or synthetic oils with lipophilic or hydrophilic surfactants and co-solvents are required in SEDDS. The ability of rapid emulsification generates a high surface area of interaction between GI fluids and drug-lipid formulation, which leads to enhanced drug dissolution and absorption. The other advantage is that for lipophilic drugs with intermediate partition coefficients ( $\log P = 2-4$ ), SEDDS result in increased drug loading capacity when compared with other lipid formulation.<sup>46</sup> This merit is attributed to the fact that those specific drugs are less soluble in lipids but much more soluble in amphiphilic surfactants and co-solvents. Kim et al. compared the bioavailability of indomethacin after oral administration of a SEDDS (comprising 30% Tween 85 and 70% ethyl oleate) and indomethacin suspension.<sup>47</sup> SEDDS formulation showed a significant 57% increase in  $AUC_{0-12h}$ . High drug loading and rapid release of drug were also responsible for the enhanced drug bioavailability.

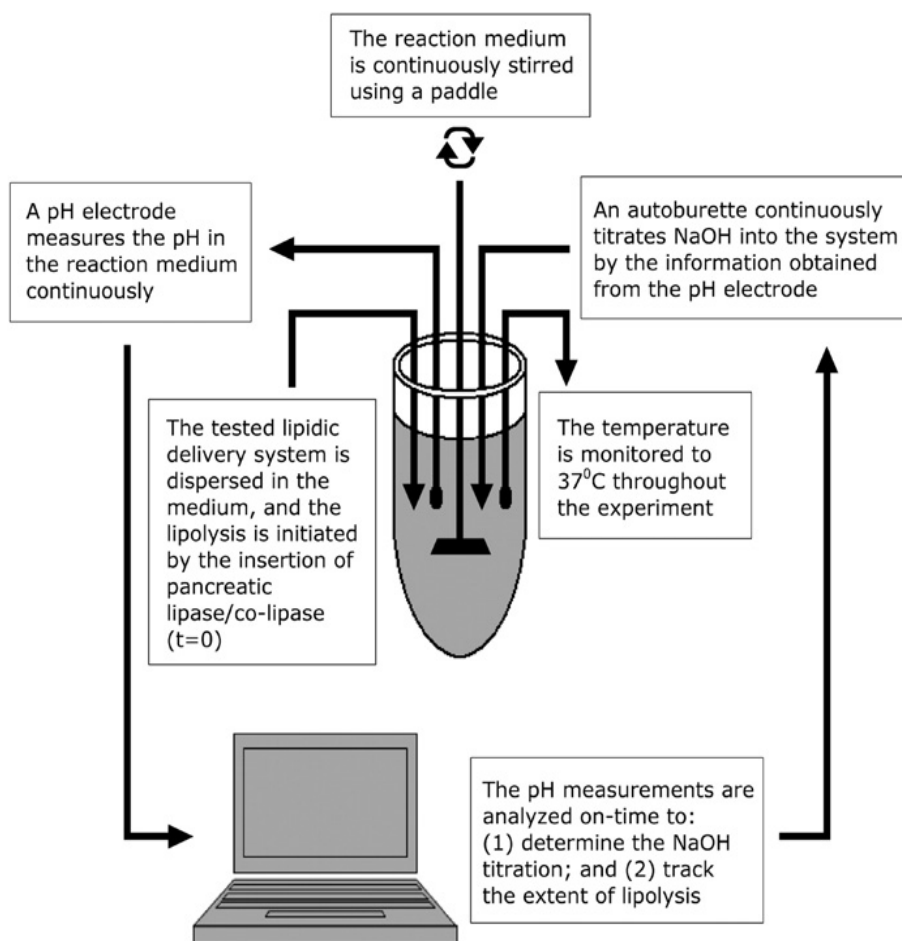


**Figure 2.4** Lipid digestion models for *in vitro* assessment of lipid-based formulations, reprinted from Dahan, A.; Hoffman, A. *J Control Release* **2008**, 129, (1), 1-10. Used with permission of Elsevier, 2008.

The limitation of lipid-based delivery system is a lack of comprehensive knowledge of the formulation parameters that are accurately predictive of *in vivo* performance for lipophilic drug candidates. Therefore only a few human studies have been reported in the literature comparing to conventional dosage forms. Recently, some valuable information could be obtained from the *in vitro* lipolysis simulation model (**Fig. 2.4**), which will potentially alter the lipid-based systems from empirical study to commercial development.

### 2.3.4 Micellar solubilization – The use of artificial surfactants as excipients

The use of surface active agents as excipients in the dosage form has been a common

approach to improve the apparent aqueous solubility of lipophilic drugs. Commonly applicable surfactants include sodium dodecyl sulfate, dodecyltrimethylammonium bromide, polysorbates, polyoxyethylated glycerides, lauroyl macroglycerides, mono- and di-fatty acid esters of low molecular weight polyethylene glycols.<sup>48</sup> They are generally composed of a hydrophilic (polar) moiety called as *head* and a hydrophobic (nonpolar) moiety known as *tail*. Above the critical micelle concentration (CMC, which is in the range of 0.05-0.1% for most surfactants), the hydrophobic tails assemble to the interior to avoid contact with water and the heads stay on the outside interacting with water. Therefore, surfactants can incorporate lipophilic drug into micelles, which can lead to extraordinary increases in apparent solubility.<sup>49</sup> The effectiveness of surfactants in micellar solubilization of drugs depends on several factors including chemical structure of surfactants and/or drugs, temperature, pH and ionic strength as described below.

1. Due to lower CMC values, nonionic surfactants are typically more capable of solubilizing lipophilic drugs than ionic surfactant.
2. Drug solubility is enhanced with the increase in temperature.<sup>50</sup> It was reasoned that the thermal agitation led to the increase in the space for drug solubilization in the micelle, apart from the solubility increase of drug itself at elevated temperature.
3. Increased ionic strength usually gives rise to solubility enhancement, especially in the case of ionic surfactants. The addition of salt decreases the repulsion between like-charged groups and then decreases the CMC and increases the aggregation numbers and free volume of the micelles. Thereby hydrophobic drugs are preferentially solubilized in the core of the micelle.<sup>51</sup>
4. pH change in the micellar solution also affects the extent of drug solubility. However, this is entirely attributed to the nature of the drug. As shown previously, pH adjustment may change the equilibrium between ionized and un-ionized forms of some drugs.<sup>52,53</sup> Certainly, the drug solubility increases as drug ionization increases.

Recently, polymeric micelles for drug solubilization have gained increased attention. They are derived from block co-polymers consisting of hydrophobic core (such as polypropylene oxide) and hydrophilic shell (such as polyethylene oxide). Well-designed polymeric micelles exhibit better solubilization capacity than conventional surfactant micelles, mostly thanks to higher number and larger cores of micelles formed.<sup>54</sup> Kataoka and Kabanov are the leading groups in the



development of polymeric micelles. The aqueous solubility of free doxorubicin (an anticancer drug, DOX) is less than 50 µg/mL. Kataoka et al. prepared and studied PEO-*b*-poly(L-aspartic acid)-DOX conjugates. PEO-poly(aspartic acid)-DOX was able to form micellar structure with a diameter of ~50 nm with a narrow distribution in phosphate-buffered saline.<sup>55</sup> The micellar conjugates exhibited nearly 3 times suppression against C26 murine tumor cells growth when compared with the effect after injecting same amount of free DOX, and prolonged life span of the entire group of treated mice.<sup>56</sup> Later, Kabanov et al. also investigated antitumor effects of DOX after formulated with PEO-PPO-PEO block co-polymers (Pluronic®).<sup>57</sup> After optimizing the ratio between hydrophobic and hydrophilic segments, treatment with these micelles considerably extended the lifespan of the mice (>150%) and inhibited tumor growth (>90%), when compared with animals treated with free drug.

In another example, the aqueous solubility of free paclitaxel (an antitumor drug) is only 1 µg/mL. Biodegradable polymeric micelles made of PEO-*b*-poly(D,L-lactic acid-*co*-caprolactone) have been utilized to incorporate paclitaxel.<sup>58</sup> After administration, the polymeric micellar formulation of paclitaxel produced a 5-fold increase in the maximum tolerated dose compared with conventional formulation with Cremophor EL. Micellar paclitaxel-treated animals possessed an increased survival time, and long-term survivors (20% of those tested) existed only in the polymeric paclitaxel formulation group.

One drawback of micellar solubilization for oral administration of BCS class II drugs is that surfactants can decrease the free fraction of drug, resulting in decreased intestinal membrane permeability.<sup>59</sup> Furthermore, barriers to use of polymeric micelles such as low drug loading efficiency, poor stability after administration, and difficulty in transporting through membranes are still being resolved, in order to reach a maximal bioavailability.<sup>60</sup>

### **2.3.5 Amorphous solid dispersions**

It has been discovered that solubility disadvantages often can be successfully overcome by formulation of drugs as amorphous solid dispersions (ASD) in polymer matrices.<sup>15</sup> When entrapped in a high energy, metastable amorphous form, drug molecules do not have to overcome the heat of fusion to dissolve. Studies from Taylor et al. have revealed that the incorporation of a

miscible polymer forms a molecular dispersion, disrupting the crystal lattice of the drug, which increases the dissolution rate and extent, and thus enhances the oral bioavailability.<sup>61</sup> In addition, enhanced drug solubility enabled by ASD relies more on supersaturation than solubilization.<sup>62</sup> As a result, recent publications showed that ASD formulations increased apparent solubility without the sacrifice of intestinal membrane permeability while other formulation methods including cyclodextrin complexation, micellar solubilization or co-solvents addition did have a trade-off effect between solubility and permeability.<sup>59, 63, 64</sup> Detailed information will be given in the next section.

Several review papers discussed multiple manufacturing processes for ASD formulations, dividing into two categories: hot melt and solvent methods.<sup>65</sup> In the hot melt process, the drug and the carrier should be miscible in the molten form. After homogenization and extrusion, the drug/polymer mixture can be re-shaped into tablets, pellets, granules or powder. Poly(ethylene glycol), ethyl cellulose, hydroxypropylmethyl cellulose and other polymers have been used for the production of ASDs with a wide range of pharmaceutical ingredients.<sup>66</sup> However, the limitation with hot melt methods is that the drug and the polymer should be both thermo-stable against degradation and chemical reactions above the temperature of the melt. This also suggests that the processing window must be wide enough for hot melt manufacturing of solid dispersions. There are numerous techniques for preparing ASDs by solvent methods. For small scale pre-screening, solvent evaporation is widely used. The drug and the polymer are dissolved in a common solvent and then the solvent is evaporated by spin-coating, rotary evaporation under reduced pressure, or dialysis followed by lyophilization. Co-precipitation can also be utilized to prepare ASDs through precipitating micro-particles of the polymer and drug from a co-solvent into a common non-solvent. For large scale especially in industry, spray-drying method is most commonly used, producing fairly dry powder by rapid drying with a hot nitrogen gas. A scheme of spray-drying and the image of a Mini Spray Dryer B-290 is shown in **Fig. 2.5**. This process has broad applicability to drug candidates and flexible ability to scale —scaling from tens of milligrams to metric tons.

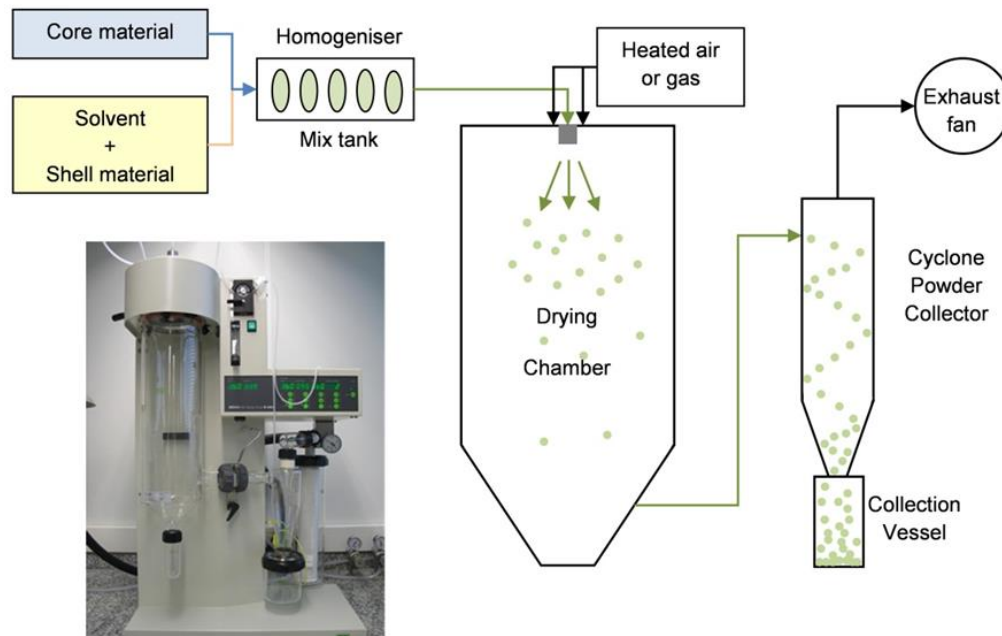


**Figure 2.5** Spray-drying process and the image of a Mini Spray Dryer B-290, reprinted from Chavarri, M.; Maranon, I.; Villaran, M. C. *Probiotics* **2012**, 501-540. Used with open access from InTech, 2012.

## 2.4 Polymer Matrices for Amorphous Dispersion Formulations

Polymers have to meet certain appropriate requirements to be utilized for amorphous matrix formulations.

Most importantly, polymers and potential side-products through chemical or enzymatic breakdown in the human body should be non-toxic. For oral medications, they have to possess good compatibility with the GI tract and do not inhibit drugs from reaching the systemic circulation. In addition, it is essential that the polymer should have the capability of forming a miscible complex with the drug in amorphous dispersion. Specific interactions between polymer and drug such as hydrogen bonding are needed to aid the miscibility and avoid phase separation. Furthermore, due to its high energy state, the amorphous drug may crystallize over time. Even trace amounts of crystallinity in the amorphous solid would promote rapid crystal growth and eventually diminish the effectiveness and shorten the shelf-life of the dosage form. Therefore, in

ASD formulation polymers must prevent or severely retard drug crystallization via complexation, and of course they should not crystallize themselves. High glass transitions and molecular-level interactions with specific drugs are usually favored and thus, the polymer-drug formulation could be stable even in hot, humid environments for years. Additionally, since the solubility of the drug is greatly enhanced in the amorphous form, polymers must have the ability to prevent the drug from precipitating in supersaturated aqueous solution in the GI lumen.

These polymers can have other beneficial effects such as a targeted and controlled release mechanism. A precisely-targeted release enables the drug to be released when inside the specific site (an organ or tumor) where it takes effect.<sup>67</sup> Since the small intestine is the main site for drug and nutrient absorption, this functionality is often achieved by pH-triggered mechanism upon moving from stomach to small intestine. On the other hand, controlled release may reduce side effects and toxicity of the active drugs by sustaining a stable rate of drug administration at or just above the effective dose needed to treat the ailment. Controlled release also provides the patient with longer periods of time in between treatments, ideally permitting once-daily dosing which is optimal for patient compliance.

## **2.4.1 Synthetic polymers**

### **Water-soluble polymers: Poly(vinyl pyrrolidone) (PVP), poly(ethylene glycol)**

Poly(vinyl pyrrolidone) (PVP) and poly(ethylene glycol) have often been used to prepare amorphous dispersions. These water-soluble synthetic polymers are commonly used to stabilize the amorphous state during storage.<sup>68</sup> PVP has a relatively high glass transition temperature (177°C). It has been concluded that the stabilizing ability of those polymers is attributed to their high  $T_g$ s. That is, the dispersions formed have higher  $T_g$  than the pure drugs which could also be predicted by using the Couchman-Karasz equation,<sup>15</sup> and thus achieved limited molecular mobility, inhibited crystallization together with longer shelf-life. This is not the only reason. Studies also showed the significant inhibition of crystallization even at relatively low levels of PVP incorporated. Taylor et al. reasoned that the formation of specific molecular level drug-polymer interactions,<sup>69</sup> for example, the formation of hydrogen bonding between the PVP amide carbonyl

and the indomethacin (drug) carboxylic acid hydroxyl, also contributes to physical stabilization.

Water has a low  $T_g$  (135 K, -138 °C). So if the polymer matrix absorbs water, moisture could reduce formulation  $T_g$  and thereby destabilize the drug with regard to mobility and crystallization. The complex is plasticized when water is absorbed into the internal amorphous structure. Based on the Fox equation, a rule of thumb is that 1% water will decrease  $T_g$  by about 10 °C. Molecular mobility increases thereby, facilitating crystallization even at ambient temperature. Marsac et al. confirmed that the hydrophilic polymer PVP is very hygroscopic which increases water sorption.<sup>70</sup> Thus, the effect of escalating hygroscopicity counteracts the inhibition of crystallization imparted by the high  $T_g$  polymer. It was observed that nifedipine and felodipine (anti-hypertension drugs) recrystallized in these meta-stable amorphous matrices. In comparison with other drug-polymer (hydropropyl methylcellulose, hydropropyl methylcellulose acetate succinate) blends, the PVP solid matrix had much more water affinity, which partly resulted in easier and faster crystallization of the drug.<sup>71</sup>

Previous work showed that PEG-amorphous ritonavir solid dispersions improved the intrinsic dissolution rate of the poorly soluble drug by at least 10-fold vs. crystalline ritonavir.<sup>72</sup> However, it was also reported that solubility enhancement of PEG solid dispersions was less than that of PVP dispersions.<sup>73</sup> This is reasoned as limited H-bonding interaction between PEG with flavonoids and thus part of the drug still remains in crystalline form. Zhu et al. also demonstrated that the onset of crystallization of API in the solid dispersions could be delayed and the crystallization rate could be reduced only if there were favorable interactions between the drug and PEG (as for benzocaine).<sup>74</sup> What's worse, the form of PEG in the dispersions is primarily crystalline.<sup>75</sup> PEG crystallizes rapidly even before reaching room temperature during the melt-quench cool process. The dissolution of amorphous drugs is not largely hampered by this highly crystallized carrier just because an increase in the surface area of drugs in solid dispersions. However, the degree of crystallinity of drug increases in storage, and this results in unacceptable changes in formulation performances, for example, a sharp decrease in solubility. For example, spray-dried lactose/PEG with PEG present as 10% by weight was found to be amorphous, and it was confirmed crystallization of lactose was retarded at low PEG concentrations. But the product recrystallized rapidly over time, and the rate of transformation from amorphous lactose to the

crystalline monohydrate form was highly dependent on temperature and humidity.<sup>76</sup>

Crystallization kinetics in semi-crystalline solid dispersions are complicated.<sup>77</sup> As for PEG, it could delay, promote or have no effect on crystallization of different APIs. For example, the induction time of ibuprofen in a PEG matrix was actually shorter than that of pure drug, and this was attributed to crystalline PEG that behaves as a heterogeneous nucleation site to accelerate the crystallization.<sup>74</sup> Moreover, the API in turn greatly influences the crystallization behavior of PEG matrix. Therefore it can be difficult to produce a PEG-based solid dispersion with consistent, stable properties.

### **Methacrylate-based copolymers: Eudragit® L, S, E.**

Eudragit® was first developed by Rohm & Haas GmbH (Evonik) in Darmstadt, Germany in 1953. Eudragit polymers are copolymers derived from esters of acrylic and methacrylic acid. While Eudragits with pH-independent behaviors such as RL, RS series (containing quaternary ammonium groups) are used for sustained release dosage forms due to their water-swallowable/permeable nature, in pharmaceutical applications, pH-dependent Eudragit polymers have received more attention.

Eudragit L and S series are two main anionic polymers for GI targeting. The active group (carboxylic moiety) percentage in Eudragit L 100 (48.3%) is higher than that in Eudragit S 100 (29.2%). The difference here results in the difference in pH-dependent solubility. L 100 is ionized at pH 5.5 while S 100 becomes ionized and water-soluble at pH 7.0.<sup>78</sup> To reduce the burst release by L 100 matrix and enhance the poor release observed from S 100 in the enteric environment (pH 6.8), combined systems of these two polymers were manufactured with poorly water-soluble drugs by hot melt extrusion (plasticizers are usually needed) or spray-drying. Mehta et al. discussed the release performance of leukotriene D<sub>4</sub> antagonist from this amorphous two-unit matrix.<sup>79</sup> Much enhanced release was achieved, and more importantly, zero-order release from such system occurred, which was controllable by alternating the ratio between those two polymers.

The pH-dependent Eudragit polymers are mainly used in gastro-resistant dosage forms.

The exception is the methacrylate aminoester copolymer - Eudragit E. It is soluble in gastric fluid up to pH 5.0. The cationic feature could provide modified release properties. Spray-dried solid dispersions of itraconazole with pH-dependent hydrophilic polymer Eudragit E 100, resulted greater increase in drug solubility (146.9-fold increase) over those prepared with pH-independent hydrophilic polymers, PEG 20,000, PVP and HPMC (range from 41.8 to 92.5-fold increase) in simulated gastric juice.<sup>80</sup> In general, due to the wide variety of Eudragits, in formulation processes usually a combination of anionic, cationic or neutral methacrylate copolymers (multi-units) is employed to enhance the physical and chemical properties of solid dispersions.

#### **2.4.2 Conventional pH-independent cellulose esters and ethers**

The utility of PVP and PEG as amorphous polymer matrices is undoubtedly limited and the research focus has been shifted to novel cellulose derivatives.<sup>67</sup> Because of their high molecular weights and other physicochemical properties, most cellulose ethers and esters cannot be absorbed from the gastrointestinal tract. Even if a small degree of hydrolysis were to occur by chemical or lipase-catalysis, the by-products (cellulose, acetic/propionic acid, glucose) are endogenous or dietary. These facts make conventional, non-ionic cellulose derivatives such as ethyl cellulose, cellulose acetate, or mixed cellulose esters (e.g. cellulose acetate propionate and cellulose acetate butyrate) exceptionally safe as hydrophobic matrices in drug delivery applications.<sup>12</sup>

However because of water-insolubility, cellulose esters are not generally used in amorphous solid dispersions (at least not used as single components). Instead of forming ASDs, cellulose esters such as CA, CAP and CAB are well-suited for osmotic delivery for sustained drug release.<sup>67</sup> Since water insoluble polymers do not erode away over time, the release of the drug is dependent on the diffusion of aqueous fluids to slowly permeate through the membrane. Those cellulose esters are permeable to water, and the permeability can be easily adjusted to fit a particular API by alternating ester degree of substitution, chain length and the type of plasticizer. Changes in pH or salt content of the surrounding physiological environment do not influence the delivery rate due to the impermeability of the polymer membrane to salt and drug. For example, cellulose diacetate (weight percent acetyl of approximately 39.8%) was primarily used as a semi-permeable membrane for sustained release of acetaminophen,<sup>81</sup> theophylline, dyphylline, and proxyphylline.<sup>82</sup> Regarding drug release rate, increasing the percentage of cellulose acetate in the

dosage form (CA-to-drug weight ratio) could further prolong the release of the drugs as expected. Release can be further controlled in osmotic pump systems by porosity during the formulation.<sup>83</sup> In order to do this, the solid dispersions were pressurized under carbon dioxide gas to form porous bubble upon release of pressure. Microspheres with large internal cavities showed higher release rate. As can be predicted, solid dispersion blends of those pH-independent cellulosic polymers with pH-dependent ones (e.g. C-A-P, HPMCP) (properties in **Table 2.1**) are being developed for desirable drug release properties.<sup>84</sup>

**Table 2.1** Properties of cellulose esters used in pharmaceutical formulation, reprinted from Edgar, K. J. *Cellulose* **2007**, 14, (1), 49-64. Used with permission of Springer, 2006.

CE	Abbrev.	DS (Ac)	R	DS (R)	T <sub>g</sub> (°C)	Solvents	M <sub>n</sub> (/1000)
Cellulose acetate	CA-398- NF	2.5	NA	NA	185	Acetone	40
Cellulose acetate butyrate	CAB- 171-15	2.0	Butyryl	0.8	161	Acetone, ethyl acetate	65
Cellulose acetate phthalate	C-A-P	2.1	Phthaloyl	0.9	175	Acetone/water, ethanol/water	13
Hydroxypropyl methyl cellulose phthalate	HPMCP 55	NA	Hydroxypropyl Methyl Phthaloyl	0.3 1.9 1.7	135	Acetone/water, ethanol/water	20

### Hydroxypropylmethylcellulose (HPMC)

Cellulose ethers, including carboxymethylcellulose, methyl/ethyl cellulose (MC) and derivatives, hydroxyethyl/propyl cellulose and derivatives, perform a variety of functions such as thickening, binding, water retention, and acting as an emulsifier and viscosity-control agent in pharmaceuticals and personal care products. For solubility enhancement, hydroxypropylmethylcellulose (HPMC) is probably the sole pH-independent cellulose derivative which has been widely used as an ASD polymeric matrix.



HPMC, also referred to as hypromellose, is a non-ionic, hydrophilic cellulose ether derivative. It is generally prepared by processing pulp cellulose in sodium hydroxide solution, followed by reaction with methyl chloride and racemic propylene oxide at the same time in a heterogeneous process, targeting for methyl and hydroxypropyl substituents respectively.<sup>85</sup> A review of the literature regarding the use of HPMC in sustained release forms, including drug release mechanisms and release rates, has been published by Li et al.<sup>86</sup> Oral formulations with HPMC are usually manufactured by pressing a tablet of a mixture of a powder of the polymer, the drug, and other excipients. When the HPMC comes in contact with water, it forms a gel through which the drug molecules must pass to be released. Over time, the outer layer of the HPMC gel dissolves in water, allowing a secondary mechanism for drug release by membrane erosion.<sup>87</sup> The release rate of the drug is affected by such factors as the drug solubility, the concentration of HPMC, the viscosity of the selected HPMC, and the inclusion of other excipients in the formulation.<sup>88</sup>

HPMC also has been widely formulated with drugs having limited bioavailability in the form of ASDs. Studies with ER-34122, a poorly water-soluble dual 5-lipoxygenase/Cyclooxygenase inhibitor, showed a surprising 100-fold increase in both  $C_{max}$  and AUC in bioavailability compared with the pure drug using male beagle dogs.<sup>89</sup> HPMC can further stabilize the drug in the amorphous state, even though the solid dispersion absorbed 2 wt% moisture when equilibrated at 75% RH, which might induce recrystallization. Suzuki et al. compared nifedipine (a calcium-channel agent) solid dispersions with 4 water-soluble polymers, HPMC, PVP, partially hydrolyzed polyvinyl alcohol (PVA) and pullulan.<sup>90</sup> HPMC showed great compatibility with nifedipine and thus provided the highest supersaturation level in dissolution studies. Solubility parameter (SP) was introduced here as a criterion for selection of the polymeric matrix; in this case the SP value of HPMC was the closest to that of nifedipine.

A commercial product, Intelence<sup>®</sup> (etravirine, a anti-HIV drug) was produced by Janssen Pharma in 2008. The polymer matrix they used for spray drying was HPMC. Etravirine is an extremely poor glass former and the amorphous state is very unstable given its high  $T_g$ . Evidenced by powder XRD, solid-state NMR, as well as visualization techniques including SEM and AFM, it turned out that spray-drying with HPMC is the only method to yield high level of stabilization of amorphous etravirine, and hence high bioavailability.<sup>91</sup> The higher the percentage of HPMC

present in the solid dispersion, the better solid-phase stability observed. A recent paper from Taylor's group further studied the impact of HPMC on inhibiting recrystallization of felodipine from supersaturated solutions.<sup>92</sup> The presence of a small amount of pre-dissolved HPMC (as low as 0.5 µg/mL) could inhibit both nucleation and growth of felodipine crystals (delaying nucleation was more evident here), and the effectiveness depended on the extent of supersaturation.

### 2.4.3 pH-dependent cellulose derivatives

As mentioned, cellulose derivatives are highly useful as matrix polymers, because of their low toxicity, generally high glass transition temperatures to prevent drug migration and crystallization, and the ability to tailor the structure to achieve compatibility with drugs.<sup>93</sup> To stabilize the drugs and protect them from immediate release, those cellulose derivatives must retain the ability to disperse in water. There are two common ways of achieving water swellability for cellulose esters: remove sufficient ester groups and expose sufficient hydroxyls, or incorporate highly polar, ionizable groups. Often what is needed is a largely hydrophobic cellulose derivative, which still contains pendent carboxylic acids to provide a trigger mechanism (pH sensitivity) for swelling and drug release.<sup>67</sup> These polar groups also provide energetically favorable specific interactions by hydrogen-bonding with the drug molecule.<sup>94</sup> Therefore, carboxylated cellulose esters also containing some hydrophobic substituents are desirable synthetic targets.

Due to their pKa values (e.g. succinate groups of HPMCAS have a pKa of ~5,<sup>95</sup> carboxymethyl groups of CMC have a pKa of ~3.7<sup>96</sup>), carboxylated polymers are fully protonated and therefore insoluble in the low pH (1-3) of the stomach, but ionized in the higher pH (5.5-7) of the small intestine. In order to target drug delivery to the small intestine, a polymer matrix-drug dosage form should remain intact when passing through the stomach to avoid direct contact between drug and gastric acid or digestive enzymes, which can easily migrate into the dosage form, but swell or dissociate to enable the active contents to dissolve, release and be absorbed in the small intestine. More valuable benefits have been discovered using carboxyl-incorporated cellulose for modern drug delivery applications. To begin with, it was proved that the polymer significantly enhanced drug solubility by entrapping the drug in metastable amorphous form dispersed in the matrix.<sup>95</sup> The hydrophobic substituents, such as propionate, butyrate, promote

miscibility of highly hydrophobic drug in the polysaccharide matrix. Furthermore, the high  $T_g$  of cellulose derivatives, together with the specific interactions such as hydrogen bonding between the polymer and drug, help to enhance the stability of amorphous dispersions.<sup>93</sup> It was also suggested that zero-order release could be achieved by ionizing the polymer matrix in solution, which permits constant blood concentration of the drug over long time periods and may reduce dosing frequency and side effects.<sup>97</sup> Detailed examples of those effective drug carriers are as follows.

### **Cellulose acetate phthalate (C-A-P) and hydroxypropylmethylcellulose phthalate (HPMCP)**

Cellulose acetate phthalate (C-A-P) was identified as a pH sensitive coating by Malm et al. at Eastman Kodak Company 70 years ago.<sup>98</sup> A pH sensitive coating is defined as a material which is insoluble at low pH and swells and/or dissolves at neutral to high pH. C-A-P is well-suited to this application because it is soluble in organic solvents and acts as a good film-former, furthermore, it has the ability to form water-soluble salts readily with ammonia. The preparation of this phthalic acid ester of cellulose was accomplished by the reaction of cellulose acetate ( $DS_{\text{acetyl}} = 1.41$ ) in glacial acetic acid with phthalic anhydride.<sup>99</sup> The esterification was catalyzed by sodium acetate or pyridine. Phthalyl content ranging from 21 to 38% was introduced but complete phthalation could not be attained. C-A-P is a high  $T_g$  cellulose ester and consequently, Malm and others pursued the coating of mixtures of drug and inactive diluents such as microcrystalline cellulose with C-A-P films. Due to the fact that it's ionized at a relatively low pH value of 5, and the potential as a concentration enhancing polymer, C-A-P was utilized and evaluated as a matrix for amorphous dispersions.<sup>100</sup> *In vivo* testing conducted in Sprague-Dawley rats demonstrated a significant 2-fold improvement in oral bioavailability from a C-A-P /itraconazole matrix (an antifungal drug, 2:1 polymer-to-drug ratio) compared to Sporanox, the current marketed dosage form of itraconazole. Moreover, C-A-P formulations also provided longer duration of supersaturation.

Hydroxypropylmethylcellulose phthalate (HPMCP) dissolves in water at either pH 5 or pH 5.5, depending on the grade. Therefore, at stomach pH, the dispersion in HPMCP does not release the drug, while at pH 6.5 it releases drug very effectively. Kai et al. studied the oral bioavailability improvement of MFB-1041 (a triazol antifungal agent) by formulating ASD with HPMCP (5:1 polymer-to-drug ratio).<sup>101</sup> The maximum drug concentration at pH 6.8 was increased by a factor

of 12.5 as compared to that of micronized drug powder, and the oral bioavailability was enhanced by nearly 17 times. HPMCP enhanced the dissolution rate but was unable to inhibit recrystallization. Maximum concentration was achieved within 5 min followed by rapid desupersaturation, resulting in only 3-fold increase in apparent solubility vs. that of a microcrystalline dosage form after 4 hours. This is probably due to lack of H-bonding interactions using phthalate-based cellulosic polymers.

However, there are only a few reports on this application mainly because C-A-P or HPMCP has relatively limited miscibility with organic drug molecules. Therefore, exploration of other more effective cellulose derivatives is necessary.

### Carboxymethyl cellulose acetate butyrate (CMCAB)

The most important anionic, water-soluble cellulose ether, carboxymethylcellulose (CMC), is produced in large quantities by etherification of activated alkaline cellulose with chloroacetic acid.<sup>102</sup> Conversion of carboxymethylcellulose into hydrophobic ester derivatives like acetate, propionate and butyrate has been reported by inventors from Eastman Chemical Company (**Fig. 2.6**).<sup>103</sup>

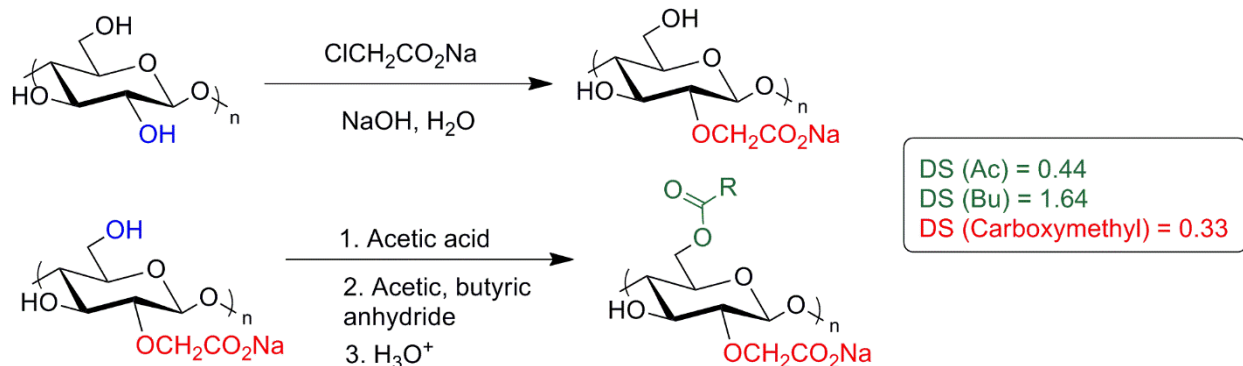


**Figure 2.6** Two-step preparation of CMCAB with DS of carboxymethyl 0.33

The resulting carboxymethylcellulose mixed esters were reported by Allen et al. with various DS values of three substituent groups, depending on the feed ratios and reaction conditions.<sup>103, 104</sup> Usually commercially available CMCAB polymers are produced with a DS of carboxymethyl of 0.29 to 0.35, a DS of butyryl group of 1.37 to 1.64 and a DS of acetyl group of

0.30 to 0.55.<sup>12</sup> The inherent viscosity  $[\eta]$  was measured in 60/40 (wt./wt.) solution of phenol/tetrachloroethane at 25°C, and the determined values were around 0.30-0.65 dL/g. Specifically, **Fig. 2.6** also shows the chemical structure and specific DS values of each substituent for Eastman CMCAB-641-0.2. The high DS of acyl groups makes the polymer miscible with hydrophobic drugs. The pendent carboxymethyl groups make it pH sensitive, but the rather low DS (0.33) of carboxymethyl causes the polymer to have limited water solubility, even at pH above 7. CMCAB swells at neutral and higher pH.

Posey-Dowty et al. described two distinct but highly effective methods of using CMCAB for oral dosage forms in drug delivery.<sup>97, 105</sup> The first and easiest way is to make physical blends with drugs by direct compression using a single tablet press. Ibuprofen is poorly soluble at low pH but has much better solubility at elevated pH. Physical blends of ibuprofen with CMCAB gave extended, zero-order drug release at pH 6.8 (**Fig. 2.7**), which confirmed that it was a simple and inexpensive way to create once-a-day pills for enhanced patient compliance and adherence. In contrast, the complete dissolution of ibuprofen from physical blend with microcrystalline cellulose within 30 min at pH 6.8 indicated a combined effect of fast matrix disintegration in buffer solution and poor compatibility of the drug and polymer matrix.

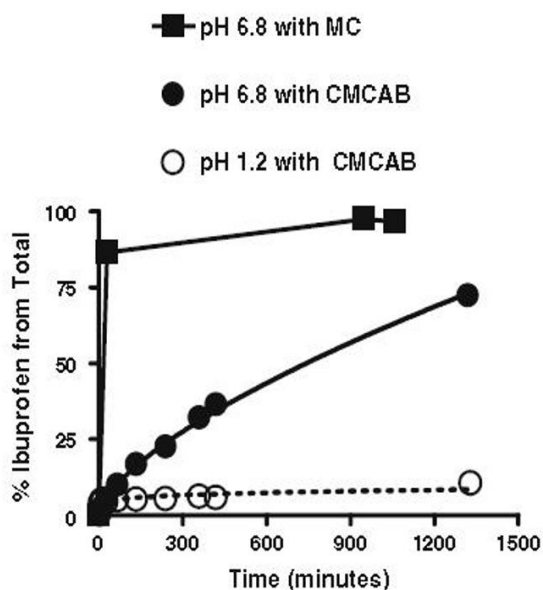


**Figure 2.7** Ibuprofen release with physical blends of CMCAB and microcrystalline cellulose (MC), reprinted from Posey-Dowty, J. D.; Watterson, T. L.; Wilson, A. K.; Edgar, K. J.; Shelton, M. C.; Lingerfelt, L. R. *Cellulose* **2007**, 14, (1), 73-83. Used with permission of Springer, 2006.

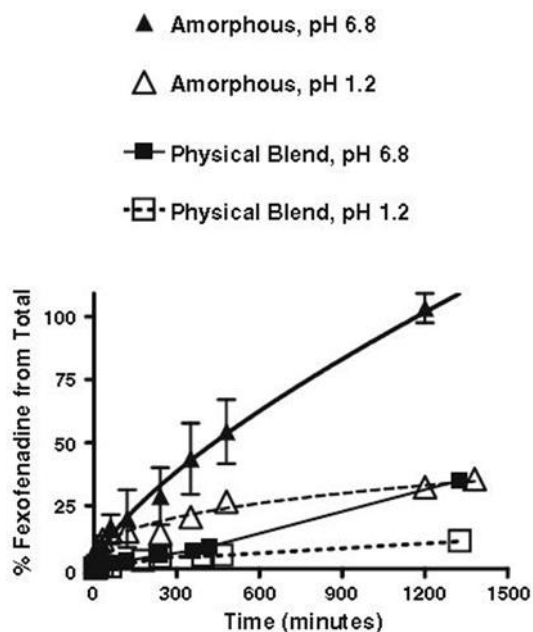


**Figure 2.8** Comparison of Fexofenadine HCl release from a compression tablet of a physical blend of CMCAB/drug with capsule containing amorphous formulation, reprinted from Shelton, M. C.; Posey-Dowty, J. D.; Lingerfelt, L. R.; Kirk, S. K.; Klein, S.; Edgar, K. J. *Polysaccharide Materials: Performance by Design* **2009**. Used with permission of American Chemical Society, 2010.

For poorly water soluble drugs, for example feoxofenadine HCl (an antihistamine drug used in the treatment of hay fever, allergy symptoms and urticarial), the second method by amorphous formulation is more effective and preferred. Molecular blends afford largely or entirely amorphous drug intimately blended with CMCAB. The drug and CMCAB were dissolved in an organic solvent first and the ASDs were prepared by a number of techniques including co-precipitation and solvent evaporation (rotary evaporation under reduced pressure, spray drying or film casting).<sup>105</sup> CMCAB is thermodynamically miscible with many pharmaceutical actives, which was predicted by using Hansen 3D solubility parameters. DSC measurement also detected only a single glass transition temperature further indicating good compatibility. It was identified that release from these molecular blends was rapid for water-soluble drugs, but slow and nearly zero-order for poorly soluble drugs. In general, drug solubility was substantially enhanced in amorphous complexes while the physical blends gave poor dissolution performance in low or neutral pH

buffers (**Fig. 2.8**).

Carboxymethylcellulose esters are very attractive materials for drug delivery and coatings applications.<sup>106</sup> However, this industrial synthesis of CMCAB creates a concern about possible crosslinking. To convert CMC into fundamentally hydrophobic CMC esters using mixed anhydrides, strong acid catalysis (e.g. sulfuric acid) and elevated temperature (40-55 °C) must be applied. However, the pendent carboxyl group could easily react with free hydroxyls to form a crosslinked gel. CMC may also get crosslinked by multivalent ions during the manufacturing process (**Fig. 2.9**). In manufacturing process, variations have been observed in organic solubility among CMCAB batches or over time within one batch due to the potential of crosslinking. There are also concerns about CMCAB crosslinking after manufacture, in storage or in use, by similar mechanisms.

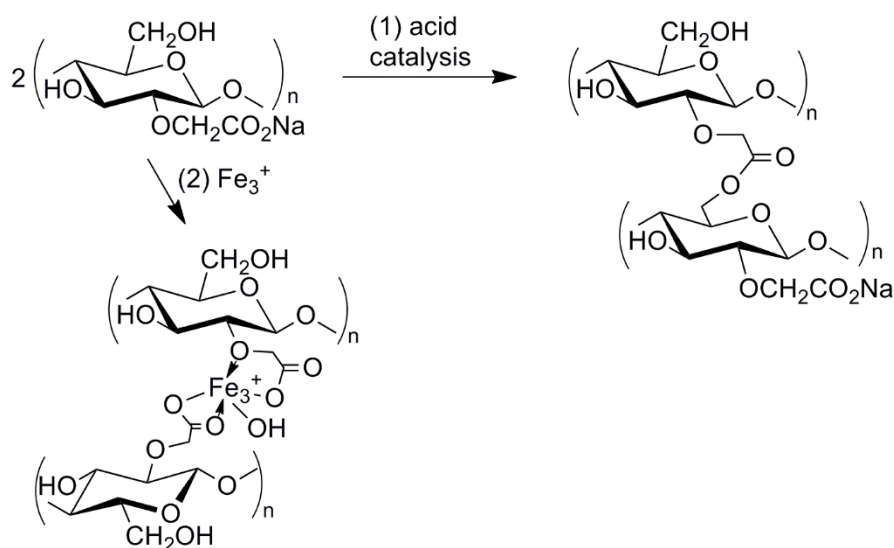


**Figure 2.9** CMCAB crosslink mechanisms of (1) acid-catalyzed crosslink (2) multivalent ions crosslink

### Cellulose succinate derivatives – hydroxypropyl methylcellulose acetate succinate (HPMCAS)

McCormick<sup>107</sup>, Liu and Li<sup>108, 109</sup> successfully synthesized cellulose succinate homogeneously using different solvent systems: polar aprotic organic liquids/lithium salt, and molten organic salts (ionic liquids) respectively. The reason to run the homogeneous reactions is that the homogeneity can offer excellent control of the substitution patterns of the hydroxyls on the cellulose backbone, for the preparation of partially regioselective derivatives directly.<sup>110</sup> Furthermore, the dissolution process destroys most of the extensive intramolecular and intermolecular cellulose H-bonds, leading to higher overall accessibility and reactivity to hydroxyl groups.

In contrast to heterogeneous treatments, the polar aprotic solvent *N,N*-dimethylacetamide (DMAc) combined with lithium chloride was widely used as solvent system for derivatization of cellulose to achieve excellent control of substitutions.<sup>111</sup> The lithium atoms of lithium chloride interact with the oxygen atoms of hydroxyls of cellulose and thus disrupt and prevent reformation of cellulose H-bonding network (**Fig. 2.10**). And then polar, aprotic solvents such as DMAc or *N*-methyl-2-pyrrolidone (NMP) further stabilize the lithium cation by strong coordination. The esterification of *in situ* activated cellulose in DMAc/LiCl using carboxylic acid anhydrides and chlorides was a typical polysaccharide modification under homogeneous conditions.<sup>112, 113</sup>

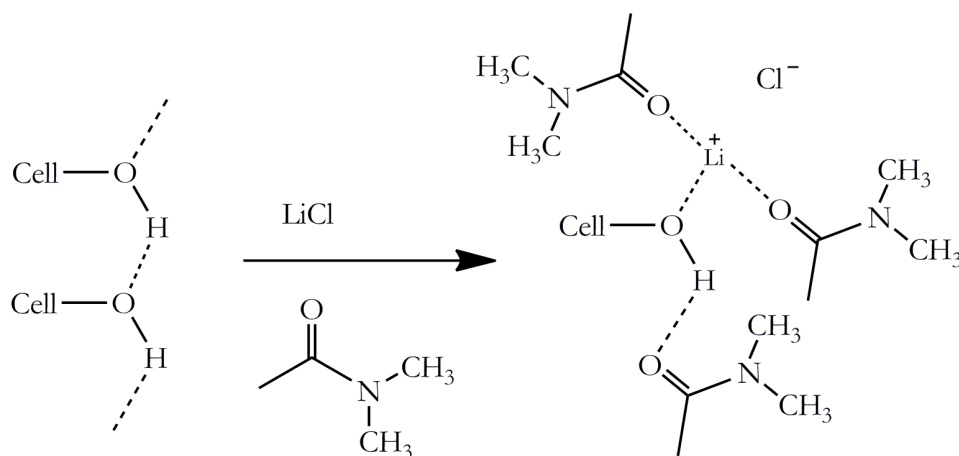


**Figure 2.10** Mechanism of cellulose dissolution in DMAc/ LiCl by Gray et al (1995).<sup>114</sup>

Cyclic succinic anhydride was successfully used to esterify cellulose in solution using a tertiary amine as catalyst and acid scavenger in the reactions.<sup>107</sup> The cellulose succinate monoester



with DS of succinate (Su) 1.4 was synthesized in 2.5 hours at 80 °C in the presence of pyridine. The resulting polymer was soluble in acetone and the salt form was water soluble. Altering of the base catalyst to triethylamine showed an interesting result that TEA salt of the cellulose monoester with a DS (Su) 1.1 precipitated from DMAc/LiCl solvent system in less than 10 minutes at ambient temperature. The product was also water soluble though it had a lower DS of half-acid ester moiety due to the fast precipitation. The regioselectivity of succinate group attachment wasn't described by these authors.

Rogers et al. discovered that the ionic liquids containing 1-butyl-3-methylimidazolium cations ([Bmim]<sup>+</sup>) with various anions (Cl<sup>-</sup>, Br<sup>-</sup>, SCN<sup>-</sup>, [BF<sub>4</sub>]<sup>-</sup> and [PF<sub>6</sub>]<sup>-</sup>) could be used as non-derivatizing solvents for cellulose.<sup>115</sup> Ionic liquids, defined as having melting points below 100°C, are attractive as “green” solvents because they have no or very low measurable vapor pressures. Therefore ionic liquids show great potential for minimizing air pollution and worker exposure during the dissolution and subsequent derivatization process<sup>116</sup>. The investigation of different imidazolium based ILs as reaction media for cellulose chemistry has been extensive, especially the acylation of cellulose including the synthesis of cellulose half-acid esters.<sup>117, 118</sup>

Succinylation of sugarcane bagasse cellulose (DP of 1277) has been carried out in 1-allyl-3-methyl-imidazolium chloride ([Amim]Cl) under various conditions.<sup>119</sup> The investigators concluded that DS (succinate) increased with increasing reaction temperature, duration and molar ratio of succinic anhydride (SA)/AGU. And the use of catalyst for acylation of alcohols, such as 4-dimethylaminopyridine (DMAP),<sup>108</sup> *N*-bromosuccinimide (NBS)<sup>109</sup> could greatly raise the DS of succinylated cellulosic derivatives from a maximum of 0.22 (without any catalyst) to 2.3 under the same reaction conditions. The actual role of NBS as a catalyst for the acylation is not clear, one reasonable explanation was proposed by Liu et al. that NBS activates the carbonyl groups and opens up the succinic anhydride ring, to form a more reactive acylating agent.<sup>109</sup> From the regioselective substitution perspective, because succinate group is not bulky enough, it was found that the substitution at C-6 is only slightly preferred to substitution at C-2 and C-3 positions.

Water-dispersible polymer cellulose succinate mixed esters were firstly reported as CAB-SU160 by Eastman Chemical Company.<sup>120</sup> Cellulose acetate butyrate (CAB-553-0.4) is prepared by acid-

catalyzed bulk reaction with butyric anhydride in acetic acid. The CAB reacted in a separate step with succinic anhydride under mild alkaline condition to afford cellulose acetate butyrate succinate (CAB-SU) (**Fig. 2.11**). The purpose of the use of basic catalysis is to avoid acid-catalyzed crosslink of hydroxyl group on one chain and carboxyl end on the other chain. The carboxyls of the succinyl groups ( $DS_{Su} = 0.38$ ) introduced water affinity into these cellulose esters, particularly when ionized by amines, while the hydrophobic acetate and butyrate groups ( $DS_{Ac} = 1.9$ ,  $DS_{Bu} = 0.1$ ) make the un-ionized material insoluble in water.<sup>12</sup>

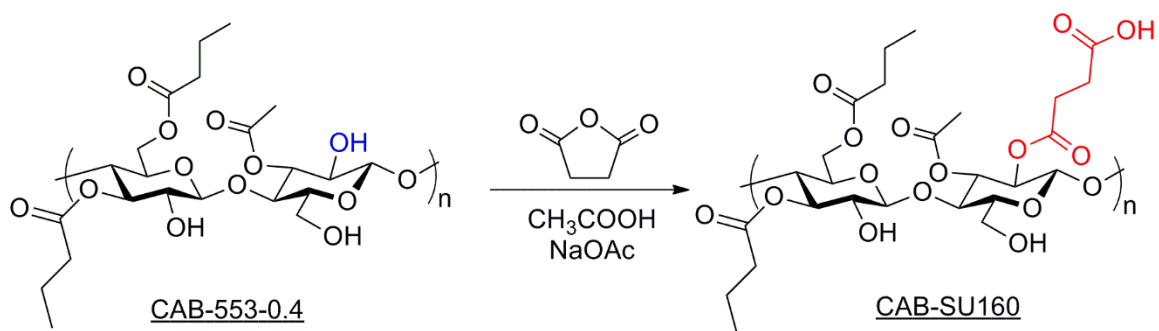


**Figure 2.11** Industrial preparation of CAB-SU160 starting from CAB-553-0.4

Hydroxypropyl methylcellulose acetate succinate (HPMCAS) is derived from reacting hydroxypropyl methylcellulose (HPMC) with acetic anhydride and succinic anhydride.<sup>121</sup> Four types of moieties are semi-randomly substituted on the hydroxyls with varied DS to affect the chemical and physical properties of the cellulosic polymer. (**Fig. 12**; **Table 2.2**) Unlike cellulose succinate, it is water-insoluble when  $pH < 5$  due to the presence of relatively hydrophobic methyl and acetate groups, and remains colloidally stable against hydrophobic aggregation when the succinate group is largely ionized at intestine pH (6.0-7.5).<sup>95</sup> In conclusion, the amphiphilic nature of HPMCAS enables strong interaction with hydrophobic drugs, and enables it to form stable dispersions in aqueous media.

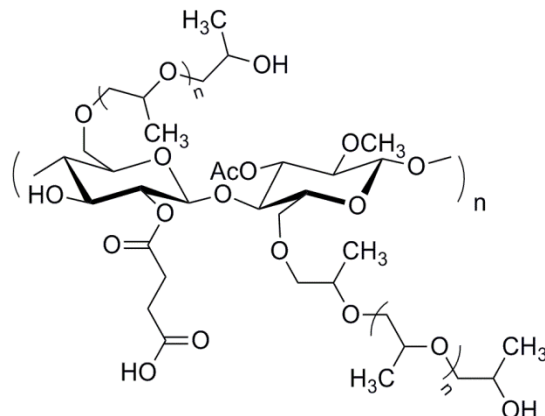


**Figure 2.12** Chemical structure of HPMCAS

**Table 2.2** Degree of substitution of HPMCAS<sup>122</sup>

Substituent	Degree of substitution
Methoxy + hydroxypropyl	2.17
Acetate	0.31-0.51
Succinate	0.12-0.33

HPMCAS was further shown to be a very promising candidate for use in ASD. This application was developed and patented by Pfizer Inc. with the collaboration from Bend Research.<sup>123</sup> It was reported that the enhancement of the solubility of basic or zwitterionic drugs, such as ziprasidone hydrochloride, by just admixing with HPMCAS in solution is at least 1.5-fold. Other studies showed a 28-fold increase in dissolution rate for amorphous solid dispersion of HPMCAS with AMG 517 (a highly selective TRPV1 antagonist) compared to crystalline form only, and nearly 2-fold increase compared to amorphous drug.<sup>124</sup>

HPMCAS was identified as a highly effective drug carrier in a solid dispersion of nifedipine.<sup>125</sup> Firstly, to achieve an amorphous solid dispersion, the required amount of cellulosic polymer including HPMCAS was less than in the case of PVP or methacrylic acid ethyl acrylate copolymer (MAEA). Secondly, the HPMCAS-based solid dispersion demonstrated the best drug

dissolution enhancement. The drug release behavior could also be manipulated by altering the ratio of succinoyl and acetyl moieties. Moreover, HPMCAS stabilized nifedipine against recrystallization from a supersaturated solution in pH 6.8 buffer fluid.

The hydrophilic substituents of HPMCAS lead to moisture absorption, which plasticizes the solid dispersion and may increase drug mobility. However, it was still identified that HPMCAS absorbed much less water than PVP and PEG.<sup>71</sup> Despite the increased hygroscopicity of the ASD system, the nucleation rate is still much lower than that of amorphous drug only.<sup>93</sup> These features resulted in excellent physical and chemical stability of HPMCAS-based amorphous dispersions.

In general, drugs in spray-dried HPMCAS-based dispersions were stable against crystallization in both the solid state and after dissolution. Friesen et al. showed that the homogeneous solid dispersion of torcetrapib/HPMCAS (w/w: 1:3) with a relatively high  $T_g$  (82 °C; drug alone 29 °C; polymer alone 119 °C) remained amorphous and finely dispersed during storage.<sup>95</sup> SEM images showed that no crystallization occurred in the solid dispersion over the course of years. When the dispersion was introduced to an *in vitro* solution that simulates the fluid in the duodenum and small intestine, drug/polymer nanostructures and nanoaggregates were formed, an enhanced and sustained free-drug concentration that far exceeded crystalline drug solubility was then generated. In conclusion, HPMCAS has the ability to form stable amorphous drug/polymer nanostructures by the spray-drying method. It is expected to offer enhanced and sustained dissolution of drug in the small intestine and reach excellent bioavailability. It must be noted that use of HPMCAS for this ASD application was already patented by Pfizer, manufacturing is somehow uncontrollable due to chain extension feature of hydroxypropyl group (OH end group reacts with more ethylene oxide) and it is difficult to simultaneously control the substitution of four substituents in large-scale production which could be an obstacle to get FDA approval.

Furthermore, the hydrolytic stability of the succinate groups in CAB succinate and other cellulose succinate derivatives in aqueous solutions is always a potential concern in many applications, especially for automotive coating. Kinetic studies have been performed by Edgar et al. using aqueous solutions of cellulose acetate butyrate succinate (CAB-SU160) in the presence of dimethylaminoethanol (DMEA).<sup>126</sup> The results demonstrated that the succinyl groups were

hydrolyzed off at an alarming rate under neutral or alkaline conditions (**Fig. 2.13**), and increasing concentration of amine promoted the hydrolysis. It was reasoned by us that such autocatalyzed hydrolysis of succinyl group would be promoted by a quite favorable 5-membered ring transition state.<sup>127</sup> The succinic anhydride generated would be converted quickly to succinic acid in the presence of aqueous medium which accelerates the hydrolysis process. Consequently, the authors indicated that the acceptable stability of CAB-SU could only be achieved by minimizing alkalinity.

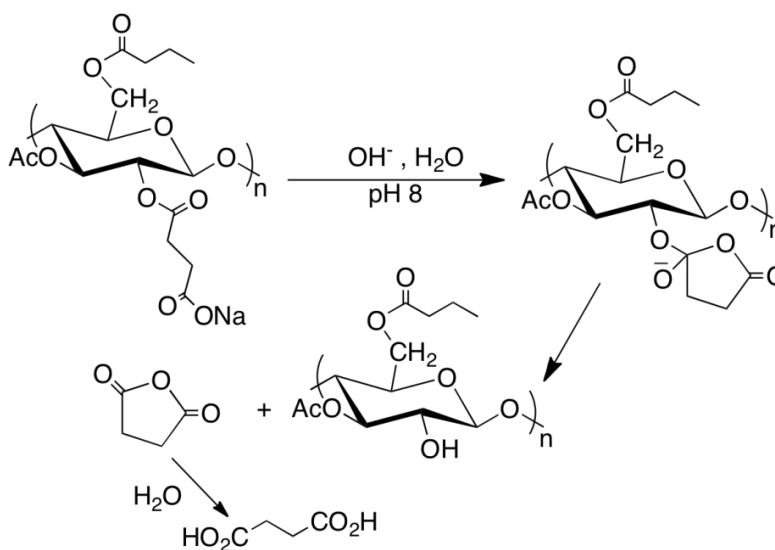


**Figure 2.13** Proposed CAB-Su Hydrolysis Mechanism<sup>126</sup>

## 2.5 Concluding Remarks

Amorphous solid dispersion formulation is a very potent technology. Drugs are intimately blended with suitable polymeric additives to form amorphous solids, which typically lead to supersaturated solutions upon release. The increase in solution concentration creates high diffusion of drug actives across epithelium into the bloodstream and hence the bioavailability enhancement. Unlike many traditional strategies to increase the equilibrium solubility of highly crystalline, lipophilic drugs including cyclodextrin complexation, micellar solubilization and cosolvent addition, the equilibrium drug solubility increase is no longer accompanied by a concurrent decrease in permeability by the ASD method.

The utility of cellulose ethers and esters in oral drug delivery applications, especially for amorphous solid dispersion discussed above has been well-established in the literature. Drug solubilization, drug stabilization and enhanced drug release provided by the polymeric additives including those cellulose derivatives are of great importance in this research. However, enhancing solubility and bioavailability of lipophilic active pharmaceutical ingredients as amorphous solid dispersions is still a difficult, mostly unresolved frontier. Each drug candidate has its own physical and chemical properties, therefore, there is no universal formulation and polymer selection is a vital process. As described above, synthetic polymers (PVP, PEG) and pH-dependent cellulose derivatives (CMCAB, HPMCAS) are not specifically designed for ASD and thus do have a number of limitations as described. Designing and producing novel carboxyl-containing cellulosic materials with enhanced properties (e.g. easier manufacturing process, better chemical stability, higher level of molecular interactions with drugs) will allow pharmaceutical scientists to maximize the advantages of amorphous solid dispersions. Moreover, it is anticipated that developing a broad family of these cellulose derivatives with easy-to-tune structures will further result in better control over the performance of oral drug formulations.

## 2.6 References

1. Sturcova, A.; Davies, G. R.; Eichhorn, S. J., Elastic Modulus and Stress-Transfer Properties of Tunicate Cellulose Whiskers. *Biomacromolecules* **2005**, 6, (2), 1055-1061.
2. Alvarez, A. I.; Real, R.; Perez, M.; Mendoza, G.; Prieto, J. G.; Merino, G., Modulation of the activity of ABC transporters (P-glycoprotein, MRP2, BCRP) by flavonoids and drug response. *J Pharm Sci* 99, (2), 598-617.
3. Romling, U., Molecular biology of cellulose production in bacteria. *Res Microbiol* **2002**, 153, (4), 205-12.
4. Stocker, M., Biofuels and biomass-to-liquid fuels in the biorefinery: catalytic conversion of lignocellulosic biomass using porous materials. *Angew. Chem., Int. Ed.* **2008**, 47, (48), 9200-9211.
5. Bolhuis Gerad, K.; Armstrong, N. A., Excipients for direct compaction--an update. *Pharm Dev Technol* **2006**, 11, (1), 111-24.
6. Kondo, T., Hydrogen bonds in cellulose and cellulose derivatives. *Polysaccharides (2nd Ed.)* **2005**, 69-98.
7. Klemm, D.; Philip, B.; Heinze, T.; Heinze, U.; Wagenknecht, W., *Comprehensive Cellulose Chemistry, Volume 1: General Principles & Analytical Methods*. 1998; p 300 pp.
8. Knill, C. J.; Kennedy, J. F., Degradation of cellulose under alkaline conditions. *Carbohydr. Polym.* **2002**, 51, (3), 281-300.
9. Sata, H.; Murayama, M.; Shimamoto, S., Properties and applications of cellulose triacetate film. *Macromol. Symp.* **2004**, 208, (Cellulose Acetates), 323-333.
10. Buchanan, C. M.; Edgar, K. J.; Hyatt, J. A.; Wilson, A. K., Preparation of cellulose [1-C-13]acetates

- and determination of monomer composition by NMR spectroscopy. *Macromolecules* **1991**, 24, (11), 3050-3059.
11. Buchanan, C. M.; Edgar, K. J.; Wilson, A. K., Preparation and characterization of cellulose monoacetates - the relationship between structure and water solubility. *Macromolecules* **1991**, 24, (11), 3060-3064.
  12. Edgar, K. J.; Buchanan, C. M.; Debenham, J. S.; Rundquist, P. A.; Seiler, B. D.; Shelton, M. C.; Tindall, D., Advances in cellulose ester performance and application. *Progress in Polymer Science* **2001**, 26, (9), 1605-1688.
  13. Rajinikanth, P. S.; Mishra, B., Stomach-site specific drug delivery system of clarithromycin for eradication of *Helicobacter pylori*. *Chem. Pharm. Bull.* **2009**, 57, (10), 1068-1075.
  14. Hauss, D. J., Oral lipid-based formulations. *Adv. Drug Delivery Rev.* **2007**, 59, (7), 667-676.
  15. Rumondor, A. C.; Ivanisevic, I.; Bates, S.; Alonzo, D. E.; Taylor, L. S., Evaluation of Drug-Polymer Miscibility in Amorphous Solid Dispersion Systems. *Pharm Res* **2009**, 26, (11), 2523-2534.
  16. Serajuddin, A. T. M., Salt formation to improve drug solubility. *Adv. Drug Delivery Rev.* **2007**, 59, (7), 603-616.
  17. Bender, M. L.; Komiyama, M., *Cyclodextrin Chemistry*. 1978; p 96 pp.
  18. Szejtli, J., Introduction and General Overview of Cyclodextrin Chemistry. *Chem. Rev. (Washington, D. C.)* **1998**, 98, (5), 1743-1753.
  19. Connors, K. A., The stability of cyclodextrin complexes in solution. *Chemical Reviews* **1997**, 97, (5), 1325-1357.
  20. Kim, Y.; Oksanen, D. A.; Masefski, W., Jr.; Blake, J. F.; Duffy, E. M.; Chrnyk, B., Inclusion Complexation of Ziprasidone Mesylate with  $\beta$ -Cyclodextrin Sulfobutyl Ether. *J. Pharm. Sci.* **1998**, 87, (12), 1560-1567.
  21. Johnson, M. D.; Hoesterey, B. L.; Anderson, B. D., Solubilization of a Tripeptide HIV Protease Inhibitor Using a Combination of Ionization and Complexation with Chemically Modified Cyclodextrins. *J. Pharm. Sci.* **1994**, 83, (8), 1142-6.
  22. Duchene, D.; Wouessidjewe, D., Pharmaceutical uses of cyclodextrins and derivatives. *Drug Dev. Ind. Pharm.* **1990**, 16, (17), 2487-99.
  23. Tinwalla, A. Y.; Hoesterey, B. L.; Xiang, T. X.; Lim, K.; Anderson, B. D., Solubilization of thiazolobenzimidazole using a combination of pH adjustment and complexation with 2-hydroxypropyl  $\beta$ -cyclodextrin. *Pharm. Res.* **1993**, 10, (8), 1136-43.
  24. Miyake, K.; Arima, H.; Hirayama, F.; Yamamoto, M.; Horikawa, T.; Sumiyoshi, H.; Noda, S.; Uekama, K., Improvement of solubility and oral bioavailability of rutin by complexation with 2-hydroxypropyl- $\beta$ -cyclodextrin. *Pharm. Dev. Technol.* **2000**, 5, (3), 399-407.
  25. Boudad, H.; Legrand, P.; Lebas, G.; Cheron, M.; Duchene, D.; Ponchel, G., Combined hydroxypropyl- $\beta$ -cyclodextrin and poly(alkyl cyanoacrylate) nanoparticles intended for oral administration of saquinavir. *Int. J. Pharm.* **2001**, 218, (1-2), 113-124.
  26. Buchanan, C. M.; Alderson, S. R.; Cleven, C. D.; Dixon, D. W.; Ivanyi, R.; Lambert, J. L.; Lowman, D. W.; Offerman, R. J.; Szejtli, J.; Szente, L., Synthesis and characterization of water-soluble hydroxybutenyl cyclomaltooligosaccharides (cyclodextrins). *Carbohydr. Res.* **2002**, 337, (6), 493-507.
  27. Buchanan, C. M.; Buchanan, N. L.; Edgar, K. J.; Lambert, J. L.; Posey-Dowty, J. D.; Ramsey, M. G.; Wempe, M. F., Solubilization and dissolution of tamoxifen-hydroxybutenyl cyclodextrin complexes. *J. Pharm Sci* **2006**, 95, (10), 2246-55.
  28. Buchanan, C. M.; Buchanan, N. L.; Edgar, K. J.; Little, J. L.; Malcolm, M. O.; Ruble, K. M.; Wachter, V. J.; Wempe, M. F., Pharmacokinetics of tamoxifen after intravenous and oral dosing of tamoxifen-hydroxybutenyl-beta-cyclodextrin formulations. *J. Pharm Sci* **2007**, 96, (3), 644-60.
  29. Buchanan, C. M.; Buchanan, N. L.; Edgar, K. J.; Ramsey, M. G., Solubility and dissolution studies of antifungal drug : hydroxybutenyl-beta-cyclodextrin complexes. *Cellulose* **2007**, 14, (1), 35-47.

30. Buchanan, C. M.; Buchanan, N. L.; Edgar, K. J.; Klein, S.; Little, J. L.; Ramsey, M. G.; Ruble, K. M.; Wachter, V. J.; Wempe, M. F., Building new drug delivery systems: in vitro and in vivo studies of drug-hydroxybutenyl cyclodextrin complexes. In *Polysaccharide Materials: Performance by Design*, Edgar, K. J.; Buchanan, C. M.; Heinze, T., Eds. American Chemical Society: Washington, D.C., 2009.
31. Buchanan, C. M.; Buchanan, N. L.; Edgar, K. J.; Little, J. L.; Ramsey, M. G.; Ruble, K. M.; Wachter, V. J.; Wempe, M. F., Pharmacokinetics of saquinavir after intravenous and oral dosing of saquinavir: hydroxybutenyl-beta-cyclodextrin formulations. *Biomacromolecules* **2008**, *9*, (1), 305-13.
32. Prentice, A. G.; Glasmacher, A., Making sense of itraconazole pharmacokinetics. *J. Antimicrob. Chemother.* **2005**, *56*, (Suppl. 1), i17-i22.
33. Stella, V. J.; He, Q., Cyclodextrins. *Toxicol. Pathol.* **2008**, *36*, (1), 30-42.
34. El-Shabouri, M. H., Nanoparticles for improving the dissolution and oral bioavailability of spironolactone, a poorly-soluble drug. *S.T.P. Pharma Sci.* **2002**, *12*, (2), 97-101.
35. Merisko-Liversidge, E.; Liversidge, G. G.; Cooper, E. R., Nanosizing: a formulation approach for poorly-water-soluble compounds. *Eur J Pharm Sci* **2003**, *18*, (2), 113-20.
36. Itoh, K.; Pongpeerapat, A.; Tozuka, Y.; Oguchi, T.; Yamamoto, K., Nanoparticle formation of poorly water-soluble drugs from ternary ground mixtures with PVP and SDS. *Chem Pharm Bull (Tokyo)* **2003**, *51*, (2), 171-4.
37. Takatsuka, T.; Endo, T.; Jianguo, Y.; Yuminoki, K.; Hashimoto, N., Nanosizing of poorly water soluble compounds using rotation/revolution mixer. *Chem. Pharm. Bull.* **2009**, *57*, (10), 1061-1067.
38. Hornig, S.; Heinze, T., Efficient Approach To Design Stable Water-Dispersible Nanoparticles of Hydrophobic Cellulose Esters. *Biomacromolecules* **2008**, *9*, (5), 1487-1492.
39. Liu, Y.; Cheng, C.; Prud'homme, R. K.; Fox, R. O., Mixing in a multi-inlet vortex mixer (MIVM) for flash nano-precipitation. *Chemical Engineering Science* **2008**, *63*, (11), 2829-2842.
40. Heng, D.; Cutler, D. J.; Chan, H.-K.; Yun, J.; Raper, J. A., What is a suitable dissolution method for drug nanoparticles? *Pharm. Res.* **2008**, *25*, (7), 1696-1701.
41. Porter, C. J. H.; Trevaskis, N. L.; Charman, W. N., Lipids and lipid-based formulations: optimizing the oral delivery of lipophilic drugs. *Nat. Rev. Drug Discovery* **2007**, *6*, (3), 231-248.
42. Dahan, A.; Hoffman, A., Rationalizing the selection of oral lipid based drug delivery systems by an in vitro dynamic lipolysis model for improved oral bioavailability of poorly water soluble drugs. *J Control Release* **2008**, *129*, (1), 1-10.
43. Porter, C. J. H.; Pouton, C. W.; Cuine, J. F.; Charman, W. N., Enhancing intestinal drug solubilization using lipid-based delivery systems. *Adv. Drug Delivery Rev.* **2008**, *60*, (6), 673-691.
44. Behrens, D.; Fricker, R.; Bodoky, A.; Drewe, J.; Harder, F.; Heberer, M., Comparison of Cyclosporin A Absorption from LCT and MCT Solutions following Intrajejunal Administration in Conscious Dogs. *J. Pharm. Sci.* **1996**, *85*, (6), 666-668.
45. Caliph, S. M.; Charman, W. N.; Porter, C. J. H., Effect of short-, medium-, and long-chain fatty acid-based vehicles on the absolute oral bioavailability and intestinal lymphatic transport of halofantrine and assessment of mass balance in lymph-cannulated and non-cannulated rats. *J. Pharm. Sci.* **2000**, *89*, (8), 1073-1084.
46. Pouton, C. W., Lipid formulations for oral administration of drugs: non-emulsifying, self-emulsifying and 'self-microemulsifying' drug delivery systems. *Eur. J. Pharm. Sci.* **2000**, *11*, (Suppl. 2), S93-S98.
47. Kim, J. Y.; Ku, Y. S., Enhanced absorption of indomethacin after oral or rectal administration of a self-emulsifying system containing indomethacin to rats. *Int. J. Pharm.* **2000**, *194*, (1), 81-89.
48. Vemula, V. R.; Lagishetty, V.; Lingala, S., Solubility enhancement techniques. *Int. J. Pharm. Sci. Rev. Res.* **2010**, *5*, (1), 41-51.
49. Rangel-Yagui, C. O.; Pessoa, A., Jr.; Tavares, L. C., Micellar solubilization of drugs. *J. Pharm. Pharm. Sci.* **2005**, *8*, (2), 147-163.



50. Alkhamis, K. A.; Allaboun, H.; Al-Momani, W. a. Y., Study of the solubilization of gliclazide by aqueous micellar solutions. *J. Pharm. Sci.* **2003**, 92, (4), 839-846.
51. Torchilin, V. P., Structure and design of polymeric surfactant-based drug delivery systems. *J. Controlled Release* **2001**, 73, (2-3), 137-172.
52. Li, P.; Zhao, L., Solubilization of flurbiprofen in pH-surfactant solutions. *J. Pharm. Sci.* **2003**, 92, (5), 951-956.
53. Li, P.; Tabibi, S. E.; Yalkowsky, S. H., Solubilization of Ionized and Un-ionized Flavopiridol by Ethanol and Polysorbate 20. *J. Pharm. Sci.* **1999**, 88, (5), 507-509.
54. Kataoka, K.; Harada, A.; Nagasaki, Y., Block copolymer micelles for drug delivery: design, characterization and biological significance. *Adv. Drug Delivery Rev.* **2001**, 47, (1), 113-131.
55. Yokoyama, M.; Miyauchi, M.; Yamada, N.; Okano, T.; Sakurai, Y.; Kataoka, K.; Inoue, S., Characterization and anticancer activity of the micelle-forming polymeric anticancer drug Adriamycin-conjugated poly(ethylene glycol)-(aspartic acid) block copolymer. *Cancer Res.* **1990**, 50, (6), 1693-700.
56. Yokoyama, M.; Okano, T.; Sakurai, Y.; Ekimoto, H.; Shibazaki, C.; Kataoka, K., Toxicity and antitumor activity against solid tumors of micelle-forming polymeric anticancer drug and its extremely long circulation in blood. *Cancer Res.* **1991**, 51, (12), 3229-36.
57. Batrakova, E. V.; Dorodnych, T. Y.; Klinskii, E. Y.; Kliushnenkova, E. N.; Shemchukova, O. B.; Goncharova, O. N.; Arjakov, S. A.; Alakhov, V. Y.; Kabanov, A. V., Anthracycline antibiotics non-covalently incorporated into the block copolymer micelles: in vivo evaluation of anti-cancer activity. *Br. J. Cancer* **1996**, 74, (10), 1545-1552.
58. Zhang, X.; Burt, H. M.; Von Hoff, D.; Dexter, D.; Mangold, G.; Degen, D.; Oktaba, A. M.; Hunter, W. L., An investigation of the antitumor activity and biodistribution of polymeric micellar paclitaxel. *Cancer Chemother. Pharmacol.* **1997**, 40, (1), 81-86.
59. Miller, J. M.; Beig, A.; Krieg, B. J.; Carr, R. A.; Borchardt, T. B.; Amidon, G. E.; Amidon, G. L.; Dahan, A., The solubility-permeability interplay: Mechanistic modeling and predictive application of the impact of micellar solubilization on intestinal permeation. *Mol. Pharmaceutics* **2011**, 8, (5), 1848-1856.
60. Kim, S.-W.; Shi, Y.-Z.; Kim, J.-Y.; Park, K.-N.; Cheng, J.-X., Overcoming the barriers in micellar drug delivery: Loading efficiency, in vivo stability, and micelle-cell interaction. *Expert Opin. Drug Delivery* **2010**, 7, (1), 49-62.
61. Marsac, P. J.; Konno, H.; Taylor, L. S., A comparison of the physical stability of amorphous felodipine and nifedipine systems. *Pharm Res* **2006**, 23, (10), 2306-16.
62. Miller, J. M.; Beig, A.; Carr, R. A.; Spence, J. K.; Dahan, A., A Win-Win Solution in Oral Delivery of Lipophilic Drugs: Supersaturation via Amorphous Solid Dispersions Increases Apparent Solubility without Sacrifice of Intestinal Membrane Permeability. *Mol. Pharmaceutics* **2012**, 9, (7), 2009-2016.
63. Beig, A.; Miller, J. M.; Dahan, A., Accounting for the solubility-permeability interplay in oral formulation development for poor water solubility drugs: The effect of PEG-400 on carbamazepine absorption. *Eur. J. Pharm. Biopharm.* **2012**, 81, (2), 386-391.
64. Miller, J. M.; Beig, A.; Carr, R. A.; Webster, G. K.; Dahan, A., The Solubility-Permeability Interplay When Using Cosolvents for Solubilization: Revising the Way We Use Solubility-Enabling Formulations. *Mol. Pharmaceutics* **2012**, 9, (3), 581-590.
65. Leuner, C.; Dressman, J., Improving drug solubility for oral delivery using solid dispersions. *Eur J Pharm Biopharm* **2000**, 50, (1), 47-60.
66. Coppens, K. A.; Hall, M. J.; Mitchell, S. A.; Read, M. D., Hypromellose, ethyl cellulose, and polyethylene oxide use in Hot melt extrusion. *Pharm. Technol.* **2006**, 30, (1), 62,64,66,68,70.
67. Edgar, K. J., Cellulose esters in drug delivery. *Cellulose* **2007**, 14, (1), 49-64.
68. Yoshioka, M.; Hancock, B. C.; Zograf, G., Inhibition of Indomethacin Crystallization in Poly(vinylpyrrolidone) Coprecipitates. *J. Pharm. Sci.* **1995**, 84, (8), 983-6.
69. Taylor, L. S.; Zograf, G., Spectroscopic characterization of interactions between PVP and

- indomethacin in amorphous molecular dispersions. *Pharm. Res.* **1997**, 14, (12), 1691-1698.
70. Marsac, P. J.; Konno, H.; Rumondor, A. C.; Taylor, L. S., Recrystallization of nifedipine and felodipine from amorphous molecular level solid dispersions containing poly(vinylpyrrolidone) and sorbed water. *Pharm Res* **2008**, 25, (3), 647-56.
71. Rumondor, A. C. F.; Konno, H.; Marsac, P. J.; Taylor, L. S., Analysis of the moisture sorption behavior of amorphous drug-polymer blends. *J. Appl. Polym. Sci.* **2010**, 117, (2), 1055-1063.
72. Law, D.; Schmitt, E. A.; Marsh, K. C.; Everitt, E. A.; Wang, W.; Fort, J. J.; Krill, S. L.; Qiu, Y., Ritonavir-PEG 8000 amorphous solid dispersions: in vitro and in vivo evaluations. *J. Pharm. Sci.* **2004**, 93, (3), 563-570.
73. Kanaze, F. I.; Kokkalou, E.; Niopas, I.; Georgakis, M.; Stergiou, A.; Bikiaris, D., Dissolution Enhancement of Flavonoids by Solid Dispersion in PVP and PEG Matrixes: A Comparative Study. *J Appl Poly Sci* **2006**, 102, 460-471.
74. Zhu, Q.; Harris Michael, T.; Taylor Lynne, S., Modification of crystallization behavior in drug/polyethylene glycol solid dispersions. *Mol Pharm* **2012**, 9, (3), 546-53.
75. Gines, J. M.; Arias, M. J.; Moyano, J. R.; Sanchez-Soto, P. J., Thermal investigation of crystallization of polyethylene glycols in solid dispersions containing oxazepam. *Int. J. Pharm.* **1996**, 143, (2), 247-253.
76. Corrigan, D. O.; Healy, A. M.; Corrigan, O. I., The effect of spray drying solutions of polyethylene glycol (PEG) and lactose/PEG on their physicochemical properties. *Int. J. Pharm.* **2002**, 235, (1-2), 193-205.
77. Zhu, Q.; Harris Michael, T.; Taylor Lynne, S., Time-resolved SAXS/WAXS study of the phase behavior and microstructural evolution of drug/PEG solid dispersions. *Mol Pharm* **2011**, 8, (3), 932-9.
78. Gallardo, D.; Skalsky, B.; Kleinebudde, P., Controlled Release Solid Dosage Forms Using Combinations of (meth)acrylate Copolymers. *Pharm. Dev. Technol.* **2008**, 13, (5), 413-423.
79. Mehta, K. A.; Kislalioglu, M. S.; Phuapradit, W.; Malick, A. W.; Shah, N. H., Release performance of a poorly soluble drug from a novel, Eudragit-based multi-unit erosion matrix. *Int. J. Pharm.* **2001**, 213, (1-2), 7-12.
80. Jung, J. Y.; Yoo, S. D.; Lee, S. H.; Kim, K. H.; Yoon, D. S.; Lee, K. H., Enhanced solubility and dissolution rate of itraconazole by a solid dispersion technique. *Int. J. Pharm.* **1999**, 187, (2), 209-218.
81. Schultz, P.; Kleinebudde, P., A new multiparticulate delayed-release system. Part I: Dissolution properties and release mechanism. *J. Controlled Release* **1997**, 47, (2), 181-189.
82. Guyonnet, T.; Brossard, C.; Lefort des Ylouses, D., Prolongation of release of theophylline derivatives from cellulose acetate-based tablets. *J. Pharm. Belg.* **1990**, 45, (2), 111-19.
83. Stithit, S.; Chen, W.; Price, J. C., Development and characterization of buoyant theophylline microspheres with near zero order release kinetics. *J. Microencapsulation* **1998**, 15, (6), 725-737.
84. Menjoge, A. R.; Kulkarni, M. G., Blends of Reverse Enteric Polymer with Enteric and pH-Independent Polymers: Mechanistic Investigations for Tailoring Drug Release. *Biomacromolecules* **2007**, 8, (1), 240-251.
85. Chan, L. W.; Wong, T. W.; Chua, P. C.; York, P.; Heng, P. W. S., Anti-tack action of polyvinylpyrrolidone on hydroxypropyl methyl cellulose solution. *Chem. Pharm. Bull.* **2003**, 51, (2), 107-112.
86. Li, C. L.; Martini, L. G.; Ford, J. L.; Roberts, M., The use of hypromellose in oral drug delivery. *J. Pharm. Pharmacol.* **2005**, 57, (5), 533-546.
87. Colombo, P.; Bettini, R.; Santi, P.; De Ascentiis, A.; Peppas, N. A., Analysis of the swelling and release mechanisms from drug delivery systems with emphasis on drug solubility and water transport. *J. Controlled Release* **1996**, 39, (2,3), 231-237.
88. Tahara, K.; Yamamoto, K.; Nishihata, T., Overall mechanism behind matrix sustained-release (SR) tablets prepared with hydroxypropyl methyl cellulose 2910. *J. Controlled Release* **1995**, 35, (1), 59-66.
89. Kushida, I.; Ichikawa, M.; Asakawa, N., Improvement of dissolution and oral absorption of ER-34122, a poorly water-soluble dual 5-lipoxygenase/cyclooxygenase inhibitor with anti-inflammatory activity by preparing solid dispersion. *J. Pharm. Sci.* **2002**, 91, (1), 258-266.

90. Suzuki, H.; Sunada, H., Influence of water-soluble polymers on the dissolution of nifedipine solid dispersions with combined carriers. *Chem. Pharm. Bull.* **1998**, 46, (3), 482-487.
91. Weuts, I.; Van Dycke, F.; Voorspoels, J.; De Cort, S.; Stokbroekx, S.; Leemans, R.; Brewster, M. E.; Xu, D.; Segmuller, B.; Turner, Y. T. A.; Roberts, C. J.; Davies, M. C.; Qi, S.; Craig, D. Q. M.; Reading, M., Physicochemical properties of the amorphous drug, cast films, and spray dried powders to predict formulation probability of success for solid dispersions: Etravirine. *J. Pharm. Sci.* **2011**, 100, (1), 260-274.
92. Alonzo, D. E.; Raina, S.; Zhou, D.; Gao, Y.; Zhang, G. G. Z.; Taylor, L. S., Characterizing the Impact of Hydroxypropylmethyl Cellulose on the Growth and Nucleation Kinetics of Felodipine from Supersaturated Solutions. *Cryst. Growth Des.* **2012**, 12, (3), 1538-1547.
93. Konno, H.; Taylor, L. S., Ability of different polymers to inhibit the crystallization of amorphous felodipine in the presence of moisture. *Pharm Res* **2008**, 25, (4), 969-78.
94. Kennedy, M.; Hu, J.; Gao, P.; Li, L.; Ali-Reynolds, A.; Chal, B.; Gupta, V.; Ma, C.; Mahajan, N.; Akrami, A.; Surapaneni, S., Enhanced Bioavailability of a Poorly Soluble VR1 Antagonist Using an Amorphous Solid Dispersion Approach: A Case Study. *Mol Pharm* **2008**.
95. Friesen, D. T.; Shanker, R.; Crew, M.; Smithey, D. T.; Curatolo, W. J.; Nightingale, J. A., Hydroxypropyl methylcellulose acetate succinate-based spray-dried dispersions: an overview. *Mol Pharm* **2008**, 5, (6), 1003-19.
96. Arguelles-Monal, W.; Peniche-Covas, C., Study of the interpolyelectrolyte reaction between chitosan and carboxymethyl cellulose. *Makromol. Chem., Rapid Commun.* **1988**, 9, (10), 693-7.
97. Posey-Dowty, J. D.; Watterson, T. L.; Wilson, A. K.; Edgar, K. J.; Shelton, M. C.; Lingerfelt, L. R., Zero-order release formulations using a novel cellulose ester. *Cellulose* **2007**, 14, (1), 73-83.
98. Malm, C. J.; Fordyce, C. R., Cellulose esters of dibasic organic acids. *J. Ind. Eng. Chem. (Washington, D. C.)* **1940**, 32, 405-8.
99. Malm, C. J.; Mench, J. W.; Fulkerson, B.; Hiatt, G. D., Preparation of phthalic acid esters of cellulose. *J. Ind. Eng. Chem. (Washington, D. C.)* **1957**, 49, 84-8.
100. DiNunzio, J. C.; Miller, D. A.; Yang, W.; McGinity, J. W.; Williams, R. O., Amorphous Compositions Using Concentration Enhancing Polymers for Improved Bioavailability of Itraconazole. *Mol. Pharmaceutics* **2008**, 5, (6), 968-980.
101. Kai, T.; Akiyama, Y.; Nomura, S.; Sato, M., Oral absorption improvement of poorly soluble drug using solid dispersion technique. *Chem. Pharm. Bull.* **1996**, 44, (3), 568-71.
102. Heinze, T.; Koschella, A., Carboxymethyl Ethers of Cellulose and Starch - A Review. *Macromolecular Symposia* **2005**, 223, 13-39.
103. Allen, J. M.; Wilson, A. K.; Lucas, P. L.; Curtis, L. G. Carboxyalkyl Cellulose Esters. 5,668,273, September 16, 1997.
104. Allen, J. M.; Wilson, A. K.; Lucas, P. L.; Curtis, L. G. Process for Preparing Carboxyalkyl Cellulose Esters. 5,792,856, August 11, 1998.
105. Shelton, M. C.; Posey-Dowty, J. D.; Lingerfelt, L. R.; Kirk, S. K.; Klein, S.; Edgar, K. J., Enhanced dissolution of poorly soluble drugs from solid dispersions in carboxymethylcellulose acetate butyrate matrices. In *Polysaccharide Materials: Performance by Design*, Edgar, K. J.; Heinze, T.; Liebert, T., Eds. American Chemical Society: Washington, D.C., 2009.
106. Posey-Dowty, J. D.; Wilson, A. K.; Curtis, L. G.; Swan, P. M.; Seo, K. S. Carboxyalkyl Cellulose Esters for Use in Aqueous Pigment Dispersions. 5,994,530, November 30, 1999.
107. McCormick, C. L.; Dawsey, T. R., Preparation of Cellulose Derivatives via Ring-Opening Reactions with Cyclic Reagents in Lithium Chloride/N,N-Dimethylacetamide. *Macromolecules* **1990**, 23, 3606-3610.
108. Li, W. Y.; Jin, A. X.; Liu, C. F.; Sun, R. C.; Zhang, A. P.; Kennedy, J. F., Homogeneous modification of cellulose with succinic anhydride in ionic liquid using 4-dimethylaminopyridine as a catalyst. *Carbohydrate Polymers* **2009**, 78, (3), 389-395.
109. Liu, C. F.; Zhang, A. P.; Li, W. Y.; Yue, F. X.; Sun, R. C., Homogeneous Modification of Cellulose in

Ionic Liquid with Succinic Anhydride Using N-Bromosuccinimide as a Catalyst. *Journal of Agricultural and Food Chemistry* **2009**, 57, (5), 1814-1820.

110. Klemm, D. O., Regiocontrol in Cellulose Chemistry: Principles and Examples of Etherification and Esterification. In *Cellulose Derivatives*, Heinze, T. J.; Glasser, W. G., Eds. American Chemical Society: Washington, D.C., 1998; pp 19-37.
111. Edgar, K. J.; Arnold, K. M.; Blount, W. W.; Lawniczak, J. E.; Lowman, D. W., Synthesis and Properties of Cellulose Acetoacetates. *Macromolecules* **1995**, 28, (12), 4122-4128.
112. Dawsey, T. R.; McCormick, C. L., The Lithium Chloride/Dimethylacetamide Solvent for Cellulose: A Literature Review. *Polymer Reviews* **1990**, 30, 405-440.
113. McCormick, C. L.; Callais, P. A., Derivatization of cellulose in lithium chloride and N,N-dimethylacetamide solutions. *Polymer* **1987**, 28, (13), 2317-23.
114. Petrus, L.; Gray, D. G.; BeMiller, J. N., Homogeneous alkylation of cellulose in lithium chloride/dimethyl sulfoxide solvent with dimethyl sodium activation. A proposal for the mechanism of cellulose dissolution in lithium chloride/DMSO. *Carbohydr. Res.* **1995**, 268, (2), 319-23.
115. Swatloski, R. P.; Spear, S. K.; Holbrey, J. D.; Rogers, R. D., Dissolution of cellulose with ionic liquids. *J. Am. Chem. Soc.* **2002**, 124, (18), 4974-4975.
116. Heinze, T.; Schwikal, K.; Barthel, S., Ionic liquids as reaction medium in cellulose functionalization. *Macromol Biosci* **2005**, 5, (6), 520-5.
117. Barthel, S.; Heinze, T., Acylation and carbanilation of cellulose in ionic liquids. *Green Chem.* **2006**, 8, (3), 301-306.
118. Granstroem, M.; Kavakka, J.; King, A.; Majoinen, J.; Maekelae, V.; Helaja, J.; Hietala, S.; Virtanen, T.; Maunu, S.-L.; Argyropoulos, D. S.; Kilpelainen, I., Tosylation and acylation of cellulose in 1-allyl-3-methylimidazolium chloride. *Cellulose (Dordrecht, Neth.)* **2008**, 15, (3), 481-488.
119. Liu, C. F.; Sun, R. C.; Zhang, A. P.; Ren, J. L.; Wang, X. A.; Qin, M. H.; Chao, Z. N.; Luo, W., Homogeneous modification of sugarcane bagasse cellulose with succinic anhydride using an ionic liquid as reaction medium. *Carbohydrate Research* **2007**, 342, (7), 919-926.
120. Walker, K. R. Aqueous coating composition with cellulose ester and preparation thereof. 1993-US2679, 9319136, 19930302., 1993.
121. Onda, Y.; Muto, H.; Maruyama, K. Coating materials for solid pharmaceuticals. 1977-116328 54049318, 19770928., 1979.
122. Tezuka, Y.; Imai, K.; Oshima, M.; Ito, K., Carbon-13 NMR structural studies on cellulose ethers by means of their acylated derivatives. 6. Carbon-13 NMR structural study on an enteric pharmaceutical coating cellulose derivative having ether and ester substituents. *Carbohydr. Res.* **1991**, 222, 255-9.
123. Curatolo, W. J.; Nightingale, J. A. S.; Shanker, R. M.; Sutton, S. C. Basic drug compositions containing cellulose derivatives with enhanced bioavailability. 2000-300587, 20000126, 2000.
124. Kennedy, M.; Hu, J.; Gao, P.; Li, L.; Ali-Reynolds, A.; Chal, B.; Gupta, V.; Ma, C.; Mahajan, N.; Akrami, A.; Surapaneni, S., Enhanced Bioavailability of a Poorly Soluble VR1 Antagonist Using an Amorphous Solid Dispersion Approach: A Case Study. *Mol. Pharmaceutics* **2008**, 5, (6), 981-993.
125. Tanno, F.; Nishiyama, Y.; Kokubo, H.; Obara, S., Evaluation of Hypromellose Acetate Succinate (HPMCAS) as a Carrier in Solid Dispersions. *Drug Dev. Ind. Pharm.* **2004**, 30, (1), 9-17.
126. Edgar, K. J., Cellulose esters in waterborne coatings. *Polymer Paint and Colour Journal* **1993**, 183, 564-571.
127. Kar, N.; Liu, H.; Edgar, K. J., Synthesis of Cellulose Adipate Derivatives. *Biomacromolecules* **2011**, 12, (4), 1106-1115.

# CHAPTER 3 PIONEERING STUDIES ON SYNTHESIS OF CELLULOSE ADIPATE DERIVATIVES

Adapted with permission from Kar, N.; Liu, H.; Edgar, K. J. *Biomacromolecules*, **2011**, 12, 1106-1115. Copyright 2011 American Chemical Society.

## 3.1 Abstract

Cellulose esters containing adipates and other ester groups are synthesized by the reaction of commercially available cellulose esters in solution with the benzyl monoester of adipoyl chloride. The products, cellulose adipate esters in which the distal end of the adipate moiety is a benzyl ester, were easily converted to cellulose adipate derivatives by Pd-catalyzed hydrogenation. These cellulose adipate derivatives are promising biopolymers for drug delivery and other applications in which water-dispersion or swelling are desired.

## 3.2 Introduction

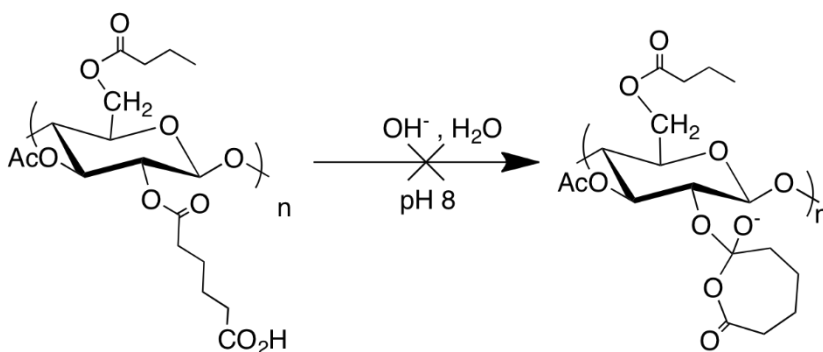
The synthesis of water-dispersible derivatives of cellulose has long been a difficult problem, of significant scientific and commercial importance. Synthesis of water-soluble cellulose derivatives is relatively well-understood, for example by acylation followed by extensive back-hydrolysis<sup>1</sup>, or by reaction of cellulose with various alkylating agents under base catalysis, to make derivatives like methylcellulose,<sup>2, 3</sup> carboxymethylcellulose,<sup>4</sup> hydroxyethylcellulose,<sup>5</sup> or ethylcellulose.<sup>6, 7</sup> These methods take advantage of the native hydrophilicity of cellulose, and the fact that a low DS of nearly any substituent can render cellulose water-soluble, by disrupting hydrogen bonding and crystallinity. For many applications, the ability to swell or disperse in water is far more desirable than water solubility. For example, in coatings applications, the low viscosity of aqueous dispersions permits the formulation of high-solids coatings, reducing drying time and transportation costs by minimizing the water content of the coating dispersion. One of the most

straightforward ways to make an aqueous dispersion that can then coalesce into a film is to incorporate carboxyl groups into the molecule; these can be deprotonated by volatile amines, enhancing the dispersability of the polymer.<sup>8</sup> Upon drying, the amine evaporates, promoting the formation of a continuous film. Polysaccharides that are fundamentally hydrophobic, but contain carboxyl groups that enable swelling or dissolution at neutral pH, are also highly useful for drug delivery applications.<sup>9</sup> Recent studies have shown that not only are such polysaccharide derivatives useful for traditional drug delivery applications such as pH-controlled release to avoid contact between drug and stomach,<sup>9</sup> but they also provide more valuable functional benefits. Recently, for example, hydroxypropylmethylcellulose acetate succinate (HPMCAS)<sup>10</sup> has proved to be a promising polymer for drug delivery formulations that significantly enhance drug solubility by entrapping the drug in metastable amorphous form dispersed in the polysaccharide matrix. Another pertinent example is carboxymethylcellulose acetate butyrate (CMCAB), which has been recently shown to combine several desirable drug delivery functions; pH-controlled release,<sup>11, 12</sup> zero-order release (which is of great value since it can permit constant blood concentration of the drug over long time periods, minimizing side effects and reducing dosing frequency), and solubility enhancement by the amorphous dispersion method.<sup>13-17</sup> CMCAB and HPMCAS function by swelling in the neutral pH of the small intestine and colon, because of ionization of the carboxyl groups; this swelling promotes drug release. The carboxyl groups of both cellulose derivatives and the hydrophobic substituents, particularly of CMCAB, promote miscibility of hydrophobic drugs in the polysaccharide matrix, helping to stabilize amorphous dispersions of otherwise poorly water-soluble drugs.<sup>15</sup> The kinetic stability of the thermodynamically metastable amorphous drug in the polymer matrix, for up to several years of storage at relatively high temperatures and humidity, is a critical performance feature of the amorphous dispersion formulations which are showing such promise for enhancing bioavailability of poorly water-soluble drugs (there is at least one commercial amorphous formulation, of the HIV drugs lopinavir and the CYP3A4 inhibitor ritonavir<sup>18</sup>). Such kinetic stability should be enhanced both by the high  $T_g$  of cellulose derivatives, and by the specific and hydrophobic interactions provided by hydrophobic cellulose derivatives that contain ionizable carboxyl groups.

Unfortunately, there are a limited number of methods available for synthesis of carboxyl-containing polysaccharides, and particularly carboxyl-containing cellulose derivatives. The most

well-known synthesis of carboxyl-containing cellulose derivatives is that of the commercial aqueous thickener carboxymethylcellulose. Typically cellulose is reacted with chloroacetic acid in water in the presence of sodium hydroxide as base. Conversion of carboxymethylcellulose into hydrophobic ester derivatives like acetate, propionate and butyrate has been reported.<sup>19, 20</sup> While the resulting carboxymethylcellulose esters are very interesting materials for coatings and drug delivery applications,<sup>21</sup> there must be concern with acid-catalyzed esterification of a polymer which contains both carboxyl and hydroxyl groups; the potential for cross-linking by esterification must always be considered. Another method is the reaction of cellulose or a cellulose derivative with a cyclic anhydride, usually employing a basic catalyst such as pyridine or triethylamine. In this way, carboxyl-substituted derivatives of cellulose such as cellulose acetate phthalate<sup>22</sup> and cellulose acetate butyrate succinate<sup>23</sup> have been synthesized. The known carboxyl-substituted cellulose derivatives prepared by this cyclic anhydride ring-opening chemistry suffer from limited stability in aqueous systems, which is of course a drawback for polymers designed to work in aqueous media. The stability of cellulose acetate butyrate succinate in neutral to alkaline media, for example, is limited.<sup>24</sup> The authors of that study speculated that the particular instability of derivatives like succinate arises from their ability to catalyze their own hydrolysis.

Cellulose adipate derivatives may be expected to possess superior properties to those of the cellulose phthalates and succinates synthesized in earlier work. They are likely to be less prone to autocatalyzed hydrolysis, since this would require an unfavorable 7-membered ring transition state (**Scheme 3.1**). They will be more hydrophobic than the corresponding succinate or phthalate derivatives, and thus would be expected to be more compatible with hydrophobic drugs. To date, there have been no reports of the synthesis of well-characterized cellulose adipates. Polysaccharide materials have been subjected to surface treatments with adipic acid in order to crosslink and strengthen those materials,<sup>25-28</sup> but the products were not fully characterized and no discrete cellulose derivatives were described.



**Scheme 3.1** Predicted hydrolytic stability of cellulose adipate esters

Adipic anhydride would be the directly analogous reagent to consider for ring-opening reaction with cellulose to produce cellulose adipates. Adipic anhydride is highly reactive due to its relatively strained 7-membered ring structure. It is prone to homopolymerization, and has most commonly been used to synthesize polyanhydrides<sup>29</sup> and polyesters.<sup>30</sup> Given its reactivity, we hoped that adipic anhydride would react with the poorly nucleophilic cellulose in solution,<sup>31</sup> providing that we could find an appropriate solvent and catalyst system. We report herein the unexpected difficulties we encountered in direct reaction of cellulose with adipic anhydride, and how those were overcome by employing monofunctional adipate reagents to develop the first successful synthesis of cellulose adipate esters, which will permit the synthesis of a broad range of cellulose adipate alkanooates.

## 3.3 Experimental Section

### 3.3.1 Materials

The high-purity hardwood pulp used in these experiments was Sulfatate HJ from Rayonier. Cellulose acetate propionate (CAP-504-0.2), cellulose acetate butyrate (CAB-553-0.4) and cellulose acetate (CA-320S) were from Eastman Chemical Co. Methyl ethyl ketone (MEK) was dried by refluxing over potassium carbonate. Other purchased reagents were used as received. Adipic anhydride was synthesized by following earlier reported procedures.<sup>31</sup> 10% Pd/C and 20% Pd(OH)<sub>2</sub>/C were purchased from Sigma Aldrich. Adipic acid, *p*-toluenesulfonic acid (PTSA), 1,3-dimethyl-2-imidazolidinone (DMI), oxalyl chloride and triethylamine (Et<sub>3</sub>N) were purchased from



ACROS Organics. Benzyl alcohol, toluene, *N,N*-dimethylformamide (DMF), *N,N*-dimethylacetamide (DMAc), dichloromethane, lithium chloride, and glacial acetic acid were purchased from Fisher Scientific. DMAc and DMI were dried over 4Å molecular sieves. Anhydrous tetrahydrofuran was purchased from Sigma Aldrich. All other reagents were synthesized by procedures described later in the experimental section.

### 3.3.2 Measurements

DSC analyses were obtained using a TA Instruments Q100. Neat powders (1-3 mg) were loaded into aluminum hermetic pans. Dry N<sub>2</sub> was used as the purge gas at 50 mL/min. Samples were equilibrated at -40 °C then ramped with a heat/cool/heat procedure between -40 °C and 160 °C, at a heating rate of 10 °C/min and a cooling rate of 5 °C/min. All tests were performed in triplicate. T<sub>g</sub> values were recorded as the step-change inflection point from 2<sup>nd</sup> heat scans. IR spectra were obtained on a Nicolet 8700 instrument. Proton NMR spectra were acquired on INOVA 400 spectrometer operating at 400 MHz. The sample tube size was 5 mm and the sample concentrations were ca. 10 mg/ml in CDCl<sub>3</sub> or DMSO-*d*<sub>6</sub>. CP/MAS <sup>13</sup>C NMR was carried out using a Bruker Avance II 300 instrument using 2048 scans at 27 °C. Elemental analyses were carried out by Micro-Analysis, Inc. Size exclusion chromatography (SEC) was used to determine the molecular weights of the polymers at 50 °C in DMF with 0.05 M LiBr at 1 mL min<sup>-1</sup> flow rate. The DMF SEC system was equipped with a Waters 717 plus autosampler, a Waters 1525 HPLC pump, two Waters Styragel HR5E (DMF) columns, and a Waters 2414 differential refractive index detector. Number average molecular weights relative to polystyrene standards are reported. Dynamic light scattering (DLS) was used to confirm the absence of polymer aggregates in solution. Solutions were prepared at a concentration of 1.0 mg/mL in pure DMF and DMF with 0.01 M LiBr and analyzed in a quartz cuvette at 20.0 °C. DLS measurements were performed on a Malvern ZetaSizer Nano Series Nano-ZS instrument using Dispersion Technology Software (DTS) version 6.01 at a wavelength of 633 nm using a 4.0 mW, solid state He-Ne laser at a back-scattering angle of 173 °. The experiments were performed at a temperature of 20 °C, in triplicate. Solubility testing on cellulose ester samples was performed by adding 10 mg of sample to a glass vial, then adding 2 mL of solvent. The mixture was subjected to vortex mixing for 5-10 min at room temperature, then solubility was judged by visual examination.

### 3.3.3 Reaction of cellulose in DMAc/LiCl solution with adipic anhydride

This procedure (**Scheme 3.2**) is typical for entries listed in **Table 3.1**. Cellulose (8.00 g, 49.3 mmol) was dissolved in DMAc (300 mL) and lithium chloride (15 g) by the procedure reported earlier.<sup>32</sup> To this solution, at 80 °C under nitrogen was added dropwise a solution of adipic anhydride (6.31 g, 49.3 mmol) in 20 mL DMAc (entry 1, **Table 3.1**). After 45 min it was observed that the solution gelled, and the gel broke up into small, translucent balls (*ca.* 1-2 cm in diameter) with mechanical stirring. The product was isolated by adding the reaction mixture to methanol, filtration of the gel-like product, and then extensive washing of the product with methanol, then with water. The product was insoluble in all solvents tried, including DMSO and chloroform. Analysis of the dried product by infrared spectroscopy and by solid-phase <sup>13</sup>C spectroscopy revealed that it was a cellulose adipate, which was cross-linked. Solid state <sup>13</sup>C NMR (**Fig. 3.1**) showed adipate peaks but the IR spectrum (**Fig. 3.2**) showed no prominent COOH absorption, indicating the lack of pendent carboxylic acid groups and affirming the presence of ester cross-links. Solid-state CP/MAS <sup>13</sup>C NMR: 173.5 (C=O), 104.6 (C-1), 83.1 (C-4), 74.8 (C-5, C-2, C-3), 62.7 (C-6), 33.8-38.5 (COCH<sub>2</sub>CH<sub>2</sub>CH<sub>2</sub>CH<sub>2</sub>CO of adipate), 21.7-24.6 (COCH<sub>2</sub>CH<sub>2</sub>CH<sub>2</sub>CH<sub>2</sub>CO of adipate). IR (cm<sup>-1</sup>): 1812, 1742 (anhydride doublet).

### 3.3.4 Synthesis of benzyl-protected cellulose adipate mixed esters

**Synthesis of Monobenzyl Adipate (Scheme 3.4).** Prepared by the procedure of English, *et al.*,<sup>33</sup> as follows. Adipic acid (73 g, 0.5 mol), benzyl alcohol (81 g, 0.75 mol), PTSA (0.95 g, 5 mmol), and toluene (400 mL) were combined in a flask equipped with Dean-Stark trap and heated at reflux until the theoretical amount of H<sub>2</sub>O (13.5 mL, 0.75 mol) was obtained. The solution was then cooled, 300 mL of H<sub>2</sub>O added, and the pH adjusted to 8 with 6 N NaOH. The aqueous layer was separated and washed with ether (2 x 100 mL), 200 mL of fresh ether was added, and the pH was adjusted to 2.0 with 6 N HCl. The ether layer was separated, dried (Na<sub>2</sub>SO<sub>4</sub>), and concentrated to yield 47 g of monobenzyl adipate (40%) as a colorless oil: <sup>1</sup>H NMR (CDCl<sub>3</sub>, **Fig. S3.1**, Supplementary Material): 1.68 (m, 4 H), 2.36 (m, 4 H), 5.09 (s, 2 H), 7.32 (m, 5 H).

**Synthesis of Monobenzyl Adipoyl Chloride (Scheme 3.4).** Prepared by the procedure of Abell, *et al.* as follows.<sup>34</sup> A solution of monobenzyl adipate (20 g, 0.08 mol) and DMF (1 drop) in dichloromethane was cooled to 0 °C and oxalyl chloride (57.15 g, 0.45 moles) was added slowly.

After 30 min at 15 °C, the solvent was removed under reduced pressure. Toluene (200 mL) was added to the resultant oil and again the solvent was removed to yield the acid chloride as an oil that was not purified further. <sup>1</sup>H NMR (CDCl<sub>3</sub>, **Fig. S3.2**, Supplementary Material): 1.73 (m, 4 H), 2.39 (t, 2 H), 2.90 (t, 2 H), 5.12 (s, 2 H), 7.32 (m, 5 H).

**Example Procedure for the Reaction of CAP with Monobenzyl Adipoyl Chloride (Scheme 3.5).** CAP-504-0.2 (entry 1, **Table 3.2**) (1 g, 3.52 mmol) was dissolved in MEK (10 mL) and the solution was heated to 60 °C with stirring under nitrogen. Et<sub>3</sub>N (0.53 mL, 3.87 mmol, 1.1 equiv) was added all at once, then monobenzyl adipoyl chloride (0.89 g, 3.52 mmol, 1 equiv) was added. An immediate precipitate (presumed to be triethylammonium chloride) was observed. The solution was stirred at 60 °C for 20 h. The reaction mixture was filtered, then added dropwise to isopropyl alcohol at room temperature with stirring. The precipitate was collected by filtration and washed with water. It was redissolved in chloroform and precipitated with hexane. The product was washed with hexane and vacuum-dried at 50 °C.

A similar procedure was followed for the reaction of CAB with monobenzyl adipoyl chloride.

**Benzyl Cellulose Acetate Adipate Propionate.** <sup>1</sup>H NMR (CDCl<sub>3</sub>): 1.02-1.20 (m, COCH<sub>2</sub>CH<sub>3</sub> of propionate), 1.66 (broad s, COCH<sub>2</sub>CH<sub>2</sub>CH<sub>2</sub>CH<sub>2</sub>CO of adipate), 2.16-2.35 (m, COCH<sub>2</sub>CH<sub>3</sub> of propionate, COCH<sub>3</sub> of acetate and COCH<sub>2</sub>CH<sub>2</sub>CH<sub>2</sub>CH<sub>2</sub>CO of adipate), 3.25-5.24 (cellulose backbone), 5.10 (CH<sub>2</sub>C<sub>6</sub>H<sub>5</sub>), 7.33 (CH<sub>2</sub>C<sub>6</sub>H<sub>5</sub>). Degree of substitution (DS) by <sup>1</sup>H NMR: adipate 0.33, propionate 2.09, acetate 0.04. Yield: 58%.

**Benzyl Cellulose Acetate Adipate Butyrate.** <sup>1</sup>H NMR (CDCl<sub>3</sub>): 0.89-0.98 (m, COCH<sub>2</sub>CH<sub>2</sub>CH<sub>3</sub> of butyrate), 1.54-1.64 (m, COCH<sub>2</sub>CH<sub>2</sub>CH<sub>3</sub> of butyrate, COCH<sub>2</sub>CH<sub>2</sub>CH<sub>2</sub>CH<sub>2</sub>CO of adipate), 2.14-2.31 (m, COCH<sub>2</sub>CH<sub>2</sub>CH<sub>3</sub> of butyrate, COCH<sub>3</sub> of acetate and COCH<sub>2</sub>CH<sub>2</sub>CH<sub>2</sub>CH<sub>2</sub>CO of adipate), 3.25-5.31 (cellulose backbone), 5.10 (CH<sub>2</sub>C<sub>6</sub>H<sub>5</sub>), 7.33 (CH<sub>2</sub>C<sub>6</sub>H<sub>5</sub>). DS by <sup>1</sup>H NMR: adipate 0.5, butyrate 1.99, acetate 0.14. Yield: 60%.

**Procedure for the Reaction of CA-320S with Monobenzyl Adipoyl Chloride.** CA-320S (entry 4, **Table 3.2**) (1 g, 4.18 mmol) was dissolved in N, N- dimethylimidazolidinone (DMI, 10 mL) and the solution was heated to 100 °C with stirring under nitrogen. Triethylamine (0.63 mL, 4.59 mmol, 1.1 equiv) was added all at once, then monobenzyl adipoyl chloride (2.12 g, 8.36 mmol, 2 equiv) was added. The solution was stirred at 100 °C for 20 h. The reaction mixture was filtered

to remove the needle shaped crystals of triethylammonium chloride. The filtrate was added dropwise to water at room temperature in a high shear mixer. The precipitate was redissolved in isopropanol and precipitated with water. The product, benzyl cellulose acetate adipate, was washed with water and vacuum-dried.  $^1\text{H}$  NMR ( $\text{CDCl}_3$ ): 1.66 (br s,  $\text{COCH}_2\text{CH}_2\text{CH}_2\text{CH}_2\text{CO}$  of adipate), 1.94-2.09 (m,  $\text{COCH}_3$  of acetate), 2.37 (br s,  $\text{COCH}_2\text{CH}_2\text{CH}_2\text{CH}_2\text{CO}$  of adipate), 3.25-5.31 (cellulose backbone), 5.10 ( $\text{CH}_2\text{C}_6\text{H}_5$ ), 7.33 ( $\text{CH}_2\text{C}_6\text{H}_5$ ). DS by  $^1\text{H}$  NMR: adipate 0.7, acetate 1.8. Yield: 82%.

**Procedure for the Hydrolysis of CAP-504-0.2 and Reaction of Hydrolyzed Product with Monobenzyl Adipoyl Chloride.** CAP-504-0.2 (3 g, 10.69 mmol) was dissolved in propionic acid (50 mL), then sulfuric acid (0.6 g, 0.66 mL) and water (6 mL) were added together into the solution. The solution was stirred at 80 °C for 3.5 h. The product was collected by precipitating into 300 mL water. The white compound was then washed with 300 mL water, 200 mL 0.5 M  $\text{Na}_2\text{CO}_3$  aqueous solution and again with 200 mL water. Yield: 1.09 g. DS of propionate 1.68 was determined by  $^1\text{H}$  NMR in  $\text{DMSO}-d_6$ .

Hydrolyzed cellulose propionate (1 g, 3.91 mmol based on DS 1.68) was fully dissolved in DMI, the solution was heated to 100 °C with stirring under nitrogen. Triethylamine (0.60 mL, 4.30 mmol, 1.1 equiv) was added all at once, then monobenzyl adipoyl chloride (1.00 g, 3.91 mmol, 1 equiv) was added. The solution was stirred at 100 °C for 20 h. The reaction mixture was filtered to remove triethylammonium chloride. The filtrate was dialyzed against water and freeze-dried. The yellow product was washed with isopropanol twice before vacuum drying.  $^1\text{H}$  NMR ( $\text{DMSO}-d_6$ ): 0.70-1.10 (m,  $\text{COCH}_2\text{CH}_3$  of propionate), 1.51 ( $\text{COCH}_2\text{CH}_2\text{CH}_2\text{CH}_2\text{CO}$  of adipate), 2.02-2.45 (m,  $\text{COCH}_2\text{CH}_3$  of propionate and  $\text{COCH}_2\text{CH}_2\text{CH}_2\text{CH}_2\text{CO}$  of adipate), 2.95-5.15 (cellulose backbone), 5.06 ( $\text{CH}_2\text{C}_6\text{H}_5$ ), 7.33 ( $\text{CH}_2\text{C}_6\text{H}_5$ ). DS by  $^1\text{H}$  NMR: adipate 0.48. Yield: 59 %.

**Procedure for the Reaction of Cellulose with Monobenzyl Adipoyl Chloride.** Cellulose (0.63 g, 3.88 mmol) was dissolved in DMAC/LiCl by an earlier reported procedure.<sup>32</sup> To this solution at 60 °C was added triethylamine (0.59 mL, 1.1 equiv). Then the monobenzyl adipoyl chloride (3 g, 11.64 mmol, 3 equiv) was added dropwise at 60 °C. The reaction mixture was stirred for 20 h at that temperature, and then cooled to room temperature. It was filtered and then added to isopropyl alcohol to precipitate the product. The product benzyl cellulose adipate was washed with water, and then was vacuum-dried at 40 °C to afford 1.83 g (78% yield) of white powder.  $^1\text{H}$

NMR (DMSO-*d*<sub>6</sub>): 1.47 (br s, COCH<sub>2</sub>CH<sub>2</sub>CH<sub>2</sub>CH<sub>2</sub>CO of adipate), 2.37 (br s, COCH<sub>2</sub>CH<sub>2</sub>CH<sub>2</sub>CH<sub>2</sub>CO of adipate), 3.25-5.31 (cellulose backbone), 5.10 (CH<sub>2</sub>C<sub>6</sub>H<sub>5</sub>), 7.33 (CH<sub>2</sub>C<sub>6</sub>H<sub>5</sub>). DS by <sup>1</sup>H NMR: adipate 2.0. Yield: 78%.

### 3.3.5 Deprotection of benzyl cellulose adipate esters

**Example Procedure for the Pd/C Hydrogenation of the Benzyl Cellulose Ester.** Benzyl cellulose acetate adipate propionate (200 mg) was dissolved in THF and to this solution was added 10% palladium on carbon (100 mg). A hydrogen balloon was attached to the flask and the solution was stirred overnight under a hydrogen atmosphere at room temperature. The mixture was filtered through Celite and evaporated to afford the product. The product was dissolved in chloroform and reprecipitated into hexane. The product (150 mg, 82% yield) was soluble in DMSO, and insoluble in water.

**Cellulose Acetate Adipate Propionate.** <sup>1</sup>H NMR (CDCl<sub>3</sub>): 1.02-1.20 (m, COCH<sub>2</sub>CH<sub>3</sub> of propionate), 1.66 (broad s, COCH<sub>2</sub>CH<sub>2</sub>CH<sub>2</sub>CH<sub>2</sub>CO of adipate), 2.16-2.35 (m, COCH<sub>2</sub>CH<sub>3</sub> of propionate, COCH<sub>3</sub> of acetate and COCH<sub>2</sub>CH<sub>2</sub>CH<sub>2</sub>CH<sub>2</sub>CO of adipate), 3.25-5.24 (cellulose backbone). DS by <sup>1</sup>H NMR: adipate 0.33, propionate 2.09, acetate 0.04. <sup>13</sup>C NMR (DMSO-*d*<sub>6</sub>): 172.0-175.0 (C=O), 99.6 (C-1), 75.1 (C-4), 72.8 (C-3), 72.1 (C-2, C-5), 62.8 (C-6), 33.2-34.0 (COCH<sub>2</sub>CH<sub>2</sub>CH<sub>2</sub>CH<sub>2</sub>CO of adipate), 26.8-27.6 (COCH<sub>2</sub>CH<sub>3</sub> of propionate), 24.0-24.8 (COCH<sub>2</sub>CH<sub>2</sub>CH<sub>2</sub>CH<sub>2</sub>CO of adipate), 23.1 (COCH<sub>3</sub> of acetate), 9.1 (COCH<sub>2</sub>CH<sub>3</sub> of propionate). Yield: 82%. Elemental analysis: Calculated C 53.24%, H 6.53%, O 40.23%; Found C 53.10%, H 6.61%, O 40.22%.

**Cellulose Acetate Adipate Butyrate.** <sup>1</sup>H NMR (CDCl<sub>3</sub>): 0.89-0.98 (m, COCH<sub>2</sub>CH<sub>2</sub>CH<sub>3</sub> of butyrate), 1.54-1.64 (m, COCH<sub>2</sub>CH<sub>2</sub>CH<sub>3</sub> of butyrate, COCH<sub>2</sub>CH<sub>2</sub>CH<sub>2</sub>CH<sub>2</sub>CO of adipate), 2.14-2.31 (m, COCH<sub>2</sub>CH<sub>2</sub>CH<sub>3</sub> of butyrate, COCH<sub>3</sub> of acetate and COCH<sub>2</sub>CH<sub>2</sub>CH<sub>2</sub>CH<sub>2</sub>CO of adipate), 3.25-5.31 (cellulose backbone). DS by <sup>1</sup>H NMR: adipate 0.5, butyrate 1.99, acetate 0.14. <sup>13</sup>C NMR (DMSO-*d*<sub>6</sub>): 171.2-175.0 (C=O), 99.9 (C-1), 76.5 (C-4), 72.0-73.0 (C-2, C-3, C-5), 63.1 (C-6), 35.9 (COCH<sub>2</sub>CH<sub>2</sub>CH<sub>3</sub> of butyrate), 34.1 (COCH<sub>2</sub>CH<sub>2</sub>CH<sub>2</sub>CH<sub>2</sub>CO of adipate), 24.8 (COCH<sub>2</sub>CH<sub>2</sub>CH<sub>2</sub>CH<sub>2</sub>CO of adipate), 21.0 (COCH<sub>3</sub> of acetate), 18.2-18.6 (COCH<sub>2</sub>CH<sub>2</sub>CH<sub>3</sub> of butyrate), 13.9 (COCH<sub>2</sub>CH<sub>2</sub>CH<sub>3</sub> of butyrate). Yield: 85%. Elemental analysis: Calculated C 55.69%, H 7.14%, O 37.17%; Found C 55.59%, H 7.11%, O 36.89%.

**Cellulose Acetate Adipate.**  $^1\text{H}$  NMR (DMSO-*d*6): 1.47 (s,  $\text{COCH}_2\text{CH}_2\text{CH}_2\text{CH}_2\text{CO}$  of adipate), 1.84-2.05 (m,  $\text{COCH}_3$  of acetate), 2.18 (s,  $\text{COCH}_2\text{CH}_2\text{CH}_2\text{CH}_2\text{CO}$  of adipate), 2.95-5.15 (cellulose backbone). DS by  $^1\text{H}$  NMR: adipate 0.7, acetate 1.8.  $^{13}\text{C}$  NMR (DMSO-*d*6): 168.0-175.0 (C=O), 99.5 (C-1), 76.4 (C-4), 70.3-73.7 (C-2, C-3, C-5), 62.8 (C-6), 33.2-34.0 ( $\text{COCH}_2\text{CH}_2\text{CH}_2\text{CH}_2\text{CO}$  of adipate), 24.0-24.5 ( $\text{COCH}_2\text{CH}_2\text{CH}_2\text{CH}_2\text{CO}$  of adipate), 20.3-21.3 ( $\text{COCH}_3$  of acetate). Yield: 88%. Elemental analysis: Calculated C 50.61%, H 5.87%, O 43.52%; Found C 46.73%, H 6.07%, O 45.66%.

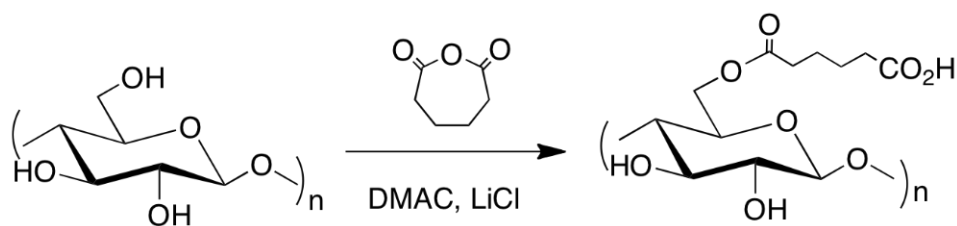
**Example Procedure for the  $\text{Pd}(\text{OH})_2/\text{C}$  Hydrogenation of the Benzyl Cellulose Ester.** To a solution of 200 mg benzyl cellulose acetate adipate propionate dissolved in 30 ml anhydrous THF/acetic acid (1:1, v/v), 100 mg palladium hydroxide, 20 wt. % Pd (dry basis) on carbon was added. A hydrogen balloon was attached to the flask and the solution was stirred overnight under hydrogen atmosphere at room temperature. The mixture was filtered through Celite and concentrated. The product was dissolved in dichloromethane and precipitated into hexane. The precipitate was collected and dried under vacuum. Yield: 130 mg (71%).

## 3.4 Results and Discussion

### 3.4.1 Direct synthesis using adipic anhydride and crosslinking problem

We initially explored the solution phase reaction of cellulose with adipic anhydride in DMAC/LiCl (**Scheme 3.2**), which is one of the best understood and most broadly useful solvent systems for reactions in which cellulose is a nucleophile.<sup>35, 36</sup> We found in earlier studies<sup>32</sup> that cellulose reacts smoothly in DMAC/LiCl with carboxylic anhydrides (cyclic or otherwise) at 80 °C or higher, without the need for added catalyst. Therefore we added adipic anhydride dropwise to cellulose in DMAC/LiCl solution at 80 °C (entry 1, **Table 3.1**). We were surprised to observe that the solution gelled almost immediately upon commencement of adipic anhydride addition. The gelled product was insoluble in all solvents tried, including DMSO and chloroform. While it is possible that the observed gelation could have been caused by inherent poor solubility of cellulose adipate, this would not be predicted from previous observations of carboxyalkyl cellulose ester solubility,<sup>37</sup> and was not supported by subsequent observations of the solubility of cellulose adipates prepared in other ways (*vide infra*). Analysis of the dried product by infrared

spectroscopy and solid-phase  $^{13}\text{C}$  spectroscopy revealed that it was a cellulose adipate, which was cross-linked. Solid-state  $^{13}\text{C}$  NMR (**Fig. 3.1**) showed adipate peaks at  $\delta$  21.7-24.6 and 33.8-38.5 and the IR (**Fig. 3.2**) spectrum showed no prominent COOH absorption, indicating the lack of pendent carboxylic acid groups. Interestingly, a doublet characteristic of anhydrides (in this case due to poly(adipic anhydride))<sup>36</sup> was seen at 1812 and 1742  $\text{cm}^{-1}$  in the infrared spectrum.



**Scheme 3.2** Reaction of cellulose with adipic anhydride

**Table 3.1** Synthesis of cellulose adipate under different conditions using adipic anhydride

entry	adipic anhydride (equiv)	temperature ( $^{\circ}\text{C}$ )	remarks
1	1	80	Cross-linked
2	1	40	No Reaction
3	3.5	60	Cross-linked

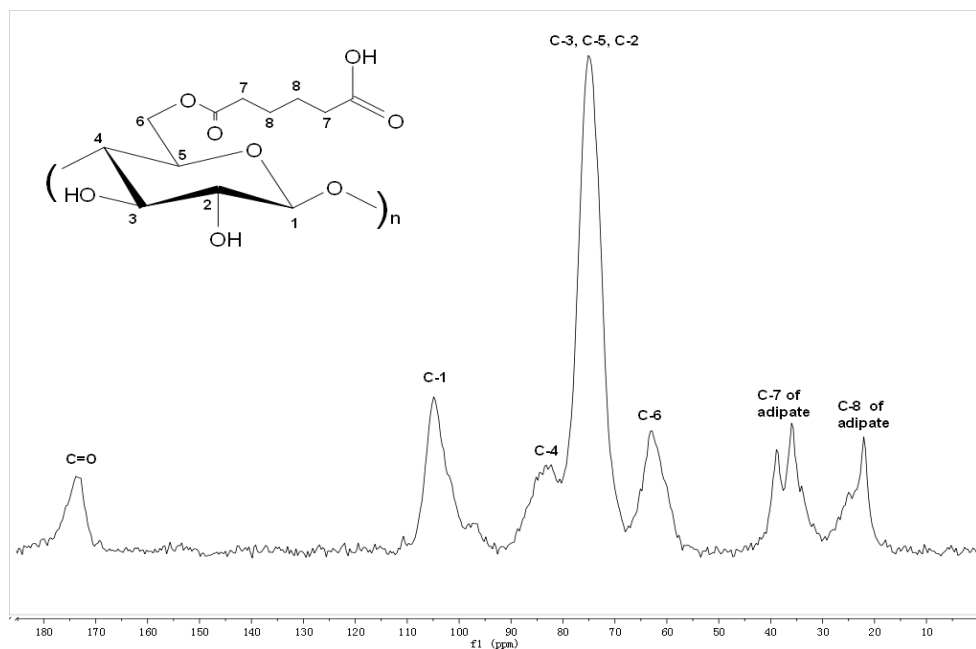


**Figure 3.1** CP/MAS  $^{13}\text{C}$  NMR spectrum of cross-linked cellulose adipate

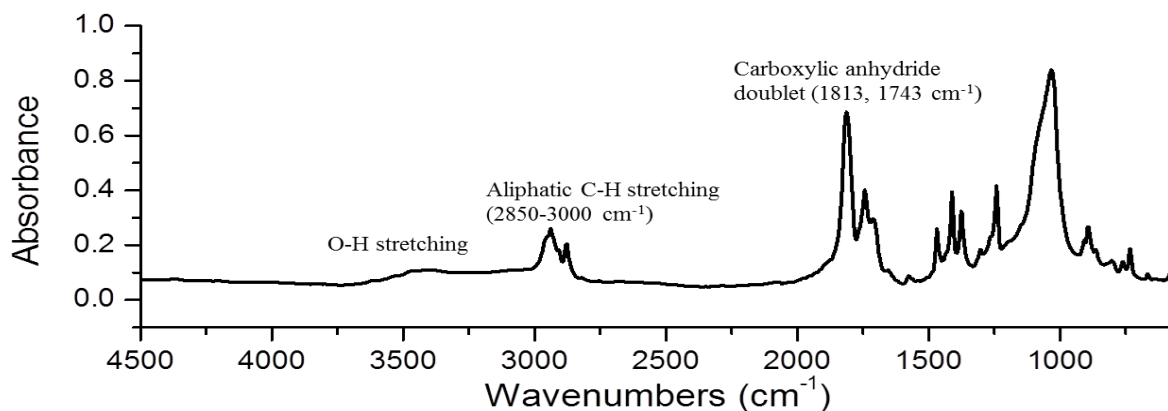
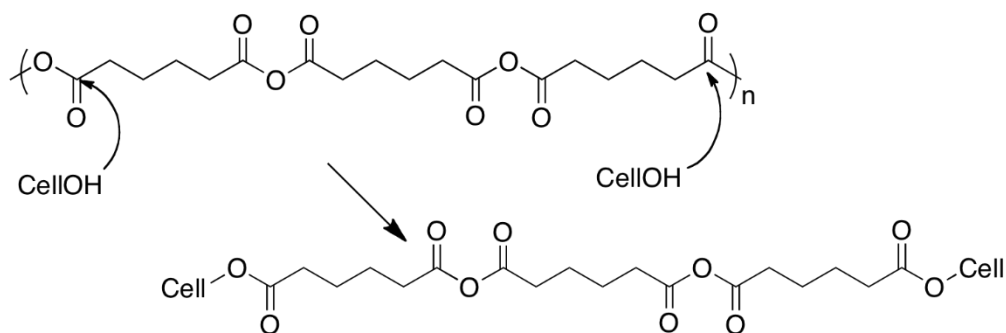


**Figure 3.2** IR spectrum of cross-linked cellulose adipate

The cross-linking observed is extraordinarily rapid; furthermore, no such cross-linking is observed when employing succinic anhydride as the electrophile under otherwise identical conditions.<sup>37</sup> Thus, it seems extremely unlikely that the rapid gelation observed could be caused by condensation between the pendent carboxyl group of adipate groups attached to cellulose, and free hydroxyl groups on cellulose (nor would such ester cross-links be consistent with the IR and  $^{13}\text{C}$  analyses of the product). Rather, we postulate that the cross-linking is being caused by reaction between cellulose and poly(adipic anhydride) (**Scheme 3.3**), in which each poly(adipic anhydride)



chain reacts on average with more than one cellulose molecule. We have observed that even freshly prepared adipic anhydride contains a measurable amount of poly(adipic anhydride) by  $^1\text{H}$  NMR spectroscopy (poly(adipic anhydride) gave signals at 1.75 and 2.5 ppm due to  $-\text{CH}_2\text{CH}_2-$  and  $\text{CH}_2\text{-CO-O-CO-CH}_2$  protons, respectively, and adipic anhydride signals appeared at 2.8 and 2.0 ppm), and that this amount grows over the course of days as the adipic anhydride is stored, even if refrigerated. This postulate is consistent with the observed anhydride carbonyl absorbances in the IR spectrum ( $1812, 1742\text{ cm}^{-1}$ ). These poly(anhydride) cross-links would not be expected to hydrolyze rapidly (even though thermodynamically labile), due to the hydrophobicity of the adipate group and the poor solubility of these high molecular weight cross-linked species.<sup>38, 39</sup>



**Scheme 3.3** Reaction of cellulose with poly(adipic anhydride)

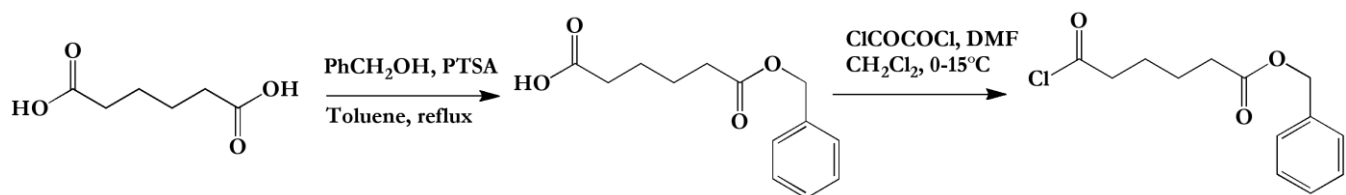
We made several attempts to circumvent the apparent cross-linking problem by adjusting reaction conditions. **Table 3.1** shows the results of several of these attempts. Lower temperature ( $40\text{ }^\circ\text{C}$ , entry 2) condensation was attempted in an effort to enhance reaction selectivity and minimize cross-linking, but at that low temperature no desired esterification was observed. We thought that by increasing the number of equivalents of adipic anhydride (entry 3) and employing rapid anhydride addition, we might block all of the hydroxyls as adipate esters, preventing cross-linking. This approach also was unsuccessful; gelation of the reaction mixture occurred even before adipic anhydride addition was complete.

If ester cross-linking by condensation of carboxyls on one cellulose chain with hydroxyls on another cellulose chain was the problem, bases like triethylamine and pyridine might be useful, to convert the initial product cellulose adipate carboxylic acid into a carboxylate anion, making condensation with a cellulosic hydroxyl to form an ester linkage far less favorable. However, the use of organic bases was not pursued, because of our evidence that reaction with poly(adipic

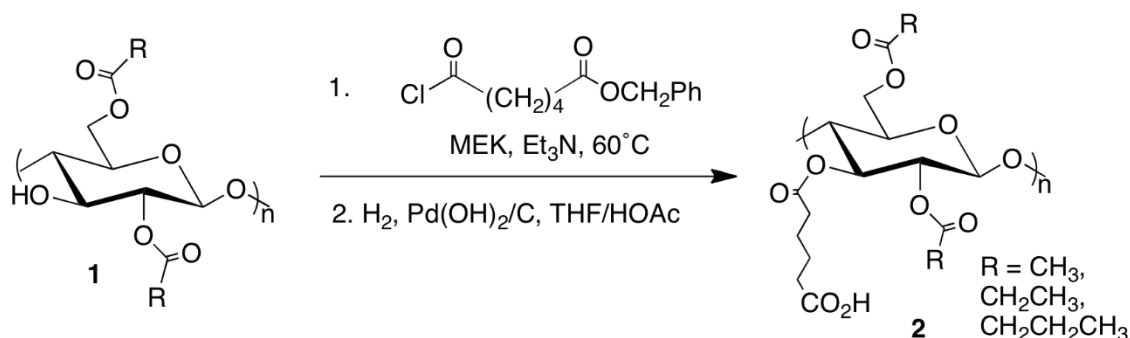
anhydride) was in fact the issue, and because of reports<sup>40</sup> that triethylamine can initiate ring-opening polymerization of adipic anhydride to polyadipic anhydride at room temperature.

### 3.4.2 Two-step synthesis using monobenzyl ester mono acid chloride

If our conclusions about the mechanism for the cross-linking observed with adipic anhydride were sound, then a sure-fire way to avoid cross-linking would be to replace adipic anhydride with a monofunctional equivalent. Fortunately for us, there were reports in the literature of the monobenzyl ester of adipic acid,<sup>33</sup> and the conversion of that ester to the monobenzyl ester monoacid chloride (benzyl 6-chloro-6-oxohexanoate, **Scheme 3.4**).<sup>34</sup> We knew from prior reports<sup>3,41,42</sup> that the removal of benzyl ether groups from cellulose by hydrogenation was feasible, and were hopeful that our adipate benzyl ester groups would be at least as easily removed by hydrogenation. We first examined the reaction of monobenzyl adipoyl chloride with commercial cellulose esters of relatively low degree of substitution; this permitted us to work in solvents of moderate polarity. Reaction of monobenzyl adipoyl chloride with CAP-504-0.2 (DS (propionyl) 2.09, DS(acetyl) 0.04) (entry 1, **Table 3.2**) in MEK at 60 °C for 20 h cleanly afforded benzyl cellulose acetate adipate propionate, with no evidence of gelation or cross-linking. The benzyl adipate substituent was then hydrogenated to remove the benzyl groups and deprotect the adipate groups; again the reaction went smoothly and no cross-linking was observed, affording cellulose acetate adipate propionate (**Scheme 3.5**; note that no regioselectivity is implied by the structures in this scheme; we have no conclusive information at this time about the regioselectivity of the reaction). We found that hydrogenation using Pd/C was always successful, but sluggish in larger scale (multigram) reactions. The use of Pd(OH)<sub>2</sub>/C gave more rapid hydrogenations at the gram scale and eliminated the occasional necessity for multiple hydrogenations to attain complete debenylation.



**Scheme 3.4** Monobenzyl adipoyl chloride synthesis



**Scheme 3.5** Synthesis of cellulose adipates via acid chloride

**Table 3.2** Synthesis of benzyl cellulose adipate derivatives using monobenzyl adipoyl chloride (MAC)

entry	substrate	MAC (equiv/ AGU)	solvent	temp. ( $^\circ\text{C}$ )	DS			solubility
					Ad	other	total	
1	CAP-504- 0.2	1	MEK	60	0.33	Pr 2.09 Ac 0.04	2.46	THF, $\text{CHCl}_3$ , DMSO
2	CAP- 504-0.2	3	MEK	60	0.50	Pr 2.09 Ac 0.04	2.63	THF, $\text{CHCl}_3$ , DMSO
3	CAB-553- 0.4	1	MEK	60	0.25	Bu 1.99 Ac 0.14	2.38	THF, $\text{CHCl}_3$ , DMSO
4	CA- 320S	2	DMI	100	0.70	Ac 1.80	2.50	THF, $\text{CHCl}_3$ , DMSO
5	CP (hydrolyzed)	1	DMI	100	0.48	Pr 1.68	2.16	THF, DMSO
6	Cellulose	3	DMAc/ LiCl	60	2.00	None	2.00	Sparingly soluble in DMSO

Ac = acetate, Bu = butyrate, Pr = propionate. CAP-504-0.2 is commercial cellulose acetate propionate from Eastman (DS(Pr) = 2.09, DS(Ac) = 0.04). CAB-553-0.4 is commercial cellulose acetate butyrate from Eastman (DS(Bu) = 1.99, DS(Ac) = 0.14). CA-320S is commercial cellulose acetate from Eastman (DS(Ac) = 1.80).

The formation of these products was confirmed by proton NMR studies. **Fig 3.3** shows the  $^1\text{H}$  NMR spectrum of benzyl cellulose acetate adipate propionate. One of the adipate peaks ( $\text{COCH}_2\text{CH}_2\text{CH}_2\text{CH}_2\text{CO}$ ) appears as a broad singlet at 1.66 ppm. The other adipate peak ( $\text{COCH}_2\text{CH}_2\text{CH}_2\text{CH}_2\text{CO}$ ) merges with the  $\text{COCH}_3$  and  $\text{COCH}_2\text{CH}_3$  peaks from CAP at 2.16 - 2.35 ppm. The benzyl protons appear at 5.1 ( $\text{CH}_2$ ) and 7.33 (Ph). **Fig. 3.4** shows the  $^1\text{H}$  NMR spectrum of the hydrogenation product, cellulose acetate adipate propionate. The success of the hydrogenation is confirmed by disappearance of the benzyl aromatic signals, and the spectrum clearly indicates that cellulose acetate adipate propionate has been formed. The  $^{13}\text{C}$  NMR spectrum (**Fig 3.5**) also clearly indicates the nearly complete absence of benzyl signals (aromatic signals 110 – 130 ppm), and the presence of the adipate groups. Thus the use of the monofunctional reagent has indeed resulted in smooth preparation of an uncross-linked cellulose adipate product, as predicted.

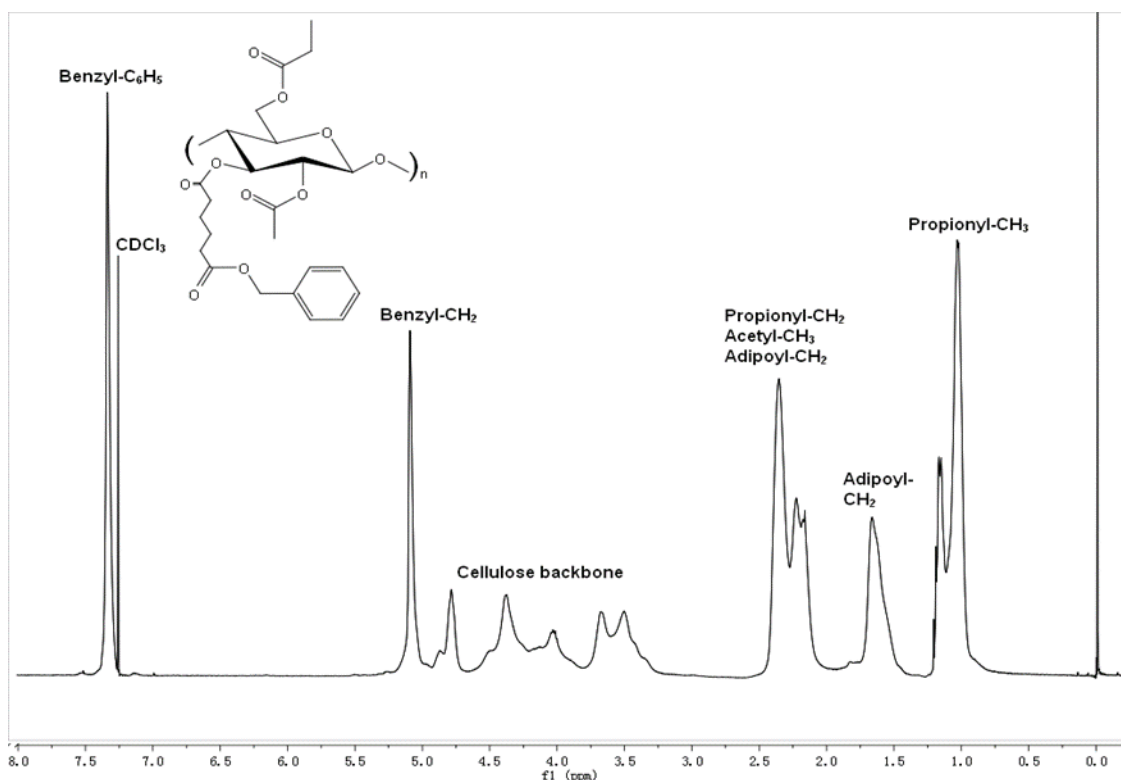


**Figure 3.3**  $^1\text{H}$  NMR spectrum of benzyl cellulose acetate adipate propionate in  $\text{CDCl}_3$

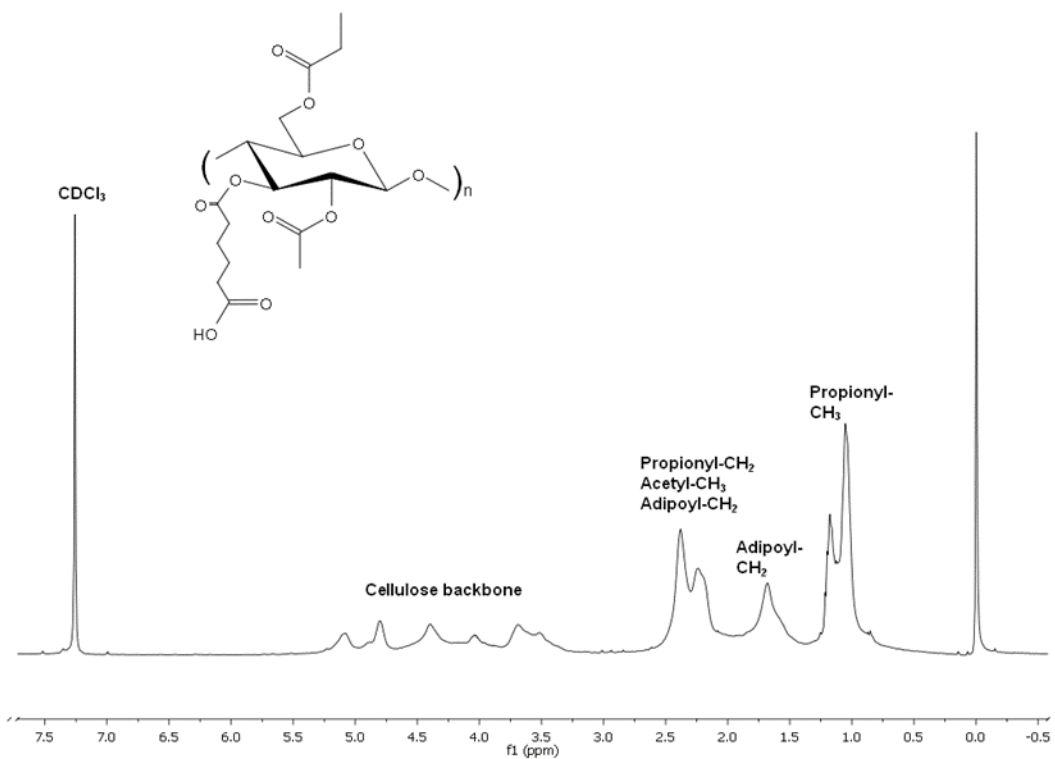


**Figure 3.4**  $^1\text{H}$  NMR spectrum of cellulose acetate adipate propionate in  $\text{CDCl}_3$

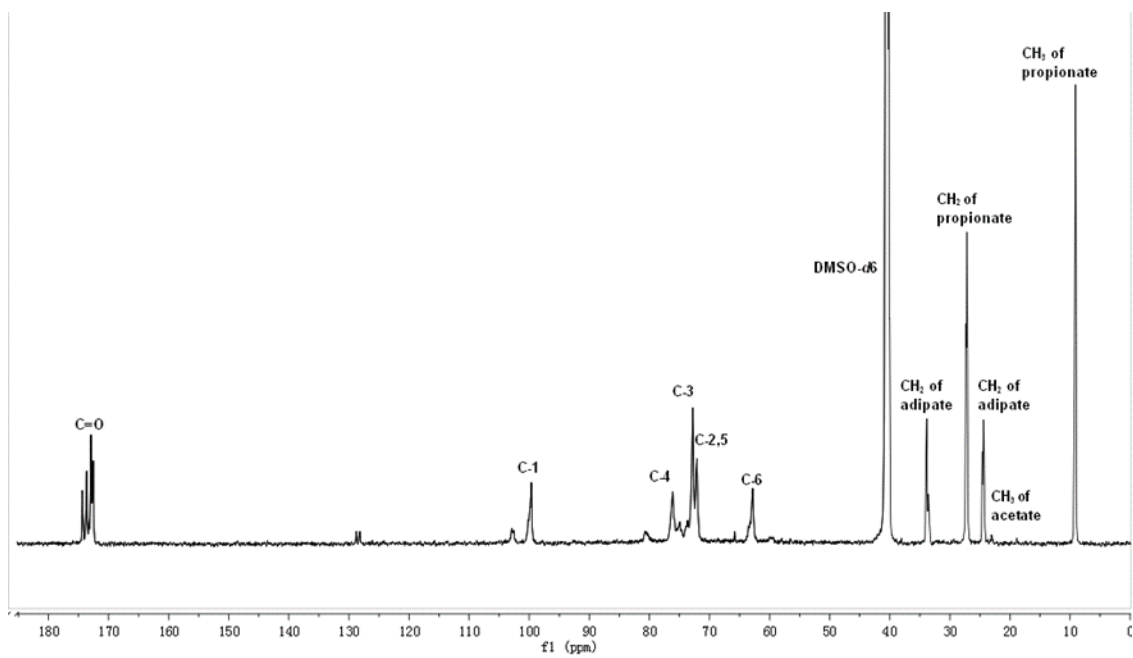


**Figure 3.5**  $^{13}\text{C}$  NMR spectrum of cellulose acetate adipate propionate in  $\text{DMSO}-d_6$

**Table 3.2** shows the results of several attempts to apply this chemistry to other cellulose derivatives, expanding the range of adipate derivatives available. MEK was used as a solvent for reaction of monobenzyl adipoyl chloride with cellulose acetate propionate (CAP-504-0.2; entry 1, **Table 3.2**) and cellulose acetate butyrate (CAB-553-0.4; entry 3, **Table 3.2**). The cellulose acetate used (CA-320S) and the hydrolysis product of CAP-504-0.2 (CP) were not soluble in MEK, so reactions of CA and CP were carried out in the polar aprotic solvent DMI. In each case, rather low DS commercial cellulose esters were used as starting materials in order to provide a higher DS of available OH groups for reaction with the adipate derivative. Triethylamine was employed as catalyst and acid scavenger. The product benzyl adipate derivatives of CAP, CAB, CA and CP were each soluble in THF. Hydrogenation of each of these four products at room temperature using a hydrogen balloon proceeded smoothly, resulting in benzyl deprotection to afford the respective cellulose adipate derivatives (**Scheme 3.5**). However, hydrogenation of benzyl cellulose adipate (DS(adipate) = 2.00, entry 6, **Table 3.2**) could not be carried out due to limited solubility of the product in common organic solvents. Synthesis of cellulose adipate alkanooates from cellulose in solution in solvents like DMAc/LiCl and ionic liquids should overcome this product solubility problem. Our results on synthesis of cellulose adipates in ionic liquids will be discussed in a forthcoming paper.

The degrees of substitution (DS) of the products were assigned from the proton NMR spectra, using the ratios of appropriate acyl proton integrations to the backbone proton integration. For example, DS (adipate) 0.33 was achieved by reaction between CAP-504-0.2 and 1 equivalent of monobenzyl adipoyl chloride (entry 1, **Table 3.2**). The level of carboxyalkanoyl substituent achieved is promising for the use of this cellulose adipate derivative for oral dosage forms in drug delivery, or for water-borne dispersions. For comparison,<sup>11</sup> carboxymethylcellulose acetate butyrate (*Eastman* CMCAB-641-0.2, DS of carboxymethyl = 0.33) can be readily dispersed in aqueous media, and swells at near-neutral pH. CMCAB with that DS carboxyl-containing substituent was also found to provide an excellent matrix for pH-controlled drug release, zero-order drug release, and solubility enhancement. Therefore we anticipate that cellulose adipate alkanooates may be valuable biopolymers for pharmaceutical formulations. Higher DS (adipate) can be achieved, although with some reduction in efficiency; using 3 equiv of monobenzyl adipoyl chloride (entry 2, **Table 3.2**) afforded CAP adipate of DS (adipate) 0.5. Reaction of cellulose

acetate butyrate with 1 equivalent of monobenzyl adipoyl chloride afforded the anticipated cellulose acetate adipate butyrate, with adipate DS 0.25. Reaction of monobenzyl adipoyl chloride with CA-320S, which has less bulky substituents and a higher DS(OH) than CAP-504-0.2 and CAB-553-0.4, afforded the expected product with a higher adipate DS of 0.7. The benzyl ester products and their characteristics are summarized in **Table 3.2**; deprotected cellulose ester adipate properties are summarized in **Table 3.3**.

For amorphous dispersion formulations of drugs in polymer matrices, high polymer glass transition temperature ( $T_g$ ) is an advantage.<sup>43</sup> If the polymer remains in the glassy state, even at high ambient temperatures and at high humidity, then the mobility of the drug molecules is restricted and their crystallization is suppressed. Therefore it was of interest to investigate the thermal properties of our cellulose adipate esters. **Table 3.3** summarizes the results of differential scanning calorimetry<sup>44</sup> studies of the respective adipates, and **Fig. 3.6** displays the DSC traces. All cellulose ester adipates prepared had glass transition temperatures in excess of 90 °C, and the CA and CAP adipates had  $T_g$  well in excess of 120 °C, indicating promise for amorphous dispersion formulations. We also observed low temperature transitions for these cellulose ester adipates, well below ambient temperature, which were not evident in the starting materials. We speculate that these transitions may be due to cooperative motions of the relatively long adipate side chains, similar to those observed by Glasser and co-workers for cellulose long-chain esters.<sup>45</sup>

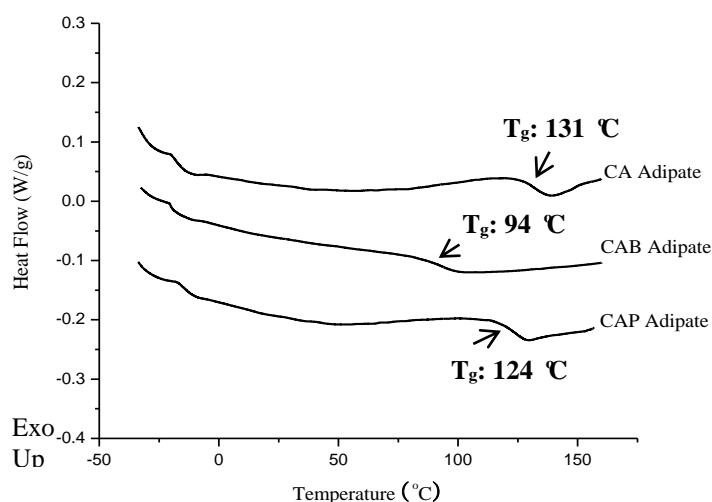


**Figure 3.6** DSC curves of cellulose adipate derivatives at heating rate 10 °C/min (2nd heat)

**Table 3.3** Properties of starting materials and deprotected cellulose ester adipates

starting material data					product data			
Entry	starting material	T <sub>g</sub> <sup>2nd</sup> Heat (°C)	T <sub>m</sub> (°C)	M <sub>n</sub> /10 <sup>3</sup> (SEC) <sup>a</sup>	product	T <sub>g</sub> <sup>2nd</sup> Heat (°C)	M <sub>n</sub> /10 <sup>3</sup> (SEC)	solubility
1	CAP-504-0.2	158	188	15.0	CAP Adipate	-14; 124	10.8	CHCl <sub>3</sub> , NMP, DMSO
2	CAB-553-0.4	100	155	20.0	CAB Adipate	-17; 94	61.0	CHCl <sub>3</sub> , NMP, DMSO
3	CA-320S	180	230- 250	38.0	CA Adipate	-18; 131	<sup>b</sup>	NMP, DMSO

<sup>a</sup>Reported by supplier, versus polystyrene standards. <sup>b</sup>M<sub>n</sub> could not be measured by SEC.

Molecular weight characterization of these cellulose adipate materials was challenging. We first explored size-exclusion chromatography (SEC) in an NMP/LiCl solvent system, but did not observe polymer signals in the column eluent. Some samples showed aggregation by laser light scattering studies in NMP/LiCl solvent, whereas other samples did not. Apparently these cellulose adipates are somewhat prone to aggregation, and have high affinity for the styrene beads of the SEC column. Finally, we found that SEC in DMF containing 0.05 M LiBr was successful for the CAP and CAB adipates; the less soluble CA was still problematic in this system. Generally the M<sub>n</sub> results (**Table 3.3**) obtained indicate no more than moderate chain degradation during the adipate ester preparation, consistent with the relatively mild conditions used.

### 3.5 Conclusions

We have developed a general process for the synthesis of cellulose adipates, with or without other ester groups, by reaction of cellulose in DMAC/LiCl solution, or cellulose esters in MEK solution, with a monofunctional adipate reagent, monobenzyl adipoyl chloride, followed by removal of the benzyl group by mild hydrogenation. We have observed no limitation on the type



of alkanooate group that may be present. In some cases we have achieved high DS of adipate, so there is no apparent limitation on achievable adipate DS. Suitable starting materials include cellulose, and esters of cellulose; ethers and other cellulose derivatives are also likely to be suitable. This process circumvents the cross-linking problems seen when using adipic anhydride, and leads to soluble cellulose (ester) adipate derivatives. We anticipate that these new cellulose derivatives will be useful in aqueous coatings systems, and for controlled release of drugs and other active molecules. Studies of the utility of these cellulose adipate esters in drug delivery are under way.

### 3.6 Supplementary Material

Supplementary information available for this chapter includes  $^1\text{H}$  NMR spectra of our intermediates monobenzyl adipate (**Fig. S3.1**) and monobenzyl adipoyl chloride (**Fig. S3.2**).

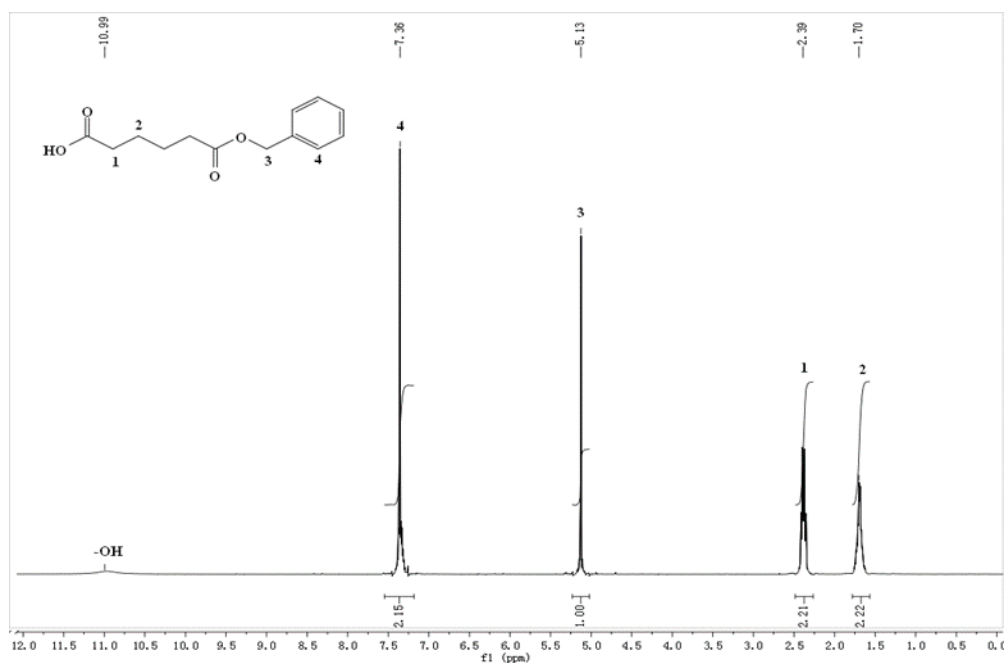


**Figure S3.1**  $^1\text{H}$  NMR spectrum of monobenzyl adipate

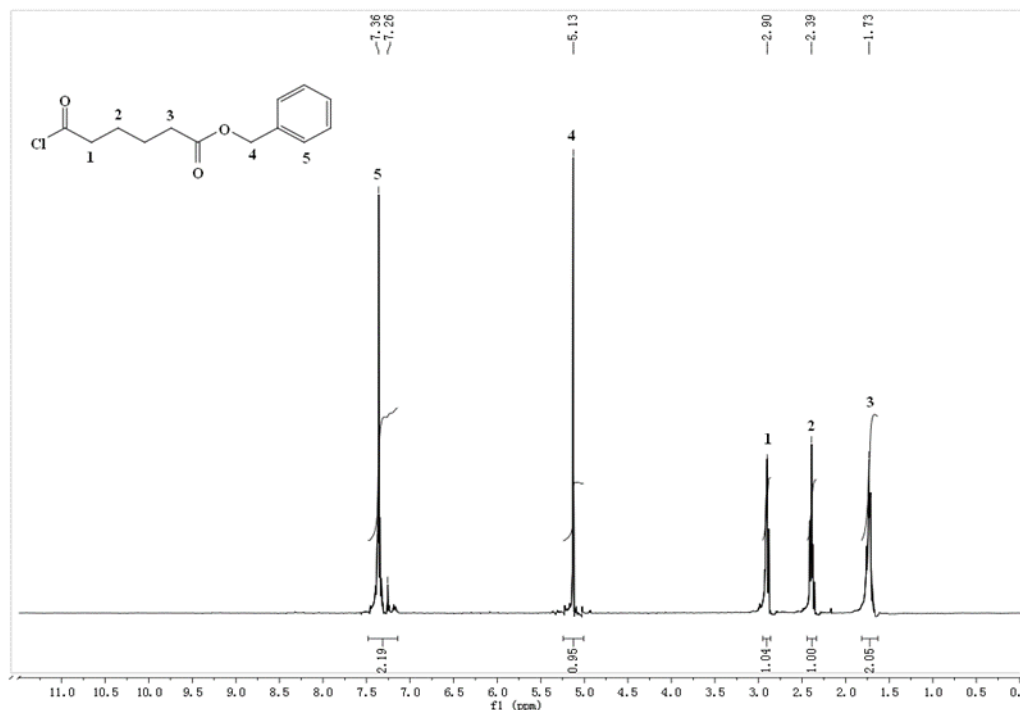


**Figure S3.2** <sup>1</sup>H NMR spectrum of monobenzyl adipoyl chloride

### 3.7 Acknowledgements

The authors thank the Eastman Chemical Company and Rayonier, Inc. for their kind donations of the cellulose ester starting materials, and high-purity hardwood dissolving pulp used in this work, respectively. We thank the National Science Foundation and the US Department of Agriculture for funding this work, and the Macromolecules and Interfaces Institute and the Institute for Critical Technologies and Applied Science at Virginia Tech for their support. We also thank Tianyu Wu of Virginia Tech for performing SEC analyses.

### 3.8 References

1. Buchanan, C. M.; Edgar, K. J.; Hyatt, J. A.; Wilson, A. K., Preparation of cellulose [1-C-13]acetates and determination of monomer composition by NMR spectroscopy. *Macromolecules* **1991**, 24, (11), 3050-3059.
2. Kamitakahara, H.; Nakatsubo, F.; Klemm, D., Block co-oligomers of tri-O-methylated and

unmodified cello-oligosaccharides as model compounds for methylcellulose and its dissolution/gelation behavior. *Cellulose* **2006**, 13, 375-392.

3. Kamitakahara, H.; Koschella, A.; Mikawa, Y.; Nakatsubo, F.; Heinze, T.; Klemm, D., Syntheses and comparison of 2,6-di-O-methyl celluloses from natural and synthetic celluloses. *Macromolecular Bioscience* **2008**, 8, (7), 690-700.
4. Heinze, T.; Koschella, A., Carboxymethyl Ethers of Cellulose and Starch - A Review. *Macromolecular Symposia* **2005**, 223, 13-39.
5. Arisz, P.; Thai, H. T. T.; Boon, J. J.; Salomons, W. G., Changes in substituent distribution patterns during the conversion of cellulose to O-(2-hydroxyethyl)celluloses. *Cellulose* **1996**, 3, 45-61.
6. Rekhi, G. S.; Jambhekar, S. S., Ethylcellulose - A Polymer Review. *Drug Development and Industrial Pharmacy* **1995**, 21, 61-77.
7. Koschella, A.; Fenn, D.; Heinze, T., Water soluble 3-mono-O-ethyl cellulose: synthesis and characterization. *Polymer Bulletin* **2006**, 57, 33-41.
8. Junior, J. A.; Kawano, Y.; Petri, D. F. S., Thin films of carbohydrate based surfactants and carboxymethylcellulose acetate butyrate mixtures: Morphology and thermal behavior. *Materials Science & Engineering C-Biomimetic and Supramolecular Systems* **2009**, 29, (2), 420-425.
9. Edgar, K. J., Cellulose esters in drug delivery. *Cellulose* **2007**, 14, (1), 49-64.
10. Friesen, D. T.; Shanker, R.; Crew, M.; Smithey, D. T.; Curatolo, W. J.; Nightingale, J. A., Hydroxypropyl methylcellulose acetate succinate-based spray-dried dispersions: an overview. *Mol Pharm* **2008**, 5, (6), 1003-19.
11. Posey-Dowty, J. D.; Watterson, T. L.; Wilson, A. K.; Edgar, K. J.; Shelton, M. C.; Lingerfelt, L. R., Zero-order release formulations using a novel cellulose ester. *Cellulose* **2007**, 14, (1), 73-83.
12. Shelton, M. C.; Posey-Dowty, J. D.; Lingerfelt, L. R.; Kirk, S. K.; Klein, S.; Edgar, K. J., Enhanced dissolution of poorly soluble drugs from solid dispersions in carboxymethylcellulose acetate butyrate matrices. In *Polysaccharide Materials: Performance by Design*, Edgar, K. J.; Heinze, T.; Liebert, T., Eds. American Chemical Society: Washington, D.C., 2009.
13. Alonzo, D. E.; Zhang, G. G.; Zhou, D.; Gao, Y.; Taylor, L. S., Understanding the behavior of amorphous pharmaceutical systems during dissolution. *Pharm Res* **2010**, 27, (4), 608-18.
14. Konno, H.; Taylor, L. S., Influence of different polymers on the crystallization tendency of molecularly dispersed amorphous felodipine. *J Pharm Sci* **2006**, 95, (12), 2692-705.
15. Konno, H.; Taylor, L. S., Ability of different polymers to inhibit the crystallization of amorphous felodipine in the presence of moisture. *Pharm Res* **2008**, 25, (4), 969-78.
16. Konno, H.; Handa, T.; Alonzo, D. E.; Taylor, L. S., Effect of polymer type on the dissolution profile of amorphous solid dispersions containing felodipine. *Eur J Pharm Biopharm* **2008**, 70, (2), 493-9.
17. Leuner, C.; Dressman, J., Improving drug solubility for oral delivery using solid dispersions. *Eur J Pharm Biopharm* **2000**, 50, (1), 47-60.
18. Klein, C. E.; Chiu, Y. L.; Awni, W.; Zhu, T.; Heuser, R. S.; Doan, T.; Breitenbach, J.; Morris, J. B.; Brun, S. C.; Hanna, G. J., The tablet formulation of lopinavir/ritonavir provides similar bioavailability to the soft-gelatin capsule formulation with less pharmacokinetic variability and diminished food effect. *J Acquir Immune Defic Syndr* **2007**, 44, (4), 401-10.
19. Allen, J. M.; Wilson, A. K.; Lucas, P. L.; Curtis, L. G. Carboxyalkyl Cellulose Esters. 5,668,273, September 16, 1997.
20. Allen, J. M.; Wilson, A. K.; Lucas, P. L.; Curtis, L. G. Process for Preparing Carboxyalkyl Cellulose Esters. 5,792,856, August 11, 1998.
21. Posey-Dowty, J. D.; Wilson, A. K.; Curtis, L. G.; Swan, P. M.; Seo, K. S. Carboxyalkyl Cellulose Esters for Use in Aqueous Pigment Dispersions. 5,994,530, November 30, 1999.
22. Cook, P. M.; Smith, J. V. Cellulose Acetate Phthalate Enteric Coating Compositions. 5,888,550, March 30, 1999.

23. Cook, P. M.; Lambert, J. L. pH-Sensitive Modified Cellulose Ester. 5,925,181, July 20, 1999.
24. Edgar, K. J., Cellulose Esters in Waterborne Coatings. *Polymers Paint and Colour Journal* **1993**, 183, 564-571.
25. Seidel, C.; Kulicke, W.-M.; Hess, C.; Hartmann, B.; Lechner, M. D.; Lazik, W., Influence of the Cross-linking Agent on the Gel Structure of Starch Derivatives. *Starch* **2001**, 53, 305-310.
26. Coma, V.; Sebt, I.; Pardon, P.; Pichavant, F. H.; Deschamps, A., Film Properties from Crosslinking of Cellulosic Derivatives with a Polyfunctional Carboxylic Acid. *Carbohydrate Polymers* **2003**, 51, 265-271.
27. Mitchell, G. R.; Guo, W.; Davis, F. J., Liquid crystal elastomers based upon cellulose derivatives. *Polymer* **1992**, 33, 68-74.
28. Thomas, R., Ein neues Verfahren zur Teilveresterung von Zellulose mit Carbonsauren unter Praxisbedingungen. *Textilveredlung* **1970**, 5, 361-368.
29. Morello, A. P., 3rd; Forbes, N.; Mathiowitz, E., Investigating the effects of surfactants on the size and hydrolytic stability of poly(adipic anhydride) particles. *J Microencapsul* **2007**, 24, (1), 40-56.
30. Carnahan, M. A.; Grinstaff, M. W., Synthesis of Generational Polyester Dendrimers Derived from Glycerol and Succinic or Adipic Acid. *Macromolecules* **2006**, 39, 609-616.
31. Albertsson, A.-C.; Lundmark, S., Synthesis of Poly(Adipic Anhydride) by Use of Ketene. *Journal of Macromolecular Science - Chemistry* **1988**, A25, 247-258.
32. Edgar, K. J.; Arnold, K. M.; Blount, W. W.; Lawniczak, J. E.; Lowman, D. W., Synthesis and Properties of Cellulose Acetoacetates. *Macromolecules* **1995**, 28, (12), 4122-4128.
33. English, A. R.; Girard, D.; Jasys, V. J.; Martingano, R. J.; Kellogg, M. S., Orally Effective Prodrugs of the Beta-Lactamase Inhibitor Sulbactam. *Journal of Medicinal Chemistry* **1990**, 33, 344-347.
34. Abell, A. D.; Morris, K. B.; Litten, J. C., Synthesis and Deprotection of [1-(Ethoxycarbonyl)-4-[(diphenylmethoxy)carbonyl]-1-methyl-2-oxobutyl]triphenylphosphonium Chloride: A Key Intermediate in the Wittig Reaction Between a Cyclic Anhydride and a Stabilized Ylide. *Journal of Organic Chemistry* **1990**, 55, 5217-5221.
35. Dawsey, T. R.; McCormick, C. L., The Lithium Chloride/Dimethylacetamide Solvent for Cellulose: A Literature Review. *Polymer Reviews* **1990**, 30, 405-440.
36. El Seoud, O. A.; Koschella, A.; Fidale, L. C.; Dorn, S.; Heinze, T., Applications of ionic liquids in carbohydrate chemistry: a window of opportunities. *Biomacromolecules* **2007**, 8, (9), 2629-47.
37. McCormick, C. L.; Dawsey, T. R., Preparation of Cellulose Derivatives via Ring-Opening Reactions with Cyclic Reagents in Lithium Chloride/N,N-Dimethylacetamide. *Macromolecules* **1990**, 23, 3606-3610.
38. Ron, E.; Turek, T.; Mathiowitz, E.; Chasin, M.; Hageman, M.; Langer, R., Controlled release of polypeptides from polyanhydrides. *Proc Natl Acad Sci U S A* **1993**, 90, (9), 4176-80.
39. Mathiowitz, E.; Jacob, J. S.; Jong, Y. S.; Carino, G. P.; Chickering, D. E.; Chaturvedi, P.; Santos, C. A.; Vijayaraghavan, K.; Montgomery, S.; Bassett, M.; Morrell, C., Biologically erodable microspheres as potential oral drug delivery systems. *Nature* **1997**, 386, (6623), 410-4.
40. Albertsson, A. C.; Carlfors, J.; Stureson, C., Preparation and characterisation of Poly(adipic anhydride) Microspheres for Ocular Drug Delivery. *Journal of Applied Polymer Science* **1996**, 62, 695-705.
41. Nakatsubo, F.; Kamitakahara, H.; Hori, M., Cationic Ring-Opening Polymerization of 3,6-Di-O-benzyl-alpha-D-glucose 1,2,4-Orthopivalate and the First Chemical Synthesis of Cellulose. *Journal of the American Chemical Society* **1996**, 118, 1677-1681.
42. Kamitakahara, H.; Nakatsubo, F.; Klemm, D., New Class of Carbohydrate-based Nonionic Surfactants: Diblock Co-oligomers of Tri-O-methylated and Unmodified Cello-oligosaccharides. *Cellulose* **2007**, 14, 513-528.
43. Weuts, I.; Van Dycke, F.; Voorspoels, J.; De Cort, S.; Stokbroekx, S.; Leemans, R.; Brewster, M. E.; Xu, D.; Segmuller, B.; Turner, Y. T.; Roberts, C. J.; Davies, M. C.; Qi, S.; Craig, D. Q.; Reading, M., Physicochemical properties of the amorphous drug, cast films, and spray dried powders to predict formulation probability of success for solid dispersions: etravirine. *J Pharm Sci* **2011**, 100, (1), 260-74.

44. Bindschedler, L. V.; Tuerck, J.; Maunders, M.; Ruel, K.; Petit-Conil, M.; Danoun, S.; Boudet, A. M.; Joseleau, J. P.; Bolwell, G. P., Modification of hemicellulose content by antisense down-regulation of UDP-glucuronate decarboxylase in tobacco and its consequences for cellulose extractability. *Phytochemistry* **2007**, 68, (21), 2635-2648.
45. Sealey, J. E.; Samaranayake, G.; Todd, J. G.; Glasser, W. G., Novel Cellulose Derivatives. IV. Preparation and Thermal Analysis of Waxy Esters of Cellulose. *J Polymer Science: Part B: Polymer Physics* **1996**, 34, 1613-1620.

# CHAPTER 4 DIRECT SYNTHESIS OF CELLULOSE ADIPATE DERIVATIVES USING ADIPIC ANHYDRIDE

Adapted with the permission from: Liu, H.; Kar, N.; Edgar, K. J. *Cellulose*, **2012**, 19:1279–1293. Copyright 2012 Springer Science and Business Media.

## 4.1 Abstract

The poor aqueous solubility of many drugs can be overcome by formulation as amorphous solid dispersions (ASD) in cellulosic-based polymer matrices. Cellulose esters containing adipates and other ester groups have shown great promise as new ASD polymers. Previous attempts to synthesize these cellulose adipate esters by direct reaction of cellulose derivatives with adipic anhydride failed due to crosslinking and gelation, caused by formation of poly(adipic anhydride) and subsequent reaction of the poly(anhydride) with cellulosic hydroxyls. In order to develop direct, efficient syntheses of these pH-sensitive cellulose adipate derivatives, we have developed new synthetic procedures that cleanly afford soluble ester products by direct condensation with adipic anhydride, that show no evidence of crosslinking. A series of cellulose ester adipates has been synthesized by this direct route, containing substantial adipate DS (up to 0.53). This new method requires no complex solvents or protective groups, and is an effective and versatile route to these useful materials.

## 4.2 Introduction

Cellulose derivatives that are inherently hydrophobic but are also designed to be pH-responsive are of significant current interest for functional applications, including water-borne coatings and drug delivery systems. In pharmaceutical applications, hydrophobic cellulose derivatives are very useful because of their low toxicity, their miscibility with hydrophobic drugs, and their slow release characteristics. The added feature of pH responsiveness permits release targeted to the small intestine (the primary organ for absorption of nutrients and drugs from the

gastrointestinal (GI) tract into the circulation), and minimization of interaction between drug and stomach (for cases where the drug is prone to decomposition in the environment of the stomach, or may cause stomach irritation).<sup>1</sup>

Synthesis of cellulose derivatives containing pendent carboxyl groups is challenging, with only a few existing useful methods. Synthesis of carboxymethylcellulose (CMC) is straightforward, because it can be carried out under anionic conditions using chloroacetic acid as the carboxyl synthon. Esterified derivatives of CMC with acetic, propionic or butyric moieties have been synthesized and are of interest for both coatings and ASD drug delivery applications.<sup>2-3</sup> However, the acid-catalyzed attachment of hydrophobic ester groups to the remaining hydroxyls of CMC<sup>4,5</sup> may cause crosslinking by ester formation between carboxymethyl and residual OH groups. Oxidation of residual free 6-OH groups of a partially esterified cellulose derivative to carboxyls is another recently explored option;<sup>6,7</sup> however the products are uronic acids, and the instability of uronic acids with respect to molecular weight loss is well-known and would be of concern in some usage situations.<sup>8</sup> Synthesis of carboxyl-containing cellulose derivatives by ring-opening of cyclic anhydrides is well-known and commercially successful, for 5- and 6-membered anhydrides. Important examples include the synthesis of cellulose acetate phthalate (CAPHth) by base-catalyzed reaction of cellulose acetate with phthalic anhydride, and the synthesis of cellulose succinates by the ring-opening reaction of cellulose or cellulose esters with succinic anhydride in the presence of an organic base catalyst, or even without a catalyst.<sup>9-11</sup> CAPHth has been known for over 70 years.<sup>12</sup> Although it is frequently used in pharmaceutical applications as a pH-controlled release coating, and also for amorphous dispersions,<sup>13</sup> CAPHth has limited miscibility with organic materials. Pendent carboxyls attached to cellulose by ester linkages can be prone to relatively rapid, autocatalyzed hydrolysis in cases like succinate where a favorable ring size intermediate (5 or 6) is accessible,<sup>14</sup> which may be problematic for polymers meant to perform in aqueous media.

Recently there has been strong interest in methods for solubility enhancement of drugs, because of the high proportion of new and existing drugs and drug candidates with poor aqueous solubility (estimated as high as 40-70%).<sup>15</sup> One of the most promising methods for solubility enhancement (and for the numerous drugs belonging to Biopharmaceutical Classification System

(BCS) Class 2, bioavailability enhancement) is that of amorphous solid dispersion (ASD). In this approach the drug molecule is distributed throughout a polymer matrix, with drug domain size approaching that of a single molecule, eliminating drug crystal lattice energy as a barrier to drug dissolution.<sup>16</sup> Elimination of this energy barrier can afford strong solubility enhancement and the simplicity of formulation (e.g., spray-drying from an organic solution of drug and polymer, or co-extrusion) makes this approach very attractive.<sup>17, 18</sup> Polysaccharide derivatives are well-suited as the continuous matrix polymers for ASDs, since they have high glass transition temperatures, tend to be non-toxic, are not absorbed from the GI tract, and can be modified so as to enhance polymer-drug miscibility.<sup>19</sup> Carboxylated polysaccharides are especially useful since the polar carboxyl groups also provide energetically favorable specific interactions by hydrogen-bonding with the drug molecule.<sup>20</sup> To date the polymers commonly used for this purpose have been selected from those already used in pharmaceutical formulations. For example, hydroxypropylmethylcellulose acetate succinate (HPMCAS) has proved quite valuable for ASDs,<sup>19, 21</sup> as has poly(vinylpyrrolidone) (for drugs whose isolation from the stomach is not a major issue).

Our hypothesis has been that rational design of a polysaccharide derivative for use in ASD systems could provide a polymer with superior performance characteristics. There are three critical things that an effective ASD polymer has to do: 1) stabilize the drug against crystallization in the solid phase; 2) stabilize the drug against crystallization from aqueous solution, during the time period between drug release and drug absorption into the enterocytes; 3) release the drug at a sufficient rate to enable the dose to be efficiently absorbed. Recently we prepared a series of novel cellulose adipate esters. It was reasoned that the tetramethylene chain of the adipate group, in combination with additional hydrophobic ester or ether substituents, would provide the desired hydrophobicity to enhance miscibility with hydrophobic drugs and to provide slow release. The pendent adipate carboxyl would provide pH sensitivity, enabling stable dispersion and pH responsive release. The adipate group was selected vs. other possible  $\omega$ -carboxy cellulose esters since it is the shortest chain possible that would provide an unfavorable transition state (7-membered ring in this case) for autocatalysis of the ester linkage, promoting good hydrolytic stability. Synthesis of pure, well-characterized cellulose adipates had to our knowledge been unknown in the literature, prior to our recent work;<sup>22</sup> the only pertinent prior reports dealt with reaction of cellulose fibers and surfaces with adipic acid to cross-link and modify textile



properties.<sup>23, 24</sup> Kar and co-workers reported that a direct approach to the synthesis of cellulose adipate esters, by reaction of cellulose or cellulose esters in solution with adipic anhydride, was plagued by problems of rapid gelation. Their investigation showed that gelation was a result of crosslinking by means of reaction of two or more cellulosic chains with each molecule of poly(adipic anhydride) impurity; it was found that this impurity was present in adipic anhydride either purchased or synthesized by literature methods, and that the percentage of the homopolymeric impurity increased upon storage even at low temperatures. They circumvented crosslinking by transforming adipic acid to a monoprotected, monofunctional reagent. This was synthesized by benzylation of one carboxyl and conversion of the other carboxyl to an acid chloride.<sup>25, 26</sup> Reaction of cellulose esters such as cellulose acetate propionate with this reagent afforded benzyl-protected cellulose adipate derivatives. Hydrogenation of these benzyl esters to free adipates was successful using palladium catalysis at atmospheric pressure. In spite of the less direct pathway, this method proved to be a versatile route to cellulose adipate derivatives for structure-property studies. This paper will describe successful efforts to overcome the earlier crosslinking issues and develop a direct, efficient route to these promising cellulose adipate materials by reaction with adipic anhydride.

## 4.3 Experimental Section

### 4.3.1 Materials

Microcrystalline cellulose (MCC, Avicel PH-101, Fluka) was dried under reduced pressure at 50 °C overnight prior to use. Cellulose acetate propionate (CAP-504-0.2), cellulose acetate butyrate (CAB-553-0.4) and cellulose acetate (CA 320S and CA-398-30) were from Eastman Chemical Co and vacuum dried at 50 °C overnight. Adipic acid (99%, Acros Organics) was recrystallized from ethanol and vacuum dried. Methyl ethyl ketone (MEK, Fisher Scientific) was dried by refluxing over potassium carbonate for 3 hours before using. *N,N*-dimethylacetamide (DMAc, Fisher Scientific) and 1,3-dimethyl-2-imidazolidinone (DMI, 98%, Acros Organics) were dried over 4 Å molecular sieves. Commercial adipic anhydride (Wako Chemical, Ltd.), acetic anhydride (99+%, Acros Organics), zinc acetate dihydrate (Fisher Scientific) and lithium chloride (LiCl, Fisher Scientific) were used as received.

### 4.3.2 Characterization

**NMR Spectroscopy.**  $^1\text{H}$  NMR spectra were acquired on an INOVA 400 spectrometer operating at 400 MHz. Samples were analyzed as solutions in  $\text{CDCl}_3$  or  $\text{DMSO-}d_6$  (ca. 10 mg/mL) at 25 °C in standard 5 mm o.d. tubes. A drop of trifluoroacetic acid was added to shift the water peak of  $\text{DMSO-}d_6$  downfield from the spectral region of interest. 32 scans were obtained for each sample.  $^{13}\text{C}$  NMR spectra were obtained on Bruker Avance 500 MHz spectrometer with a minimum of 5,000 scans in  $\text{DMSO-}d_6$  (ca. 50 mg/mL) at 80 °C. Solid state CP/MAS  $^{13}\text{C}$  NMR was recorded with a Bruker Avance II 300 instrument using 2048 scans at frequency of 75.468 MHz and 27 °C.

**IR Analysis.** Dried samples (5 mg) were finely dispersed in 200 mg of KBr and pressed. The IR spectra were obtained with a Nicolet 8700 FT-IR spectrometer with  $\text{N}_2$  purge in transmission mode. 64 scans were obtained for each spectrum.

**Differential Scanning Calorimetry.** DSC was performed on a TA Instruments Q2000 apparatus. Dry powders (2-5 mg) were loaded in Tzero™ aluminum hermetic pans. Samples were equilibrated at 25 °C. Each run consisted of a 10 °C/min heating ramp to 200°C, followed by a 20 °C/min cooling ramp back to -50 °C, and then a second heating ramp at 10 °C/min to 160 °C. All tests were performed in triplicate and the thermal transitions were recorded from the second heating cycle.

**Size Exclusion Chromatography (SEC).** The DMF SEC system was equipped with a Waters 717 plus autosampler, a Waters 1525 HPLC 155 pump, and two Waters Styragel HR5E columns. The column effluent was monitored using a Waters 2414 156 differential refractive index detector. The sample concentrations in DMF/0.05M LiBr were ca. 1-1.5 mg/mL. The collected data provided number average molecular weights relative to polystyrene.

**Solubility Testing.** Dried sample (~10mg) was added to a 10 mL glass vial, then 2-3 mL of solvent was added. The mixture was subjected to vortex mixing for 5-10 min (moderate heating was applied); then, solubility at room temperature was determined by visual examination.

### 4.3.3 Synthesis of cellulose adipates esters

**Reaction of Cellulose in DMAc/LiCl Solution with Commercial Adipic Anhydride.** MCC (8 g, 49.3 mmol) was completely dissolved in DMAc (300 mL) and LiCl (15 g) by a literature procedure.<sup>27</sup> A pre-mixed solution of commercial adipic anhydride (6.31 g, 49.3 mmol) in DMAC (20 mL) was added dropwise to this solution at 80 °C under nitrogen. After approximately 45 min the solution gelled. The product was isolated by adding the reaction mixture to methanol, filtration of the gel-like material, and then extensive washing of the gel with methanol, then with water. The vacuum-dried product was insoluble in all solvents tried, including DMSO and chloroform. Product analysis was by infrared spectroscopy and solid state <sup>13</sup>C NMR.

Solid-state CP/MAS <sup>13</sup>C NMR: 21.7-24.6 (COCH<sub>2</sub>CH<sub>2</sub> CH<sub>2</sub>CH<sub>2</sub>CO of adipate), 33.8-38.5 (COCH<sub>2</sub>CH<sub>2</sub>CH<sub>2</sub>CH<sub>2</sub>CO of adipate), 62.7 (C-6), 74.8 (C-5,C-2,C-3), 83.1 (C-4), 104.6 (C-1), 173.5 (C=O). IR (cm<sup>-1</sup>): 1812, 1742 (anhydride doublet).

**Preparation of Adipic Anhydride.** Adipic anhydride was synthesized by adapting a previously reported procedure.<sup>28, 29</sup> Adipic acid (15 g, 0.1026 mol) was dissolved in acetic anhydride (150 mL) in a three-neck round bottom flask. The reaction vessel was heated under reflux for 4 h with a continuous nitrogen purge. The by-product acetic acid and the excess acetic anhydride were removed by short path distillation under vacuum.

The residue containing a small amount of acetic anhydride was transferred to a Claisen flask, and the depolymerization catalyst zinc acetate dihydrate (150 mg, 0.68 mmol) was added. The temperature was slowly raised under vacuum (1 mbar). The pure adipic anhydride fraction was collected at 80 to 95°C, and condensed in a flask cooled with an ice bath. Yield: 55%.

<sup>1</sup>H NMR (CDCl<sub>3</sub>, ppm): 2.65 (-CH<sub>2</sub>(CO)-, 4H), 1.89 (-CH<sub>2</sub>-, 4H).

**Procedure for the Reaction of CAP with Adipic Anhydride.** CAP-504-0.2 (1 g, 3.56 mmol) was dissolved in dry solvent (10 mL, MEK or DMI) and the solution was heated to 60 °C or 90 °C with stirring under nitrogen. Freshly synthesized adipic anhydride (0.396 g, 1 eq per free hydroxyl group) was first dissolved in additional dry solvent (3 mL, MEK or DMI) and then added dropwise to the CAP solution. The resulting solution was stirred at 60 °C or 90 °C. At timed intervals, aliquots of the reaction solution were withdrawn and added dropwise to isopropyl alcohol at room

temperature with vigorous stirring. Each precipitate was collected by filtration. Each precipitate was further purified by re-dissolving in acetone, reprecipitating into water, then this precipitate was twice reslurried in hot water (90 °C) for 1 h each time, and each time recovered by filtration in order to remove residual adipic acid and poly(adipic anhydride). The final product was isolated by filtration, and vacuum-dried at 40 °C.

<sup>1</sup>H NMR (DMSO-*d*<sub>6</sub>, ppm): 0.70-1.18 (COCH<sub>2</sub>CH<sub>3</sub> of propionate), 1.35-1.65 (broad s, COCH<sub>2</sub>CH<sub>2</sub>CH<sub>2</sub>CH<sub>2</sub>CO of adipate), 1.85-2.50 (COCH<sub>2</sub>CH<sub>3</sub> of propionate, COCH<sub>3</sub> of acetate and COCH<sub>2</sub>CH<sub>2</sub>CH<sub>2</sub>CH<sub>2</sub>CO of adipate), 3.20-5.30 (cellulose backbone).

<sup>13</sup>C NMR (DMSO- *d*<sub>6</sub>, ppm): 173.8 (C=O of adipate), 172.0-173.2 (C=O of propionate), 101.9, 99.1 (C-1), 75.7 (C-4), 71.6-73.1 (C-2, C-3, C-5), 62.5 (C-6), 33.3 (COCH<sub>2</sub>CH<sub>2</sub>CH<sub>2</sub>CH<sub>2</sub>CO of adipate), 26.7 (COCH<sub>2</sub>CH<sub>3</sub> of propionate), 23.8 (COCH<sub>2</sub>CH<sub>2</sub>CH<sub>2</sub>CH<sub>2</sub>CO of adipate), 8.6 (COCH<sub>2</sub>CH<sub>3</sub> of propionate).

FTIR (KBr pellet method): 3482 cm<sup>-1</sup>, O-H stretching; 2850-3000 cm<sup>-1</sup>, aliphatic C-H stretching; 1738 cm<sup>-1</sup>, ester and carboxylic acid C=O stretching.

A similar procedure was followed for the reactions of CAB-553-0.4 (1 g, 3.26 mmol) with freshly prepared adipic anhydride (0.363 g, 1 eq per free hydroxyl group).

#### **CAAdB Analytical Data:**

<sup>1</sup>H NMR (DMSO-*d*<sub>6</sub>, ppm): 0.57-0.94 (COCH<sub>2</sub>CH<sub>2</sub>CH<sub>3</sub> of butyrate), 1.27-1.66 (COCH<sub>2</sub>CH<sub>2</sub>CH<sub>3</sub> of butyrate, COCH<sub>2</sub>CH<sub>2</sub>CH<sub>2</sub>CH<sub>2</sub>CO of adipate), 1.85-2.50 (COCH<sub>2</sub>CH<sub>2</sub>CH<sub>3</sub> of butyrate, COCH<sub>3</sub> of acetate and COCH<sub>2</sub>CH<sub>2</sub>CH<sub>2</sub>CH<sub>2</sub>CO of adipate), 3.20-5.30 (cellulose backbone).

<sup>13</sup>C NMR (DMSO-*d*<sub>6</sub>, ppm): 173.8 (C=O of adipate), 172.0-173.2 (C=O of butyrate and acetate), 102.2, 99.5 (C-1), 75.5 (C-4), 71.3-72.3 (C-2, C-3, C-5), 62.4 (C-6), 35.2 (COCH<sub>2</sub>CH<sub>2</sub>CH<sub>3</sub> of butyrate), 33.3 (COCH<sub>2</sub>CH<sub>2</sub>CH<sub>2</sub>CH<sub>2</sub>CO of adipate), 23.9 (COCH<sub>2</sub>CH<sub>2</sub>CH<sub>2</sub>CH<sub>2</sub>CO of adipate), 20.3 (COCH<sub>3</sub> of acetate), 17.5 (COCH<sub>2</sub>CH<sub>2</sub>CH<sub>3</sub> of butyrate), 13.2 (COCH<sub>2</sub>CH<sub>2</sub>CH<sub>3</sub> of butyrate).

FTIR (KBr pellet method): 3460 cm<sup>-1</sup>, O-H stretching; 2830-3020 cm<sup>-1</sup>, aliphatic C-H stretching; 1741 cm<sup>-1</sup>, ester and carboxylic acid C=O stretching.

**Procedure for the Reaction of CA-398-30 with Adipic Anhydride.** CA-398-30 (1 g, 3.76 mmol) was dissolved in DMI (20 mL) and the solution was heated to 90 °C with stirring under nitrogen. Then freshly prepared adipic anhydride (0.766 g, 3 eq per free hydroxyl group) was pre-dissolved

in dry DMI (3 mL) and added dropwise. The solution was stirred at 90 °C for 20 h. The reaction mixture was then added to water at room temperature with stirring. The precipitate was collected by filtration and washed with hot water (90 °C). The product was further purified by Soxhlet extraction with isopropyl alcohol for 5 h, isolated by filtration, and finally vacuum-dried overnight at 40 °C.

<sup>1</sup>H NMR (DMSO-*d*<sub>6</sub>, ppm): 1.34-1.59 (COCH<sub>2</sub>CH<sub>2</sub>CH<sub>2</sub>CH<sub>2</sub>CO of adipate), 1.68-2.13 (COCH<sub>3</sub> of acetate), 2.13-2.24 (COCH<sub>2</sub>CH<sub>2</sub>CH<sub>2</sub>CH<sub>2</sub>CO of adipate), 3.20-5.20 (cellulose backbone).

<sup>13</sup>C NMR (DMSO-*d*<sub>6</sub>, ppm): 173.8 (C=O of adipate), 172.0-173.2 (C=O of acetate), 102.2, 99.5 (C-1), 75.5 (C-4), 71.3-72.3 (C-2, C-3, C-5), 62.4 (C-6), 33.3 (COCH<sub>2</sub>CH<sub>2</sub>CH<sub>2</sub>CH<sub>2</sub>CO of adipate), 23.9 (COCH<sub>2</sub>CH<sub>2</sub>CH<sub>2</sub>CH<sub>2</sub>CO of adipate), 20.3 (COCH<sub>3</sub> of acetate).

FTIR (KBr pellet method): 3464 cm<sup>-1</sup>, O-H stretching; 2800-3040 cm<sup>-1</sup>, aliphatic C-H stretching; 1740 cm<sup>-1</sup>, ester and carboxylic acid C=O stretching.

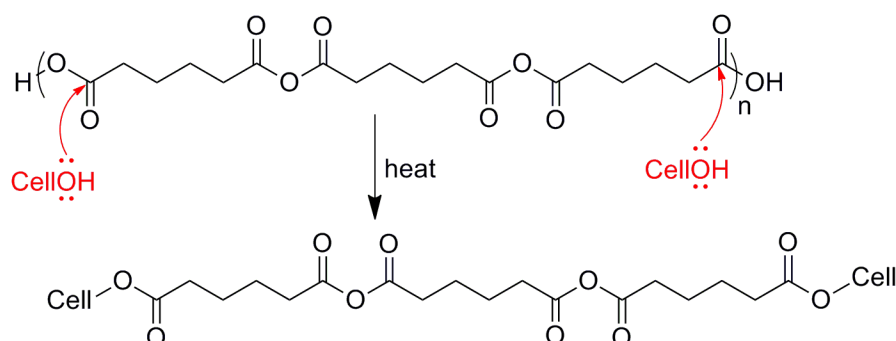
A similar procedure was followed for the reaction of CA-320S (1 g, 4.19 mmol) with freshly prepared adipic anhydride (0.633 g, 1 eq per free hydroxyl group). The reaction medium gelled within 2 h, and the product was not analyzed.

## 4.4 Results and Discussion

### 4.4.1 Crosslinking issue and mechanistic understanding

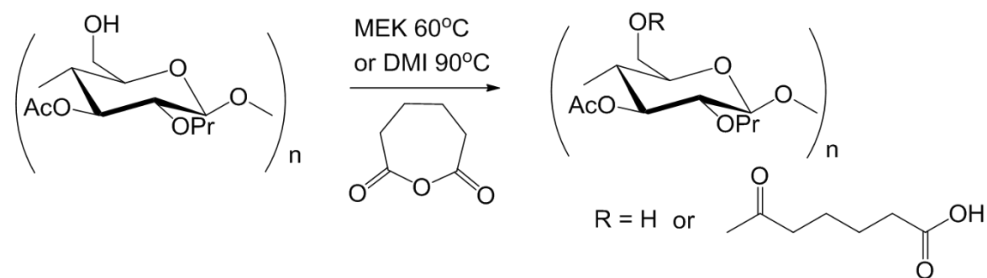
In our previous work, we found that adipic anhydride either purchased or synthesized by literature procedures<sup>30</sup> routinely contained substantial amounts of poly(adipic anhydride) (pAA), and that even freshly prepared adipic anhydride stored at 0 °C continued to homopolymerize. Adipic anhydride and pAA can be quantified by <sup>1</sup>H NMR. pAA has proton resonances at 1.75 and 2.5 ppm, corresponding to -CH<sub>2</sub>CH<sub>2</sub>- and CH<sub>2</sub>-CO-O-CO-CH<sub>2</sub> protons, respectively, while the corresponding adipic anhydride signals appear at 2.0 and 2.8 ppm, respectively. Adipic anhydride from these sources contained 5-15 mole% of pAA, as determined by peak integrations. Using this adipic anhydride containing >5% homopolymer, we observed rapid gelation upon reaction either with cellulose (DMAc/LiCl) or preformed cellulose esters (in MEK, for example). This gelation

was attributed to attack by multiple cellulose hydroxyls on each pAA chain (**Scheme 4.1**). This attribution was supported by solid-state  $^{13}\text{C}$  NMR and IR analysis of the crosslinked product.<sup>22</sup>



**Scheme 4.1** Proposed crosslinking mechanism

Employing this mechanistic understanding, we wished to modify the reaction with adipic anhydride in a rational way to minimize or eliminate crosslinking, so as to create a more efficient and direct route to cellulose adipate derivatives. First, we sought a method to make pAA-free adipic anhydride. Highly pure adipic anhydride was synthesized by adapting a procedure from Albertsson et al.,<sup>28, 29</sup> employing double distillation of the adipic anhydride product. The white oil after double distillation was collected in an ice bath to prevent rapid homopolymerization.  $^1\text{H}$  NMR analysis indicated success; the complete absence of pAA within the limits of  $^1\text{H}$  NMR detection (Supplementary Material, **Fig. S4.1**). We focused initially on using this more highly purified reagent to modify commercially available cellulose esters, since we knew these esters could be reacted with adipic anhydride in neutral organic solvents like MEK (there was concern that the slightly basic solvents, like DMAc, required to dissolve cellulose (higher temperatures needed to overcome high solution viscosity could also be a problem) could cause more rapid homopolymerization of adipic anhydride *in situ*). Adipic anhydride is prone to homopolymerization in the presence of weak bases.<sup>29</sup> Commercial cellulose acetate propionate (CAP-504-0.2), cellulose acetate butyrate (CAB-553-0.4), and cellulose acetate (CA-398-30, CA 320s) afforded lower solution viscosities in neutral solvents and so were our initial focus.



**Scheme 4.2** Reaction of CAP with freshly prepared adipic anhydride

CAP-504-0.2 ( $\text{DS}_{\text{Pr}}$  2.09,  $\text{DS}_{\text{Ac}}$  0.04, determined by  $^1\text{H}$  NMR) was selected for the initial reactions in MEK (**Scheme 4.2**). We were at first discouraged by the fact that we observed gelation after the addition of freshly-prepared adipic anhydride (1 eq or 3 eq/free CAP hydroxyl group) within 80 or 23 minutes, respectively. We knew from our previous study that uncrosslinked cellulose acetate adipate propionates have good organic solubility.<sup>22</sup> The sol fraction was removed by Soxhlet extraction with isopropanol, and the insoluble gel fraction was analyzed by solid-state  $^{13}\text{C}$  NMR. The spectrum showed two adipate methylene peaks at 21-23 and 32-38 ppm, and an adipate carbonyl peak at 168-170 ppm (**Fig. 4.1**). The result was consistent with the hypothesis that cellulose acetate adipate propionate (CAAdP) was formed, but that subsequent crosslinking occurred. This could be the result of adipic anhydride homopolymerization *in situ*, followed by reaction with cellulose. Alternatively, adipic anhydride could react with adipate groups already attached to the cellulose backbone, creating anhydride linkages with which cellulosic hydroxyls could react to form crosslinks (**Scheme 4.3**).

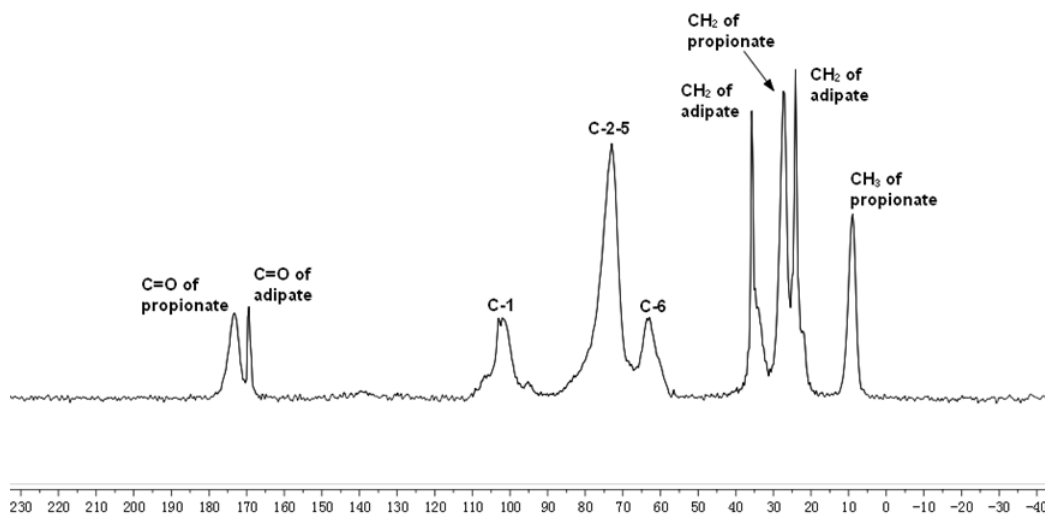
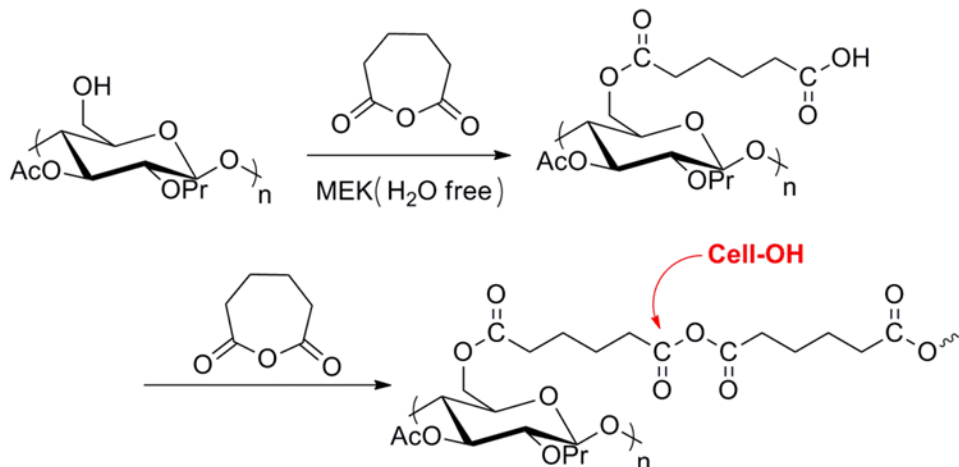


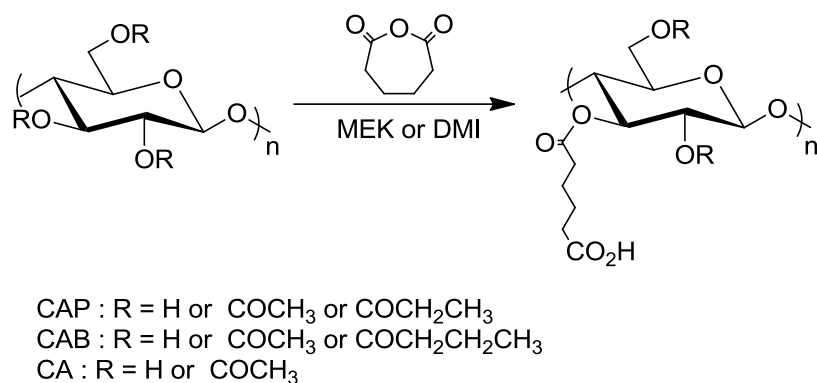
**Figure 4.1** CP/MAS  $^{13}\text{C}$  NMR spectrum of cross-linked CAAdP



**Scheme 4.3** Alternative proposed crosslinking mechanism

It was concluded that even with pure adipic anhydride, thermally-driven homopolymerization still occurred quickly *in situ*, even in neutral solvents, causing the formation of pAA (possibly initiated by cellulose adipate) and concomitant crosslinking of the cellulosic polymer. This competition between ring-opening esterification and anhydride homopolymerization is controlled by unknown variables. We reasoned that dilution of the added adipic anhydride could decrease the homopolymerization rate by decreasing the adipic anhydride concentration at the instant of the drop hitting the hot reaction mixture. We further reasoned that kinetic studies could be useful; since reaction of alcohols with adipic anhydride should be faster than reaction with weaker carboxyl nucleophiles, it could be possible to identify the time to gelation for a particular set of reaction conditions, and use this information to stop the reaction before gelation, to obtain soluble cellulose adipate products. Thus, to obtain organic-soluble cellulose adipate alkanooates applicable to amorphous matrix formulations,<sup>2</sup> the following reactions were monitored and stopped before the onset of gelation (**Scheme 4.4**).





**Scheme 4.4** Reactions of cellulose esters with freshly prepared adipic anhydride

#### 4.4.2 Synthesis of organo-soluble cellulose adipate esters

CAP could be readily dissolved in MEK, and upon the addition of the diluted adipic anhydride (1 eq/free CAP hydroxyl group) solution at 60 °C, the desired condensation took place smoothly and no gelation occurred within the first 5 h. After the work-up to remove by-products, the isolated cellulose acetate adipate propionates (Sample 1-2, **Table 4.1**) are fully soluble in DMSO, acetone, THF, acetic acid and partly soluble in CHCl<sub>3</sub>. <sup>1</sup>H NMR revealed that pAA was in fact generated during the reaction and that the crude isolated product contained pAA (Supplementary Material, **Fig. S4.2**). The products were washed extensively with hot water to remove the co-product pAA,<sup>30,31</sup> and IR and NMR spectra confirmed the absence of pAA in the purified final product. These results indicated that the combination of adipic anhydride purification, reagent dilution, and careful control of reaction duration successfully produced soluble CAAdP, devoid of detectable cross-links. The use of three equivalents of adipic anhydride led to more rapid gelation, predictably; the higher adipic anhydride concentration likely induced more rapid homopolymerization.

It was found in past studies that DMI is an excellent solvent for esterification reactions of cellulose or intermediate cellulose esters at higher temperatures,<sup>32,33</sup> it has advantages vs. DMAc in some cases, being less prone to side reactions.<sup>34</sup> CAP was completely soluble in DMI at elevated temperatures. Therefore, DMI was used as a solvent for this condensation reaction, despite some concerns that, as a slightly alkaline solvent, it might promote adipic anhydride

homopolymerization. In the event, the reaction mixture did not gel over 20 hours at 90 °C, and organo-soluble products could be isolated after timed intervals (Sample 4-7, **Table 4.1**). These results suggested that the higher temperature might be useful in providing ring-opening esterification rates that compete effectively with that of gel formation. Encouraged by these results, we carried out a kinetic study using 3 equiv adipic anhydride per free CAP OH group in DMI (samples 8-10, **Table 4.1**), to see whether higher DS(Ad) values might be accessible in this more powerful solvent. Indeed, increasing DS values were obtained from 1-20 h, with no evidence of gelation even after 20 h. At 20 h, a product was obtained with DS(Ad) 0.53 and total DS 2.62 (Sample 10, **Table 4.1**). Kinetic studies in both MEK and DMI before onset of gelation, by the indication that magnetic bar stopped stirring, are summarized in **Fig. 4.2**. Clearly, DMI was a more effective solvent for obtaining a high DS(Ad) product and for preventing gelation of the reaction mixture.

**Table 4.1** Synthesis of CAP-504-0.2 adipates and full DS information<sup>a</sup>

Sample	Adipic Anhydride (eq.)	Solvent	Temp (°C)	Reaction Time (h)	Degree of Substitution (DS)			
					Ad	Pr	Ac <sup>b</sup>	Total
1	1	MEK	60	2	0.03	2.03	0.04	2.10
2	1	MEK	60	5	0.13	2.03	0.04	2.20
3	3	MEK	60	2	0.16	2.05	0.04	2.25
4	1	DMI	90	2	0.25	2.05	0.04	2.34
5	1	DMI	90	5	0.27	2.05	0.04	2.36
6	1	DMI	90	10	0.30	2.03	0.04	2.37
7	1	DMI	90	20	0.37	2.03	0.04	2.44
8	3	DMI	90	1	0.30	2.10	0.04	2.44
9	3	DMI	90	2	0.39	2.10	0.04	2.53
10	3	DMI	90	20	0.53	2.05	0.04	2.62

<sup>a</sup> Starting material CAP-504-0.2 is commercial cellulose acetate propionate ( $DS_{Pr} = 2.09$ ,  $DS_{Ac} = 0.04$ ).

<sup>b</sup> DS (Ac) is directly adopted from the DS of starting material. It is not determined by NMR, the associated resonance is difficult to pick out in the spectrum due to very low substitution, and the overlap of peaks of acetyl  $CH_3$ , propionyl  $CH_2$  and adipoyl  $CH_2$  with  $DMSO-d_6$  solvent peak (**Fig. 4.3**).

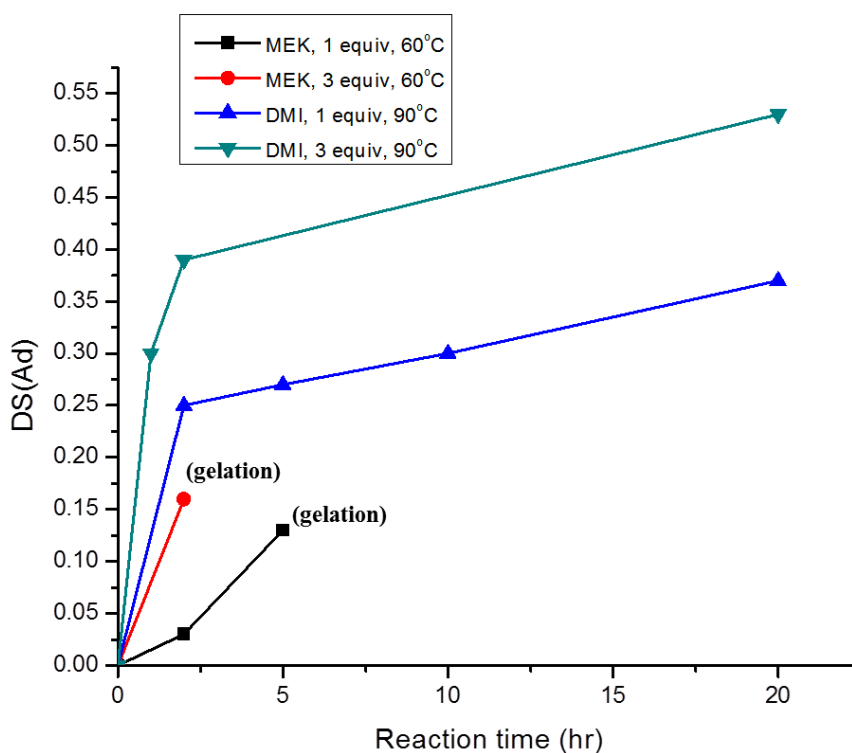


**Figure 4.2** CAAdP DS(Ad) vs. reaction time under different reaction conditions

Formation of the desired CAAdP products was confirmed by  $^1H$  NMR (**Fig. 4.3** and Supplementary Material, **Fig. S4.3**). One of the adipate peaks ( $COCH_2CH_2CH_2CH_2CO$ ) appeared as a broad singlet at  $\sim 1.35$ - $1.65$  ppm. The other adipate peak ( $COCH_2CH_2CH_2CH_2CO$ ) overlapped with the  $COCH_3$  and  $COCH_2CH_3$  peaks from CAP at  $1.85$ - $2.50$  ppm. The absence of anhydride crosslinks was further confirmed by the fact that the CAAdP samples are soluble in a wide range of organic solvents such as acetone, DMSO and THF, while the previously synthesized crosslinked products were insoluble in all common organic solvents. The  $^{13}C$  NMR spectrum for CAAdP

(Sample 7, **Table 4.1**) is shown in **Fig. 4.4**. Three different types of ester group are substituted on the C-6 position, resulting in a broad peak which shifts downfield to 62.5 ppm compared with unmodified cellulose C-6 at ~60.0 ppm. The large peaks at 9 and 27 ppm indicate the presence of a high DS of propionate esters.<sup>35</sup> The low DS of acetate esters ( $DS_{Ac} = 0.04$ ) means that associated resonances are difficult to pick out in the spectrum. The three peaks around 172-173 ppm suggest the random substitution of propionate esters on O-2, 3, and 6 positions. The methylene groups from pendent adipate esters show up as two peaks at 24 and 33 ppm respectively. The carbonyl carbons from adipate groups resonate at 174 ppm. In comparison to the  $^{13}C$  spectrum of CAAdP synthesized in our previous paper, no additional peaks of poly(adipic anhydride) are observed, further confirming the absence of crosslinks.

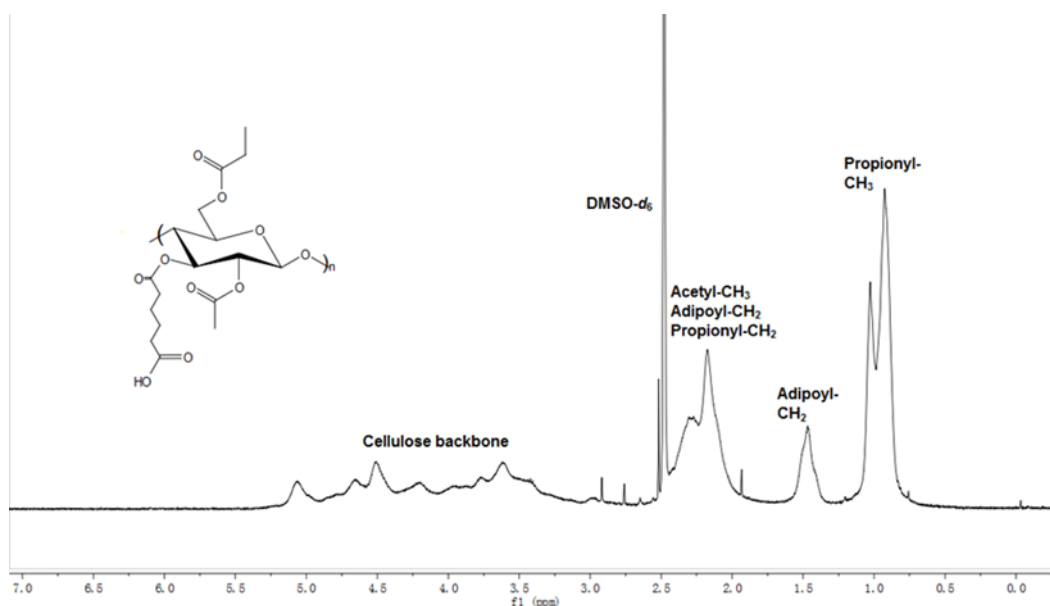


**Figure 4.3**  $^1H$  NMR spectrum of CAAdP (Sample 7, Table 4.1) in  $DMSO-d_6$

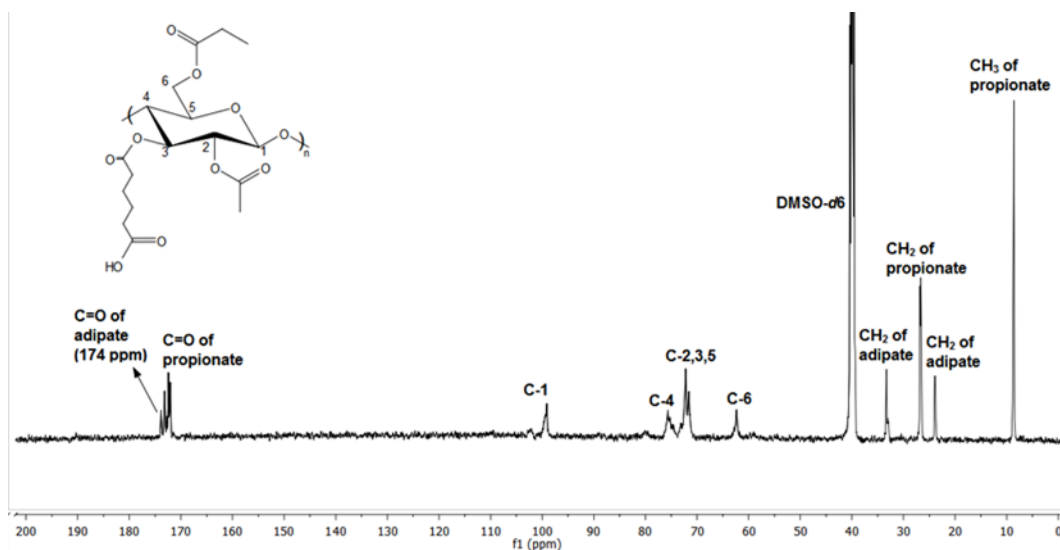


**Figure 4.4**  $^{13}\text{C}$  NMR spectrum of CAAdP (Sample 7, Table 4.1) in  $\text{DMSO-}d_6$

FT-IR spectra of unmodified CAP-504-0.2 and CAAdP (Samples 2 and 7, **Table 4.1**) are displayed in **Fig. 4.5**. The relative peak intensities of characteristic bands are of interest. The carbonyl of the pendent carboxyl group usually gives a peak at  $1712\text{ cm}^{-1}$ , which closely overlaps with the absorption band by carbonyl bonds in esters at  $1750\text{ cm}^{-1}$ .<sup>36</sup> This overlap results in a strong peak centered at  $1738\text{ cm}^{-1}$ . More importantly, the spectra also provide further evidence of the lack of crosslinking. Samples 2 and 7 show no evidence of the characteristic anhydride carbonyl doublet at  $1800\text{ cm}^{-1}$  and  $1740\text{ cm}^{-1}$ .<sup>37</sup>

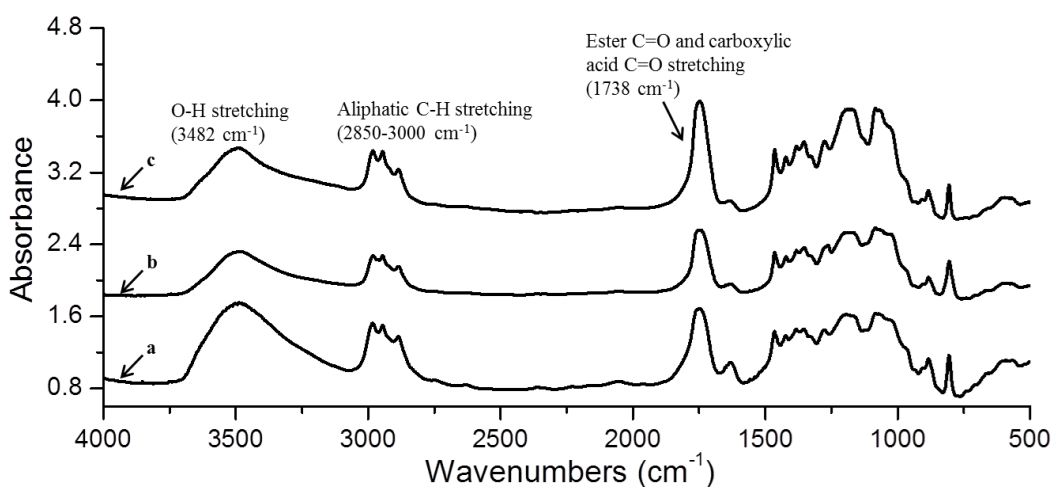


**Figure 4.5** FT-IR spectra of starting material CAP-504-2 (spectrum a), and two lab-synthesized CAAdP samples with lower (spectrum b, sample 2) or higher DSAd (spectrum c, sample 7)

The intensity of peaks at  $\sim 1745\text{ cm}^{-1}$  for ester C=O and carboxylic acid C=O stretching increased with increasing DS of pendent adipate groups. In the O-H stretching region, the band intensity decreased from spectrum a to spectrum c, which coincides with the reduction of hydroxyl DS as adipate substitution increases.

Using pAA-free adipic anhydride and the same dilution protocol, CAB-553-0.4 ( $DS_{Bu} = 1.99$ ,  $DS_{Ac} = 0.14$ ) was reacted in MEK and DMI solvents. Smooth condensation occurred with no gelation observed over the course of 20 hours. The reaction was faster at  $90\text{ }^{\circ}\text{C}$  in DMI, reaching completion within 5 h. Cellulose acetate adipate butyrates (CAADB) of similar DS were obtained in the two solvents. Moreover, the CAADB (Sample 11-16, **Table 4.2**) products were readily soluble in many organic solvents. Proton,  $^{13}\text{C}$  and FTIR spectra all supported the lack of poly(anhydride) crosslinks.

**Table 4.2** Synthesis of CAB-553-0.4 adipates and full DS information<sup>a</sup>

Sample	Adipic Anhydride (eq.)	Solvent	Temp ( $^{\circ}\text{C}$ )	Reaction Time (h)	Degree of Substitution (DS)			
					Ad	Bu	Ac <sup>b</sup>	Total
11	1	MEK	60	5	0.02	1.99	0.14	2.15
12	1	MEK	60	10	0.13	1.99	0.14	2.26
13	1	MEK	60	20	0.13	1.96	0.14	2.23
14	1	DMI	90	5	0.14	1.99	0.14	2.27
15	1	DMI	90	10	0.14	1.96	0.14	2.24
16	1	DMI	90	20	0.14	1.96	0.14	2.24

<sup>a</sup> Starting material CAB-553-0.4 is commercial cellulose acetate butyrate ( $DS_{Bu} = 1.99$ ,  $DS_{Ac} = 0.14$ ).

<sup>b</sup> DS (Ac) is directly adopt from the DS of starting material. It is not determined by NMR, the associated resonance is difficult to pick out in the spectrum due to very low substitution, and the overlap of peaks of acetyl  $\text{CH}_3$ , propionyl  $\text{CH}_2$  and adipoyl  $\text{CH}_2$  with  $\text{DMSO-}d_6$  solvent peak.

To enable further tailoring of the hydrophobic/hydrophilic balance of the cellulose adipate esters, reaction of less hydrophobic cellulose acetates (CA) with adipic anhydride was also investigated. Even though CAs have a much narrower range of organic solubility than CAPs and CABs, the polar aprotic solvent DMI proved to be good medium for reaction with adipic anhydride in solution. Condensation of CA-398-30 (DS(Ac) 2.5) with excess adipic anhydride (3 eq.) in DMI at 90 °C was achieved in 20 hours without gelation, affording a DS (Ad) of 0.28 and a total DS of 2.75. We did not find conditions for obtaining cellulose adipate alkanooates of total DS 3.0 by condensation with adipic anhydride, perhaps due to suboptimal reactivity of the cyclic anhydride in the absence of a catalyst. The formation of the CA-398-30 adipate was confirmed by <sup>1</sup>H NMR (**Fig. 4.6**). Product structure and the absence of poly(anhydride) crosslinks were supported also by FTIR and <sup>13</sup>C spectra.

Surprisingly, even using only 1 eq of adipic anhydride per hydroxyl group, reaction with lower DS cellulose acetate (CA 320S, DS(Ac) 1.82) proved unsuccessful (Sample 18, **Table 4.3**), despite the fact that this CA possesses a higher DS (OH) per AHG. The reaction mixture formed a transparent gel within one hour. This negative result could be a consequence of the fact that the higher DS (OH) means that at a given number of equivalents of adipic anhydride per OH group, the solution concentration of adipic anhydride is greater for CA 320S than with the other cellulose esters investigated. Pursuing this hypothesis, we found that by reducing the amount of adipic anhydride to 0.5 eq per OH group (and thus reducing the adipic anhydride solution concentration in the reaction mixture), the crosslinking problem could be avoided and organo-soluble CAAd was obtained with DS (Ad) 0.27. It is noteworthy that when using CA with higher DS (Ac) (CA-398-30, DS(Ac) 2.47, DS(OH) 0.53), a larger excess of adipic anhydride (3 eq.) was required to achieve a similar adipate DS (compare samples 17 and 19, **Table 4.3**).

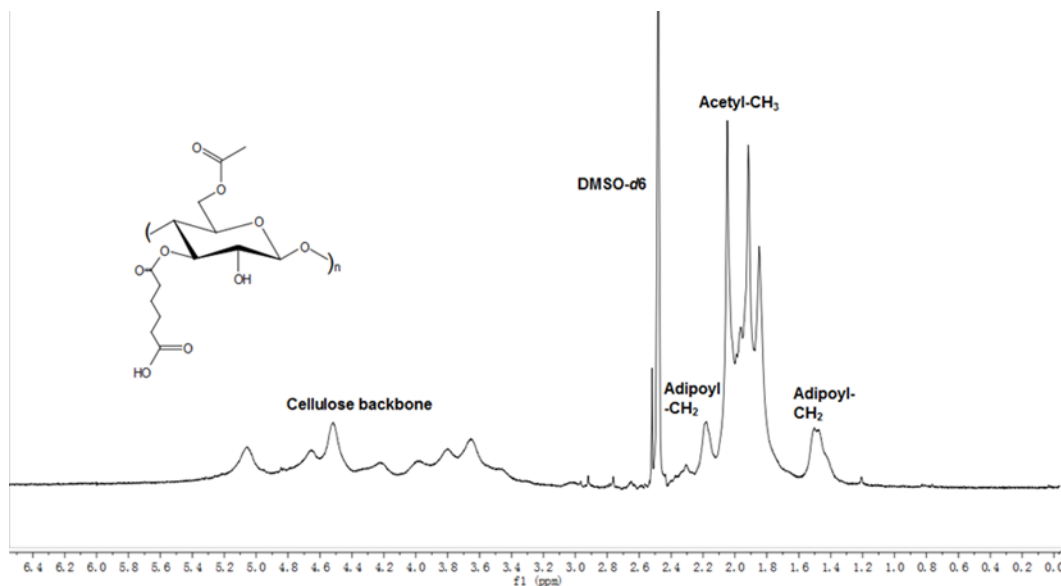
**Table 4.3** Synthesis of CA adipates and full DS information<sup>a,b</sup>

Sample	Cellulose Ester	Adipic Anhydride (eq.)	Solvent	Temp ( °C)	Reaction Time (h)	DS		
						Ad	Other	Total
17	CA-398-30	3	DMI	90	20	0.28	Ac 2.47	2.75
18	CA 320S *	1	DMI	90	<2	n.d.	Ac 1.82	n.d.
19	CA 320S	0.5	DMI	90	20	0.27	Ac 1.82	2.09

n.d. – not determined

<sup>a</sup> Starting material CA-398-30 is commercial cellulose acetate ( $DS_{Ac} = 2.47$ ).

<sup>b</sup> Starting material CA 320S is commercial cellulose acetate ( $DS_{Ac} = 1.82$ ).

**Figure 4.6** <sup>1</sup>H NMR spectrum of CA-398-30 adipate (Sample 17, Table 4.3) in DMSO-d<sub>6</sub>

Overall, reactions of cellulose esters with adipic anhydride proceeded smoothly under the new reaction conditions, avoiding measurable crosslinking and affording soluble products. The DS(Ad) was in each case moderate, and short of the theoretical amount possible given the DS(OH)



of the starting cellulose ester, despite the presence of adequate to excess adipic anhydride in every case. This could be in part due to reaction with water; all reagents were dried prior to use but certainly some adventitious water may have been present. Another limiting factor could be siphoning off of adipic anhydride into pAA, which was then reacted and removed from the product by the hot water extraction. We consider it likely that this played some role.<sup>38,39</sup> Further refinement of solvent and temperature conditions may make it possible to prepare higher DS(Ad) derivatives. Even so, the products with DS(Ad) ranging from 0.25 to 0.37 achieved by the reaction between CAP-504-0.2 and 1 eq of adipic anhydride in DMI at 90 °C over 20 hours promise to be quite useful. Comparison with other carboxyl-containing cellulose derivatives is instructive; a DS of carboxymethyl of approximately 0.33 was adequate to confer both water-dispersibility and favorable ASD characteristics upon carboxymethylcellulose acetate butyrate<sup>2</sup>, while DS(succinate) of 0.38 was adequate to confer water dispersibility upon cellulose acetate butyrate succinate, allowing it to form stable aqueous dispersions useful for automotive waterborne basecoat coating formulations.<sup>40</sup> Therefore the DS(Ad) achieved herein is promising for applications like industrial water-based dispersion coatings and ASDs for oral drug delivery. Indeed, we have observed excellent ASD performance by CAAdP with DS(Ad) of 0.3.<sup>41</sup> While it is important not to draw overly broad conclusions based on the current data, which pertains only to adipic anhydride reaction with the limited range of commercial esters, it appears that the achievable DS may also depend on steric hindrance caused by the other ester groups. The achievable DS(Ad) with CABs and their larger ester substituents has not exceeded 0.15 (**Table 4.2**). With the less hindered acetates of CA-398-30, total DS of 2.75 was attainable (vs. maximum of 2.66 for CAAdP derivatives and 2.27 for CAAdB). It was also notable that long-chain adipate substitution had a generally mildly positive impact on organic solubility; for example, CAAdP became more soluble in CHCl<sub>3</sub> than starting CAP-504-0.2, while CAAdB acquired enhanced ethanol solubility vs. the starting CAB-553-0.4 as a result of the adipate substitution (**Table 4.4**).

**Table 4.4** Solubility of starting cellulose esters and cellulose adipate esters

Ester (DS(Ad))	Solubility								
	DMK	ACN	CHCl <sub>3</sub>	DMSO	EtOAc	EtOH	MeOH	THF	Tol
CAP-504-0.2	+	+	-	+	+	*	+	+	-
CAAdP (0.37)	+	+	<b>S</b>	+	+	*	+	+	-
CAAdP (0.53)	+	+	+	+	+	*	+	+	-
CAB-553-0.4	+	+	+	+	+	*	+	+	-
CAAdB (0.14)	+	+	+	+	+	+	+	+	<b>S</b>
CA-398-30	+	+	-	+	<b>S</b>	-	-	+	-
CAAd <sup>1</sup> (0.28)	+	+	-	+	+	-	-	+	-
CA-320 S	-	-	-	+	-	-	-	-	-
CAAd <sup>2</sup> (0.27)	-	-	-	+	-	-	-	<b>S</b>	-

Solvent abbreviations: DMK-acetone, ACN-acetonitrile, DMSO-dimethylsulfoxide, EtOAc-ethyl acetate, THF-tetrahydrofuran, MeOH-methanol, EtOH-ethanol, Tol-toluene

+ Soluble; - Insoluble; S Swells; \* insoluble at room temperature, becomes soluble when heat is applied. <sup>1</sup>Prepared from CA-398-30. <sup>2</sup>Prepared from CA 320S

#### 4.4.3. Property evaluation of cellulose adipate esters

In designing polysaccharide derivatives for use in ASDs, one important polymer characteristic is glass transition temperature; high T<sub>g</sub> can prevent premature drug crystallization from the solid phase under conditions of high ambient humidity and temperature.<sup>19, 42</sup> High T<sub>g</sub> is

also useful in coatings applications, since it aids in faster hardening of coatings films as solvent evaporates.<sup>40</sup> For these reasons it was important to assess the impact of adipate substitution on cellulose ester  $T_g$ . **Fig. 4.7** shows the DSC second heating curves for the cellulose adipate ester of each type with the highest DS value. All starting esters are amorphous and the adipate products remain so, as expected. Glass transition values of the synthesized cellulose adipate esters are ~30-50 °C lower than those of the corresponding starting cellulose esters (**Table 4.5**). This is presumably a plasticization effect of incorporation of the adipate tetramethylene chain, increasing the spacing between cellulose chains, which, in turn, enhances chain mobility leading to a decrease in  $T_g$ .<sup>43</sup> Even so, all cellulose adipate alkanooates possess  $T_g$  values above 100 °C. The moderate DS(Ad) demonstrated by this direct route may be adequate for introduction of desired thermal, solubility, compatibility, dispersibility and release properties.

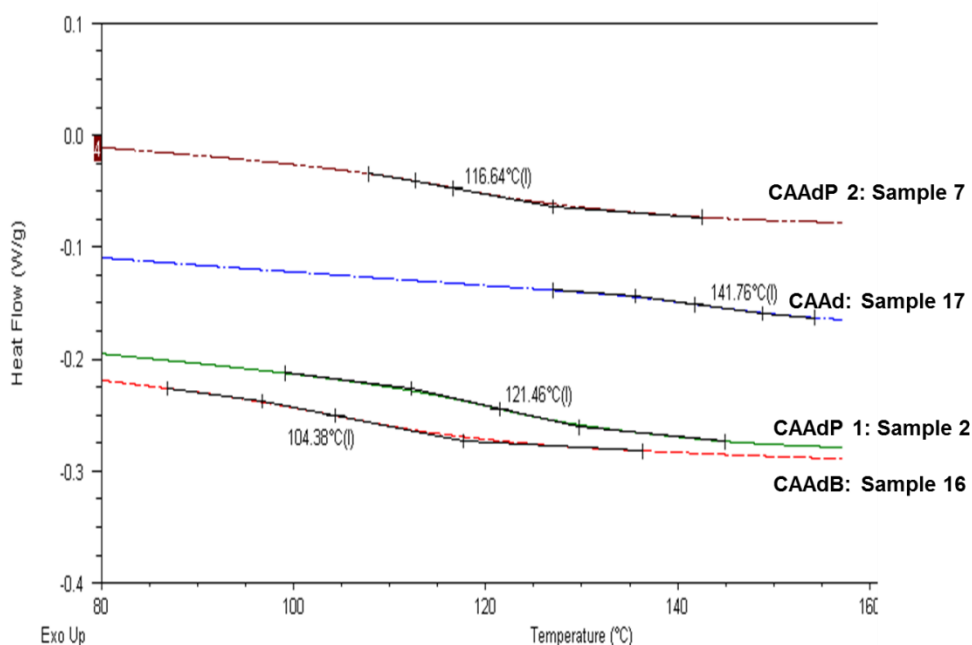


**Figure 4.7** DSC thermograms (2nd heating scan) of cellulose adipate mixed esters

**Table 4.5** Properties of starting materials and cellulose adipate mixed esters

Cellulose Ester	T <sub>g</sub> (°C)	M <sub>n</sub> (*10 <sup>3</sup> )	DP	Products	T <sub>g</sub> (°C) <sup>a</sup>	M <sub>n</sub> (*10 <sup>3</sup> ) <sup>b</sup>	DP
CAP-504-0.2	159	15.0	53	<b>2</b> ; DS(Ad) 0.13	121	n.d.	n.d.
CAP-504-0.2	159	15.0	53	<b>7</b> ; DS(Ad) 0.37	117	12.0	37
CAB-553-0.4	136	20.0	65	<b>16</b> ; DS(Ad) 0.14	104	18.3	56
CA-398-30	189	50.0	188	<b>17</b> ; DS(Ad) 0.28	142	20.5	68

<sup>a</sup> Determined by DSC

<sup>b</sup> Determined by SEC. The molecular weight of product 2 CAAdP was not determined.

Number-average molecular weights of selected cellulose adipate alkanooate products (Sample 7, 16, and 17) ranged between 12.0k and 20.5k (DP 37-68) by SEC. Comparing to the DP values of starting materials (also by SEC), the data indicate some apparent cellulose chain degradation during reaction with adipic anhydride at relatively high temperature (90 °C), particularly in the case of CAAd.

## 4.5 Conclusion

We have developed a one-pot process for the synthesis of cellulose adipate alkanooates, by reaction of preformed cellulose esters in MEK or DMI solution with freshly prepared adipic anhydride. Critical process factors included the use of redistilled adipic anhydride, since poly(adipic anhydride), a universal contaminant in crude or aged adipic anhydride, resulted in cross-linked cellulose adipates. Dilution of the added adipic anhydride with solvent and careful kinetic studies to identify, and avoid, the onset of gelation are other essential elements to synthesis of a soluble cellulose adipate alkanooate that is not crosslinked. The absence of crosslinks is confirmed both by spectroscopic analysis and product solubility. In fact, the cellulose adipate alkanooates synthesized using this procedure exhibit slightly enhanced organic solubility compared with their precursor cellulose esters. They have glass transition temperatures that, while reduced 30-50 °C in comparison with those of their precursor cellulose esters, nonetheless exceed 100 °C

for all derivatives made in this work. The use of these derivatives as polymeric matrices in amorphous solid dispersions is under active investigation in ongoing collaborative work.

## 4.6 Supplementary Material

Supplementary information available for this chapter includes  $^1\text{H}$  NMR spectra of pure adipic anhydride (**Fig. S4.1**), CAAAdP sample 3 prior to and after hot water washing (**Fig. S4.2** and **Fig. S4.3**).

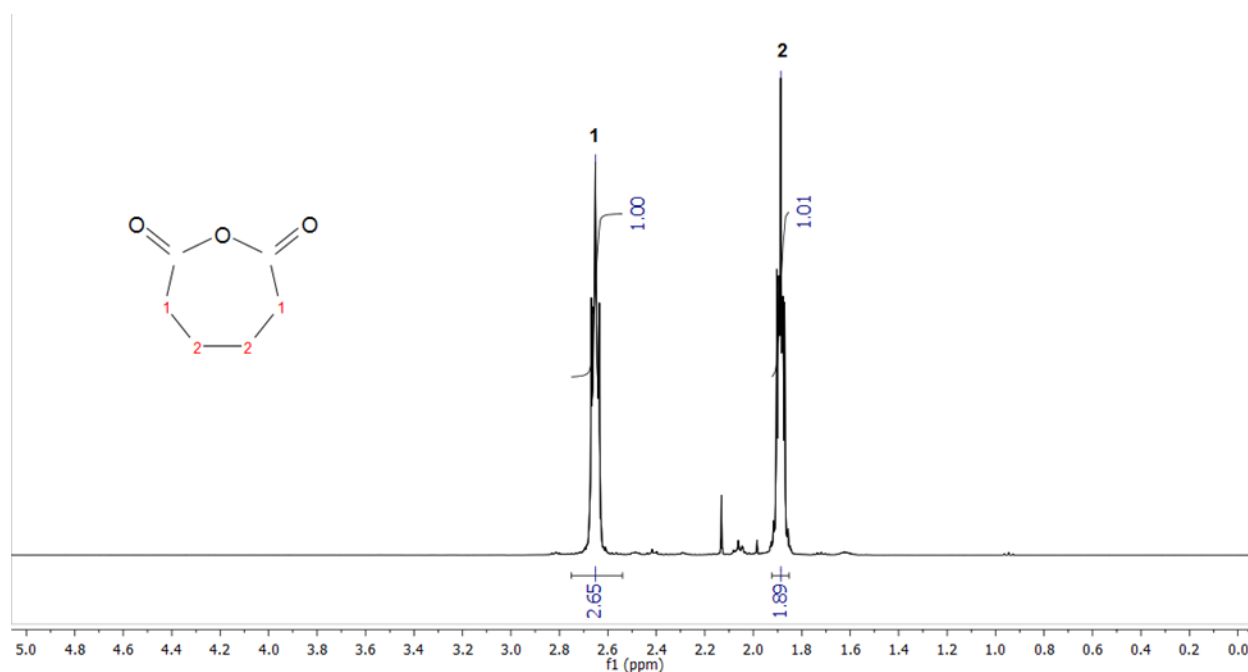


**Figure S4.1**  $^1\text{H}$  NMR spectrum of pure adipic anhydride

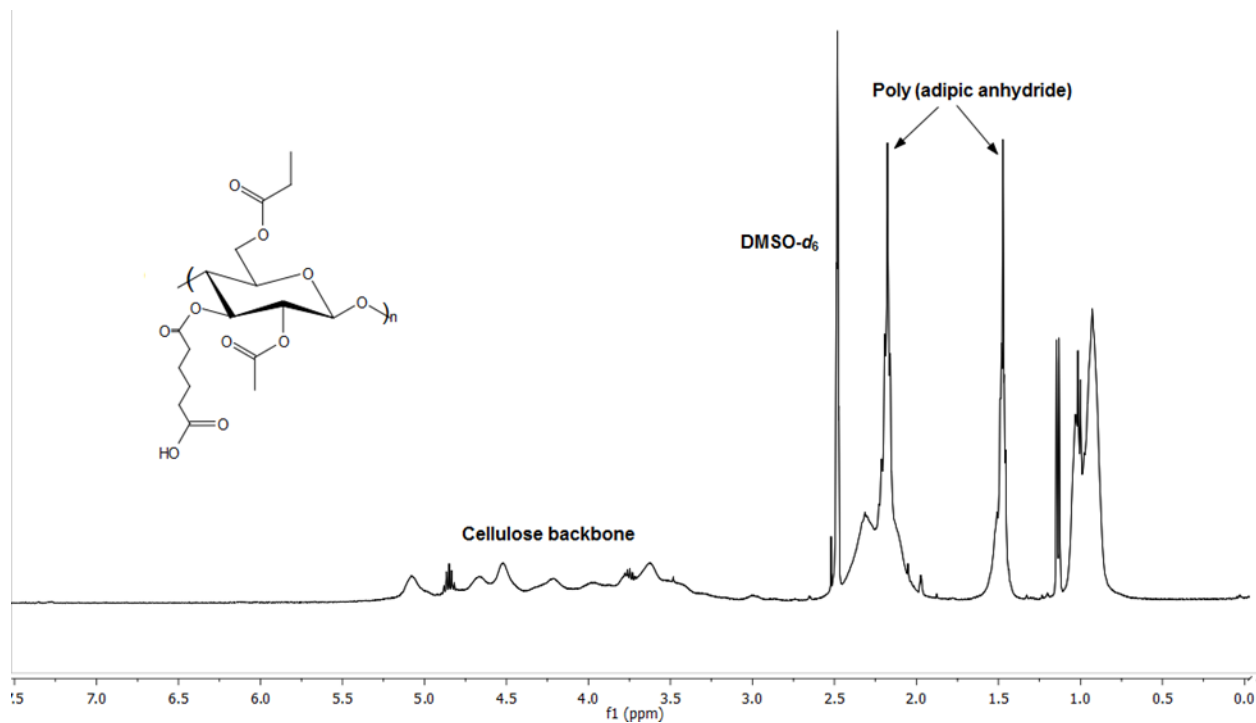


**Figure S4.2**  $^1\text{H}$  NMR of CAAdP (Sample 3, Table 4.1) before the hot water wash step

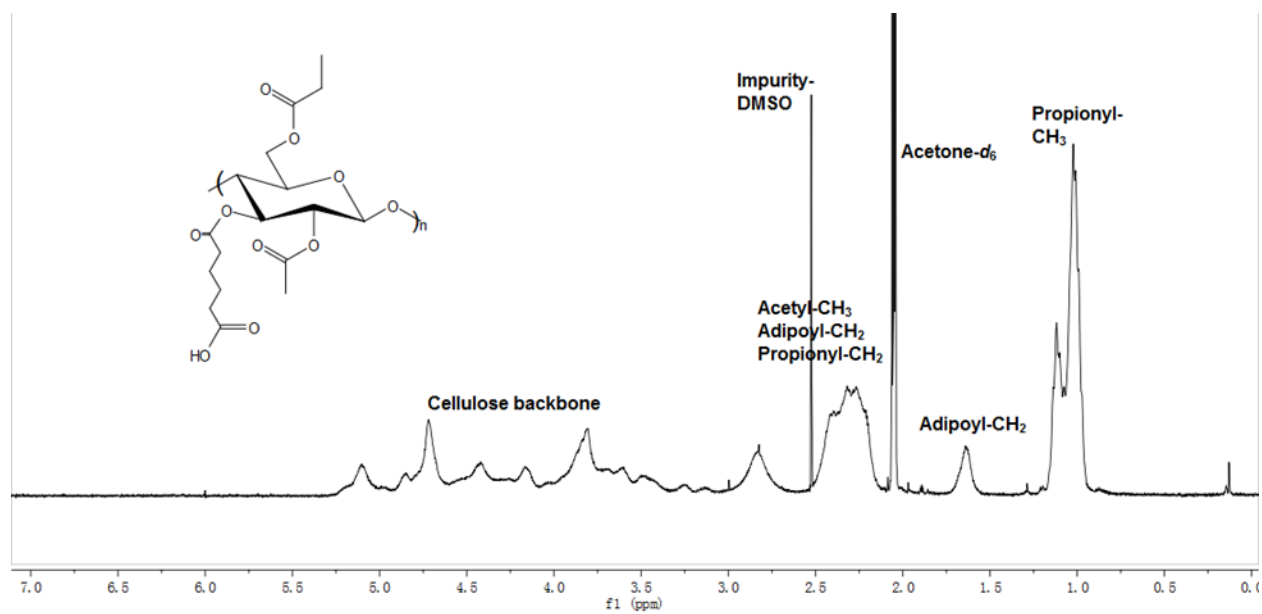


**Figure S4.3**  $^1\text{H}$  NMR spectrum of CAAdP (Sample 3, Table 4.1) in acetone- $d_6$

## 4.7 Acknowledgements

This project was supported primarily by a grant from the National Science Foundation (NSF, grant number DMR-0804501). The authors would like to thank the Eastman Chemical Company for their kind donation of the cellulose esters used in this work. We would also like to thank the Macromolecules and Interfaces Institute and the Institute for Critical Technologies and Applied Science at Virginia Tech for their support, and Tianyu Wu for running the SEC analyses.

## 4.8 References

1. Edgar, K. J., Cellulose esters in drug delivery. *Cellulose* **2007**, 14, (1), 49-64.
2. Posey-Dowty, J. D.; Watterson, T. L.; Wilson, A. K.; Edgar, K. J.; Shelton, M. C.; Lingerfelt, L. R., Zero-order release formulations using a novel cellulose ester. *Cellulose* **2007**, 14, (1), 73-83.
3. Shelton, M. C.; Posey-Dowty, J. D.; Lingerfelt, L. R.; Kirk, S. K.; Klein, S.; Edgar, K. J., Enhanced dissolution of poorly soluble drugs from solid dispersions in carboxymethylcellulose acetate butyrate matrices. In *Polysaccharide Materials: Performance by Design*, Edgar, K. J.; Heinze, T.; Liebert, T., Eds. American Chemical Society: Washington, D.C., 2009.
4. Allen, J. M.; Wilson, A. K.; Lucas, P. L.; Curtis, L. G. Carboxyalkyl Cellulose Esters. 5,668,273, September 16, 1997.
5. Allen, J. M.; Wilson, A. K.; Lucas, P. L.; Curtis, L. G. Process for Preparing Carboxyalkyl Cellulose Esters. 5,792,856, August 11, 1998.
6. Gomez-Bujedo, S.; Fleury, E.; Vignon, M. R., Preparation of Cellouronic Acids and Partially Acetylated Cellouronic Acids by TEMPO/NaClO Oxidation of Water-Soluble Cellulose Acetate. *Biomacromolecules* **2003**, 5, (2), 565-571.
7. Buchanan, C. M.; Buchanan, N. L.; Carty, S. N.; Kuo, C. M.; Lambert, J. L.; Posey-Dowty, J. D.; Watterson, M. D.; Malcolm, M. O.; Lindblad, M. S. Cellulose interpolymers and method of oxidation. 7,879,994, 2011.
8. Shibata, I.; Isogai, A., Depolymerization of celluronic acid during TEMPO-mediated oxidation. *Cellulose (Dordrecht, Neth.)* **2003**, 10, (2), 151-158.
9. Yoshimura, T.; Matsuo, K.; Fujioka, R., Novel biodegradable superabsorbent hydrogels derived from cotton cellulose and succinic anhydride: Synthesis and characterization. *J Appl Poly Sci* **2006**, 99, 3251-3256.
10. McCormick, C. L.; Dawsey, T. R., Preparation of Cellulose Derivatives via Ring-Opening Reactions with Cyclic Reagents in Lithium Chloride/N,N-Dimethylacetamide. *Macromolecules* **1990**, 23, 3606-3610.
11. Liu, C. F.; Sun, R. C.; Zhang, A. P.; Ren, J. L.; Wang, X. A.; Qin, M. H.; Chao, Z. N.; Luo, W., Homogeneous modification of sugarcane bagasse cellulose with succinic anhydride using a ionic liquid as reaction medium. *Carbohydrate Research* **2007**, 342, (7), 919-926.
12. Malm, C. J.; Fordyce, C. R., Cellulose Esters of Dibasic Organic Acids. *Ind. Eng. Chem.* **1940**, 32, 405-408.
13. DiNunzio, J. C.; Miller, D. A.; Yang, W.; McGinity, J. W.; Williams, R. O., 3rd, Amorphous compositions using concentration enhancing polymers for improved bioavailability of itraconazole. *Mol Pharm* **2008**, 5, (6), 968-80.

14. Edgar, K. J., Cellulose esters in waterborne coatings. *Polymer Paint and Colour Journal* **1993**, 183, 564-571.
15. Hauss, D. J., Oral lipid-based formulations. *Adv. Drug Delivery Rev.* **2007**, 59, (7), 667-676.
16. Rumondor, A. C.; Ivanisevic, I.; Bates, S.; Alonzo, D. E.; Taylor, L. S., Evaluation of Drug-Polymer Miscibility in Amorphous Solid Dispersion Systems. *Pharm Res* **2009**, 26, (11), 2523-2534.
17. Taylor, L. S.; Zografis, G., Spectroscopic characterization of interactions between PVP and indomethacin in amorphous molecular dispersions. *Pharm. Res.* **1997**, 14, (12), 1691-1698.
18. Marsac, P. J.; Konno, H.; Taylor, L. S., A comparison of the physical stability of amorphous felodipine and nifedipine systems. *Pharm Res* **2006**, 23, (10), 2306-16.
19. Konno, H.; Taylor, L. S., Ability of different polymers to inhibit the crystallization of amorphous felodipine in the presence of moisture. *Pharm Res* **2008**, 25, (4), 969-78.
20. Kennedy, M.; Hu, J.; Gao, P.; Li, L.; Ali-Reynolds, A.; Chal, B.; Gupta, V.; Ma, C.; Mahajan, N.; Akrami, A.; Surapaneni, S., Enhanced Bioavailability of a Poorly Soluble VR1 Antagonist Using an Amorphous Solid Dispersion Approach: A Case Study. *Mol Pharm* **2008**.
21. Friesen, D. T.; Shanker, R.; Crew, M.; Smithey, D. T.; Curatolo, W. J.; Nightingale, J. A., Hydroxypropyl methylcellulose acetate succinate-based spray-dried dispersions: an overview. *Mol Pharm* **2008**, 5, (6), 1003-19.
22. Kar, N.; Liu, H.; Edgar, K. J., Synthesis of Cellulose Adipate Derivatives. *Biomacromolecules* **2011**, 12, (4), 1106-1115.
23. Campbell, H. J.; Francis, T., The Cross-linking of Cotton Cellulose by Aliphatic Dicarboxylic Acids. *Textile Research Journal* **1965**, 35, 260-270.
24. Rowland, S. P.; Brannan, M. F., Mobile Ester Cross Links for Thermal Creasing of Wrinkle-Resistant Cotton Fabrics. *Textile Research Journal* **1968**, 38, 634-643.
25. English, A. R.; Girard, D.; Jasys, V. J.; Martingano, R. J.; Kellogg, M. S., Orally Effective Prodrugs of the Beta-Lactamase Inhibitor Sulbactam. *Journal of Medicinal Chemistry* **1990**, 33, 344-347.
26. Abell, A. D.; Morris, K. B.; Litten, J. C., Synthesis and Deprotection of [1-(Ethoxycarbonyl)-4-[(diphenylmethoxy)carbonyl]-1-methyl-2-oxobutyl]triphenylphosphonium Chloride: A Key Intermediate in the Wittig Reaction Between a Cyclic Anhydride and a Stabilized Ylide. *Journal of Organic Chemistry* **1990**, 55, 5217-5221.
27. Edgar, K. J.; Arnold, K. M.; Blount, W. W.; Lawniczak, J. E.; Lowman, D. W., Synthesis and Properties of Cellulose Acetoacetates. *Macromolecules* **1995**, 28, (12), 4122-4128.
28. Albertsson, A. C.; Lundmark, S., Melt Polymerization of Adipic Anhydride (Oxepane-2,7-Dione). *Journal of Macromolecular Science-Chemistry* **1990**, A27, (4), 397-412.
29. Albertsson, A. C.; Eklund, M., Short methylene segment crosslinks in degradable aliphatic polyanhydride: Network formation, characterization, and degradation. *Journal of Polymer Science Part a-Polymer Chemistry* **1996**, 34, (8), 1395-1405.
30. Albertsson, A.-C.; Lundmark, S., Synthesis of Poly(Adipic Anhydride) by Use of Ketene. *Journal of Macromolecular Science - Chemistry* **1988**, A25, 247-258.
31. Albertsson, A. C.; Carlfors, J.; Stureson, C., Preparation and characterisation of Poly(adipic anhydride) Microspheres for Ocular Drug Delivery. *Journal of Applied Polymer Science* **1996**, 62, 695-705.
32. Edgar, K. J., Direct Synthesis of Partially Substituted Cellulose Esters. In *Polysaccharide Materials: Performance by Design*, Edgar, K. J.; Buchanan, C. M.; Heinze, T., Eds. American Chemical Society: Washington, D.C., 2009; pp 213-229.
33. Takaragi, A.; Minoda, M.; Miyamoto, T.; Liu, H. Q.; Zhang, L. N., Reaction characteristics of cellulose in the lithium chloride/1,3-dimethyl-2-imidazolidinone solvent system. *Cellulose (Dordrecht, Neth.)* **1999**, 6, (2), 93-102.
34. Furuhashi, K.; Koganei, K.; Chang, H.-S.; Aoki, N.; Sakamoto, M., Dissolution of cellulose in lithium bromide-organic solvent systems and homogeneous bromination of cellulose with N-bromosuccinimide



- triphenylphosphine in lithium bromide - N,N-dimethylacetamide. *Carbohydr Res* **1992**, 230, 165-177.
35. Fox, S. C.; Edgar, K. J., Synthesis of regioselectively brominated cellulose esters and 6-cyano-6-deoxycellulose esters. *Cellulose (Dordrecht, Neth.)* **2011**, 18, (5), 1305-1314.
36. Liu, C. F.; Zhang, A. P.; Li, W. Y.; Yue, F. X.; Sun, R. C., Homogeneous Modification of Cellulose in Ionic Liquid with Succinic Anhydride Using N-Bromosuccinimide as a Catalyst. *Journal of Agricultural and Food Chemistry* **2009**, 57, (5), 1814-1820.
37. Albertsson, A. C.; Carlfors, J.; Stureson, C., Preparation and characterisation of poly(adipic anhydride) microspheres for ocular drug delivery. *Journal of Applied Polymer Science* **1996**, 62, (4), 695-705.
38. Liebert, T.; Pfeiffer, K.; Heinze, T., Carbamoylation applied for structure determination of cellulose derivatives. *Macromol. Symp.* **2005**, 223, (Cellulose and Cellulose Derivatives), 93-108.
39. Liebert, T.; Hussain, M. A.; Heinze, T., Structure determination of cellulose esters via subsequent functionalization and NMR spectroscopy. *Macromol. Symp.* **2005**, 223, (Cellulose and Cellulose Derivatives), 79-91.
40. Edgar, K. J.; Buchanan, C. M.; Debenham, J. S.; Rundquist, P. A.; Seiler, B. D.; Shelton, M. C.; Tindall, D., Advances in cellulose ester performance and application. *Progress in Polymer Science* **2001**, 26, (9), 1605-1688.
41. Ilevbare, G. L., H.; Edgar, K.J.; Taylor, L.S., Manuscript in preparation on Drug Crystal Growth Inhibition by Cellulose Omega-Carboxyalkanoates. In.
42. Kennedy, M.; Hu, J.; Gao, P.; Li, L.; Ali-Reynolds, A.; Chal, B.; Gupta, V.; Ma, C.; Mahajan, N.; Akrami, A.; Surapaneni, S., Enhanced Bioavailability of a Poorly Soluble VR1 Antagonist Using an Amorphous Solid Dispersion Approach: A Case Study. *Mol. Pharmaceutics* **2008**, 5, (6), 981-993.
43. Sealey, J. E.; Samaranayake, G.; Todd, J. G.; Glasser, W. G., Novel cellulose derivatives .4. Preparation and thermal analysis of waxy esters of cellulose. *Journal of Polymer Science Part B-Polymer Physics* **1996**, 34, (9), 1613-1620.

# CHAPTER 5 SYNTHESIS AND STRUCTURE-PROPERTY EVALUATION OF CELLULOSE $\omega$ -CARBOXYESTERS FOR AMORPHOUS SOLID DISPERSIONS

Adapted from: Liu, H.; Ilevbare, G. A.; Cherniawski, B. P.; Ritchie E. T.; Taylor L. S.; Edgar K. J. *Carbohydrate Polymers*, **2014**, 100, 116-125. Copyright 2014, with permission from Elsevier.

## 5.1 Abstract

The use of amorphous solid dispersions (ASDs) is an effective and increasingly widely used approach for solubility enhancement of drugs and drug candidates with poor aqueous solubility. Successful molecular dispersion of drugs in polymer matrices requires new polymers that are designed to meet all ASD requirements, including drug release and prevention of drug recrystallization in storage or from solution. We describe herein design and synthesis of a new series of cellulose  $\omega$ -carboxyalkanoates for ASDs, by reaction of cellulose with long-chain diacids that have been monoprotected as benzyl esters at one end, and monoactivated as acid chlorides at the other. Glass transition temperatures of these cellulose  $\omega$ -carboxyesters exceed ambient temperature by at least 50 °C, providing a sufficient  $\Delta T$  to prevent drug mobility and crystallization. Cellulose acetate suberates and sebacates prepared in this way are extraordinary solution crystal growth inhibitors for the poorly soluble anti-HIV drug ritonavir. These new cellulose  $\omega$ -carboxyesters have strong potential as ASD polymers for enhancement of drug solubility and bioavailability.

**Keywords:** Cellulose  $\omega$ -carboxyalkanoates, crystal growth inhibition, amorphous solid dispersion, oral drug delivery, cellulose esters, cellulose acylation

## 5.2 Introduction

Cellulose esters have a long history of effective use in pharmaceutical applications, based on their low toxicity, water permeability, essentially complete lack of ability to permeate through the enterocytes into the circulation, and the possibility of tailoring the cellulose ester structure to impart, for example, pH responsiveness.<sup>1</sup> More recently, cellulose esters have been explored as key components of advanced drug delivery systems addressing difficult issues like poor drug bioavailability<sup>2</sup> and nanoparticulate therapy.<sup>3</sup> Cellulose esters are more useful in oral drug administration than in modes like intravenous or inhalation therapy, since humans lack the ability to metabolize and clear cellulose from the circulation. Oral drug administration is generally preferred by patients, due to its unsurpassed convenience, potential for outpatient therapy, and relatively low cost, but the ability to administer drugs orally is currently limited by physical characteristics of drugs and drug candidates.

Poor drug solubility, and the low bioavailability that often results, is a particular problem in modern oral drug therapy. The process of high throughput screening of drug candidates against often hydrophobic receptor binding sites, with selection based on magnitude of binding constant, leads inevitably to a plethora of hydrophobic drug candidates. The need for purity of drug candidates leads drug developers to favor highly crystalline molecules. These two properties, hydrophobicity and high crystallinity, are inimical to water solubility. As a result, a high proportion of new and existing drugs and drug candidates has poor aqueous solubility (estimated as high as 40-70%).<sup>4</sup>

In recent years, amorphous solid dispersion has emerged as an effective approach to enhancing drug solubility.<sup>5-7</sup> To create an ASD of a particular drug, the drug is dispersed, ideally molecularly, in a polymer matrix. The creation of a miscible drug-polymer blend leads to a high-energy, amorphous state of the drug, where the polymer inhibits drug crystallization. This enhances drug solution concentration by reducing the kinetic energy barrier that must be surmounted for the drug to dissolve. The criteria for the polymer may be summarized as follows:

- Polymer and any decomposition products must be non-toxic.

- Polymer must be miscible with the active drug, and prevent drug crystallization during transport and storage, even in hot, humid ambient environments, for at least several years.<sup>8</sup>
- Must prevent or severely retard drug crystallization after release but prior to absorption, in aqueous solution.<sup>9, 10</sup>
- Must release the drug effectively in the absorptive zone of the digestive tract.<sup>1, 11</sup>

Polymers used for ASD to date have largely been selected from those already in approved pharmaceutical formulations, rather than having been designed for ASD requirements. Some of these polymers can themselves crystallize during storage (poly(ethylene glycol)), so are not suitable from a stability perspective. Poly(vinylpyrrolidinone) (PVP) is an excellent polymer for ASD of drugs, but is highly soluble in water, especially at low (gastric) pH; thus overly fast release or undesired exposure of stomach to drug can be problems. Hydroxypropyl methylcellulose acetate succinate (HPMCAS) is also quite effective in ASD of drugs. However HPMCAS is complex to synthesize and analyze; amounts of four separate substituents must be controlled, and the hydroxypropyl substituent carries the additional complication that it can form oligomeric poly(hydroxypropyl) side chains of various lengths from the cellulosic hydroxyl initiator. The overall hypothesis in the collaborative ASD work between the Taylor and Edgar groups is that, by understanding the fundamental science and specific performance requirements for ASDs and ASD polymers, we can design, synthesize and use polymers with superior performance in ASD systems that meet all system requirements.

In previous work, we have reported that cellulose esters containing adipate groups have useful combinations of properties as ASD polymers.<sup>12, 13</sup> The tetramethylene side chains of the adipate groups accentuate the already hydrophobic nature of the cellulose esters, enhancing miscibility with hydrophobic drugs and enabling slow drug release. The carboxyl end groups not only provide specific interactions with hydrogen bond acceptors on the drug, enhancing miscibility and stability, but also provide a mechanism for drug release through ionization and subsequent swelling upon reaching the neutral environment of the small intestine. In our previous studies, cellulose acetate adipate propionate (CAAdP) was found to be an effective inhibitor of crystal growth of the important, hydrophobic drug ritonavir at supersaturations lower than that generated during the dissolution of the amorphous form.<sup>10, 14</sup> Ritonavir is an important metabolic inhibitor that is a key component of several drug formulations used in human immunodeficiency virus (HIV)

therapy<sup>15</sup> and is administered as the amorphous form. These structure-property studies showed that both the hydrophobicity of the polymer and its carboxyl group content were important contributors predicting strong inhibition of ritonavir crystallization, and that crystal growth inhibition was highly sensitive to these parameters; indeed, the closely related cellulose acetate adipate butyrate (CAAdB) was ineffective in inhibiting ritonavir crystal growth. In related research in our groups, amorphous solid dispersion in CAAdP matrices has been shown not only to strongly inhibit crystallization from either solid dispersion or aqueous solution of the biologically potent but poorly soluble flavonoid curcumin, but remarkably also protected curcumin against the rapid chemical degradation (retro-aldol reaction) that occurs in the absence of polymer.<sup>16</sup>

The hypothesis of the current study is that further exploration of this ASD structure-property relationship, through synthesis of novel cellulose  $\omega$ -carboxyalkanoates bearing longer, more hydrophobic tethers between the cellulose main chain and the pendent carboxyl group, will lead to even more effective ASD polymers. In this way we hoped to expand both the breadth of our ability to enhance drug solubility and bioavailability by ASD (making it effective for an even broader range of drug structures) and enhance the stability of the drug in the ASD, permitting longer term stabilization of maximum solution concentrations attainable from amorphous drug (increasing bioavailability). This paper describes the development of methods for the synthesis and characterization of soluble, non-crosslinked cellulose esters containing suberate or sebacate groups, as well as the results of preliminary structure-property investigations that demonstrate the great promise of these new polymers for amorphous solid dispersions of poorly soluble drugs.

## 5.3 Experimental Section

### 5.3.1 Materials

Microcrystalline cellulose (MCC, Avicel<sup>®</sup> PH-101, Fluka) was dried under reduced pressure at 50 °C overnight prior to use. Cellulose acetate propionate (CAP-504-0.2), cellulose acetate butyrate (CAB-553-0.4) and cellulose acetate (CA 320S) were obtained from Eastman Chemical Co. and dried overnight under vacuum at 40 °C prior to use. *N, N*-Dimethylacetamide (DMAc) and 1,3-dimethyl-2-imidazolidinone (DMI) were purchased from ACROS Organics and

dried over 4 Å molecular sieves. Other purchased reagents were used as received. Suberic acid, sebacic acid, methyl ethyl ketone (MEK), *p*-toluenesulfonic acid (PTSA), triethylamine (Et<sub>3</sub>N), oxalyl chloride and anhydrous tetrahydrofuran were purchased from ACROS Organics. Toluene, benzyl alcohol, *N,N*-dimethylformamide (DMF), dichloromethane, lithium chloride and sodium bicarbonate were purchased from Fisher Scientific. Hydrogenolysis catalyst 20% Pd(OH)/C was obtained from Sigma Aldrich. Ritonavir was purchased from Attix Corporation, Toronto, Ontario, Canada.

### 5.3.2 Measurements

<sup>1</sup>H NMR spectra were acquired on INOVA 400 or Bruker Avance 500 spectrometers. Samples were analyzed as solutions in CDCl<sub>3</sub> or DMSO-*d*<sub>6</sub> (ca. 10 mg/mL) at 25 °C in standard 5 mm o.d. tubes. A drop of trifluoroacetic acid was added to shift the water peak of DMSO-*d*<sub>6</sub> downfield from the spectral region of interest. 32 scans were obtained for each sample. <sup>13</sup>C NMR spectra were obtained on a Bruker Avance 500 MHz spectrometer with a minimum of 5,000 scans in DMSO-*d*<sub>6</sub> (ca. 50 mg/mL) at 80 °C. DSC analyses of cellulosic polymers were performed on a TA Instruments Q2000 apparatus. Dry powders (ca. 5 mg) were loaded in Tzero™ aluminum pans. Each sample was equilibrated at 30 °C and then heated to 180 °C at 15 °C/min. The sample then was cooled at 50 °C/min to -50 °C. During the second heating cycle the sample was heated to 180 °C at 15 °C/min. All DSC measurements were verified with a duplicate run. T<sub>g</sub> values were recorded as the step-change inflection point from 2<sup>nd</sup> heat scans. IR spectra were obtained on a Nicolet 8700 instrument. Size exclusion chromatography (SEC) was performed in HPLC grade THF at 40 °C at flow rate 1 mL/min using a Waters size exclusion chromatograph equipped with an autosampler, three in-line 5 μm PLgel Mixed-C columns, and a Waters 410 refractive index (RI) detector operating at 880 nm, which was programmed to a polystyrene calibration curve. We report number average molecular weights relative to polystyrene standards. Cellulose ester solubility was tested by adding ca. 10 mg of sample into 2 mL each of various solvents. Each mixture was subjected to vortex mixing for 5-10 min at room temperature, then solubility was judged by visual examination.

Thermal analysis of the solid dispersion was carried out through the use of a modulated differential scanning calorimeter (Model Q2000, TA Instruments). The calorimeter was calibrated

with sapphire and indium standards using a nitrogen purge. For each measurement a sample of approximately 2-5 mg was heated to 180 °C at a heating rate of 20 °C/min in order to remove moisture. Then the sample was cooled to -78 °C at 50 °C/min, followed by the second heating scan to 180 °C at 20 °C/min. From this second scan the glass transition temperature ( $T_g$ ) of each solid dispersion was measured and the lack of crystallization or melting transitions was confirmed. DSC heating curves were analyzed using Universal Analysis 2000 software (TA instruments). Powder X-ray Diffraction (PXRD) data were collected using a Bruker D8 Discover X-Ray Diffractometer. Cu K $\alpha$  ( $\lambda = 0.154$  nm) radiation was at 40 kV/40 mA and the diffraction profile was detected using a locked couple 2 theta scan from 10 to 50 °scattering angle. The scan speed was 0.1 sec/step with the increment of 0.01 °. XRD samples were prepared by flattening the lyophilized solid dispersions into powder form onto a glass slide.

### 5.3.3 Methods

**Synthesis of Monobenzyl Sebacate.** The method of English, *et al.*<sup>17</sup> was adapted for the synthesis of monobenzyl sebacate. Sebacic acid (0.25 mol, 50.56 g), toluene (200 mL), benzyl alcohol (0.30 mol, 1.2 eq, 32.4 g, 31.1 mL), and p-toluene sulfonic acid (2.5 mmol, 0.475 g) were combined in a Dean-Stark apparatus and refluxed until the desired volume of H<sub>2</sub>O (0.30 mol, 5.40 mL) was collected from the Fischer esterification of the sebacic acid, indicating the end of the reaction. The mixture was allowed to cool to room temperature, then 150 mL of DI water was added. Using vigorous mixing, this mixture was adjusted to pH 9 with 6 M NaOH. The aqueous layer with the di-acid and mono-ester was separated and washed twice with 50 mL of diethyl ether; these diethyl ether washes contained primarily the dibenzyl ester by-product, and were discarded. Diethyl ether (200 mL) was combined with the aqueous layer which was acidified to pH 2.0-2.5 with 6 M HCl. The ether layer containing the mono-ester was separated. To further purify, the ether layer was washed with 1M NaHCO<sub>3</sub> solution. The ether layer then was concentrated under reduced pressure and vacuum-dried for 1.5 h to yield the final product as white, needle-like solid. Yield: 29.0% (16.96 g, 0.058 mol).

<sup>1</sup>H NMR (CDCl<sub>3</sub>): 1.29 (m, 8H), 1.62 (m, 4H), 2.33 (m, 4H), 5.11 (s, 2H), 7.35 (m, 5H).

A similar procedure was followed to synthesize monobenzyl suberate (colorless oil). Yield: 47.5% (31.35 g, 0.12 mol)

$^1\text{H}$  NMR ( $\text{CDCl}_3$ ): 1.33 (m, 4H), 1.63 (m, 4H), 2.33 (m, 4H), 5.11 (s, 2H), 7.34 (m, 5H).

**Synthesis of Monobenzyl Sebacoyl Chloride.** The procedure was adapted from Abell, *et al.*<sup>18</sup>, as follows. Monobenzyl sebacate (0.051 mol, 15.00 g) was dissolved in dichloromethane (300 mL), then DMF (5 drops) was added. The solution was cooled in an ice bath to 0 °C. Oxalyl chloride (24.42 mL, 5.6 eq) was added slowly. The ice bath was removed and the reaction proceeded at room temperature. A halt in gas evolution indicated completion, then solvent was removed under reduced pressure. Toluene (50 mL) was added and the product concentrated azeotropically under reduced pressure. The product was stored and used in this crude form without further purification. Yield: 90.1% (0.046 mol, 14.35 g).  $^1\text{H}$  NMR ( $\text{CDCl}_3$ ): 1.30 (m, 8H), 1.67 (m, 4H), 2.35 (t, 2H), 2.86 (t, 2H), 5.11 (s, 2H), 7.35 (m, 5H).

A similar procedure was followed to synthesize monobenzyl suberoyl chloride. Yield : 90.7% (0.051 mol, 14.54 g).  $^1\text{H}$  NMR ( $\text{CDCl}_3$ ): 1.34 (m, 4H), 1.66 (m, 4H), 2.36 (t, 2H), 2.86 (t, 2H), 5.12 (s, 2H), 7.35 (m, 5H).

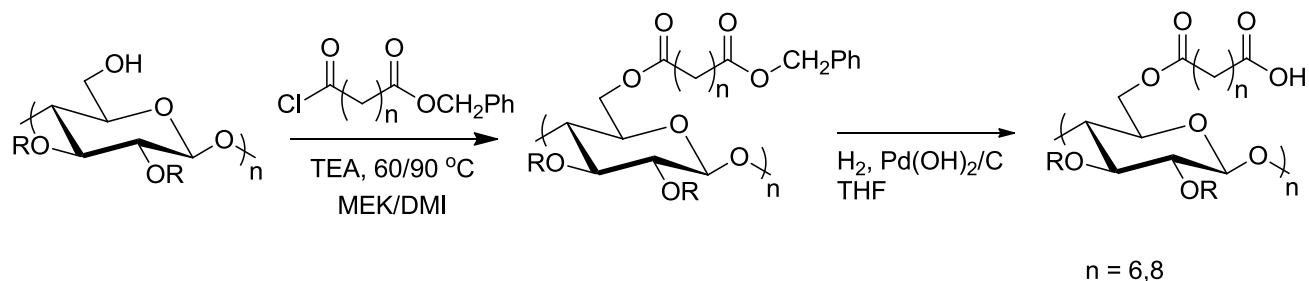
**Preparation of Benzyl Cellulose Acetate Propionate Suberate/Sebacate (Scheme 5.1).** CAP-504-0.2 (1.00 g, 3.56 mmol) was dissolved in MEK (20 mL), and the solution was heated to 60 °C with stirring under nitrogen. Triethylamine (0.54 mL, 3.92 mmol, 1.1 equiv) was added to the solution. Monobenzyl sebacoyl chloride (1.11 g, 3.56 mmol, 1 equiv) or monobenzyl suberoyl chloride (1.02 g, 3.56 mmol, 1 equiv) was added dropwise and allowed to react at 60 °C for 20 h. The reaction mixture was diluted with ~10 mL of acetone and filtered to remove *in situ* formed triethylamine chloride precipitate. The remaining solution was precipitated into 250 mL water. The precipitate was collected and washed with isopropanol. The filtered product was redissolved in a minimal amount of chloroform and reprecipitated in hexanes.

Benzyl CAP sebacate yield: 89.1% (3.17 mmol, 1.10 g).  $^1\text{H}$  NMR ( $\text{CDCl}_3$ ): 0.95-1.20 ( $\text{COCH}_2\text{CH}_3$  of propionate), 1.30 ( $\text{COCH}_2\text{CH}_2\text{CH}_2\text{CH}_2\text{CH}_2\text{CH}_2\text{CH}_2\text{CO}$  of sebacate), 1.63 ( $\text{COCH}_2\text{CH}_2\text{CH}_2\text{CH}_2\text{CH}_2\text{CH}_2\text{CH}_2\text{CH}_2\text{CO}$  of sebacate), 2.13-2.44 ( $\text{COCH}_2\text{CH}_2\text{CH}_2\text{CH}_2\text{CH}_2\text{CH}_2\text{CH}_2\text{CH}_2\text{CO}$  of sebacate,  $\text{COCH}_2\text{CH}_3$  of propionate, and  $\text{COCH}_3$  of acetate), 3.00-5.20 (cellulose backbone), 5.11 ( $\text{CH}_2\text{C}_6\text{H}_5$ ), 7.35 ( $\text{CH}_2\text{C}_6\text{H}_5$ ).



Benzyl CAP suberate yield: 78.4% (2.79 mmol, 0.97 g).  $^1\text{H NMR}$  ( $\text{CDCl}_3$ ): 0.95-1.22 ( $\text{COCH}_2\text{CH}_3$  of propionate), 1.33 ( $\text{COCH}_2\text{CH}_2\text{CH}_2\text{CH}_2\text{CH}_2\text{CH}_2\text{CO}$  of suberate), 1.63 ( $\text{COCH}_2\text{CH}_2\text{CH}_2\text{CH}_2\text{CH}_2\text{CH}_2\text{CO}$  of suberate), 2.10-2.46 ( $\text{COCH}_2\text{CH}_2\text{CH}_2\text{CH}_2\text{CH}_2\text{CH}_2\text{CO}$  of suberate,  $\text{COCH}_2\text{CH}_3$  of propionate, and  $\text{COCH}_3$  of acetate), 3.00-5.20 (cellulose backbone), 5.10 (s,  $\text{CH}_2\text{C}_6\text{H}_5$ ), 7.35 ( $\text{CH}_2\text{C}_6\text{H}_5$ ).

A similar procedure was followed for the reaction of cellulose acetate butyrate (CAB-553-0.4, 1.00 g, 3.26 mmol) with monobenzyl suberoyl/sebacoyl chloride (1 equiv).



R: H or  $\text{COCH}_3$  or  $\text{COCH}_2\text{CH}_3$  or  $\text{COCH}_2\text{CH}_2\text{CH}_3$ . Note that the ester groups are randomly distributed at O-2,3,6, the particular positions of substitution are shown in Scheme 5.1 only for convenience of depiction

**Scheme 5.1** General two-step synthetic method for  $\omega$ -carboxyalkanoate derivatives of cellulose

**Preparation of Benzyl Cellulose Acetate Suberate/Sebacate.** CA 320S (1.00 g, 4.19 mmol) was dissolved in DMI (20 mL), and the solution heated to 90 °C with stirring under  $\text{N}_2$ . Triethylamine (1.29 mL, 9.22 mmol, 2.2 equiv) was added; a condenser was used to avoid evaporative loss of the base catalyst. Monobenzyl sebacoyl chloride (2.61 g, 8.38 mmol, 2 equiv) or monobenzyl suberoyl chloride (2.41 g, 8.38 mmol, 2 equiv) was added dropwise and allowed to react at 90 °C for 20 h. The reaction mixture was then filtered, and the remaining solution was diluted with ~10 mL of acetone. The solution was precipitated in 300 mL of ethanol. The precipitate was then collected and washed with ethanol twice. The filtered product was redissolved in a minimal amount of THF and reprecipitated in hexanes.

**Reaction of Cellulose in DMAc/LiCl Solution with Monobenzyl Sebacoyl Chloride.**

Microcrystalline cellulose (1.00 g, 6.17 mmol) was dissolved in DMAc (37.5 mL) and LiCl (1.88 g) by a procedure reported earlier.<sup>19</sup> The clear solution was heated to 60 °C and triethylamine (1.1 equiv or 4 equiv) was added. Monobenzyl suberoyl chloride (1 equiv or 3 equiv) was added dropwise and allowed to react for 20 h. For 1 equiv. reaction, the mixture was precipitated in 300 mL of DI water with slow addition, filtered, and the precipitate washed twice with ethanol, then vacuum-dried. Yield: 78.6% (4.85 mmol, 1.52 g). For the 3 equiv. reaction, after precipitating in DI water, the aggregated product was ground using a mortar and pestle, Soxhlet-extracted with methanol overnight, and vacuum-dried. Yield: 94.8% (5.85 mmol, 4.09 g). Structural analysis by <sup>1</sup>H NMR was performed after peracylation.

A similar procedure was followed to synthesize benzyl cellulose suberate.

**Peracylation.** Benzyl cellulose suberate or sebacate (300 mg) was dissolved in 6 mL of pyridine, 25 mg 4-dimethylaminopyridine, and 5 mL of acetic or propionic anhydride. After stirring for 24 h at 80 °C, the product was precipitated into 250 mL water, collected by filtration, and then washed several times with water. The crude product was re-dissolved in 15 mL of CH<sub>2</sub>Cl<sub>2</sub>. This solution was added slowly with rapid stirring to 250 mL of ethanol. After filtration and washing with excess ethanol several times, the sample was dried under vacuum at 40 °C. <sup>1</sup>H NMR of peracetylated benzyl cellulose sebacate (CDCl<sub>3</sub>): 0.94-1.35 (COCH<sub>2</sub>CH<sub>2</sub>CH<sub>2</sub>CH<sub>2</sub>CH<sub>2</sub>CH<sub>2</sub>CH<sub>2</sub>CH<sub>2</sub>CO of sebacate), 1.50-1.72 (COCH<sub>2</sub>CH<sub>2</sub>CH<sub>2</sub>CH<sub>2</sub>CH<sub>2</sub>CH<sub>2</sub>CH<sub>2</sub>CH<sub>2</sub>CO of sebacate), 1.82-2.25 (COCH<sub>3</sub> of acetate), 2.32 (COCH<sub>2</sub>CH<sub>2</sub>CH<sub>2</sub>CH<sub>2</sub>CH<sub>2</sub>CH<sub>2</sub>CH<sub>2</sub>CH<sub>2</sub>CO of sebacate), 3.00-5.20 (cellulose backbone), 5.11 (CH<sub>2</sub>C<sub>6</sub>H<sub>5</sub>), 7.33 (CH<sub>2</sub>C<sub>6</sub>H<sub>5</sub>).

**Pd(OH)<sub>2</sub>/C Hydrogenolysis of the Benzyl Cellulose Ester (Scheme 5.1).** To a solution of 500 mg benzyl cellulose mixed ester dissolved in 50 mL of anhydrous THF, 500 mg palladium hydroxide, 20 wt % Pd (dry basis) on carbon was added. A hydrogen balloon was attached to the flask, and the solution stirred overnight under hydrogen at room temperature. The mixture was filtered through Celite and concentrated. The product was dissolved in dichloromethane and precipitated into hexanes. The precipitate was collected and dried under vacuum. For benzyl CA

320S suberate and sebacate esters, a second hydrogenolysis reaction was required to achieve complete cleavage of the benzyl ester bond.

CAP sebacate yield: 96.1% (1.39 mmol, 0.45 g).  $^1\text{H NMR}$  ( $d_6$ -DMSO): 0.80-1.10 (COCH<sub>2</sub>CH<sub>3</sub> of propionate), 1.22 (COCH<sub>2</sub>CH<sub>2</sub>CH<sub>2</sub>CH<sub>2</sub>CH<sub>2</sub>CH<sub>2</sub>CH<sub>2</sub>CH<sub>2</sub>CO of sebacate), 1.45 (COCH<sub>2</sub>CH<sub>2</sub>CH<sub>2</sub>CH<sub>2</sub>CH<sub>2</sub>CH<sub>2</sub>CH<sub>2</sub>CH<sub>2</sub>CO of sebacate), 2.05-2.52 (COCH<sub>2</sub>CH<sub>2</sub>CH<sub>2</sub>CH<sub>2</sub>CH<sub>2</sub>CH<sub>2</sub>CH<sub>2</sub>CH<sub>2</sub>CO of sebacate, COCH<sub>2</sub>CH<sub>3</sub> of propionate, and COCH<sub>3</sub> of acetate), 2.80-5.30 (cellulose backbone).

**Preparation of Amorphous Solid Dispersions by Co-precipitation.** Powder solid dispersion systems of 1/3 w/w ritonavir/cellulose  $\omega$ -carboxyalkanoate (50 mg/150 mg) were prepared as follows: Accurately weighed quantities of polymer and drug were dissolved in 32 mL acetone (or THF if the polymer was not soluble in acetone), then the homogeneous solution was added into 150 mL water with vigorous stirring. The organic solvent was removed under reduced pressure by rotary evaporation at 40 °C. The aqueous drug/polymer mixture was freeze-dried at -53 °C for 2 days to obtain solid powder.

***In vitro* Drug Release Profile from Prepared Solid dispersions.** Dissolution testing was performed in phosphate buffer pH 6.8 as described by Galia, *et al.*<sup>20</sup> 15 mg of drug/polymer dispersion particles were wetted in 80 mL of buffer. 1 mL of Aliquots were withdrawn every 0.5 h for the first 2 h and then every 1h for additional 6 h. After each collection, 1 mL of the same buffer was replaced. The withdrawals were centrifuged at 14,000 x g for 15 min and the supernatants were analyzed using an Agilent 1100 series HPLC. The mobile phase was acetonitrile and phosphate buffer pH 5.65. The flow rate was 1.5 mL/min and retention time was 20 minutes. A UV detector was used and signal at 240 nm was collected. The concentration was calculated based on ritonavir standard curve measured using the same HPLC method.

**Solubility Parameter (SP) of Cellulose  $\omega$ -carboxyalkanoates.** SP calculations were used to compare the relative hydrophobicities of the polymers. SP values were estimated using the method proposed by Fedors<sup>21</sup>. The method is based on group additive constants and the contribution of a

large number of functional groups was evaluated, therefore this method requires only knowledge of the structural formula of the polymer. Solubility parameter can be evaluated using:

$$\delta = \sqrt{\frac{\sum_i \Delta e_i}{\sum_i \Delta v_i}} = \sqrt{\frac{\Delta E_v}{V}} \quad (1)$$

where the  $\Delta e_i$  and  $\Delta v_i$  are the additive atomic and group contribution for the energy of vaporization and molar volume, respectively. The contributions applicable at a temperature of 25°C are presented in the reference <sup>21</sup>. For high molecular weight polymers that have a glass transition greater than 25°C, there is a deviation between the experimentally measured  $\Delta E_v$  and  $V$  and the estimated values. A small correction factor was introduced to take into account the divergence in the  $V$  values:

$$\Delta v_i = 4n, n < 3 \quad (2)$$

$$\Delta v_i = 2n, n \geq 3 \quad (3)$$

where  $n$  is the number of main chain skeletal atoms in the smallest repeating unit of the polymer.

**Crystal Growth Rate of Ritonavir.** Crystal growth rate was characterized by measuring the rate of desupersaturation in the presence of seed crystals. Crystal growth rate experiments were performed in the presence and absence of pre-dissolved cellulose derivatives and the initial ritonavir concentration was 10 µg/mL. Polymer concentrations of 5 µg/mL were used and all experiments were performed in triplicate. The solubility of crystalline ritonavir is known not to change in 5 µg/mL polymer solutions from HPLC measurement. The rate of desupersaturation of ritonavir was measured using an SI Photonics (Tuscon, Arizona) UV spectrometer coupled to a fiber optic probe (path-length 5 mm) at a constant temperature of 37 °C. Data was acquired at 5 second time intervals within wavelengths ranging from 200 – 450 nm. The ritonavir peak was detected at 240 nm. Supersaturated solutions were generated by adding a small volume of pre-dissolved ritonavir in methanol to 100 mM sodium phosphate buffer, pH 6.8. Prior to addition of solubilized ritonavir, seed crystals were added to the buffer and allowed to equilibrate at 37 °C. Data collection began immediately after generation of supersaturation. An overhead stirrer was used to stir the solution at a speed of 400 rpm. The slope of the concentration vs. time curve over the first 2 minutes of the experiment was taken as the initial crystal growth rate. In order to mitigate particle scattering effects, second derivatives (SIMCA P+ V. 12 software (Umetrics Inc., Umea Sweden) of the spectra were taken for the sample data.

## 5.4 Results and Discussion

### 5.4.1 Synthesis and characterization of cellulose $\omega$ -carboxyalkanoates.

In our previous work on synthesis of cellulose ester adipates, we found that reaction of cellulose esters with adipic anhydride could lead to crosslinked, insoluble products because of reaction of multiple cellulose chains with poly(adipic anhydride) contaminant in the adipic anhydride.<sup>12</sup> Though we later developed a carefully designed procedure that circumvented these issues and permitted use of adipic anhydride reagent to afford soluble cellulose ester adipates,<sup>13</sup> we found in the interim that there was a more forgiving, if slightly less direct approach. We found that conversion of adipic acid into a mono-functional, mono-protected reagent provided a useful route for synthesis of cellulose ester adipates for our initial structure-property studies. Fischer esterification of the diacid with benzyl alcohol afforded a mixture of diester, monoester, and starting diacid, from which the monoester could be readily isolated in reasonable yield; this was then smoothly converted using oxalyl chloride/DMF to the monoacid chloride. Commercially available cellulose esters were reacted with the product monobenzyl adipoyl chloride to generate protected cellulose ester adipates. Finally, mild hydrogenation removed the benzyl protective group to afford the cellulose adipate esters.

We planned to follow a similar approach for the synthesis of cellulose ester suberates and sebacates (suberic and sebacic anhydrides would have large and unfavorable (9 and 11 membered, respectively) ring sizes and to our knowledge are unknown). We were however cognizant that the synthesis of the monoprotected, monofunctional reagents required could be more complicated due to solubility issues, and that often reaction of longer chain reagents with cellulose can be difficult.<sup>22</sup> Indeed, we found that using the same methodology we employed for monobenzyl adipate synthesis gave exceptionally low yields of monobenzyl suberate and monobenzyl sebacate. We investigated stoichiometric as well as work up issues to improve the yields. In the monobenzyl adipate synthesis, a molar ratio of benzyl alcohol to di-acid of 1.5 was most effective, in spite of the excess benzyl alcohol that might be expected to generate an excessive amount of dibenzyl adipate. We were also concerned that the strongly basic conditions (NaOH) used in the adipate workup might be reducing yield due to ester hydrolysis. We reduced the molar ratio of benzyl alcohol to diacid to 1.2, to

minimize generation of the dibenzyl suberate or sebacate. By extracting residual diacid with aqueous 1M NaHCO<sub>3</sub>, we were able to avoid excessive hydrolysis (NaOH) or poor separation of layers (Na<sub>2</sub>CO<sub>3</sub>), while still ensuring quantitative removal of diacid (crucial since residual diacid would be converted to a diacid chloride in the ensuing step, leading to polymer crosslinking). <sup>1</sup>H NMR confirmed that the product monobenzyl esters, obtained in moderate yields, were pure and uncontaminated by dibenzyl esters or unreacted diacid.

Subsequent conversion of monobenzyl suberate and monobenzyl sebacate to the corresponding monoacid chlorides went very smoothly using oxalyl chloride/DMF, affording more than 90% yield in each case of crude products that were not purified, but were shown by <sup>1</sup>H NMR to have the desired monoprotected, monofunctional structures (Supplementary Materials, Fig. S5.1). Both products were reactive yellow liquids that were stable if stored at 4 °C.

Reactions of these monofunctional reagents with commercially available cellulose esters in common organic solvents were facile, with no sign of crosslinking. Three different commercially available cellulose esters, cellulose acetate propionate (CAP-504-0.2), cellulose acetate butyrate (CAB-553-0.4) and cellulose acetate (CA 320S), were selected due to their solvent solubility and high number of hydroxyls available for reaction (**Scheme 5.1**, and see **Table 5.1** for details on substituent DS); this also gave us a range of hydrophobicity that would facilitate our structure-property studies. CAP-504-0.2 and CAB-553-0.4 were reacted with the acid chlorides in methyl ethyl ketone (MEK). The low DS CA we used is not soluble in MEK, so instead was dissolved in warm 1,3-dimethyl-2-imidazolidinone (DMI). MEK is preferred over acetone due to its higher boiling point, permitting the reaction to be run under more energetic conditions (60 °C). The nature of this condensation reaction is such that there should be considerable flexibility with regard to reaction solvent.

**Table 5.1** Cellulose suberate/sebacate mixed-ester syntheses, DS values and properties

Sam ple	Starting CE	Carboxy -ester <sup>a</sup>	Solvent	Temp ( °C)	Molar ratio <sup>b</sup>	DS Chain	DS <sup>c</sup> Other	DS Total	T <sub>g</sub> (°C)	M <sub>n</sub> (*10 <sup>3</sup> )	DP
1	CAP- 504-0.2	Sub	MEK	60	1	0.27	Pr 2.09 Ac 0.04	2.39	120	16.7	52
2	CAP- 504-0.2	Seb	MEK	60	1	0.24	Pr 2.09 Ac 0.04	2.37	116	18.8	58
3	CAP- 504-0.2	Seb	MEK	60	3	0.67	Pr 2.09 Ac 0.04	2.80	78	19.1	47
4	CAB- 553-0.4	Sub	MEK	60	1	0.26	Bu 1.99 Ac 0.14	2.39	89	20.9	60
5	CAB- 553-0.4	Seb	MEK	60	1	0.22	Bu 1.99 Ac 0.14	2.37	89	22.6	65
6	CA 320S	Sub	DMI	90	2	0.63	Ac 1.82	2.45	101	21.2	63
7	CA 320S	Seb	DMI	90	2	0.57	Ac 1.82	2.39	117	25.0	73

<sup>a</sup> Abbreviations: suberate (Sub) and sebacate (Seb).

<sup>b</sup> Mol monobenzyl acid chloride per mol anhydroglucose unit.

<sup>c</sup> Abbreviations: acetate (Ac), propionate (Pr), butyrate (Bu),

Substituent DS values in these protected cellulose sebacate/suberate products were calculated by integrating the cellulose backbone and benzylic hydrogen peaks together and calculating the ratio to the phenyl protons (**Fig. 5.1**); (sample calculation Appendix I). As shown in **Table 5.1**, sebacate DS in cellulose acetate propionate sebacate (CAP Seb) responded in

straightforward fashion to an increase in monobenzyl sebacoyl chloride (BnSeCl) used, affording nearly 3 fold increase in DS (Seb) with a threefold increase in acid chloride. We observe that  $\omega$ -carboxyalkanoyl DS values decrease slightly for the CAB and CAP polymers as the diacid chain gets longer. This can be rationalized by steric hindrance. Similarly, CAP derivatives consistently have higher  $\omega$ -carboxyalkanoyl DS values than the corresponding CAB derivatives, with the obvious culprit being poorer accessibility of the OH groups on cellulose in the presence of the longer butyrate chains. CA 320S has less bulky substituents and higher hydroxyl content, thus by using 2 equiv monobenzyl sebacoyl chloride per CA 320S AGU, the DS of benzyl-protected carboxyester can be up to 0.57. All these benzyl-protected intermediate products are quite soluble in organic solvents, for example in THF.

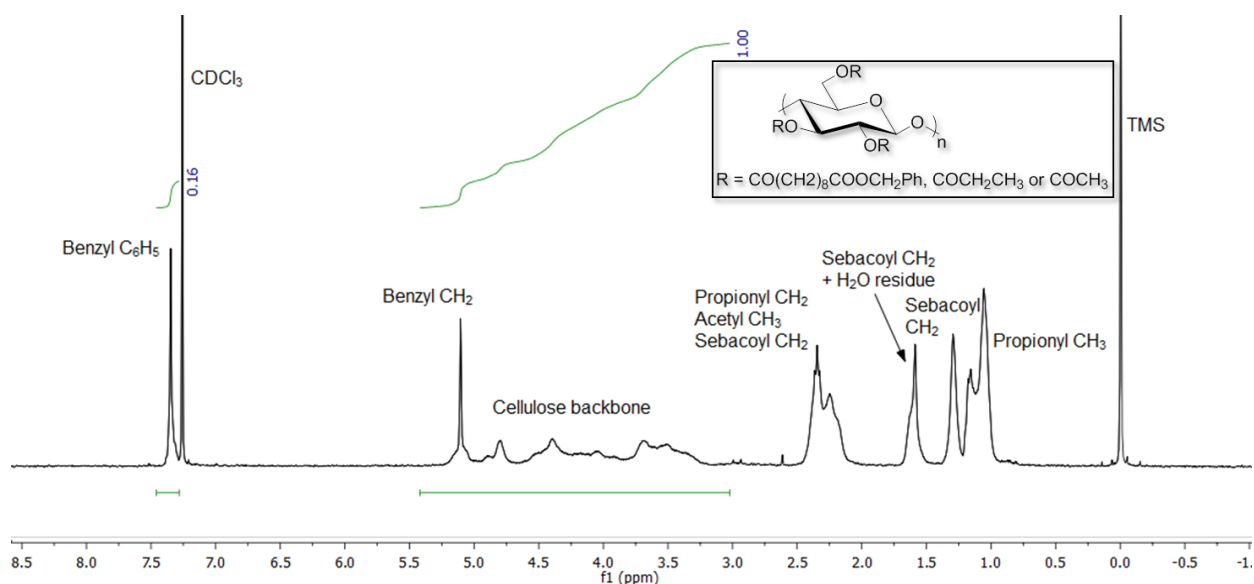


**Figure 5.1**  $^1\text{H}$  NMR of benzyl CAP-504-0.2 sebacate (DS Se = 0.24) in  $\text{CDCl}_3$ .

Hydrogenolysis of the benzyl ester groups on protected cellulose adipates, for example on protected CAAdP, can be slightly sluggish, occasionally requiring longer reaction times or re-hydrogenation. In contrast, the longer and more flexible suberate and sebacate chains are more suitable for heterogeneous catalytic hydrogenation, so that all benzyl cellulose suberate and sebacate hydrogenation reactions were facile and straightforward, achieving clean hydrogenolysis of the benzyl ester. Use of  $\text{Pd}(\text{OH})_2/\text{C}$  catalyst enables reaction completion overnight at room



temperature on the gram scale. Both  $^1\text{H}$  NMR and  $^{13}\text{C}$  NMR spectra (**Fig. 5.2a and 5.2b**) show the disappearance of benzylic and aromatic signals, without any observable residual substitution. In larger scale reactions it may be necessary to perform the hydrogenation reaction twice to obtain complete hydrogenolysis.

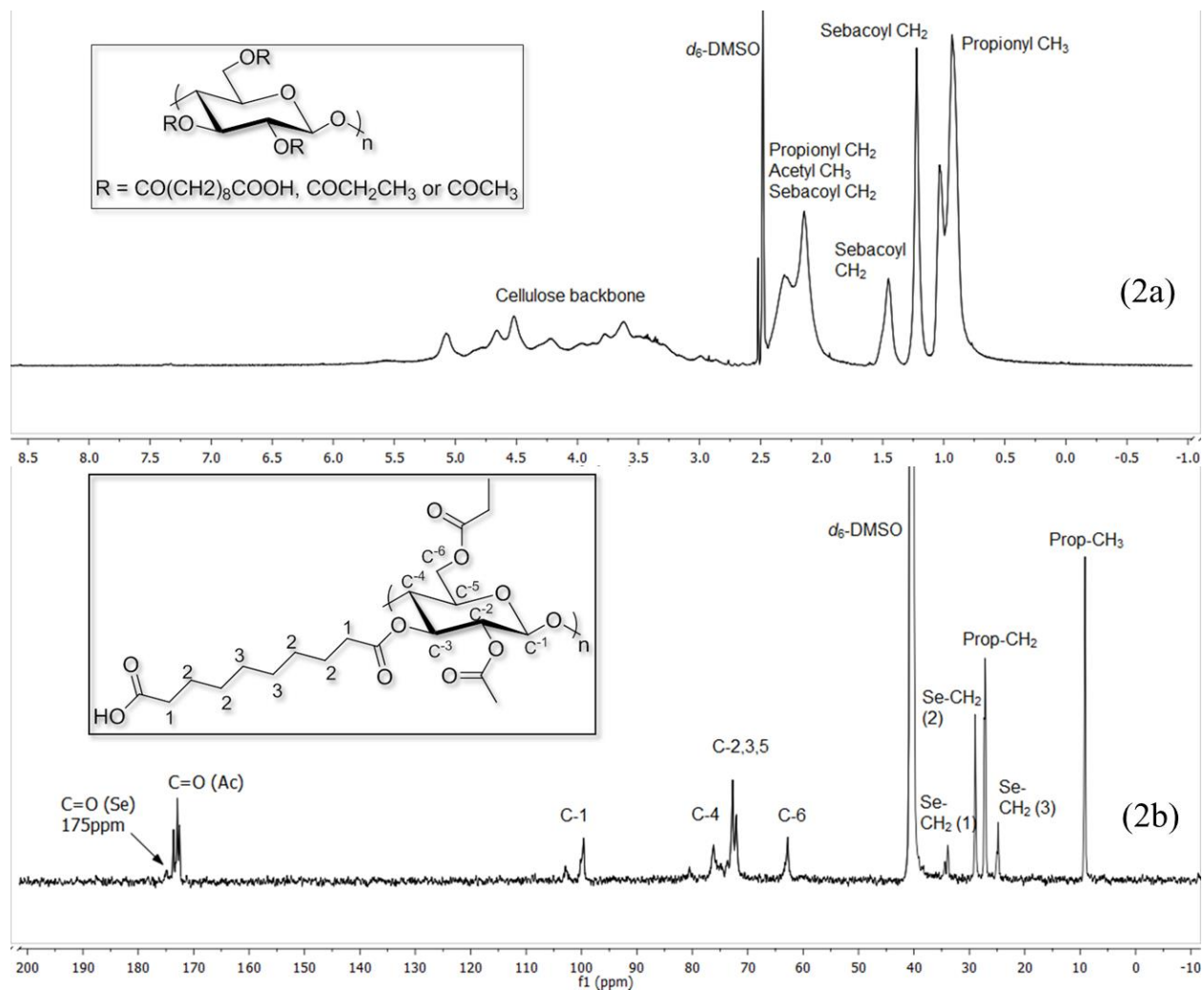


**Figure 5.2**  $^1\text{H}$  NMR (2a) and  $^{13}\text{C}$  NMR (2b) of CAP-504-0.2 sebacate (DS Se 0.24) in  $\text{DMSO-}d_6$

It was important to determine the relationship of cellulose  $\omega$ -carboxyalkanoate structure to thermal properties. Glass transition temperature ( $T_g$ ) in particular is important in ASDs; the high  $T_g$  values for most known cellulose esters are advantageous in ASD formulations, since they ensure that the formulation  $T_g$  will remain well above ambient temperature even when containing a substantial portion of drug (which may be a plasticizer) and at high ambient humidity (water will

definitely be a plasticizer). Keeping the formulation  $T_g$  well above ambient temperature ensures that the matrix is in the glassy state, preventing drug migration through the matrix that could lead to crystallization.<sup>23</sup> From the thermogram we are also able to observe whether the polymer itself has a tendency to crystallize. Thermal properties of cellulose suberate and sebacate mixed esters after deprotection are summarized in **Table 5.1**.  $T_g$  values of the products are generally 40-80 °C lower than the starting cellulose esters due to the plasticizing effect of the polymethylene chains of the pendent  $\omega$ -carboxyalkanoyl groups. DSC results showed that  $T_g$  depression increased with increasing chain length and increasing DS. Even so,  $T_g$  values of these deprotected cellulose  $\omega$ -carboxyalkanoates are at least 50 °C higher than the highest anticipated ambient temperatures, indicating adequacy for ASDs. Degree of polymerization (DP) data for CAP and CAB derivatives indicate that little or no cellulose chain degradation occurred during acylation and deprotection, consistent with the relatively mild conditions applied. It should be noted that the DP of CAP Seb (DS Se = 0.24) slightly exceeds the DP of the starting CAP (DP = 53); it is reasonable to speculate that the carboxyl-containing cellulosic polymers can self-aggregate in THF solvent.<sup>12</sup> For CA derivatives, the DPs are reduced to less than half that of the starting CA-320S, presumably due to the higher reaction temperatures employed (90 °C) in acylation of CA.

#### 5.4.2 Regioselectivity

It was of interest to explore the regioselectivity of reaction of cellulose with the monoprotected long chain diacid chlorides, since substitution regioselectivity has been shown to have powerful influence on properties like solubility, thermal properties, and optical properties<sup>24</sup> to name just a few such relationships.<sup>25</sup> To investigate regioselectivity, microcrystalline cellulose was reacted in DMAc/LiCl solution with monobenzyl suberoyl/sebacoyl chlorides. The benzyl cellulose suberate and sebacate products from acylation in DMAc/LiCl are only sparingly soluble in DMSO. To obtain a well-resolved NMR spectrum, peracetylation was performed to provide products that were readily soluble in chloroform. DS ( $\omega$ -carboxyester) was calculated based on the ratio of the integrals of benzyl ring protons to those of the benzyl methylene and the cellulose backbone overlapping from 3.00 ppm to 5.20 ppm. At a ratio of 1 equiv BnSeCl per AGU, DS 0.55 was obtained with a reaction time of 20 h at 60 °C. Using 3 equiv BnSeCl per AGU under the same conditions, higher DS (1.95) was achieved. Benzyl cellulose sebacate with high  $\omega$ -

carboxyester substitution tends to self-aggregate in water, therefore grinding and extra washing steps are necessary to remove the impurities before peracetylation.

As predicted from our previous study with very bulky acid chlorides like pivaloyl chloride<sup>26</sup>, regioselectivity was quite limited. After peracetylation of benzyl cellulose sebacate (DS Seb = 1.95), acetyl methyls at O-6 (2.10 ppm), O-2 (1.97 ppm) and O-3 (1.90 ppm) could still be observed by <sup>1</sup>H NMR (Supplementary Material, **Fig. S5.2**). **Table S5.1** in the Supplementary Material summarizes the total/partial DS values according to corresponding reaction feed ratio and substitution type.

The <sup>13</sup>C NMR spectrum of peracetylated cellulose sebacate (DS Seb = 0.55) further confirmed the lack of regioselectivity of this reaction (**Fig. 5.3**). The hydrogenated product is readily soluble in DMSO. Acetyl carbonyl carbons at 170.0, 169.1 and 168.8 ppm were correlated in heteronuclear multibond correlation spectroscopy (HMBC) with AGU protons at the sites of acetylation at O-6, O-3 and O-2, respectively<sup>27</sup>. HMBC is not sensitive enough to provide the exact distribution of sebacate group with much lower substitution, but fortunately, the sebacoyl carbonyl carbons demonstrate as well three different peaks near downfield around 171-174 ppm.

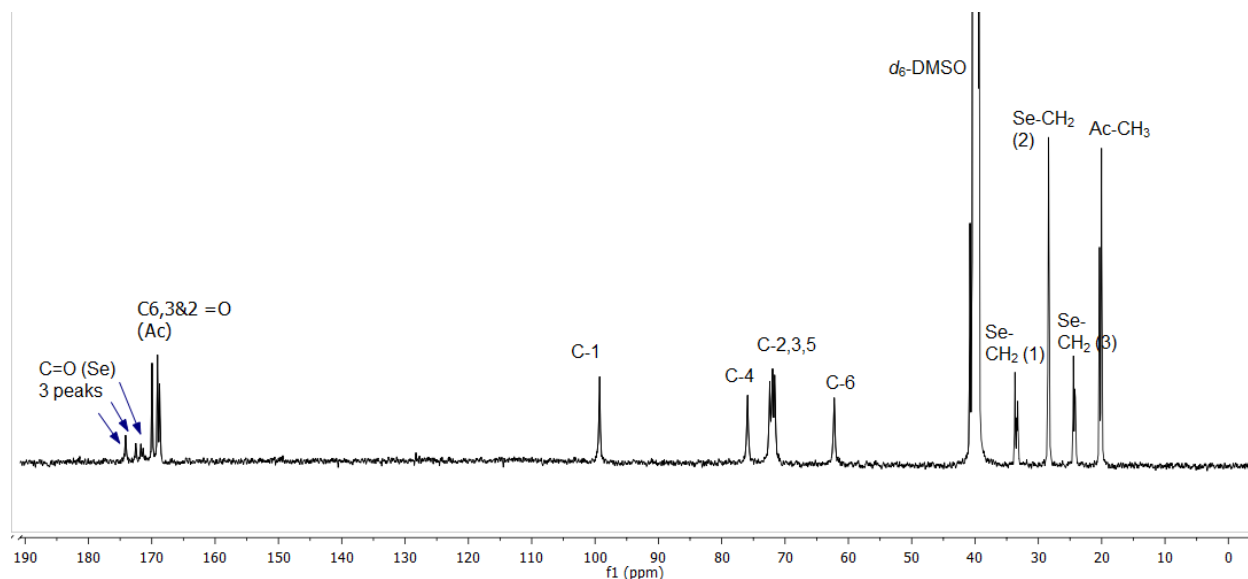


**Figure 5.3** <sup>13</sup>C NMR of fully-substituted cellulose acetate sebacate (DS Se 0.55) in DMSO-*d*<sub>6</sub>

### 5.4.3 Effect of newly synthesized polymers on solution crystal growth inhibition of ritonavir

Supersaturating dosage forms, such as amorphous solids, are attractive for improving the delivery of poorly water soluble drugs since they result in a solution with a higher thermodynamic activity which may enhance the absorption of a drug relative to a saturated solution.<sup>28</sup> However, in order to maintain supersaturation, crystallization must be prevented and hence the presence of an effective crystal growth inhibitor in solution is desirable to prolong supersaturation. While polymers are often used to fulfill this role,<sup>29-32</sup> there is little mechanistic understanding of the properties of a polymer that make it a good inhibitor of crystal growth for a given compound. In a previous study,<sup>10</sup> the effectiveness of a group of chemically diverse polymers, including a number of novel cellulose  $\omega$ -carboxyalkanoates, at inhibiting the crystal growth of ritonavir from solution was quantified. It was found that moderately hydrophobic polymers were more effective crystal growth inhibitors of the hydrophobic drug, ritonavir, than either highly hydrophilic or highly hydrophobic polymers. In addition, the novel cellulose-based polymers containing a higher DS of ionizable carboxylic acids were better inhibitors relative to less ionized cellulose polymers. We have evaluated the effectiveness of several of the newly synthesized cellulose  $\omega$ -carboxyalkanoates in inhibiting crystal growth of ritonavir from supersaturated solution, in comparison with that of previously synthesized and reported cellulose derivatives<sup>12</sup>. Ritonavir is a highly lipophilic compound with a log P value of 5.98 and melting point of 121 °C,<sup>33,34</sup> yielding an equilibrium solubility of  $1.3 \pm 0.10$   $\mu\text{g/mL}$ , at pH 6.8 (ritonavir is un-ionized at this pH) and 37 °C.

The crystal growth rate of ritonavir in the absence and presence of the novel cellulose polymers was determined using the method previously described<sup>10</sup>. The novel cellulose derivatives used in this report and some of their properties are presented in **Table 5.2**. Solubility parameters (SP), estimated according to Fedors,<sup>21</sup> were used to rank relative polymer hydrophobicity. The solubility parameter provides a numerical estimate of the intermolecular forces within a material, and can be a good indication of solubility, particularly for non-polar materials such as polymers. The hydrophobicity ranking is presented, where the least hydrophobic polymer, CP Adp is ranked #1 and #13 represents the most hydrophobic polymer, CAB Seb. DS

of carboxyl-containing substituents (DS (CO<sub>2</sub>H)) of the new cellulose esters are also listed and ranked in **Table 5.2**.

**Table 5.2** DS and SP values for cellulose derivatives and their ranking

Polymer Abbreviation	DS (CO <sub>2</sub> H)	DS (Other) <sup>a</sup>	DS (Total)	DS (CO <sub>2</sub> H) Rank	SP (MPa <sup>1/2</sup> )	SP Rank
CP Adp	0.48	Pr 1.68	2.16	6	23.28	1
CA 320S Adp	0.67	Ac 1.82	2.49	3	22.95	2
CA 320S Sub	0.63	Ac 1.82	2.45	4	22.62	3
CA 320S Seb	0.57	Ac 1.82	2.39	5	22.36	4
CAP Adp 0.85	0.85	Ac 0.04; Pr 2.09	2.98	1	21.27	5
CAB Adp 0.81	0.81	Ac 0.14; Bu 1.99	2.84	2	20.86	6
CAP Adp 0.33	0.33	Ac 0.04; Pr 2.09	2.46	7	20.56	7
CAP Seb 0.67	0.67	Ac 0.04; Pr 2.09	2.80	3	20.41	8
CAP Sub	0.27	Ac 0.04; Pr 2.09	2.39	8	20.19	9
CAB Adp 0.25	0.25	Ac 0.14; Bu 1.99	2.38	10	20.05	10
CAP Seb 0.24	0.24	Ac 0.04; Pr 2.09	2.37	11	19.94	11
CAB Sub	0.26	Ac 0.14; Bu 1.99	2.38	9	19.84	12
CAB Seb	0.22	Ac 0.14; Bu 1.99	2.35	12	19.62	13

<sup>a</sup> Abbreviations: acetate (Ac), propionate (Pr), butyrate (Bu), adipate (Adp), suberate (Sub) and sebacate (Seb).

**Fig. 5.4** shows a comparison of the growth rate ratio of ritonavir (10 µg/mL, S of 7.6) in the absence of polymer ( $R_{g0}$ ) to that in the presence of polymer ( $R_{gp}$ ). Polymers are arranged in order of increasing hydrophobicity (L to R). Polymers with an effectiveness ratio greater than 1 ( $R_{g0}/R_{gp} > 1$ ) are considered effective crystal growth inhibitors. With the exception of the data for the CA 320S sebacates and suberates, we have previously reported effectiveness ratios for the other cellulose ω-carboxyalkanoates. Out of the 13 cellulose ω-carboxyalkanoates presented, 6 were ineffective, while 7 were effective at inhibiting crystal growth, albeit to varying extents. Polymers located in the middle portion of **Fig. 5.4** (i.e., polymers with a moderate level of hydrophobicity (20.56 – 22.62 MPa<sup>1/2</sup>)) were the most effective crystal growth inhibitors. In the

previous study, CAP Adp 0.85 and CAB Adp 0.81 were identified as the most effective cellulose-based polymers.<sup>10</sup> However, two of the new cellulose  $\omega$ -carboxyalkanoate polymers, CA320S Sub and CA320S Seb, were significantly more effective at inhibiting the crystal growth of ritonavir. Together with the relatively high DS of suberate and sebacate substituents (more ionizable carboxylic acids), combining the relatively more hydrophilic cellulose ester (CA320S) with the longer chain  $\omega$ -carboxyalkanoate (e.g., suberate and sebacate) resulted in polymers with an optimal level of hydrophobicity, thus making CA320 Sub and CA320 Seb very effective crystal growth inhibitors. This further supports the importance of hydrophobicity as a key factor influencing polymer effectiveness.

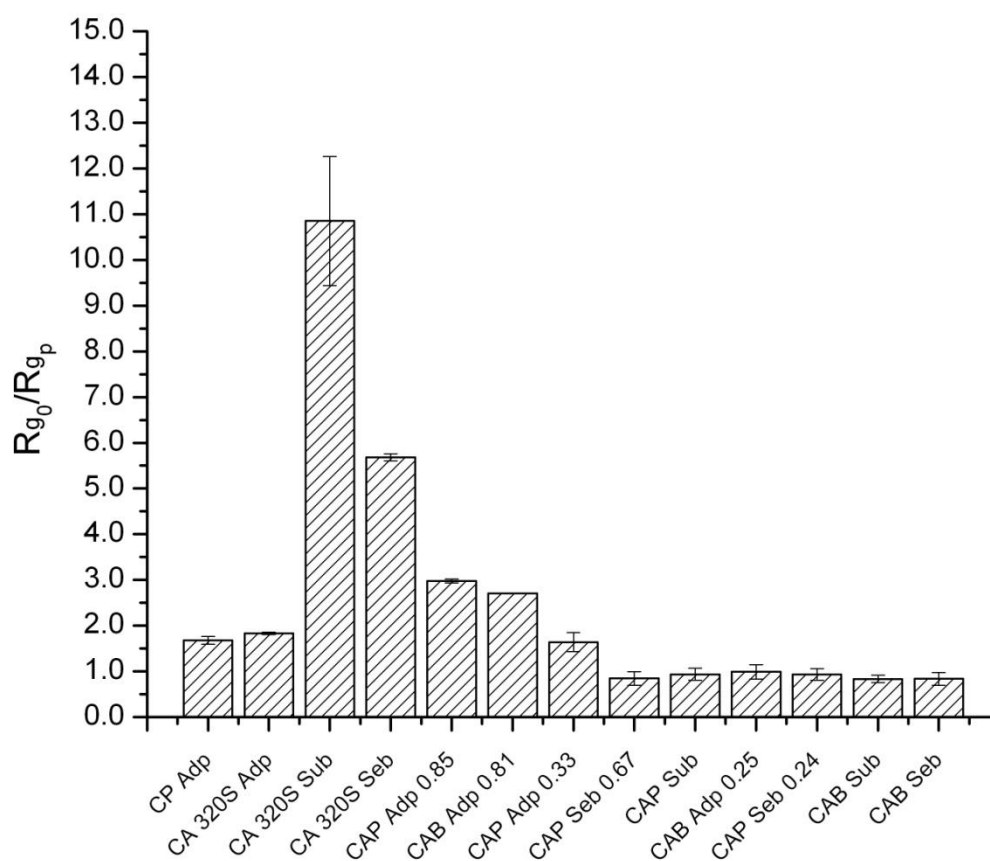


**Figure 5.4** Crystal growth rate ratio of ritonavir at an initial ritonavir concentration of 10  $\mu\text{g/mL}$ . The data is arranged in order of hydrophobicity: least hydrophobic to most hydrophobic (left to right). Crystal growth rate experiments were performed in triplicate. Each column is an average of the effectiveness ratio and error bars indicate one standard deviation. The y-axis is a ratio of the growth rate of ritonavir in the absence of polymer to growth rate of ritonavir in the presence of

polymer (5 µg/mL). Polymers with a ratio > 1 are considered effective crystal growth inhibitors. With the exception of CA 320S Sub and CA 320S Seb, the effectiveness growth ratios for all cellulose ω-carboxyalkanoates were previously reported.<sup>10</sup>

#### 5.4.4 ASDs of ritonavir in cellulose ω-carboxyalkanoate matrices

We prepared ASDs of the model drug ritonavir in cellulose ω-carboxyalkanoates by coprecipitation of a solution of drug and polymer in a common solvent (acetone or THF) into a common non-solvent, water, followed by solvent removal by rotary evaporation and lyophilization to remove water. Spray drying was not practical due to the small amounts of each novel polymer available. ASD samples were characterized by PXRD to determine the crystallinity of the ritonavir in the ASD (**Fig. 5.5**). PXRD patterns of all polymer/RTV 3/1 ASD were devoid of the diffraction peaks evident in the XRD pattern of crystalline ritonavir, indicating that ritonavir is completely amorphous in these blends. To further confirm their amorphous nature, DSC thermograms (**Fig. S5.3**, Supplementary Material) of the ASDs showed single, broad glass transitions, whereas the melting endotherm of crystalline ritonavir at ~ 125 °C was not observed. Based on our previous work and that of others, we expect that the aqueous solution concentrations of ritonavir released from these ASDs will be significantly increased vs. that from crystalline drug. Determination of solubility enhancement (the degree of supersaturation) versus time was also studied by dispersing the sample in a phosphate buffer at pH 6.8 and measured by HPLC. As seen in **Fig. 5.6**, the concentration of ritonavir in the buffer was higher for the ASDs than that of crystalline ritonavir, particularly from the CA320S Suberate-based ASDs, which offered a nearly 15-fold enhancement in apparent solubility. Furthermore, the concentration of ritonavir in the buffer was increased and sustained for the entirety of the study. This *in vitro* study shows the ability of the cellulose ω-carboxyalkanoates to trap ritonavir in an amorphous state and prevent nucleation and crystal growth in solution for at least 8 hours.

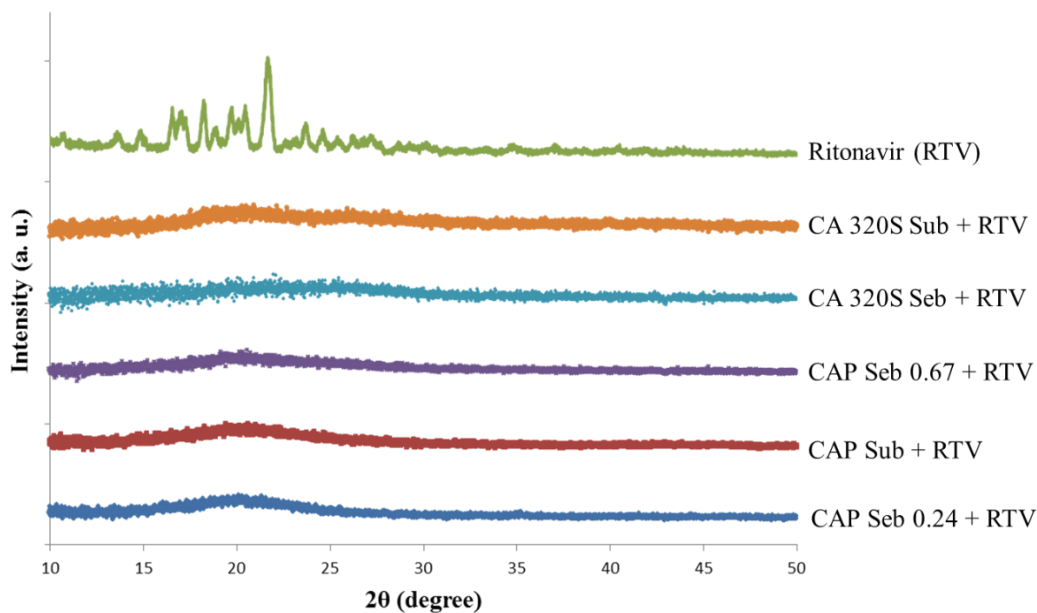


**Figure 5.5** PXR D pattern of ritonavir crystalline powder and amorphous solid dispersions prepared by co-precipitation with cellulose  $\omega$ -carboxyalkanoates

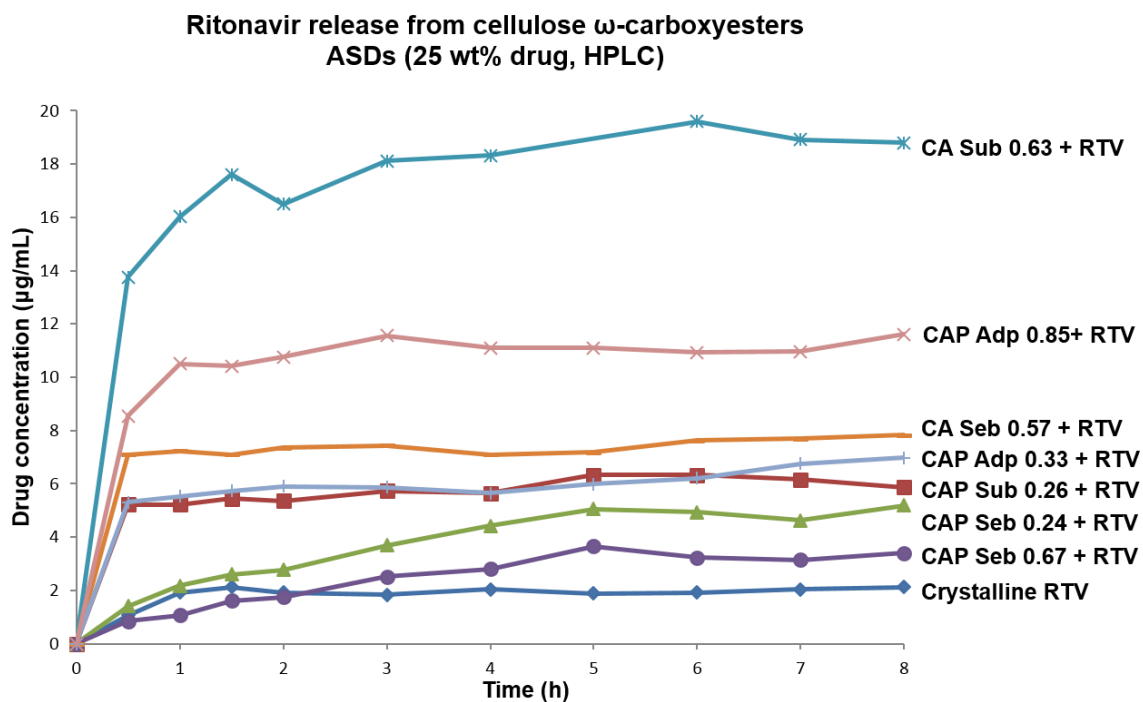


**Figure 5.6** Ritonavir in vitro release from cellulose  $\omega$ -carboxyesters-based amorphous solid dispersions, prepared by co-precipitation



## 5.5 Conclusions

Successful pathways were developed for the synthesis of cellulose  $\omega$ -carboxyalkanoates by reaction of cellulose, CAP, CAB and CA with monobenzyl suberoyl and monobenzyl sebacoyl chlorides. Barriers to synthesis of the acid chlorides were overcome to develop reasonably efficient processes. Condensation of acid chlorides with cellulose esters can be carried out in common organic solvents under mild conditions, and appears to be capable of affording a wide range of DS  $\omega$ -carboxyalkanoates. Even though a relatively bulky benzyl-protected long chain diacid was incorporated, virtually no regioselectivity of substitution was observed. Debenzylation of these long chain benzyl cellulose  $\omega$ -carboxyalkanoates was facile under mild conditions in the presence of a palladium catalyst. The resulting carboxyl-containing mixed esters are well suited as ASD polymers for oral drug delivery, and most of them form amorphous dispersions with the hydrophobic drug ritonavir. All of them possess  $T_g$  values adequate to prevent drug recrystallization in the solid phase. Most importantly, CA 320S suberate and sebacate provide at least 5-fold increased effectiveness at inhibition of ritonavir crystallization from aqueous solution versus other cellulosic and non-cellulose ASD polymers. Prepared novel cellulose  $\omega$ -carboxyalkanoates-based solid dispersion demonstrate higher degree and longer duration of apparent solubility enhancement, we will further explore the generality of cellulose  $\omega$ -carboxyalkanoates with respect to drug structure, and the mechanism of solubilization in forthcoming reports.

**Appendix 1.** The degree of substitution (DS) values were determined according to the following equation

$$\text{DS } \omega\text{-carboxyester} = 7I_{\text{phenyl}} / (5I_{\text{backbone+benzylic hydrogen}} - 2I_{\text{phenyl}})$$

## 5.6 Supplementary Material

Supplementary information available for this chapter includes  $^1\text{H}$  NMR spectra of monobenzyl adipoyl chloride (**Fig. S5.1**), fully-substituted benzyl cellulose acetate sebacate (DS

Se = 1.95) (**Fig. S5.2**), DSC thermograms of ritonavir and ritonavir-cellulose  $\omega$ -carboxyester ASDs (**Fig. S5.3**) and partial DS values of benzyl cellulose  $\omega$ -carboxyesters (**Table S5.1**)

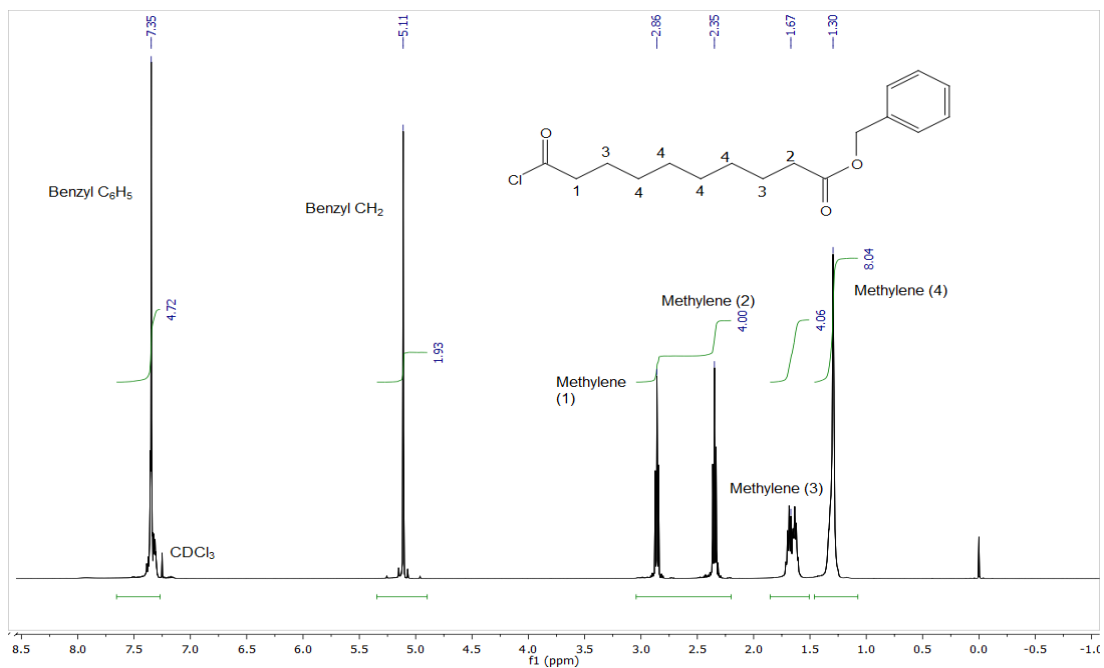


**Figure S5.1**  $^1\text{H}$  NMR of monobenzyl sebacoyl chloride in  $\text{CDCl}_3$

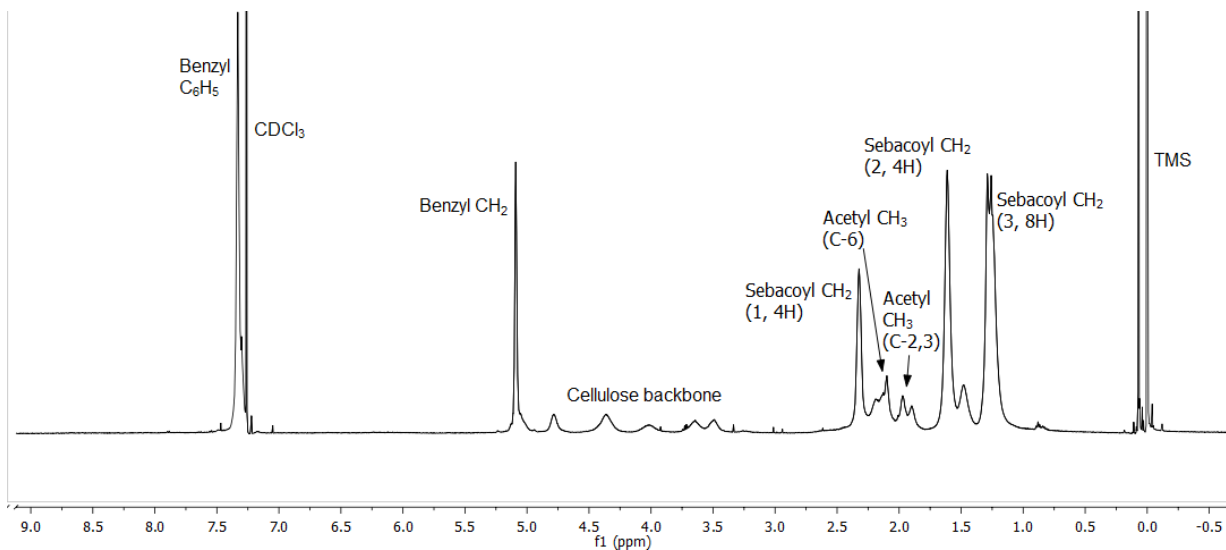


**Figure S5.2**  $^1\text{H}$  NMR of fully-substituted benzyl cellulose acetate sebacate (DS Se = 1.95) in  $\text{CDCl}_3$

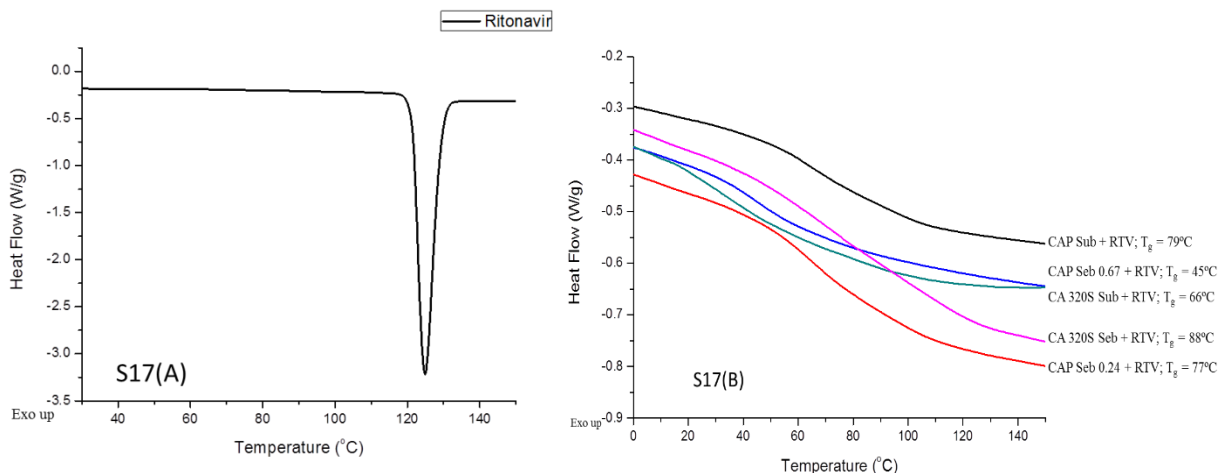


**Figure S5.3** DSC thermograms of ritonavir (A; left) and amorphous solid dispersions in cellulose  $\omega$ -carboxyalkanoates (B; right)

**Table S5.1** Partial degree of substitution values of benzyl cellulose  $\omega$ -carboxyesters

Sample	Carboxyester type	Molar ratio <sup>a</sup>	DS ( $\omega$ -carboxyester)	DS (O-6)	DS (O-2,3)
1	Suberate	1:1	0.67	0.23	0.44
2	Suberate	1:3	2.01	0.89	1.12
3	Sebacate	1:1	0.55	0.25	0.30
4	Sebacate	1:3	1.95	0.89	1.06

<sup>a</sup> Mol monobenzyl acid chloride per mol anhydroglucose unit

## 5.7 Acknowledgements

This project was supported primarily by a grant from the National Science Foundation (NSF, grant number DMR-0804501). The authors thank Eastman Chemical Company for their kind donation of the commercial cellulose esters used in this work, and the Macromolecules and Interfaces Institute and the Institute for Critical Technologies and Applied Science at Virginia

Tech for their financial, facilities, and educational support. We also thank Alison Shultz for SEC analyses, Rick Caudill for XRD experiments and Bruce Orler for some of DSC measurements.

## 5.8 References

1. Edgar, K. J.; Buchanan, C. M.; Debenham, J. S.; Rundquist, P. A.; Seiler, B. D.; Shelton, M. C.; Tindall, D., Advances in cellulose ester performance and application. *Prog. Polym. Sci.* **2001**, 26, (9), 1605-1688.
2. Friesen, D. T.; Shanker, R.; Crew, M.; Smithey, D. T.; Curatolo, W. J.; Nightingale, J. A., Hydroxypropyl methylcellulose acetate succinate-based spray-dried dispersions: an overview. *Molecular Pharmaceutics* **2008**, 5, (6), 1003-19.
3. Mawad, D.; Mouaziz, H.; Penciu, A.; Méhier, H.; Fenet, B.; Fessi, H.; Chevalier, Y., Elaboration of radiopaque iodinated nanoparticles for in situ control of local drug delivery. *Biomaterials* **2009**, 30, (29), 5667-5674.
4. Hauss, D. J., Oral lipid-based formulations. *Adv. Drug Delivery Rev.* **2007**, 59, (7), 667-676.
5. Konno, H.; Handa, T.; Alonzo, D. E.; Taylor, L. S., Effect of polymer type on the dissolution profile of amorphous solid dispersions containing felodipine. *Eur. J. Pharm. Biopharm.* **2008**, 70, (2), 493-499.
6. Alonzo, D. E.; Gao, Y.; Zhou, D.; Mo, H.; Zhang, G. G. Z.; Taylor, L. S., Dissolution and precipitation behavior of amorphous solid dispersions. *J. Pharm. Sci.* **2011**, 100, (8), 3316-3331.
7. Newman, A.; Knipp, G.; Zografi, G., Assessing the performance of amorphous solid dispersions. *J. Pharm. Sci.* **2012**, 101, (4), 1355-1377.
8. Hancock, B. C.; Shamblin, S. L.; Zografi, G., Molecular mobility of amorphous pharmaceutical solids below their glass transition temperatures. *Pharm. Res.* **1995**, 12, (6), 799-806.
9. Alonzo, D. E.; Zhang, G. G.; Zhou, D.; Gao, Y.; Taylor, L. S., Understanding the behavior of amorphous pharmaceutical systems during dissolution. *Pharmaceutical Research* **2010**, 27, (4), 608-18.
10. Ilevbare, G. A.; Liu, H.; Edgar, K. J.; Taylor, L. S., Understanding Polymer Properties Important for Crystal Growth Inhibition—Impact of Chemically Diverse Polymers on Solution Crystal Growth of Ritonavir. *Crystal Growth & Design* **2012**, 12, (6), 3133-3143.
11. Posey-Dowty, J. D.; Watterson, T. L.; Wilson, A. K.; Edgar, K. J.; Shelton, M. C.; Lingerfelt, L. R., Jr., Zero-order release formulations using a novel cellulose ester. *Cellulose (Dordrecht, Neth.)* **2007**, 14, (1), 73-83.
12. Kar, N.; Liu, H.; Edgar, K. J., Synthesis of Cellulose Adipate Derivatives. *Biomacromolecules* **2011**, 12, (4), 1106-1115.
13. Liu, H.; Kar, N.; Edgar, K. J., Direct synthesis of cellulose adipate derivatives using adipic anhydride. *Cellulose (Dordrecht, Neth.)* **2012**, 19, (4), 1279-1293.
14. Ilevbare, G.; Liu, H.; Edgar, K. J.; Taylor, L., Inhibition of Solution Crystal Growth of Ritonavir by Cellulose Polymers - Factors Influencing Polymer Effectiveness. *CrystEngComm* **2012**.
15. Cameron, W.; Japour, A. J.; Xu, Y.; Hsu, A.; Mellors, J.; Farthing, C.; Cohen, C.; Poretz, D.; Markowitz, M.; Follansbee, S.; Angel, J. B.; McMahon, D.; Ho, D.; Devanarayan, V.; Rode, R.; Salgo, M. P.; Kempf, D. J.; Granneman, R.; Leonard, J. M.; Sun, E., Ritonavir and saquinavir combination therapy for the treatment of HIV infection. *AIDS* **1999**, 13, (2), 213-224.
16. Li, B.; Konecke, S.; Wegiel, L. A.; Taylor, L. S.; Edgar, K. J., Both solubility and chemical stability of curcumin are enhanced by solid dispersion in cellulose derivative matrices. *Carbohydr. Polym.* **2013**, 98, (1), 1108-1116.
17. English, A. R.; Girard, D.; Jasys, V. J.; Martingano, R. J.; Kellogg, M. S., Orally Effective Prodrugs of

- the Beta-Lactamase Inhibitor Sulbactam. *Journal of Medicinal Chemistry* **1990**, 33, 344-347.
18. Abell, A. D.; Morris, K. B.; Litten, J. C., Synthesis and Deprotection of [1-(Ethoxycarbonyl)-4-[(diphenylmethoxy)carbonyl]-1-methyl-2-oxobutyl]triphenylphosphonium Chloride: A Key Intermediate in the Wittig Reaction Between a Cyclic Anhydride and a Stabilized Ylide. *Journal of Organic Chemistry* **1990**, 55, 5217-5221.
  19. Edgar, K. J.; Arnold, K. M.; Blount, W. W.; Lawniczak, J. E.; Lowman, D. W., Synthesis and Properties of Cellulose Acetoacetates. *Macromolecules* **1995**, 28, (12), 4122-4128.
  20. Nicolaidis, E.; Galia, E.; Efthymiopoulos, C.; Dressman, J. B.; Reppas, C., Forecasting the in vivo performance of four low solubility drugs from their in vitro dissolution data. *Pharm. Res.* **1999**, 16, (12), 1876-1882.
  21. Fedors, R. F., Method for estimating both the solubility parameters and molar volumes of liquids. *Polym. Eng. Sci.* **1974**, 14, (2), 147-54.
  22. Edgar, K. J., Direct Synthesis of Partially Substituted Cellulose Esters. In *Polysaccharide Materials: Performance by Design*, Edgar, K. J.; Buchanan, C. M.; Heinze, T., Eds. American Chemical Society: Washington, D.C., 2009; pp 213-229.
  23. Shelton, M. C.; Posey-Dowty, J. D.; Lingerfelt, L. R.; Kirk, S. K.; Klein, S.; Edgar, K. J., Enhanced dissolution of poorly soluble drugs from solid dispersions in carboxymethylcellulose acetate butyrate matrices. In *Polysaccharide Materials: Performance by Design*, Edgar, K. J.; Heinze, T.; Liebert, T., Eds. American Chemical Society: Washington, D.C., 2009.
  24. Tasaka, K.; Umeda, H.; Kuzuhara, N.; Yajima, T. Cellulose ester film, manufacturing, optical retardation film, optical compensation sheet, elliptic polarizing plate, and image display. 2002-154188 20030020208, 20020523., 2003.
  25. Fox, S. C.; Li, B.; Xu, D.; Edgar, K. J., Regioselective Esterification and Etherification of Cellulose: A Review. *Biomacromolecules* **2011**, 12, (6), 1956-1972.
  26. Xu, D.; Li, B.; Tate, C.; Edgar, K. J., Studies on regioselective acylation of cellulose with bulky acid chlorides. *Cellulose (Dordrecht, Neth.)* **2011**, 18, (2), 405-419.
  27. Iwata, T.; Azuma, J.; Okamura, K.; Muramoto, M.; Chun, B., Preparation and NMR assignments of cellulose mixed esters regioselectively substituted by acetyl and propanoyl groups. *Carbohydr Res* **1992**, 224, 277-283.
  28. Warren, D. B.; Benameur, H.; Porter, C. J. H.; Pouton, C. W., Using polymeric precipitation inhibitors to improve the absorption of poorly water-soluble drugs: A mechanistic basis for utility. *J. Drug Targeting* **2010**, 18, (10), 704-731.
  29. Alonzo, D. E.; Raina, S.; Zhou, D.; Gao, Y.; Zhang, G. G. Z.; Taylor, L. S., Characterizing the Impact of Hydroxypropylmethyl Cellulose on the Growth and Nucleation Kinetics of Felodipine from Supersaturated Solutions. *Cryst. Growth Des.* **2012**, 12, (3), 1538-1547.
  30. Zimmermann, A.; Millqvist-Fureby, A.; Elema, M. R.; Hansen, T.; Muellertz, A.; Hovgaard, L., Adsorption of pharmaceutical excipients onto microcrystals of siramesine hydrochloride: Effects on physicochemical properties. *Eur. J. Pharm. Biopharm.* **2009**, 71, (1), 109-116.
  31. Lechuga-Ballesteros, D.; Rodriguez-Hornedo, N., The influence of additives on the growth kinetics and mechanism of L-alanine crystals. *Int. J. Pharm.* **1995**, 115, (2), 139-49.
  32. Lechuga-Ballesteros, D.; Rodriguez-Hornedo, N., Effects of molecular structure and growth kinetics on the morphology of L-alanine crystals. *Int. J. Pharm.* **1995**, 115, (2), 151-60.
  33. Baird, J. A.; Van Eerdenbrugh, B.; Taylor, L. S., A classification system to assess the crystallization tendency of organic molecules from undercooled melts. *J. Pharm. Sci.* **2010**, 99, (9), 3787-3806.
  34. Murdande, S. B.; Pikal, M. J.; Shanker, R. M.; Bogner, R. H., Solubility Advantage of Amorphous Pharmaceuticals: II. Application of Quantitative Thermodynamic Relationships for Prediction of Solubility Enhancement in Structurally Diverse Insoluble Pharmaceuticals. *Pharm. Res.* **2010**, 27, (12), 2704-2714.

# CHAPTER 6 IMPACT OF CHEMICALLY DIVERSE POLYMERS ON CRYSTALLIZATION OF LIPOPHILIC DRUG COMPOUNDS FROM SUPERSATURATED SOLUTION

Adapted from with permission from:

Ilevbare, G. A.; Liu, H.; Edgar, K. J.; Taylor, L. S. *Crystal Growth & Design* **2012**, *12*, 3133-3143.

Ilevbare, G. A.; Liu, H.; Edgar, K. J.; Taylor, L. S. *Crystal Growth & Design* **2012**, *12*, 6050-6060.

Ilevbare, G. A.; Liu, H.; Edgar, K. J.; Taylor, L. S. *Crystal Growth & Design* **2013**, *13*, 740-751.

Ilevbare, G. A.; Liu, H.; Edgar, K. J.; Taylor, L. S. *Molecular Pharmaceutics* **2013**, *10*, 2381-2393.

Copyright 2012, 2013 American Chemical Society.

## 6.1 Abstract

The use of polymeric additives is an increasingly common approach for inhibiting crystallization from supersaturated solutions to enhance the delivery of poorly water-soluble drugs. Maintaining supersaturation by employing polymeric additives depends on their ability to inhibit both nucleation and crystal growth. In our series of studies, the effectiveness of a group of chemically diverse polymers, including several recently synthesized cellulose derivatives, on inhibition of crystallization (nucleation and crystal growth, individually) of three model pharmaceutical compounds (celecoxib, efavirenz and ritonavir) was quantified. Nucleation was quantified by measuring the induction time for the appearance of particulates from unseeded desupersaturation experiments. Induction times in the absence of the polymers varied from approximately 2 min for celecoxib to 2 h for ritonavir. Selected polymers were found to extend induction times by up to a factor of 5–6 at all levels of supersaturation tested. The bulk crystal growth rate was characterized by measuring the rate of desupersaturation facilitated by adding seed crystals. Specifically, three of the in-house synthesized cellulose derivatives (CA 320S Sub 0.63, CA 320S Sub 0.90, and CA 320S Seb) inhibited the crystal growth of ritonavir by a factor of 5-12.5. In general, despite the different chemical properties and structures of the model

compounds, the effectiveness of the various polymers appeared to depend on the hydrophobicity of the polymer relative to that of the drug. The hydrophobicity of the polymer most likely influences its ability to form polymer–solute interactions relative to polymer–solvent and polymer–polymer interactions. Polymer–solute interactions would be expected to hinder the reorganization of a cluster of solute molecules into an ordered crystal structure and later block crystalizing sites by adsorption onto the surface of formed crystals.

## 6.2 Introduction

The use of high energy forms, such as amorphous solids, to generate supersaturated aqueous solutions of poorly water-soluble drugs has become a common approach for improving drug delivery.<sup>1,2</sup> In the supersaturated state, the thermodynamic activity of a drug is increased beyond its solubility limit, thus there is an increased driving force for transit into and across the biological membrane.<sup>3</sup> However, due to the inherent thermodynamic instability of the supersaturated state, which will eventually lead to crystallization of the poorly water-soluble drug, prolonged maintenance of supersaturation in the gastrointestinal (GI) tract may be difficult. It has been shown that the addition of polymeric materials can be used to delay crystallization from supersaturated solutions;<sup>4-10</sup> however to date, very few predictive tools exist for the rational selection of the optimum polymer for a given solute. Stabilization of supersaturated systems by polymeric additives depends on their ability to inhibit nucleation and subsequent crystal growth. If one or both processes can be retarded or inhibited, supersaturation may be maintained for a physiologically relevant time period, leading to enhanced absorption. Although the inhibition of crystallization from aqueous supersaturated solutions by polymeric additives has been extensively documented,<sup>5,7</sup> little quantitative work has been published about the impact of these additives on nucleation and crystal growth kinetics, and probing key polymer properties that influence their inhibitory potential.

In solution crystallization, nucleation plays a decisive role in determining the final crystal properties, including crystal form and size distribution, and hence is of practical importance in pharmaceutical systems. Drug delivery challenges concerning the concentration threshold above which crystallization of an active pharmaceutical ingredient (API) occurs upon administration are

related to the kinetic stability of supersaturated solutions, which is in turn regulated by the nucleation mechanisms and kinetics.<sup>11</sup> Thus, optimum control over crystallization from supersaturated solutions is facilitated by understanding the fundamentals of nucleation kinetics and the mechanism of inhibition by additives. However, the influence of additives on nucleation is speculative, partly because the molecular-level processes involved are inaccessible to direct experimental observation. Some molecular simulations on a model system suggested that the relative strength of the pair-wise intermolecular interactions between solute, solvent and additive, as well as size factors, influence the impact of the additive on nucleation kinetics.<sup>12</sup>

Trace crystalline material in an amorphous formulation, either resulting from the manufacturing process or produced during storage, can thus potentially have a significant impact on the extent and duration of supersaturation; the presence of an effective crystal growth inhibitor in solution is therefore highly desirable to prolong supersaturation. It has been proposed that maintenance of supersaturation through the addition of polymeric additives is the result of intermolecular interactions in solution (hydrogen bonding) and/or steric hindrance of recrystallization.<sup>13-15</sup> As reported, the adsorption of additive molecules on the surface of crystal is a required step for the stabilization to occur. A polymer inhibits the introduction of drug molecules from solution into the crystal lattice by occupying growth sites and thereby acting as a steric barrier.<sup>16</sup> The interactions responsible for adsorption can be either physical or chemical in nature.<sup>17</sup> Physical adsorption is usually reversible and van der Waals forces and electrostatic forces are primarily responsible, while chemical adsorption occurs through covalent bonding and is usually strong and irreversible. Several factors, such as hydrophobicity,<sup>18-19</sup> electrostatic interaction,<sup>20,21</sup> and hydrogen bonding between the adsorbate and interfacial species<sup>17,22</sup> have been found to contribute to the adsorption process. An understanding of the mechanism of adsorption is thus essential for understanding the principal factors responsible for inhibition of crystallization by polymeric additives. Adsorption of polymeric additives onto crystal surfaces is heterogeneous as a result of the anisotropic nature of most molecular crystals. Consequently changes in morphology may result if there is a high level of adsorption and inhibition of fast growing faces. For example, hydroxypropyl cellulose (HPC) and hydroxypropyl methylcellulose (HPMC) had a significant effect on the morphology of siramesine hydrochloride.<sup>23</sup> HPC and HPMC interacted differently with the growing crystal surface whereby the morphology of crystals was dominated by the crystal faces on which adsorption occurred.



The objectives of this study was to quantify and compare the effectiveness of a group of polymers, selected based their chemical and physical attributes, in inhibiting nucleation and crystal growth from supersaturated solutions of three chemically diverse poorly water soluble compounds; celecoxib, efavirenz and ritonavir. A variety of polymers were investigated, including a number of recently synthesized cellulose polymers with greater chemical diversity than commercially available cellulose derivatives. Cellulosic polymers are amenable to chemical modification and are biologically compatible, some particular derivatives have been shown to improve the drug solubilization through stabilizing the amorphous form.<sup>24,25</sup> Nucleation was experimentally quantified by measuring the induction time for the appearance of particulates. Crystal growth was monitored in the presence and absence of predissolved polymer after adding seed crystals to solutions of known supersaturation.

## 6.3 Experimental Section

### 6.3.1 Materials

Efavirenz (**Fig. 6.1a**) and ritonavir (**Fig. 6.1b**) were purchased from Attix Corporation, Toronto, Ontario, Canada. Celecoxib (**Fig. 6.1c**) was provided by Pfizer Inc. (Groton, MA). Acetonitrile and methanol were purchased from Macron Chemicals (Phillipsburg, NJ). The commercially available polymers were obtained from various sources: poly(vinyl pyrrolidone) K29/32 (PVP), poly(acrylic acid) (PAA) and cellulose acetate phthalate (CAPH) from Sigma-Aldrich Co., St. Louis MO, poly(vinyl pyrrolidone vinyl acetate) K28 (PVPVA) from BASF, Germany, hydroxypropyl methyl cellulose 606 grade (HPMC) and hydroxypropyl methylcellulose acetate succinate AS-MF grade (HPMCAS) from Shin-Etsu Chemical Co., Ltd, poly(allylamine) and poly(N-iso-propylacrylamide) from Polysciences, Inc., Warrington, PA, hydroxypropyl cellulose from Hercules Polymer and Chemicals, Inc. Florida and carboxymethyl cellulose acetate butyrate from Eastman Chemical Company, Kingsport, TN. The synthesis of the cellulose  $\omega$ -carboxyalkanoates is described in refs 26 and 27. The abbreviations used in this report for the synthesized cellulose ester polymers (**Fig. 6.2**) are presented in **Table 6.1**.

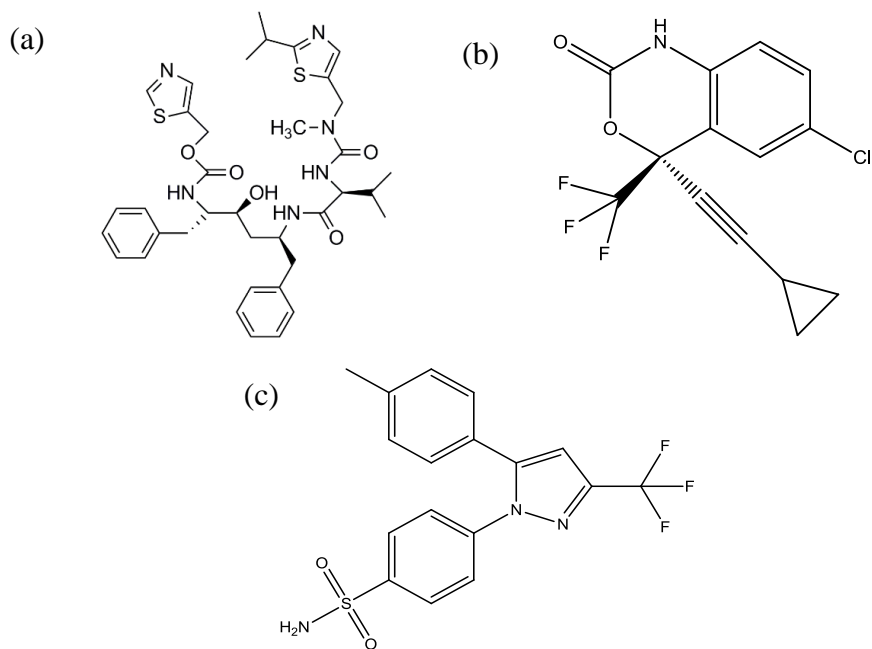


**Figure 6.1** Molecular structures of (a) ritonavir, (b) efavirenz and, (c) celecoxib

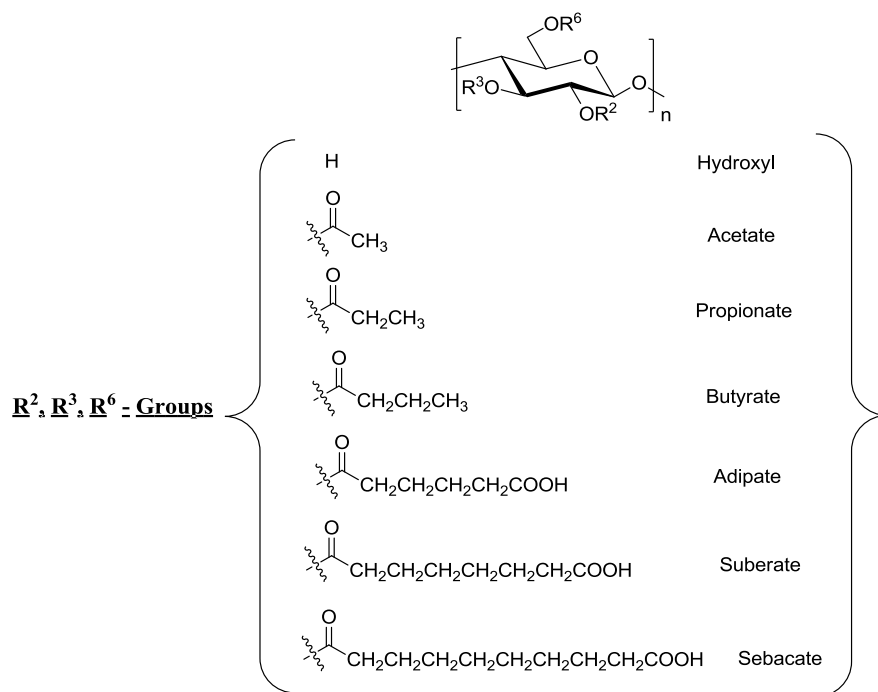


**Figure 6.2** Molecular structure of the novel synthesized cellulose derivatives and the substituent groups. These cellulose derivatives are not regioselectively substituted. The abbreviations are presented in Table 6.1.

**Table 6.1** Polymers additives and abbreviations used in this study

<b>Polymer</b>	<b>Abbreviation</b>
Poly( vinylpyrrolidone) (K 29/32)	PVP
Poly(vinylpyrrolidone vinyl acetate) (K 28)	PVPVA
Poly(allylamine)	PAIAmn
Poly(N-iso-propylacrylamide)	Pn-IPAAMD
Poly(acrylic acid)	PAA
Poly(4-vinylpyridine N-oxide)	PVPdn-O
Hydroxypropyl Cellulose	HPC
Cellulose Acetate Phthalate	CAPh
Hydroxypropyl methyl cellulose (606 grade)	HPMC
Hydroxypropyl methyl cellulose acetate succinate (AS-MF)	HPMCAS
Carboxymethyl cellulose acetate butyrate	CMCAB
Cellulose Propionate Adipate	CP Adp
Cellulose Acetate 320S Adipate	CA 320S Adp
Cellulose Acetate 320S Suberate 0.63	CA 320S Sub 0.63
Cellulose Acetate 320S Suberate 0.90	CA 320S Sub 0.90
Cellulose Acetate 320S Sebacate	CA 320S Seb
Cellulose Acetate Propionate 504-0.2 Adipate 0.85	CAP Adp 0.85
Cellulose Acetate Butyrate 553-0.4 Adipate 0.81	CAB Adp 0.81
Cellulose Acetate Propionate 504-0.2 Adipate 0.33	CAP Adp 0.33
Cellulose Acetate Butyrate 553-0.4 Adipate 0.25	CAB Adp 0.25
Cellulose Acetate Propionate Sebacate 0.24	CAP Seb
Cellulose Acetate Butyrate Sebacate	CAB Seb

## 6.3.2 Methods

### Solubility Parameter

The solubility parameter (SP) was used to characterize the relative hydrophobicity of the polymers and the model compounds. SP values were estimated using the method proposed by Fedors.<sup>28</sup> The solubility parameter can be evaluated using:

$$\delta = \sqrt{\frac{\sum_i \Delta e_i}{\sum_i \Delta v_i}} = \sqrt{\frac{\Delta E_v}{V}} \quad (6.1)$$

where the  $\Delta e_i$  and  $\Delta v_i$  are the additive atomic and group contributions to the energy of vaporization and molar volume, respectively,  $\Delta E_v$  is the energy of vaporization at a given temperature and  $V$  is the corresponding molar volume which is calculated from the known values of molecular weight and density. The method is based on group additive constants; therefore, it requires only knowledge of the structural formula of the compound. The group contributions at 25 °C are presented in ref. 28.

### Determination of Amorphous “Solubility” – Theoretical and Experimental

The theoretical amorphous solubility ( $C_{amorphous}$ ) of the model compounds was estimated using the experimentally determined crystalline solubility ( $C_{eq}$ ), the estimated free energy difference between crystalline and amorphous forms ( $\Delta G_c$ ), and the activity of the amorphous solute saturated with water ( $I(a_2)$ ):

$$C_{amorphous} = C_{eq} \cdot \exp[-I(a_2)] \cdot \exp\left[\frac{\Delta G_c}{RT}\right] \quad (6.2)$$

Using the heat of fusion ( $\Delta H_f$ ) and melting point ( $T_m$ ) determined from DSC analysis as described above, the free energy change for transformation of an amorphous solid to a crystalline solid was estimated at 37 °C ( $T$ ):<sup>29</sup>

$$\Delta G_C = \frac{\Delta H_f (T_m - T) T}{T_m^2} \quad (6.3)$$

The activity of the hydrated amorphous solute in contact with water ( $I(a_2)$ ) was estimated by applying the Gibbs-Duhem equation to the water sorption isotherm data for the amorphous solid. The detailed thermodynamic analysis is presented in ref. 30.

Amorphous samples were prepared by a solvent evaporation (spin-coating) method. Prior to use, the samples were analyzed by cross-polarized light microscopy and powder x-ray diffraction analysis to verify their amorphous nature. The experimental amorphous “solubility” of the model compounds was determined by dissolving the solid in 100 mM sodium phosphate buffer at pH 6.8, 37 °C. The glass slide was placed on a star-shaped stir bar (VWR International, LLC) and the solution stirred at a speed of 300 rpm. Solution concentration was measured using a SI Photonics (Tuscon, Arizona) UV spectrometer coupled to a fiber optic probe (path-length 5 mm). Wavelength scans (200 – 450 nm) were performed at 45 second time intervals. Second derivatives (SIMCA P+ V.12 software (Umetrics Inc., Umea Sweden) of the spectra were taken for the calibration and sample data in order to mitigate particle scattering effects. Calibration solutions (1.0 – 30.0 µg/mL) were prepared in methanol. The standard curve was linear over the aforementioned concentration range;  $r^2 > 0.999$  for the model compounds investigated.

### **Induction Time**

Crystal formation was characterized by measuring the induction time from unseeded-desupersaturation experiments. The onset of crystal formation at an equilibrium temperature (37 °C) was determined from the increase in intensity of light scattered (extinction) from the drug solutions. Light scattering was detected by monitoring the extinction, at 280 nm for ritonavir and 350 nm for celecoxib and efavirenz, using a SI Photonics UV/Vis spectrometer (Tuscon, Arizona), fiber optically coupled with a dip probe (path-length 5 mm); the compounds have no absorbance at these wavelengths. Wavelength scans (200 – 450 nm) were performed at 30 second time intervals. Solution concentration was also monitored during the desupersaturation experiments by monitoring absorption peaks. Supersaturated solutions were generated by adding a small volume of pre-dissolved drug in methanol to buffer. Solubilized drug (4 mg/mL) in methanol was titrated into buffer solution (50 – 80 mL) equilibrated at 37 °C, at a pH condition where the compound of

interest was un-ionized, using a syringe pump (Harvard Apparatus, Holliston, MA). Agitation of the solution at 300 rpm was achieved by use of a magnetic stirrer (Corning PC-420D, Fisher Scientific, Pittsburgh, PA). Induction time experiments were performed in the absence and presence of pre-dissolved polymers. A polymer concentration of 5  $\mu\text{g}/\text{mL}$  was used and all experiments were performed in triplicate. The induction times for celecoxib, efavirenz and ritonavir were determined at initial solution concentrations of 22, 19 and 20  $\mu\text{g}/\text{mL}$ , respectively. These concentration values correspond to the theoretical amorphous “solubility” of each drug. Data collection commenced immediately after the addition of the drug solution to the test medium. The effect of the ionization state of the polymer on the nucleation behavior of the solute was evaluated by performing experiments at pH 3.8 and 6.8, using 100 mM sodium acetate buffer and 100 mM sodium phosphate, respectively.

An important factor contributing to the nucleation mechanism and kinetics is the volume of solution in which nucleation occurs. Previous studies have shown that in relatively small volumes (~1 mL) and low supersaturation, the probability of nuclei formation in solution is low, leading to a large variation in induction time.<sup>31</sup> However, for the relatively large volume (50 – 80 mL) and high supersaturation ratios (2.4, 14.7 and 15.4 for efavirenz, celecoxib and ritonavir, respectively) utilized herein, it is reasonable to expect that the probability of nucleation formation will be high (due to random impurities in solution which may induce heterogeneous nucleation which has a lower energetic barrier compared to homogeneous nucleation), resulting in a relatively small variation in induction time measurements. This expectation appears to have been met as reflected by the relatively small variations (<15% error) in the values associated with the induction time measurements.

### **Crystal Growth Rate**

Crystal growth rate was characterized by measuring the rate of de-supersaturation in the presence of seed crystals. Celecoxib, efavirenz and ritonavir were used as received from the manufacturer and prior to use, the seeds were sieved to a size below 250  $\mu\text{m}$ . Crystal growth experiments were performed in a jacketed beaker connected to a digitally-controlled temperature water bath. Crystal growth rate experiments were performed at initial solution concentrations ranging from 2.5 – 20.0  $\mu\text{g}/\text{mL}$  in the absence and presence of pre-dissolved polymer present at a concentration of 5  $\mu\text{g}/\text{mL}$ . Supersaturation ratio (S) was expressed as:

$$S = \frac{C}{C_0} \quad (6.4)$$

where  $C$  is the concentration of the supersaturated solution and  $C_0$  is the equilibrium solubility at a given temperature. Here it is assumed that concentration is a reasonable substitute for thermodynamic activity because of the extremely dilute solutions involved in these studies. All experiments were performed in triplicate. Stock solutions (solubilized drug) of the drug compounds were prepared by dissolving 200 mg of drug in 50 mL of methanol to make a final stock solution of 4 mg/mL. Supersaturated solutions were generated by adding a small volume of solubilized drug in methanol to sodium phosphate buffer, pH 6.8 (50 mL); the amount of methanol added to the aqueous solution had a negligible impact on equilibrium solubility. The seeds (0.010 g) were added to the buffer and allowed to equilibrate at 37 °C prior to addition of solubilized drug in the absence/presence of selected polymer. The test solution was stirred at a constant speed of 400 rpm using a Cole Parmer (model 50000-20) overhead mixer attached to axial-flow impeller blade, with a digital mixer controller (Cole Parmer Instrument Co., Niles, IL). De-supersaturation profiles were measured using a SI Photonics UV spectrometer coupled to a fiber optic probe (path-length 5 mm) at a constant temperature of 37 °C. Wavelength scans (200 – 450 nm) were performed at 5 second time intervals. Data collection began immediately after generation of supersaturation. The slope of the concentration vs. time curve over the first 2 minutes of the experiment was taken as the initial bulk crystal growth rate ( $R_g$ ). The effect of the ionization state of the polymer on crystal growth rate was evaluated by performing experiments at pH 3.8 and 6.8, using 100 mM sodium acetate buffer and 100 mM sodium phosphate, respectively. Drug-polymer hydrophobic interactions were investigated by performing growth experiments in sodium phosphate buffer at two different ionic strengths, 50 mM and 100 mM.

## 6.4 Results

### 6.4.1 Physicochemical properties of model drug compounds

The three model compounds, celecoxib, efavirenz and ritonavir, were selected to cover a range of chemical structures and potential interactions with the polymers; their molecular structures are shown in **Fig. 6.1**. Celecoxib is an aromatic, very weakly acidic molecule (pKa

11.1).<sup>32</sup> Efavirenz is also a very weak acid (pKa 10.2), while ritonavir is a very weak base with two thiazole functional groups with pKa values of 1.8 and 2.6.<sup>33</sup> The model compounds were also selected because they possess intrinsic properties that are expected to result in poor aqueous solubility. Insolubility of pharmaceuticals results primarily from high melting point,  $T_m$  (representing lattice energy) and/or high Log P (lipophilicity).

Log P and solubility parameter (SP) values were used as indicators of hydrophobicity. In this study, Log P values were obtained from the ChemBioDraw Ultra version 12.0 (CambridgeSoft, Cambridge, MA) and literature sources, where the values were predicted using atomic contribution methods. The model compounds have different positive Log P values, indicative of varying levels of hydrophobicity. SP values provide a numerical estimate of the cohesive interactions within a material, and can provide an indication of relative polarity.<sup>28</sup> The higher the solubility parameter of a compound, the more hydrophilic it is; water has a SP value of 49.01 MPa<sup>1/2</sup>. Based on Log P and SP values (**Table 6.2**), ritonavir is the most hydrophobic of the model compounds, while celecoxib is the most hydrophilic, although all of the compounds can be characterized as being hydrophobic. Celecoxib had the highest melting point at 163.5 °C, while ritonavir had the lowest value of 122.7 °C.

**Table 6.2** Physicochemical properties of the model compounds

<b>Property</b>	<b>Ritonavir</b>	<b>Efavirenz</b>	<b>Celecoxib</b>
<b>pKa</b>	1.8 & 2.6	10.2	11.1
<b>Molecular Weight (g mol<sup>-1</sup>)</b>	720.9	315.7	381.4
<b>Log P</b>	5.6 <sup>a</sup>	4.7 <sup>a</sup>	3.5 <sup>b</sup>
<b>Solubility Parameter (MPa<sup>1/2</sup>)</b>	20.03	21.89	23.38
<b>Enthalpy of fusion (kJ mol<sup>-1</sup>)</b>	60.4	14.5	37.6
<b>Melting Point ( °C)</b>	122.7	139.0	163.5
<b>Equilibrium Solubility (µg mL<sup>-1</sup>)<sup>c</sup></b>	1.3	8.2	1.5
<b>Theoretical Amorphous “Solubility” (µg mL<sup>-1</sup>)</b>	20.6	19.8	22.6
<b>Experimental Amorphous “Solubility” (µg mL<sup>-1</sup>)</b>	19.8	12.3	2.5
<b>Crystallization Tendency Classification<sup>c</sup></b>	III	III	II

<sup>a</sup> As reported in ChemBioDraw Ultra v11.0, CambridgeSoft Corp., Cambridge, MA. <sup>b</sup> Ref. 32. <sup>c</sup> determined at pH 6.8 and 37 °C, Ref. 38. <sup>d</sup> Ref. 37.



The equilibrium solubility values of crystalline celecoxib, efavirenz and ritonavir at pH 6.8 and 37 °C, where all the molecules exist in the un-ionized form, were determined to be 1.3, 8.2 and 1.5 µg/mL, respectively; all model compounds thus have extremely poor aqueous solubility. The equilibrium solution concentrations of these compounds in the presence of selected polymers at polymer concentrations of 5 µg/mL were also measured. At this polymer concentration, the effect of polymers on the equilibrium solubility of the model compounds is negligible.

The theoretical amorphous “solubility” of the compounds, which incorporates the impact of absorbed water on the thermodynamic activity, is also summarized in **Table 6.2**. The theoretical “solubility” of an amorphous solid is rarely achieved under typical experimental conditions because of the strong driving force for crystallization in the presence of dissolution media.<sup>34</sup> There are two crystallization pathways: crystallization of the dissolving amorphous solid, and crystallization from the supersaturated solution generated following dissolution. The experimental and theoretical “solubility” values for amorphous ritonavir are quite similar, indicating that the rate of crystallization of the dissolving amorphous solid exposed to aqueous solution as well as from the supersaturated solution is relatively slow. Thus a supersaturated solution with a concentration close to the theoretical amorphous “solubility” is generated and crystallization will subsequently occur from the supersaturated solution<sup>35</sup>. In contrast, there is a notable difference between the theoretical and experimentally determined amorphous “solubility” values for both celecoxib and efavirenz. In particular, the dissolution of amorphous celecoxib generated a solution with a low maximum extent of supersaturation (*S* of 1.7) compared to the expected value, indicating that crystallization was rapid. Although ritonavir and celecoxib have comparable theoretical amorphous “solubility” values (20.6 and 22.6 µg/mL, respectively), from these results, it can be deduced that ritonavir has a much slower crystallization tendency. Previous studies have shown that different compounds have very different crystallization tendencies both upon cooling from the melt as well as during rapid solvent evaporation and compounds have been classified as fast (Class I), intermediate (Class II) or slow crystallizers (Class III) depending on the behavior shown during solidification processes.<sup>36,37</sup> These classifications are shown in **Table 6.2** for the model compounds evaluated in this study. Based upon the crystallization tendency from the undercooled melt, ritonavir and efavirenz are slow crystallizers, while celecoxib is an intermediate crystallizer. The facile crystallization of celecoxib and efavirenz following dissolution of the

amorphous solids suggests that these compounds have much more rapid nucleation rates than that of ritonavir.

#### **6.4.2 Impact of polymers on nucleation inhibition of the model compounds**

The crystallization tendencies of the drug molecules from solution can be inferred from their nucleation-induction times. At the beginning of the desupersaturation experiment, minimum turbidity (from light scattering measurements) was apparent, since the solution was initially clear and no particulates were present in solution. However, when nuclei begin to form and grow into detectable macroscopic crystals, the turbidity of the solution began to increase. The induction time,  $t_{ind}$ , was determined by plotting extinction versus time and drawing regression lines through the two distinct linear regions. The intersection point of the regression lines for these two regions was taken as the  $t_{ind}$ . Representative plots are shown in **Fig. 6.3 (a) – (f)**. During the desupersaturation experiments, solution concentration was maintained at the initial solution concentration until the onset of crystal formation (marked by an increase in extinction), after which solution concentration was observed to simultaneously rapidly decrease, as indicated by a decrease in intensity of the UV absorption peaks, towards the equilibrium solubility, due to the subsequent growth of the crystals. The average induction times of celecoxib, efavirenz and ritonavir in the absence of polymer were approximately 2, 5 and 120 min, respectively. Based on these induction times, it is apparent that the rate of nucleation of ritonavir from supersaturated solutions was much slower compared to those of celecoxib and efavirenz, most likely as a result of the higher molecular weight and greater conformational flexibility of ritonavir.

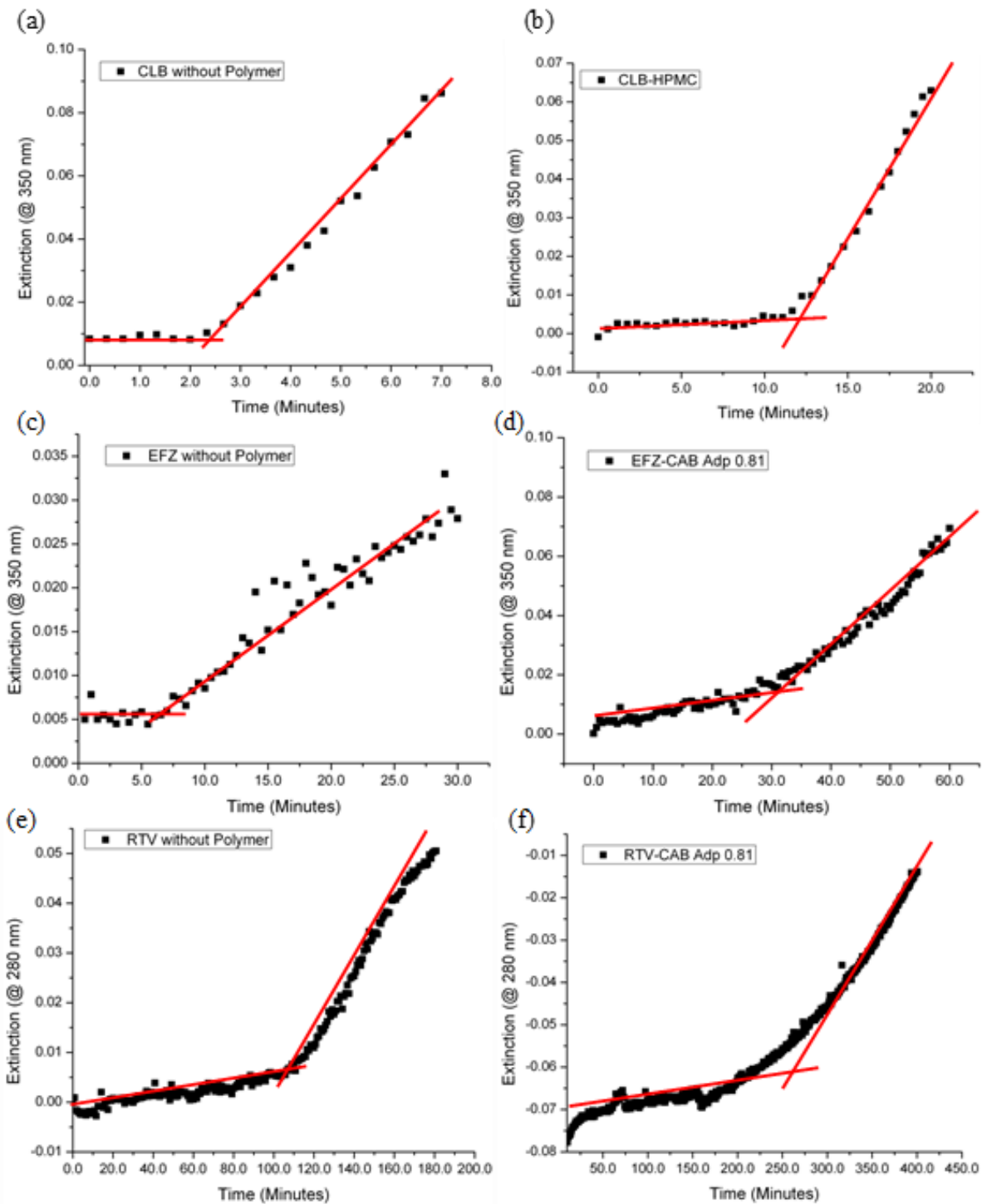


**Figure 6.3** Representative plots of extinction (which characterizes turbidity) with time from desupersaturation experiments for celecoxib (a & b), efavirenz (c & d) and ritonavir (e & f), in the absence and presence of the most effective polymers for each of the model compounds

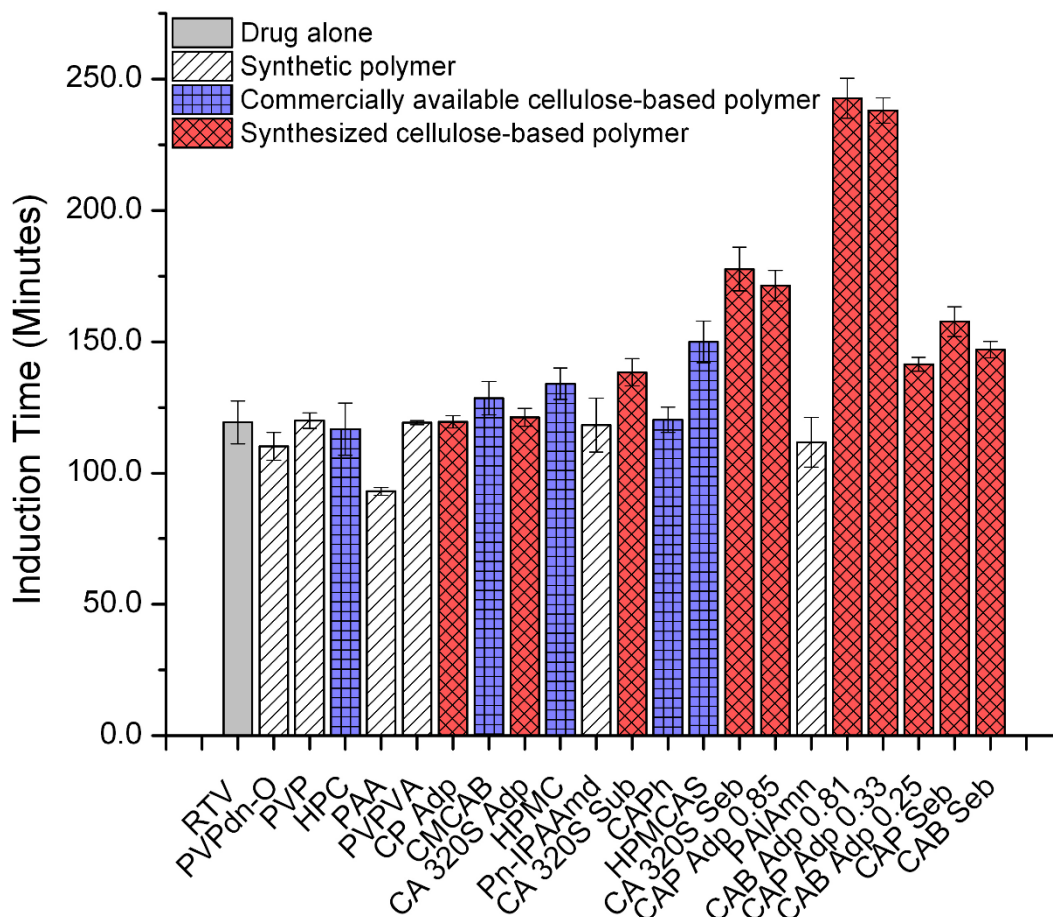


**Figure 6.4** Induction times for ritonavir, from unseeded desupersaturation experiments, in the absence and presence of polymers (n = 3). An initial concentration corresponding of 20  $\mu\text{g/mL}$  ritonavir and the polymer concentration was 5  $\mu\text{g/mL}$ .

**Fig. 6.4** shows a representative comparison of the nucleation-induction time measurements for ritonavir in the absence and presence of polymer. Results on celecoxib and Efavirenz are presented in Ref. 38. The polymers are arranged in order of increasing hydrophobicity (left to right based on decreasing SP values); the calculated SP values of the polymers tested in this study are summarized in **Table 6.3**. A wide range of polymers with different structures and properties was employed, 6 of which were synthetic polymers (white columns) while the other 15 were cellulose-based polymers (blue and red columns). Ten of the 15 cellulose-based polymers were recently synthesized cellulose esters (red columns), designed to span a wider range of hydrophobicities and chemical functionality than commercially available cellulose derivatives.<sup>27</sup> For ritonavir (**Fig. 6.4**),

9 out of the 21 investigated polymers were effective ( $t_{ind} > 120$  min), while 14 and 15 polymers had an impact on induction times for efavirenz and celecoxib (Ref 38), respectively, although to varying extents. CAB Adp 0.81, CAP Adp 0.85, CA 320 Seb and CAP Adp 0.33, four of the recently synthesized cellulose derivatives, were the most effective nucleation inhibitors for both efavirenz and ritonavir, increasing the induction time significantly relative to the commercially available and more frequently used polymers, HPMCAS, HPMC and CMCAB. For ritonavir, the induction time was increased by a factor of two from 120 minutes in the absence of a polymer, to approximately 250 min in the presence of CAB Adp 0.81, the most effective inhibitor. For efavirenz, the induction time increased by a maximum factor of approximately 5, from 5 min to 25 min with CAB Adp 0.81 again being the most effective inhibitor. The very hydrophilic polymers had no impact on induction times for either compound. For celecoxib a more chemically diverse, and more hydrophilic group of polymers – HPMC, HPMCAS and CA 320S Adp – was the most effective at extending the induction time. For celecoxib, hydrophobic polymers are ineffective, while the most hydrophilic polymers have some effect and moderately hydrophobic polymers are the most effective at increasing the induction times. Celecoxib had the shortest induction time of the three model compounds, and the most effective polymers were only able to increase the induction time from 2 min to approximately 13 min.

Summarizing, in general, the hydrophilic polymers were ineffective in inhibiting crystal formation of the more hydrophobic compounds, efavirenz and ritonavir (SP values of 20.03 and 21.89, respectively), while the more hydrophobic cellulose-based polymers (both commercially available and in-house synthesized cellulose-based polymers) were effective nucleation inhibitors. In contrast, for the more hydrophilic celecoxib (SP value of 23.38), the hydrophilic polymers and some of the moderately hydrophobic cellulose-based polymers were effective in increasing induction times, while the more hydrophobic polymers were ineffective. A side-by-side comparison of the impact of the investigated polymers on induction times of the model compounds is presented in **Table 6.3**, where the very effective, moderately effective and ineffective polymers are color coded green, yellow and pink, respectively.

**Table 6.3** Solubility parameter (SP) values of the polymers investigated; summary and comparison of the effect of polymers on the drug molecules

<b>Ritonavir</b>	<b>Efavirenz</b>	<b>Celecoxib</b>	<b>SP (MPa<sup>1/2</sup>)</b>	
CAB Seb	CAB Seb	CAB Seb	19.62	
CAP Seb	CAP Seb	CAP Seb	19.94	
CAB Adp 0.25	CAB Adp 0.25	CAB Adp 0.25	20.05	→ Ritonavir (20.03 MPa <sup>1/2</sup> )
CAP Adp 0.33	CAP Adp 0.33	CAP Adp 0.33	20.56	
PAIAmn	PAIAmn	PAIAmn	20.70	
CAB Adp 0.81	CAB Adp 0.81	CAB Adp 0.81	20.86	
CAP Adp 0.85	CAP Adp 0.85	CAP Adp 0.85	21.27	→ Efavirenz (21.89 MPa <sup>1/2</sup> )
CA 320S Seb	CA 320S Seb	CA 320S Seb	22.36	
HPMCAS	HPMCAS	HPMCAS	22.44	
CAPh	CAPh	CAPh	22.48	
CA 320S Sub	CA 320S Sub	CA 320S Sub	22.62	
Pn-IPAAmd	Pn-IPAAmd	Pn-IPAAmd	22.64	
HPMC	HPMC	HPMC	22.68	
CA 320S Apd	CA 320S Apd	CA 320S Apd	22.95	
CMCAB	CMCAB	CMCAB	23.18	
CP Adp	CP Adp	CP Adp	23.28	→ Celecoxib (23.38 MPa <sup>1/2</sup> )
PVPVA	PVPVA	PVPVA	25.77	
PAA	PAA	PAA	25.92	
HPC	HPC	HPC	25.98	
PVP	PVP	PVP	28.39	
PVPdn-O	PVPdn-O	PVPdn-O	32.24	

<sup>a</sup>The ineffective polymers, moderately and very effective polymers are color coded pink, yellow and green, respectively. The arrows indicate the approximate SP value of each model compound. RTV: (Green: > 145 min); EFZ: (Green: >17 min, yellow: 5 – 16 min); CLB: (Green > 7 min, yellow: 2 – 6 min).

### 6.4.3 Impact of polymers on crystal growth inhibition of the model drug compounds

The effectiveness of the polymers for the model compounds was investigated at an initial compound concentration of 10  $\mu\text{g/mL}$  and this initial concentration corresponds to an initial supersaturation ratio ( $S$ ) of 6.6 for celecoxib, 1.2 for efavirenz and 7.6 for ritonavir. Higher levels of inhibition by the polymers were expected for efavirenz, since crystal growth rate experiments were performed at a relatively low supersaturation. The effectiveness ( $E_g$ ) of the polymers in inhibiting crystal growth was estimated using the following equation:

$$E_g = \frac{R_{g_o}}{R_{g_p}} \quad (1)$$

where  $R_{g_o}$  and  $R_{g_p}$  are the initial bulk crystal growth rate in the absence and presence of polymer, respectively. **Fig. 6.5** shows an example of the desupersaturation rate for seeded crystal growth in the presence and absence of a polymer at an initial ritonavir concentration of 10  $\mu\text{g/mL}$ . From these data, CAP Adp 0.85 3X and CAP Adp 0.33 1X (5  $\mu\text{g/mL}$ ) are quite effective inhibitors for ritonavir at this supersaturation. On the other hand, CAB Adp 0.25 1X is shown to be ineffective crystal growth inhibitors.

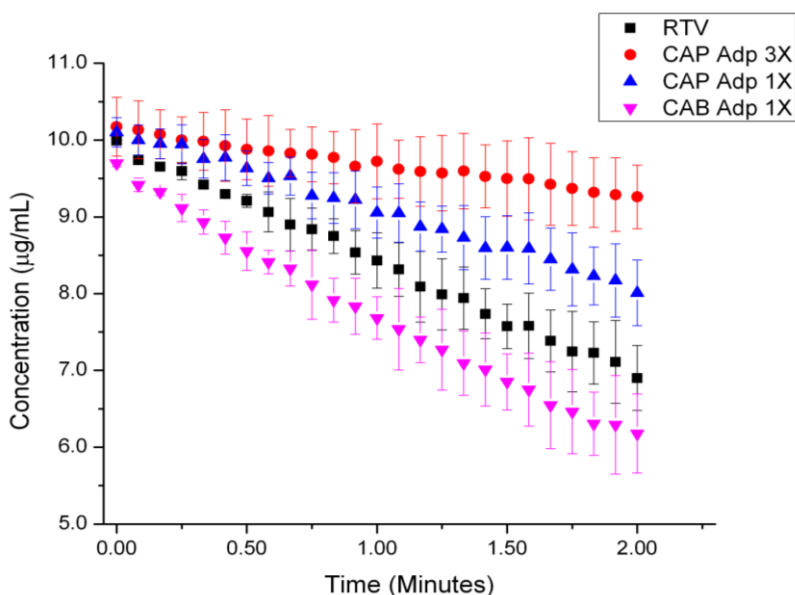


**Figure 6.5** Rate of desupersaturation of ritonavir with seed crystals in the absence and presence of

polymer at an initial concentration of 10  $\mu\text{g/mL}$  ritonavir. All experiments were performed in triplicate and errors indicate one standard deviation

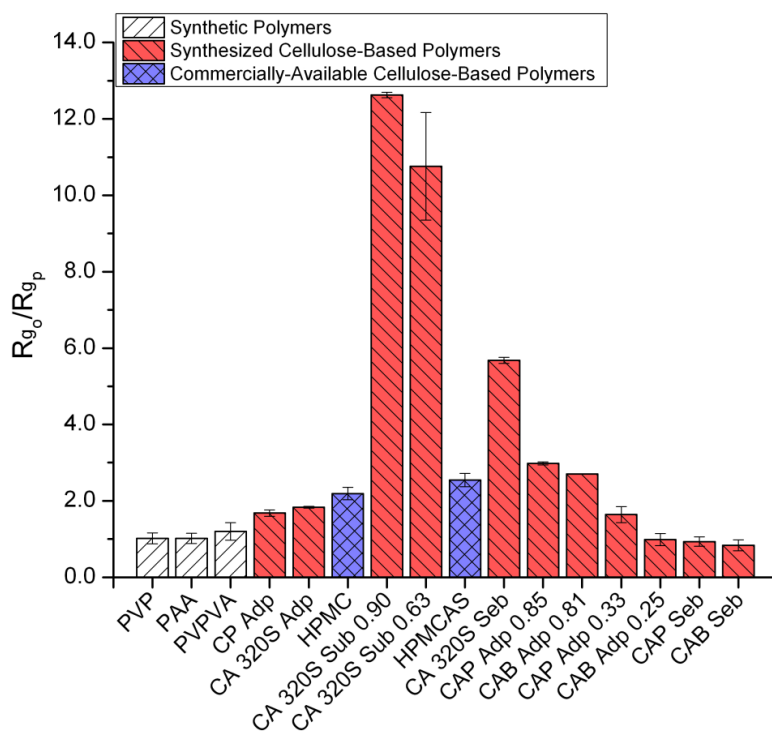


**Figure 6.6** Crystal growth rate ratio of ritonavir at an initial concentration of 10  $\mu\text{g/mL}$ . The data is arranged in order of hydrophobicity: least hydrophobic to most hydrophobic (left to right). Crystal growth rate experiments were performed in triplicate. Each column is an average of the effectiveness ratio of the polymers (5  $\mu\text{g/mL}$ ) and error bars indicate one standard deviation

**Fig. 6.6** shows a comparison of the growth rate ratios of ritonavir at an initial concentration of 10  $\mu\text{g/mL}$  in the absence of polymer ( $R_{g_0}$ ) to the growth rate in the presence of each polymers investigated ( $R_{g_p}$ ). Results on celecoxib and efavirenz are presented in Ref. 39. The polymers are arranged in order of increasing hydrophobicity (left to right based on decreasing SP values); the calculated SP values of the polymers tested in this study are summarized in **Table 6.3**. Sixteen polymers with different structures and properties were employed, 3 of which were synthetic polymers (white columns) while the other 13 were cellulose-based polymers (blue and red columns). Eleven of the 13 cellulose-based polymers were recently synthesized cellulose  $\omega$ -carboxyalkanoate esters (red columns), designed to be effective amorphous solid dispersion



polymers, and spanning a wider range of hydrophobicities and chemical functionality than commercially available cellulose derivatives (blue columns). Out of the 16 investigated polymers, 13 were effective for efavirenz, 10 were effective for ritonavir, and 12 were effective for celecoxib

$\left( \frac{R_{g_0}}{R_{g_p}} > 1 \right)$ , although to different extents. It should be noted that three of the in-house synthesized cellulose derivatives were designed based on insights into the key polymer properties responsible for effective growth rate inhibition gained during an initial study with ritonavir.<sup>27</sup> These second generation novel cellulose-based polymers, CA 320S Sub 0.63, CA 320S Sub 0.90 and CA 320S Seb 0.57 (number stands for degree of substitution of carboxylic-bearing ester) were much more effective at inhibiting the crystal growth of ritonavir compared to commercially available polymers as well as the best of the first generation cellulose derivatives that we investigated (CAP Adp 0.85 and CAB Adp 0.81). For celecoxib the moderately hydrophobic commercially available polymers were the most effective inhibitors shown in Ref. 39: HPMC > HPMCAS > PVPVA; HPMC was a very effective crystal growth inhibitor of celecoxib, inhibiting crystal growth by a factor of 10.2 while the most effective of the newly synthesized cellulose derivatives was CA 320S Sub 0.90, which inhibited the growth by a factor of about 7. A set of chemically diverse polymers was effective in inhibiting crystal growth of efavirenz shown in Ref. 39, whereby the two most effective polymers were PVPVA, a non-cellulose derivative, and the newly synthesized cellulose derivative, CA 320S Sub 0.90. The best performing polymers were: PVPVA  $\approx$  CA 320S Sub 0.90 > CAP Adp 0.85  $\approx$  HPMCAS, whereby, PVPVA and CA 320S Sub 0.90, both inhibited growth by a factor of  $\sim$ 5.0; it should be noted that for efavirenz, the initial S was very low (1.2). In contrast, for ritonavir (**Fig. 6.6**), the moderately hydrophobic newly synthesized cellulose-based polymers were most effective: CA 320S Sub 0.90 > CA 320S Sub 0.63 > CA 320S Seb > CAP Adp 0.85 > CAB Adp 0.81. The second-generation polymer, CA 320S Sub 0.90, was the most effective cellulose-based polymer for both efavirenz and ritonavir, inhibiting crystal growth by factors of 4.9 and 12.8, respectively. Interestingly, the hydrophilic and synthetic polymers, PVP and PVPVA, were effective crystal growth inhibitors for celecoxib and efavirenz but not for ritonavir, while PAA was ineffective for all the model compounds. Summarizing, in general the most hydrophobic newly synthesized cellulose  $\omega$ -carboxyalkanoate derivatives were ineffective in inhibiting crystal growth, while the moderately hydrophobic cellulose-based polymers, both those commercially

available and the new cellulose  $\omega$ -carboxyalkanoate polymers, were effective crystal growth inhibitors for the model drug compounds. The very hydrophilic synthetic polymers were highly variable in effectiveness.

## 6.5 Discussion

### 6.5.1 Impact of polymers on nucleation-induction times

Preventing crystallization is an essential component of any drug delivery strategy that utilizes supersaturation to enhance mass transport across a biological membrane. It is clear from the results of this study that polymers should not be selected arbitrarily for this purpose, and that the effectiveness of a given polymer seems to be linked to the properties of the crystallizing solute. Based on the data presented in **Fig. 6.4** and **Table 6.3**, it is apparent that the hydrophobicity of the polymer relative to that of the drug molecule appears to be a key parameter in determining the impact of a given polymer on the nucleation rate. From a theoretical perspective and considering only non-specific interactions, the hydrophobicity of the polymer relative to the drug affects the affinity of polymer segments for the drug molecules. This will impact the ability of the polymer to mix with drug pre-nucleation aggregates which in turn would be expected to influence the effectiveness of the polymer as a nucleation inhibitor. A two-step nucleation model proposes that a sufficient-sized disordered cluster of solute molecules forms first, followed by reorganization of that cluster into an ordered structure. Here we assume that polymers most likely affect nucleation by hindering the reorganization of a cluster of solute molecules into an ordered structure, which is proposed to be the rate-limiting step of the two-step nucleation model. An effective nucleation inhibitor should thus interact favorably with the solute. A strong affinity of the polymer for the solute, relative to that for the solvent and other polymer molecules in solution, not only ensures that the polymer molecules interact with the solute aggregates, but also leads to disruption of the reorganization of the solute clusters.<sup>12</sup> If a polymer is very hydrophilic relative to the solute molecules, it would be expected to have a higher affinity for water molecules, while if the polymer is too hydrophobic, it is likely to interact more favorably with other polymer molecules. Based on this reasoning, it is apparent that the ability of the polymer to inhibit crystal nucleation will be dependent on both the properties of the drug and polymer; a polymer should have hydrophobicity

similar to that of the solute to maximize non-specific interactions, or alternatively be able to form highly favorable specific interactions with the drug to be an effective nucleation inhibitor. These expectations are in general supported by the results of this study. Cellulose polymers that had a SP values close to that of the drug molecule were effective nucleation inhibitors; that is polymers with relatively similar hydrophobicity to the drug molecule were effective. For ritonavir (SP 20.03 MPa<sup>1/2</sup>), cellulose polymers with SP value ranging from 19.62 – 22.44 MPa<sup>1/2</sup> were effective crystallization inhibitors, albeit to varying extents (**Table 6.4**). The average SP value of the polymers within the aforementioned range is 20.87 MPa<sup>1/2</sup>, which is comparable to the SP value of ritonavir (20.03). In contrast, for the more hydrophilic celecoxib with a SP value of 23.38 MPa<sup>1/2</sup>, polymers with SP values ranging from 21.27 – 32.24 MPa<sup>1/2</sup> were effective, where the average SP value for this group of polymers is 24.28 MPa<sup>1/2</sup>. In general, for the three model compounds investigated in this study, the average SP value for the group of effective polymers is close to the SP value of the drug molecule (**Table 6.4**).

**Table 6.4** Comparison of the SP values of the model compounds and average SP value of the effective polymers

<b>Compound</b>	<b>SP Value of Compound<sup>a</sup></b>	<b>Effective Polymer SP Range</b>	<b>Average SP Value of Effective Polymers</b>
<b>Ritonavir</b>	20.03	19.62 -22.44	20.87
<b>Efavirenz</b>	21.89	19.62 - 23.28	21.73
<b>Celecoxib</b>	23.38	21.27 - 32.24	24.28

<sup>a</sup>SP unit in MPa<sup>1/2</sup>

For efavirenz and ritonavir, the synthetic polymers were ineffective in inhibiting nucleation, even when they had solubility parameters similar to the drug molecule as for Pn-IPAAmd and PAIAm (Fig. 6.4). However, in addition to drug-polymer interactions, the structure of the polymer monomer units may also influence the ability of the polymer to disrupt the packing of solute molecules. The ineffectiveness of the synthetic polymers perhaps can be attributed to their flexible structures compared to the relatively rigid structure of the cellulose-based polymers. Higher levels of disruption can be caused by steric effects due to the bulky substituent groups of the cellulose esters and lower degrees of freedom of the polymer molecules compared to that of the smaller-flexible synthetic polymers.<sup>12,40,41</sup>

## 6.5.2 Impact of polymers on crystal growth rate

Two important observations are highlighted here. First, a polymer that is an effective nucleation inhibitor may not have a similar impact on the inhibition of crystal growth, especially at high supersaturations. The polymers that were the most effective nucleation inhibitors for ritonavir and efavirenz (CAB Adp 0.81, CAP Adp 0.33 and CAP Adp 0.85) do not correspond to the polymer(s) that inhibit crystal growth to the greatest extent (CA 320S Sub 0.63 and CA 320S Sub 0.90), while for celecoxib, HPMC was the most effective polymer for both nucleation and crystal growth inhibition. Second, the effectiveness of a polymer as a crystal growth rate inhibitor is highly dependent on its structure. For ritonavir, a clear trend was observed between polymer hydrophobicity and effectiveness in reducing crystal growth rates, whereby very hydrophilic and very hydrophobic polymers were ineffective. This result suggests that the extent of drug-polymer hydrophobic interactions is one important factor in determining polymer effectiveness, in particular among the cellulose derivatives.

The results of the current study fully support the hypothesis that the cellulosic polymers interact with drugs via non-specific interactions. For the hydrophobic drug compounds (Log P: 3.5 – 5.6; SP values: 20.03 – 23.38 MPa<sup>1/2</sup>) investigated herein, the very hydrophobic polymers with SP values greater than 20.56 MPa<sup>1/2</sup> were ineffective, while the moderately hydrophobic polymers located in middle portion of **Fig. 6.6**, with SP values ranging from 20.56 – 23.28 MPa<sup>1/2</sup>, were effective crystal growth inhibitors. However, interestingly, the most effective cellulosic polymer does vary for different drug structures. For the more hydrophobic ritonavir and efavirenz, the second generation cellulose-based polymers (CA 320S Sub/Seb) appeared to interact with crystal most effectively while, for celecoxib, the slightly more hydrophilic HPMC was the best polymer. The recently designed polymers, CA 320S Sub 0.63 and CA 320S Sub 0.90, showed good inhibition for all three compounds, and thus appear to be interesting candidate polymers for supersaturating dosage forms. This polymer has an amphiphilic structure arising from the relatively hydrophilic cellulose acetate backbone combined with the ionizable fatty acid suberate substituent. This amphiphilic structure may promote interaction with drug substances leading to crystallization inhibition. Further exploration of the effectiveness of this cellulose ester derivative,

relative to commonly employed pharmaceutical polymers (e.g. HPMC and HPMCAS), therefore appears to be warranted.

For the synthetic, somewhat hydrophilic polymer, PVPVA, an effective inhibitor for celecoxib and efavirenz, there was no significant change in polymer effectiveness at different ionic strengths which affect the extent of drug-polymer hydrophobic interactions, suggesting a different mechanism of interaction with this polymer. Electrostatic interactions are unlikely since PVPVA and the drug compounds, celecoxib and efavirenz, are un-ionized at pH 6.8. Hence, we surmise that the main interactive force that drives adsorption of PVPVA is the formation of specific inter-molecular interactions. The amide and sulfonamide functional groups on efavirenz and celecoxib, respectively, are likely form to inter-molecular hydrogen bonds with the carbonyl-oxygen on PVPVA. The higher level of effectiveness of PVPVA in comparison to PVP, which also possesses a carbonyl-oxygen, may be attributed to the more hydrophobic nature of PVPVA compared to PVP. Evidence for the formation of specific interactions is supported by the FTIR data presented in Ref 39. The formation of specific inter-molecular interactions was also proposed to be important for crystal growth inhibition of ritonavir by poly(N-isopropylacrylamide) (Pn-IPAAmd), whereby polymer hydrophobicity alone was inadequate to explain the effectiveness of Pn-IPAAmd in inhibiting ritonavir crystal growth. Specific inter-molecular interactions have been found to contribute to the adsorption of polymer onto solids and thus, are important for controlling a number of interfacial processes such as crystal growth.<sup>17,22</sup> Based on our results, it appears that both specific and non-specific interactions are important for polymer adsorption to the crystallizing solid and both influence polymer effectiveness as a growth modifier. Thus although polymer adsorption appears to be mainly driven by hydrophobic interactions (in particular for cellulose derivatives), specific inter-molecular interactions also play an important role when the chemical structures of the drug and polymer favor their formation.

**Note:** Effects of polymer ionization, level of supersaturation, ionic strength and binary polymer combinations on drug nucleation and crystal growth from supersaturated solution, which were detailedly described in our publications, are not covered in this dissertation due to limited length.

## 6.6 Conclusion

In this study, the effectiveness of a set of structurally and chemical diverse polymers, added at low levels, on the nucleation and crystal growth of three hydrophobic poorly-water soluble compounds – celecoxib, efavirenz and ritonavir – was quantified and compared. The polymers that were effective inhibitors were found to have (1) an optimal level of hydrophobicity – the effective polymers had a similar hydrophobicity to the drug molecule, and (2) structure – the cellulose derivatives with relatively rigid structure and bulky substituent groups were more effective inhibitors compared to the synthetic polymers, even when the level of hydrophobicity of the synthetic polymers was similar to that of the cellulose-based polymers. These polymer-solute interactive forces are likely to disrupt the reorganization of a cluster of solute molecules into an ordered crystal structure and also promote polymer adsorption onto the surface of formed drug crystal.

The effectiveness of the cellulose-based polymers, in particular the synthesized cellulose-based polymers, was found to depend on the extent of ionization of the carboxylic acid substituents, the degree of supersaturation, and the inherent crystallization tendency of the drug molecule. These insights into key polymer properties that affect crystallization inhibition of chemically and structurally different drug molecules gained from this study are important for the development of new excipients with superior crystallization inhibitory properties used for enhanced oral drug delivery.

## 6.7 References

1. Kwong, A. D.; Kauffman, R. S.; Hurter, P.; Mueller, P. Discovery and development of telaprevir: an NS3-4A protease inhibitor for treating genotype 1 chronic hepatitis C virus. *Nature Biotechnology*, **2011**, 29, 933 – 1003.
2. Bollag, G.; Hirth, P.; Tsai, J.; et, al. Clinical efficacy of a RAF inhibitor needs broad target blockade in BRAF-mutant melanoma. *Nature*, **2010**, 467, 596 – 599.
3. Gao, P.; Guyton, M. E.; Huang, T.; Bauer, J. M.; Stefanski, K. J.; Lu, Q. Enhance oral bioavailability of a poorly water soluble drug PNY-91325 by supersaturatable formulations. *Drug Development and Industrial Pharmacy*, **2004**, 30, 221 – 229.
4. Simonelli, A. P.; Mehta, S.C.; Higuchi, W.I. Inhibition of sulfathiazole crystal growth by polyvinylpyrrolidone. *Journal of Pharmaceutical Sciences*, **1970**, 57, 633 – 638.

5. Vandecruys, R.; Peeters, J.; Verreck, G.; Brewster, M. E. Use of a screening method to determine excipients which optimize the extent and stability of supersaturated drug solutions and application of this system to solid formulation design. *International Journal of Pharmaceutics*, **2007**, 342, 168 – 175.
6. Simonelli, A. P.; Mehta, S. C.; Higuchi, W. I. Inhibition of sulfathiazole crystal growth by polyvinylpyrrolidone. *Journal of Pharmaceutical Sciences*, **1970**, 59, 633 – 638.
7. Alonzo, D. E.; Zhang, G. G. Z.; Zhou, D.; Gao, Y.; Taylor, L.S. Understanding the behavior of amorphous pharmaceutical systems during dissolution. *Pharmaceutical Research*, **2009**, 27, 608 – 618.
8. Dai, W. G.; Dong, L.C.; Shi, X. F.; Nguyen, J.; Evans, J.; Xu, Y. D.; Creasey, A. A. Evaluation of drug precipitation of solubility enhancing liquid formulations using milligram quantities of a new molecular entity (NME). *Journal of Pharmaceutical Sciences*, **2007**, 96, 2957 – 2969.
9. Gao, P.; Akrami, A.; Alvarez, F.; Hu, J.; Li, L.; Ma, C.; Surapaneni, S. Characterization and optimization of AMG 517 supersaturatable self-emulsifying drug delivery system (S-SEDDS) for improved oral absorption. *Journal of Pharmaceutical Sciences*, **2009**, 98, 516 – 528.
10. Alonzo, D. E.; Raina, S.; Zhou, D.; Gao, Y.; Zhang, G. G. Z.; Taylor, L. S. Characterizing the impact of hydroxypropylmethyl cellulose on the growth and nucleation kinetics of felodipine from supersaturated solutions. *Crystal Growth and Design*, 2012, 12, 1538 – 1547.
11. Rodriguez-Hornedo, N.; Murphy, D. Significance of controlling crystallization mechanisms and kinetics in pharmaceutical systems. *Journal of Pharmaceutical Sciences*, **1999**, 88, 651 – 660.
12. Anwar, J.; Boateng, P. K.; Tamaki, R.; Odedra, S. Mode of action and design rule for additives that modulate crystal nucleation. *Angewandte Chemie International Edition*, **2009**, 48, 1596 – 1600.
13. P. Gao; M. E. Guyton; T. Huang; J. M. Bauer; K. J. Stefanski; Q. Lu. Enhanced oral bioavailability of a poorly water soluble drug PNU-91325 by supersaturatable formulations. *Drug Dev. Ind. Pharm.*, **2004**, 30, 221–229.
14. H. Suzuki; H. Sunada. Influence of water-soluble polymers on the dissolution of nifedipine solid dispersions with combined carriers. *Chem. Pharm. Bull.*, **1998**, 46, 482–487.
15. Y. Yokoi; E. Yonemochi; K. Terada. Effects of sugar ester and hydroxypropyl methylcellulose on the physicochemical stability of amorphous cefditoren pivoxil in aqueous suspension. *Int. J. Pharm.*, **2005**, 290, 91–99.
16. Hasegawa, A. et al. Supersaturation mechanism of drugs from solid dispersion with enteric coating agents. *Chemical Pharmaceutical Bulletin*, **1988**, 36(12): 4941 – 4950.
17. Somasundaran, P., Krishnakumar, S. Adsorption of surfactants and polymers at the solid-liquid interface. *Colloids and Surfaces A: Physicochemical and Engineering Aspects*, **1997**, 123 – 124: 491 – 513.
18. Zimmermann, A., Millqvist-Fureby, A., Elema, M.R., Hansen, T., Mullertz, A. and Hovgaard, L. Adsorption of pharmaceutical excipients onto microcrystals of siramesine hydrochloride: Effects of physicochemical properties. *European Journal of Pharmaceutics and Biopharmaceutics*, **2009**, 71: 109 – 116.
19. Tian, F., Saville, D. J., Gordon, K. C., Strachan, C. J., Zeitler, J. A., Sander, N. Rades, T. The influence of various excipients on the conversion kinetics of carbamazepine polymers in aqueous suspension. *Journal of Pharmacy and Pharmacology*, **2007**, 59: 193 – 201.
20. Pan, Z., Campbell, A., Somasundaran, P. Polyacrylic acid adsorption and conformation in concentrated alumina suspensions. *Colloids and Surfaces A: Physicochemical and Engineering Aspects*, **2001**, 191: 71 – 78.
21. Tjipangandjara, K. F. and Somasundaran, P. Effects of changes in adsorbed polyacrylic acid conformation on alumina flocculation. *Colloids and Surfaces*, **1991**, 55: 245 – 255.
22. Somasundaran, P., Huang, L. Adsorption/aggregation of surfactants and their mixtures at solid-liquid interfaces. *Advances in Colloid and Interface Science*, **2000**, 88: 179 – 208.
23. Zimmermann, A., Millqvist-Fureby, A., Elema, M.R., Hansen, T., Mullertz, A. and Hovgaard, L. Adsorption of pharmaceutical excipients onto microcrystals of siramesine hydrochloride: Effects of

- physicochemical properties. *European Journal of Pharmaceutics and Biopharmaceutics*, **2009**, 71: 109 – 116.
24. Posey-Dowty, J. D.; Watterson, T. L.; Wilson, A. K.; Edgar, K. J.; Shelton, M. C.; Lingerfelt Jr., L. R. Zero-order release formulations using a novel cellulose ester. *Cellulose*, **2007**, 14: 73 – 83.
  25. Tanno, F.; Nishiyama, Y.; Kokubo, H.; Obara, S. Evaluation of Hypromellose Acetate Succinate (HPMCAS) as a Carrier in Solid Dispersions. *Drug Dev. Ind. Pharm.* **2004**, 30, 9.
  26. Kar, N.; Liu, H.; Edgar, K. J. Synthesis of Cellulose Adipate Derivatives. *Biomacromolecules*, **2011**, 12, 1106 – 1115.
  27. Liu, H.; Ilevbare, G. A.; Cherniawski, B. P.; Ritchie, E. T.; Taylor, L. S.; Edgar, K. J. Synthesis and Preliminary Structure-Property Evaluation of Cellulose  $\omega$ -Carboxyesters for Amorphous Solid Dispersions. *Carbohydrate Polymers*. **2012**. DOI: 10.1016/j.carb-pol.2012.11.049.
  28. Fedors, R. F. A method for estimating both the solubility parameter and molar volumes of liquids. *Polymer Engineering and Science*, **1974**, 14, 147 – 154.
  29. Hoffman, J. D. Thermodynamic driving force in nucleation and growth processes. *Journal of Chemical Physics*, **1958**, 29, 1192.
  30. Murdande, S. B.; Pikal, M. J.; Shanker, R. M.; Bogner, R. H.; Solubility advantage of amorphous pharmaceuticals I. A thermodynamic analysis. *Journal of Pharmaceutical Sciences*, **2009**, 99, 1254.
  31. Jiang, S.; Ter Horst, J. H. Crystal Nucleation Rates from Probability Distributions of Induction Times. *Crystal Growth and Design*, **2010**, 11, 256–261.
  32. Subramanian, N.; Ray, S.; Ghosal, S. K.; Bhadra, R.; Moulik, S. P. Formulation design of self-microemulsifying drug delivery systems for improved oral bioavailable of celecoxib. *Biological and Pharmaceutical Bulletin*, **2004**, 27, 1993 – 1999.
  33. Strickley, R. G. Currently marketed oral lipid-based dosage forms: Drug products and excipients. In *Oral Lipid-Based Formulations: Enhancing the Bioavailability of Poorly Water Soluble Drugs*, Edited by Hauss, D., *CRC Press*, **2007**.
  34. Hancock, B. C.; Parks, M. What is the true solubility advantage for amorphous pharmaceuticals? *Pharmaceutical Research*, **2000**, 17, 397 – 404.
  35. Alonzo, D. E.; Gao, Y.; Zhou, D.; Mo, H.; Zhang, G. G. Z.; Taylor, L. S. Dissolution and Precipitation Behavior of Amorphous Solid Dispersions. *Journal of Pharmaceutical Science*, **2011**, 100, 3316–3331.
  36. Baird, J. A.; Van Eerdenburgh, B.; Taylor, L. S. A classification system to assess the crystallization tendency of organic molecules from undercooled melts. *Journal of Pharmaceutical Science*, **2010**, 99, 3787 – 3806.
  37. Van Eerdenburgh, B.; Baird, J. A.; Taylor, L. S. Crystallization tendency of active pharmaceutical ingredients following rapid solvent-evaporation – classification and comparison with crystallization tendency from undercooled melts. *Journal of Pharmaceutical Science*, **2010**, 99, 3826 – 3838.
  38. Ilevbare, G. A.; Liu, H.; Edgar, K. J.; Taylor, L. S. Maintaining supersaturation in aqueous drug solutions: Impact of different polymers on induction times. *Crystal Growth & Design* **2013**, 13, 740–751.
  39. Ilevbare, G. A.; Liu, H.; Edgar, K. J.; Taylor, L. S. Impact of polymers on crystal growth rate of structurally diverse compounds from aqueous solution. *Molecular Pharmaceutics* **2013**, 10, 2381–2393.
  40. Shen, T.; Langan, P.; French, A. D.; Johnson, G. J.; Gnanakaran, S. Conformational flexibility of soluble cellulose oligomers: Chain length and temperature dependence. *Journal of American Chemical Society*, **2009**, 131, 14786 – 14794.
  41. Kramarenko, E. Y.; Winkler, R. G.; Khalatur, P. G.; Khokhlov, A. R.; Reineker, P. Molecular dynamics simulation study of adsorption of polymer chains with variable degree of rigidity. I. Static properties. *Journal of Chemical Physics*, **1995**, 104, 4806 – 4813.



# CHAPTER 7 AMPHIPHILIC CELLULOSE ESTERS FOR ORAL DRUG DELIVERY

## 7.1 Abstract

Polymer selection is a crucial step in the development of amorphous solid dispersions (ASD) for lipophilic drug solubilization and stabilization. The polymer matrix is required to interact strongly at the molecular level with a drug candidate to prevent drug from recrystallization, meanwhile must release drug adequately when entering the absorption milieu. Herein we report a versatile synthesis of a non-ionic, water-soluble cellulosic polymer family; cellulose trioxadecanoates, containing a hydrophilic oligo(ethylene oxide) side chain. This series of cellulose derivatives is designed to perform both functions as matrix polymers for dispersions of hydrophobic pharmaceutical actives with high crystallization tendency. These polymers also may be derivatized to append a pH-responsive functional group. Detailed structural information and structure-property relationship characterization of these amphiphilic polymers are described in our report, which may permit future evaluation of these materials as ASD polymers for enhancement of drug solubility and bioavailability.

## 7.2 Introduction

Renewable, plant-based cellulose materials are of considerable current interest for pharmaceutical applications, mostly for drug delivery.<sup>1-6</sup> Comparing with the intravenous mode, oral drug administration is a widely used approach, generally favored by patients due to its unsurpassed convenience and low expense. Cellulose derivatives are best suited for oral drug delivery, since humans lack cellulase enzymes to metabolize and clear cellulose from the blood circulation. Thus, novel cellulose derivatives have been formulated with drugs as high-energy amorphous solids to address pharmaceutical issues like poor drug aqueous solubility and

bioavailability. Typically, they are intimately mixed with active pharmaceutical actives into an amorphous, homogeneous form, called an amorphous solid dispersion (ASD).

Due to the absence of crystal lattice energy, ASDs create higher apparent solubility and faster dissolution rate of drugs. ASD may be more advantageous than other solubilization approaches including cyclodextrin complexation, micellar formation and cosolvents, because the generation of supersaturated solutions enhances drug apparent permeability across the gastrointestinal (GI) epithelial membrane, resulting in increased flux and drug exposure in circulation.<sup>7-10</sup> However, this formulation strategy can fail due to the strong driving force for re-crystallization of metastable amorphous drugs. In order to resolve this stability issue, novel cellulosic polymers are designed to interact sufficiently with the drug at the molecular level, and possess high glass transition temperatures to prevent drug mobility and resulting crystallization. Even at high storage temperature and humidity, these ASDs can be stable against crystallization for years.<sup>11, 12</sup> It was also rationalized that the effectiveness of cellulosic polymers is based on the type and strength of their intermolecular interactions with particular drugs.<sup>13</sup> For example, for a drug containing strong hydrogen bond (H-bond) donor groups, the best ASD stabilization would be observed with a polymer containing strong H-bond acceptor groups.

Beyond that, when an ASD formulation is administered orally, the supersaturated solutions generated by the dissolution of amorphous solids may lead to an increase in absorption only if the enhanced drug concentrations can be maintained long enough for drug to be absorbed. Crystallization of amorphous solids from solution, involving nucleation and subsequent crystal growth, must be prevented. Well-chosen cellulosic polymers not only can behave as effective crystallization inhibitors in the solid state, but also prolong supersaturation after ASDs are dispersed in aqueous media.<sup>14</sup> In our previous screening study, the polymers that were effective nucleation and crystal growth inhibitors were deduced to have a moderate level of hydrophobicity relative to the drug molecule and/or contain functional groups that can form specific polymer-solute intermolecular interactions, thereby disrupting the reorganizations of solute molecule back into a crystalline structure and further block the crystalizing site.<sup>15-18</sup>

In the previous approach, cellulose  $\omega$ -carboxyesters derived from various cellulose esters (cellulose acetate, cellulose acetate propionate and cellulose acetate butyrate) showed outstanding inhibitory effect on drug nucleation and crystal growth in solution.<sup>19, 20</sup> Our research group has also systematically studied ASDs of a series of flavonoids with carboxylated cellulose derivatives including in-house synthesized cellulose acetate adipate propionate (CAAdP), commercially available cellulosic polymers carboxymethylcellulose acetate butyrate (CMCAB) and hydroxypropylmethylcellulose acetate succinate (HPMCAS), along with the synthetic ASD polymer poly(vinylpyrrolidone) (PVP).<sup>21-24</sup> The drug release curves for amorphous solid dispersions were characterized by the maximum concentrations of drug achieved ( $C_{\max}$ ). For all the flavonoid compounds tested,  $C_{\max}$  values achieved from ASDs with equal drug content but different matrices follow the following sequence: PVP > HPMCAS > CMCAB  $\approx$  CAAdP, which is exactly the sequence of polymer solubility. The results suggested that more hydrophilic polymer matrices swell or dissolve more rapidly in aqueous media, leading to faster release kinetics. However, PVP formulation does not work for all drugs, especially owing to its relative inability to inhibit crystallization from supersaturated solution<sup>21</sup> and its rapid dissolution, especially at gastric pH. PVP-based solid dispersions thereby led to an early burst release of drugs in the gastric environment.<sup>24</sup>

From the above observations, the hydrophobic nature of cellulose  $\omega$ -carboxyalkanoates might impede their development as enhancers of drug release from formulated ASDs. Therefore we propose here an approach to synthesis of polymers of interest for ASD; a series of novel water-soluble cellulosic esters with varying degree of substitutions are the precursors, whose remaining hydroxyl groups are carefully derivatized with hydrophobic or pH-responsive moieties to control the hydrophilic-hydrophobic balance of the entire cellulosic polymer. The approach is in some ways analogous to the syntheses of HPMCAS and CMCAB, which also begin with a water-soluble cellulose derivative and subsequently modify its amphiphilicity. These products are designed to increase the drug  $C_{\max}$  from ASDs without sacrificing the ability to stabilize the drug against recrystallization.

Considering the synthetic method, cellulose esterification provides access to a variety of biomaterials with distinctive and valuable properties for various applications. Hydroxyls of

cellulose are rather inert to chemical modification, therefore esterification reactions are usually carried out with the reactive anhydrides or chlorides under basic catalysis. In addition, in order to make a broad scope of new cellulose esters available, alternative “one-pot” synthetic approaches of *in situ* activation of the carboxylic acid prior to reaction with cellulose have emerged and now play a very important role in cellulose modification processes.<sup>25, 26</sup>

It was reported that water-soluble, non-ionic ethylene glycolated esters of cellulose (namely cellulose trioxadecanoates) with degrees of substitution in the range from 0.11 to 3.0 were synthesized homogeneously in DMAc/LiCl using the corresponding acid chloride,<sup>27</sup> in DMAc/LiCl by *p*-toluenesulfonyl chloride activation,<sup>28</sup> or in ionic liquid by 1,1'-carbonyldiimidazole activation.<sup>29</sup> However, methods for synthesis of cellulose esters with hydrophilic oligo(ethylene oxide)-containing side chains have not been systematically studied. To our knowledge, further derivatization of water-soluble cellulose trioxadecanoates with hydrophobic or ionizable moieties to afford amphiphilic polymers and their use for amorphous solid dispersions have not been reported.

The non-ionic, water-soluble cellulose ether HPMC has been reported to inhibit both nucleation and growth of felodipine crystals even at ppm levels.<sup>30</sup> With their oligoethylene glycol-containing side chains, cellulose trioxadecanoate esters may further maximize molecular interactions with drugs containing substantial hydrogen bonding donor groups. In this paper we utilize above-mentioned synthetic route to generate a family of highly amphiphilic cellulose mixed-esters for oral drug delivery applications.

## 7.3 Experimental Section

### 7.3.1 Materials

Microcrystalline cellulose (Avicel® PH-101, Fluka, DP 260) was dried under reduced pressure at 50 °C overnight prior to use. *N,N*-Dimethylacetamide (DMAc) and 1,3-dimethyl-2-imidazolidinone (DMI) were purchased from ACROS Organics and dried over 4 Å molecular sieves. Adipic anhydride was synthesized according to a reported procedure.<sup>31</sup> Other purchased reagents were used as received. Oxalyl chloride (98%), 1,1'-carbonyldiimidazole (CDI, 97%), *p*-

toluenesulfonyl chloride (TosCl, 99+%), 4-dimethylaminopyridine (DMAP), pyridine (anhydrous, 99.0%), succinic anhydride (99%), phthalic anhydride (99%) and regenerated cellulose dialysis tubing (MW cut-off 3500 Daltons) were purchased from ACROS Organics. *N,N*-Dimethylformamide (DMF), lithium chloride, sodium hydroxide solution (0.1N, certified) and hydrochloric acid solution (0.1 N, certified) were purchased from Fisher Scientific. 2-[2-(2-Methoxyethoxy)ethoxy]acetic acid (3,6,9-trioxadecanoic acid, TODA, technical grade), propionic anhydride (97%) was purchased from Aldrich.

### 7.3.2 Analytical measurements

**NMR Spectroscopy.**  $^1\text{H}$  NMR spectra were acquired on Bruker Avance 500 spectrometers. Samples were analyzed as solutions in  $\text{CDCl}_3$ , acetone- $d_6$ , DMSO- $d_6$  or pyridine- $d_5$  (ca. 10 mg/mL) at 25 °C in standard 5 mm o.d. tubes. A drop of trifluoroacetic acid was added to shift the water peak downfield from the spectral region of interest. 16 scans were obtained for each sample.  $^{13}\text{C}$  NMR spectra were obtained on a Bruker Avance 500 MHz spectrometer with 6400 scans in  $\text{D}_2\text{O}$  (ca. 50 mg/mL) at 70 °C.

**Thermogravimetric analysis.** TGA was performed on a TA Q500. Thermal decomposition of ~10 mg dry samples was carried out at a heating rate of 15 °C/min from ambient temperature to 650 °C. Thermogravimetric (TG) and differential thermogravimetric (DTG) curves were plotted by Universal Analysis 2000 software.

**Differential scanning calorimetry.** DSC analyses were performed on a TA Q2000. Dry powders ( $8 \pm 2$  mg) were loaded in Tzero<sup>TM</sup> aluminum pans. Each sample was equilibrated at 0 °C and then heated to 180 °C at 20 °C/min and held isothermally at 180 °C for 3 min. The sample then was cooled at 100 °C/min to -50 °C and held isothermally at -50 °C for 3 min. During the second heating cycle the sample was heated to 220 °C at 20 °C/min. For the modulated method, the sample is equilibrated at -50 °C, held isothermally for 5 min, then heated at 5-7 °C/min to 220 °C with a modulation of  $\pm 1$  °C every 40 s. All DSC measurements were verified with a duplicate run.

**Ester saponification and back-titration.** Cellulose trioxadecanoate (~200 mg for DS <1 samples, ~250 mg for DS >1 samples) was carefully weighed and charged into a 50 mL 3-neck flask. An accurately measured volume of NaOH (20 mL for DS <1 samples, 25 mL for DS >1 samples) was added and stirred vigorously in a closed system at room temperature for 24 h.

The mixture was then titrated with 0.1 N HCl solution. A potentiometric probe and a conductometric probe were inserted in the two sides of the flask. Each measurement was carried out by adding 100  $\mu$ L aliquots of HCl solution, allowing the solution to stir for 20 seconds and then collecting the pH and conductivity data points.

The precipitates were washed extensively with water, vacuum dried and then analyzed by ATR spectroscopy. 64 scans were obtained for each spectrum.

**Elemental analysis.** Cellulose trioxadecanoate propionates were again washed extensively with water and vacuum dried at 40 °C for 8 h prior to elemental (C, H) analysis, carried out by Atlantic Microlab, Inc.. Equations were established using Mathematica<sup>®</sup> software to convert % C and %H in DS values. Graph was plotted in Excel 2013.

**Solubility testing.** Dried sample (~10 mg) was added to a 10 mL glass vial, then 2–3 mL of solvent was added. The mixture was subjected to vortex mixing for 5 min (moderate heating was applied) and placed on a roller overnight; the solubility was determined by visual examination.

### 7.3.3 Methods

#### **Dissolution of cellulose in DMAc/LiCl**

Microcrystalline cellulose (3.00 g, 18.5 mmol) was dissolved in DMAc (112.5 mL) and LiCl (5.63 g) by a procedure reported earlier.<sup>32</sup>

#### **Reaction of cellulose with 3,6,9-trioxadecanoyl chloride (TODCl)**

Thionyl chloride (29.2 mL, 0.4 mol) was added dropwise into TODA (35.64 g, 0.2 mol) at room temperature over 30 min. It was allowed to react for 30 min and then heated to 70 °C for

additional 2 h until the gas formation stopped. Toluene (50 mL) was added and the unreacted thionyl chloride was co-distilled out by short-path distillation. The residual liquid (TODCl) was checked by  $^1\text{H}$  NMR (absence of toluene peaks) and then used for the esterification reaction.

Then to the cellulose solution, pyridine (6.72 mL, 83.3 mmol, 4.5 mol/AGU) was injected all at once and then TODCl (10.92 g, 55.6 mmol, 3 mol/AGU) pre-diluted with DMAc (30 mL), was then added dropwise through a dropping funnel at room temperature. The mixture was then heated to 80 °C. After 3 h at 80 °C, the homogeneous solution was cooled to room temperature. The product was precipitated by adding the reaction mixture slowly to 800 mL isopropanol in an ice bath. The product was isolated by filtration and washed with 200 mL isopropanol. Then the waxy compound was redissolved in water, and dialyzed against DI water for 4 days. After the conductivity of the dialysis water reached the same level as that of DI water, the polymer solution was then freeze-dried. Yield: 6.63 g (73 %).

#### **Reaction of cellulose with 3,6,9-trioxadecanoic acid (TODA)/1,1'-carbonyldiimidazole (CDI)**

A solution of TODA (9.90 g, 3 mol/AGU) and CDI (9.00 g, 3 mol/AGU) in 30 mL of DMAc was stirred for 30 min at 80 °C. It was added to pre-dissolved cellulose solution using a dropping funnel. The mixture was then allowed to stir for 3 h at 80 °C. The homogeneous solution was cooled to room temperature and precipitated by adding slowly to 600 mL ethanol, then the solid product was isolated by filtration and washed with 200 mL ethanol. The precipitate was redissolved in water, then dialyzed against DI water for 4 days and isolated by freeze-drying. Yield: 5.20 g (74 %).

#### **Reaction of cellulose with 3,6,9 trioxadecanoic acid (TODA)/*p*-toluenesulfonyl chloride (TosCl)**

A solution of TODA (9.90 g, 55.6 mmol, 3 mol/AGU) and TosCl (10.59 g, 3 mol/AGU) in 30 mL of DMAc was stirred for 30 min at 80 °C. It was added to pre-dissolved cellulose solution using a dropping funnel. The mixture was then allowed to stir for 3 h at 80 °C. The homogeneous solution was cooled to room temperature. The product was isolated by adding the reaction mixture slowly to 800 mL of isopropanol in an ice bath. The product was isolated by filtration and washed with 200 mL isopropanol. Then the waxy compound was redissolved in water, dialyzed against DI water for 4 days, and then freeze-dried. Yield: 5.40 g (63 %).

### **Reaction of cellulose with 3,6,9-trioxadecanoic acid (TODA)/oxalyl chloride/DMF**

To prepare the iminium chloride intermediate, in a 100 mL flask equipped with a thermometer, a gas bubbler and a septum 30 mL of DMF was added and cooled to -20 °C in an isopropanol/dry ice bath. At this temperature oxalyl chloride (4.87 mL, 55.6 mmol, 3 mol/AGU) was added dropwise. During the addition, gas evolution and formation of white precipitates were observed. After gas evolution halted, TODA (9.90 g, 3 mol/AGU) was added. The temperature was increased to 0 °C and the mixture was stirred for 20 min. A clear solution of TOD iminium chloride was formed.

The obtained iminium chloride solution was added to the cellulose solution dropwise. The mixture was kept for 3 h at 80 °C. The mixture was cooled down and then added slowly to 800 mL of ethyl acetate. The product was isolated by filtration and washed with 200 mL ethyl acetate. Then the gummy compound was redissolved in water, dialyzed against DI water for 4 days and then freeze-dried. Yield: 6.96 g (82 %).

All reactions with 1-to-1 molar ratio followed the same fashion in preparation, isolation and purification procedure.

### **Perpropionylation**

Cellulose trioxadecanoate (750 mg) was dissolved in 15 mL of pyridine, 15 mL of propionic anhydride and 75 mg DMAP. After stirring for 24 h at 80 °C, the product was precipitated into 300 mL water, collected by filtration, and then washed several times with water. The crude product was redissolved in 20 mL of chloroform. This solution was added slowly with rapid stirring to 300 mL of hexanes. After filtration and washing with excess hexanes several times, the sample was dried under vacuum at 40 °C.

### **Reaction of cellulose trioxadecanoate with phthalic/succinic/adipic anhydrides**

In a typical example, cellulose trioxadecanoate (via acid chloride 1-1 molar ratio, 250 mg, 1.06 mmol) was dissolved in 10 mL anhydrous DMI, followed by adding pyridine (0.38 mL, 4.77 mmol, 4.5 mol/mol modified AGU) and phthalic anhydride (0.47 g, 3.18 mmol, 3 mol/mol modified AGU). The reaction mixture was allowed to react homogeneously at 80 °C for 20 h. After the



reaction, the solution was placed into a dialysis bag, dialyzed against water for 2 days and then freeze-dried. Yield: 302 mg (74 %).

The reaction of cellulose trioxadecanoate with adipic anhydride was performed immediately after fresh, pure adipic anhydride was synthesized, and no pyridine was added.

## 7.4 Results and Discussion

### 7.4.1 General description and comparison of different esterification approaches

Cellulose acylation with acid chloride in DMAc/LiCl binary system is a traditional method to synthesize cellulose esters. Usually pyridine, triethylamine or imidazole is co-added as base catalyst and acid scavenger. Therefore in first series of experiments, cellulose dissolved in DMAc/LiCl was allowed to react with trioxadecanoyl chloride. Trioxadecanoyl chloride was separately synthesized by reacting trioxadecanoic acid with thionyl chloride prior to the cellulose derivatization. Thionyl chloride must be co-evaporated with toluene with a higher boiling point, otherwise its residue (invisible in  $^1\text{H}$  NMR) would lead to a temporary solidification during the esterification process and much lower ester substitution. The freeze-dried products are amber yellow-colored.

For cellulose acylation, TosCl and CDI are very effective reagents for *in situ* activation of carboxylic acids. For acylation with CDI activation, the reaction has to be performed in two stages. That is, the imidazolide of the carboxylic acid should be firstly synthesized before esterification, otherwise it leads to crosslinking by carbonate formation in the presence of polyol (cellulose in our case).<sup>33</sup> The first-stage activation was controlled to  $\leq 30$  min in our experiments, to prevent imidazolide decomposition that occurs after longer activation times, resulting in decreased DS values.<sup>29</sup> No crosslinking was observed, confirming that CDI was mostly consumed within 30 min. For consistency, a mixture of TosCl and 3,6,9-trioxadecanoic acid in DMAc was heated up to 80 °C for 30 min before added dropwise into cellulose solution, even though there is usually no

need for this separate activation when TosCl is used. It is believed a mixture of anhydride and acid chloride is pre-formed that accounts for high reactivity by TosCl activation.<sup>34</sup>

The most efficient *in situ* activation method is the application of iminium chloride. Iminium chlorides can be easily synthesized by conversion of *N,N*-dimethylformamide with a variety of chlorinating agents such as oxalyl chloride. Oxalyl chloride was also used in our previous study to convert acid to reactive acid chloride.<sup>19</sup> Cellulose esterification was achieved by adding pre-formed solution of the acid iminium chloride to cellulose dissolved in DMAc/LiCl. The purification of cellulose trioxadecanoate was even simpler because most of the by-products are gaseous and reformed DMF can be readily removed together with DMAc. After precipitation, filtration and vacuum-drying, all the cellulose trioxadecanoate products were again dissolved in water, and dialyzed against water for 4 days to remove various impurities, that were prone to be entrapped into the sticky crude polymers.

#### 7.4.2 Degree of substitution (DS) determination

The water-soluble cellulose trioxadecanoates with varying DS obtained via those different approaches were examined by FT-IR; it was observed that in all cases a characteristic ester characteristic absorption band at  $1753\text{ cm}^{-1}$  was present. In order to characterize the DS of cellulose esters for structure-property elucidation, there are various analytical techniques including  $^1\text{H}$  and quantitative  $^{13}\text{C}$  NMR, saponification followed by back titration of the alkali excess, pyrrolidinolysis followed by GC analysis,<sup>35</sup> elemental analysis,<sup>36</sup> alkaline hydrolysis followed by the derivatization of the extracted products to be analyzed by gas chromatography<sup>37</sup> and transesterification with trimethylsulphonium hydroxide to afford acid methyl esters for GC analysis.<sup>38</sup>

$^1\text{H}$  NMR is usually convenient and is widely used for DS determination of cellulose derivatives; however, it is difficult to determine DS of cellulose trioxadecanoate by  $^1\text{H}$  NMR directly. Peaks for trioxadecanoate methylene and methoxy end groups at around 3.3 - 4.5 ppm strongly overlap with signals for the protons of the cellulose AGU in the range 3.5 – 5.1 ppm (**Fig.**

**7.1a).** Therefore the DS of trioxadecanoate can only be calculated by difference, subtracting DS of propionate from total available hydroxyls after perpropionylation. Complete propionylation is achieved by reaction of cellulose esters with large excess of propionic anhydride in pyridine, using DMAP as catalyst.<sup>39</sup> Ester exchange reactions have already been confirmed to be negligible. The mixed esters are all highly soluble in CDCl<sub>3</sub>, therefore regio-pattern of the substitution can be inferred by <sup>1</sup>H NMR spectrum (**Fig. 7.1b**), which shows the peaks for CH<sub>3</sub> of propionate at 0.98 – 1.12 ppm (protons at C2 and C3), 1.12 – 1.23 ppm (protons at C6).

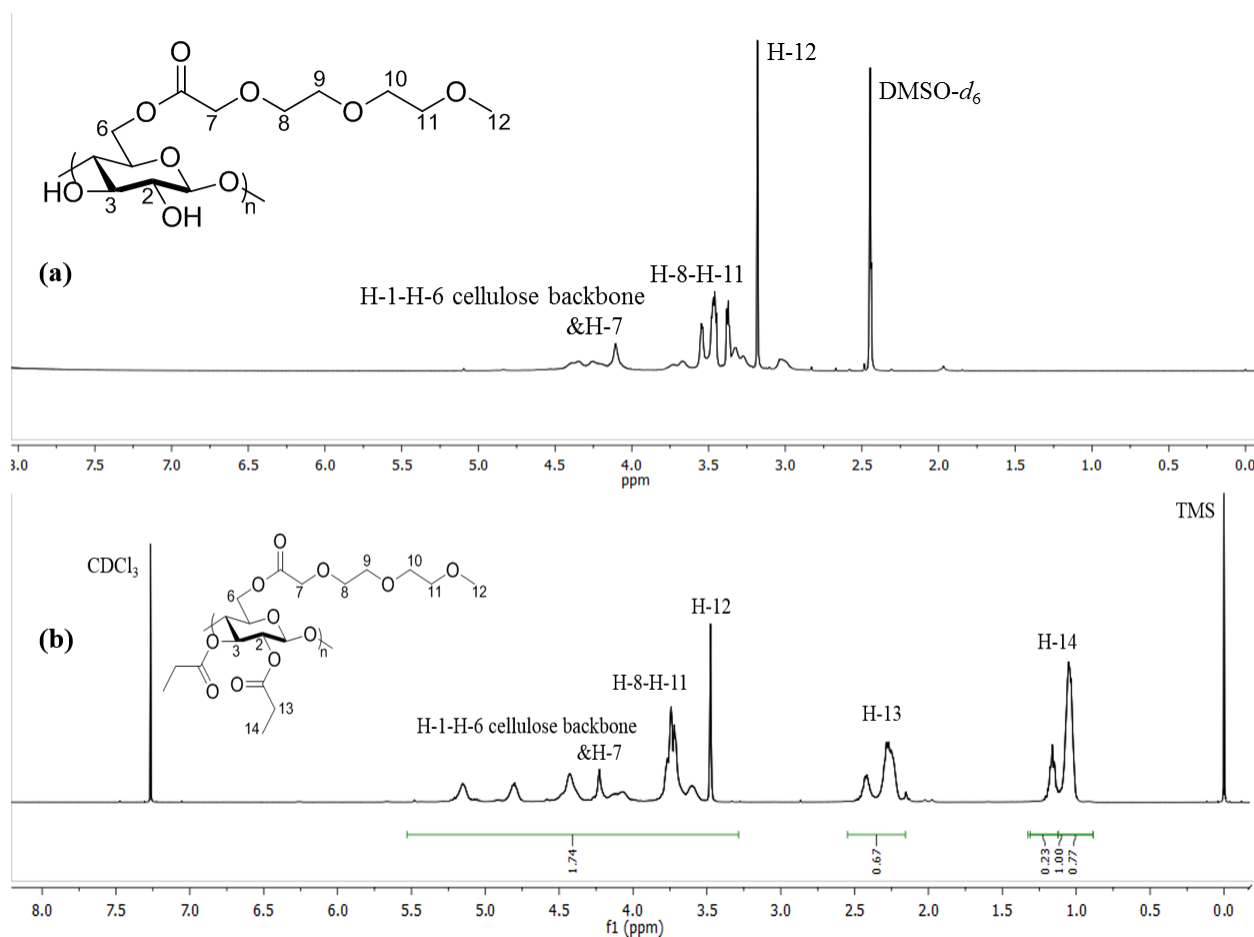


**Figure 7.1** Representative <sup>1</sup>H NMR of cellulose trioxadecanoate (a) and cellulose trioxadecanoate propionate after peracylation (b)

The DS was calculated by the following equation.

$$\frac{3(3 - DS_{TOD})}{7 + 13 DS_{TOD}} = \frac{I_{H,CH_3 \text{ of propionyl}}}{I_{AGU+TOD}}$$

$$DS_{TOD} = \frac{9 I_{AGU+TOD} - 7 I_{H,CH_3 \text{ of propionyl}}}{3 I_{AGU+TOD} + 13 I_{H,CH_3 \text{ of propionyl}}}$$

Trioxadecanoate substitution occurs preferentially at the O-6 position by all methods, especially by TosCl activation. For example, sample C3 (derived from C1) showed a partial DS at O-6 of TOD ester 0.42, while only slight O-2 and O-3 substitution was observed (total DS of TOD 0.06). The  $^{13}\text{C}$  NMR spectrum of C1 before perpropionylation also demonstrated a single carbon peak for TOD ester group at 172.5 ppm and a single signal of C-1 atom at 103 ppm, suggesting that only O-6 functionalization took place (Supplementary Material, **Fig. S7.1**). With higher molar ratio (3 mol reagent per mol modified AGU), the  $^1\text{H}$  NMR spectrum of C4 (derived from C2) showed almost no peak from propionyl esterification at the O-6 position (Supplementary Material, **Fig. S7.2**), suggesting that trioxadecanoylation at O-6 position was nearly complete.

As an alternative analytical technique, saponification of the ester groups with aqueous NaOH and back-titration of the excess base is one of the most reliable methods for DS determination of cellulose esters. Complete hydrolysis of ester groups is a prerequisite for quantitative determination. In some previous studies, severe hydrolysis conditions and co-solvent, for example, 0.5 N NaOH aqueous ethanol solution, heating 24 h at 80 °C, had to be applied for long aliphatic esters due to their steric bulk and hydrophobic character.<sup>37</sup>

Complete hydrolysis of cellulose ester derivatives can be confirmed by infrared spectroscopy (**Fig. 7.2**). Decreased intensities of the aliphatic C-H stretching band (2800-3000  $\text{cm}^{-1}$ ) and bending vibrations (900-1200  $\text{cm}^{-1}$ ) are indications of the occurrence of the ester hydrolysis. More importantly, following the disappearance of the ester carbonyl (C=O) band at 1753  $\text{cm}^{-1}$  suggested that complete saponification of all cellulose trioxadecanoates could be easily achieved using 0.1 N NaOH standard solution at 25 °C for 24 h. The result suggested that the hydrophilic nature of cellulose trioxadecanoate facilitated the deacylation process, overriding any problems caused by steric bulk. The optimized alkali concentration and mild temperature reduced the likelihood of side reactions.

Back-titration with 0.1 N HCl solution was used to measure the excess sodium hydroxide, and the volume of added HCl was plotted against the pH change (**Fig. 7.3**). The peak in the

derivative graph indicated the equilibrium point and it coincided with the inflexion point by conductometric measurements (Supplementary Material, **Fig. S7.3**).

The DS was calculated by the following equation.

$$DS_{TOD} = \frac{(V_1 - V_2) \times 0.1 \times (162 + 160DS_{TOD})}{1000 m}$$

$$DS_{TOD} = \frac{16.2 (V_1 - V_2)}{1000 m - 16 (V_1 - V_2)}$$

Where  $V_1$ ,  $V_2$  are the volumes of 0.1 N NaOH and 0.1 N HCl solution (in mL) used during the titration,  $m$  is the mass of added cellulose trioxadecanoate (in g).

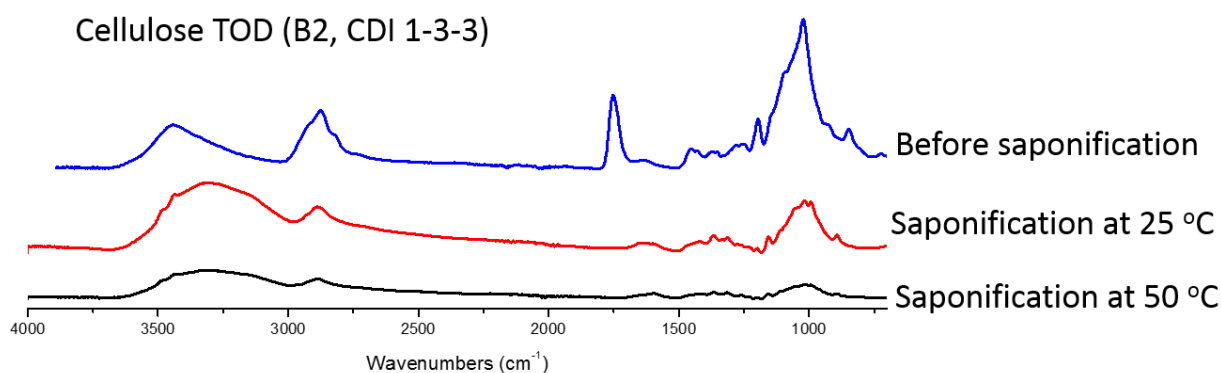


**Figure 7.2** ATR spectra of cellulose trioxadecanoate (B2, via CDI activation 1-3-3), before and after saponification at 25 °C and 50 °C for 24 h

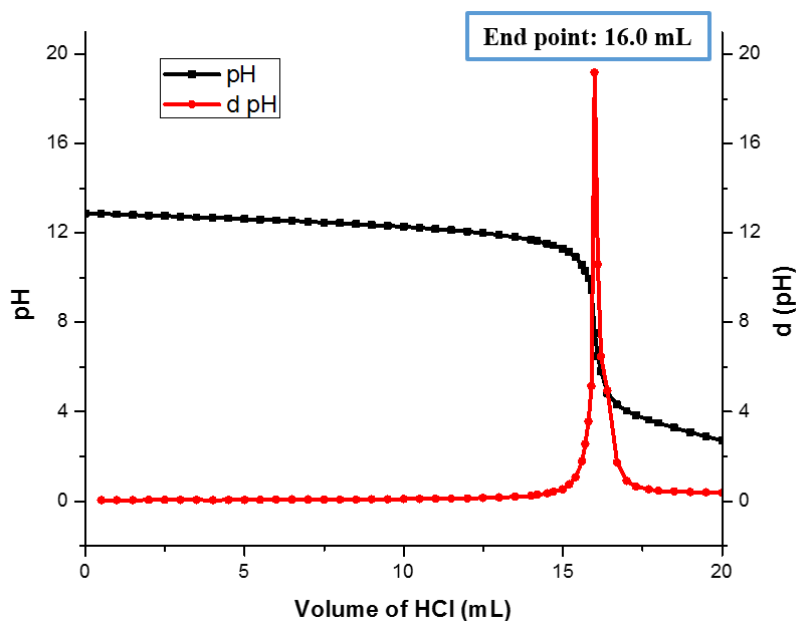


**Figure 7.3** Potentiometric titration and its derivative curve of cellulose trioxadecanoate (B1, via CDI activation 1-1-1) after saponification at 25 °C for 24 h

Even under mild alkaline conditions, cellulose sample might undergo some side reactions during saponification. It was difficult to establish the correlation between NaOH consumption with those unknown reactions, which lead to inaccuracy (usually higher DS) by titrimetry. Accurate DS determination by  $^1\text{H}$  NMR works best with fully substituted cellulose esters, therefore we were unable to determine DS of partially substituted cellulose trioxadecanoate propionate by  $^1\text{H}$  NMR spectroscopy.

We also attempted determination of DS of the mixed cellulose esters by elemental analysis. Using this method, DS values of the two ester types can be calculated with precision of  $\pm 0.10$  if the accuracy of the hydrogen measurement is within  $\pm 0.1\%$ .<sup>36</sup> However, % H determinations do not typically reach that level of accuracy (%H accuracy is typically ca.  $\pm 0.3\%$ ), which could result in inaccurate DS values as shown in **Fig. S7.4** (Supplementary Material). These polymers are quite hygroscopic (displaying a prominent water peak in “anhydrous”  $\text{CDCl}_3$  in the  $^1\text{H}$  NMR spectrum), which also led to variation during %CHN measurement. Thus 2-dimensional DS calculation by elemental analysis was not applied, instead, to reduce uncertainty, only %C data were used for

calculation of DS (TOD) calculation, presuming that the perpropionylation is complete and relying on the fact that DS calculations based on %C is less sensitive than %H to the same level of measurement error. For instance, +0.05% in measured values of %C and H% for cellulose trioxadecanoate DS 2.0 sample would result in the DS calculations to 1.95 and 2.44, respectively.

The DS of TOD ester was calculated by the following equation.

$$\%C = \frac{12.011 [6 + 7DS_{TOD} + 3(3 - DS_{TOD})]}{12.011 [6 + 7DS_{TOD} + 3(3 - DS_{TOD})] + 1.008 [10 + 12DS_{TOD} + 4(3 - DS_{TOD})] + 15.999[5 + 4DS_{TOD} + (3 - DS_{TOD})]}$$

$$DS_{TOD} = \frac{180.185 - \%C \times 330.333}{\%C \times 104.105 - 48.044}$$

A summary of reaction paths, conditions and results is given in **Table 7.1**. The DS values were determined either by <sup>1</sup>H NMR spectroscopy after perpropionylation, by saponification and back-titration, or by elemental analysis of propionylated products employing %C values. From the results, the DS values obtained from titrimetry and elemental analysis are quite consistent with each other and higher than the DS calculated from NMR spectra, but still we cannot rule out the factors that might lead to artificially high DS numbers. 1) For titrimetry, NaOH consumption caused by chain degradation and free acid residue in the cellulose product would increase DS 2) for elemental analysis, hygroscopic nature of the polymer would decrease the C% value, which in turn increases the DS. Using the synthesized acid chloride for esterification, in comparison with the three other *in situ* activation esterification methods, CDI activation demonstrated the lowest product DS.

**Table 7.1** Reaction conditions and the degree of substitution (DS) determined by 3 analytical methods.

No.	Reaction conditions		Cellulose trioxadecanoate		
	Reagents	molar ratio <sup>a</sup>	DS <sup>b</sup>	DS <sup>c</sup>	DS <sup>d</sup>
A1	TODCl	1:1	0.46	0.55	0.56
A2	TODCl	1:3	2.04	2.15	2.14
B1	TODA/CDI	1:1	0.39	0.45	0.50
B2	TODA/CDI	1:3	1.40	1.50	1.62
C1	TODA/TosCl	1:1	0.48	0.59	0.59
C2	TODA/TosCl	1:3	2.02	2.11	2.10
D1	TODA iminium chloride	1:1	0.58	0.60	0.68
D2	TODA iminium chloride	1:3	1.88	2.02	2.35 <sup>e</sup>

- Moles of anhydroglucose units / moles of reagents
- Determined by <sup>1</sup>H NMR spectroscopy after perpropionylation.
- Determined by saponification and back-titration.
- Determined by elemental analysis (C%) after perpropionylation.
- Abnormal DS. Data obtained from elemental analysis is highly sensitive to moisture and other contaminants.

### 7.3.3 Investigation on physiochemical properties

As previously reported,<sup>27</sup> cellulose trioxadecanoates within a certain DS range undergo a phase transition in water. From our results, A2, C2, D2 with DS (TOD) higher than 1.8 can be soluble in water at room temperature, but precipitate out of solution when heated, independent of the activation method used. The phase transition between precipitation and solution in water is reversible, controlled by the temperature. B2 via CDI activation with a slightly lower DS (1.40 by NMR spectroscopy) does not show the precipitation behavior, indicating this phenomenon is highly DS-dependent.



From thermogravimetric data, cellulose trioxadecanoates and their propionate derivatives are all highly thermally stable. The onsets of degradation take place from 277 to 344 °C, which are close to the thermal degradation temperature of starting microcrystalline cellulose. The DSC (or mDSC) thermograms of the cellulose trioxadecanoates with low/high DS and their propionates (C1, C2, C3, C4) were shown in **Fig. 7.4**. For cellulose trioxadecanoate with low substitution (ABCD1, and B2 with DS of TOD 1.40), glass transition temperature could not be detected in the temperature range of -50 – 220 °C (**Fig. 7.4a**), mostly due to the presence of sufficient hydroxyls, which lead to extensive hydrogen bonding and molecular packing. Further perpropionylation eliminated this problem, glass transitions from 71 – 93 °C were found clearly (**Fig. 7.4c**). In the case of C2 with the degree of substitution 2.02,  $T_g \sim 91$  °C can be confirmed by the application of mDSC (**Fig. 7.4b**). Interestingly, its propionylated product did show a characteristic melting and crystallization peak from the cooling and 2<sup>nd</sup> heating scan (**Fig. 7.4d**). Previous studies also identified this thermal phenomenon in fully substituted cellulose trioxadecanoate and related it to the formation of columnar liquid crystalline mesophase.<sup>27</sup> We did not observe the same thermogram pattern in our highly substituted cellulose trioxadecanoates (DS 2.0), but only in their derived propionate esters. Therefore, we hypothesize that this thermal behavior is attributable to the crystallization of the oligo(oxyethylene) substituents. Side chain cooperative motions, observed by melting and crystallization transitions, have been reported in waxy esters of cellulose.<sup>40</sup> It is likely that the remaining hydroxyls of partially substituted cellulose trioxadecanoate (DS 2.0) can retard the tendency for oligo(ethylene oxide) side chains to crystallize through hydrogen bonding. Polyethylene glycol has melting temperature ranging up to 62 °C, depending on its molecular weight. Due to the postulated H-bonding of the trioxadecanoate chain with the stiff cellulose backbone, we hypothesize that restricted side chain motion results in the shift to a higher melting temperature.

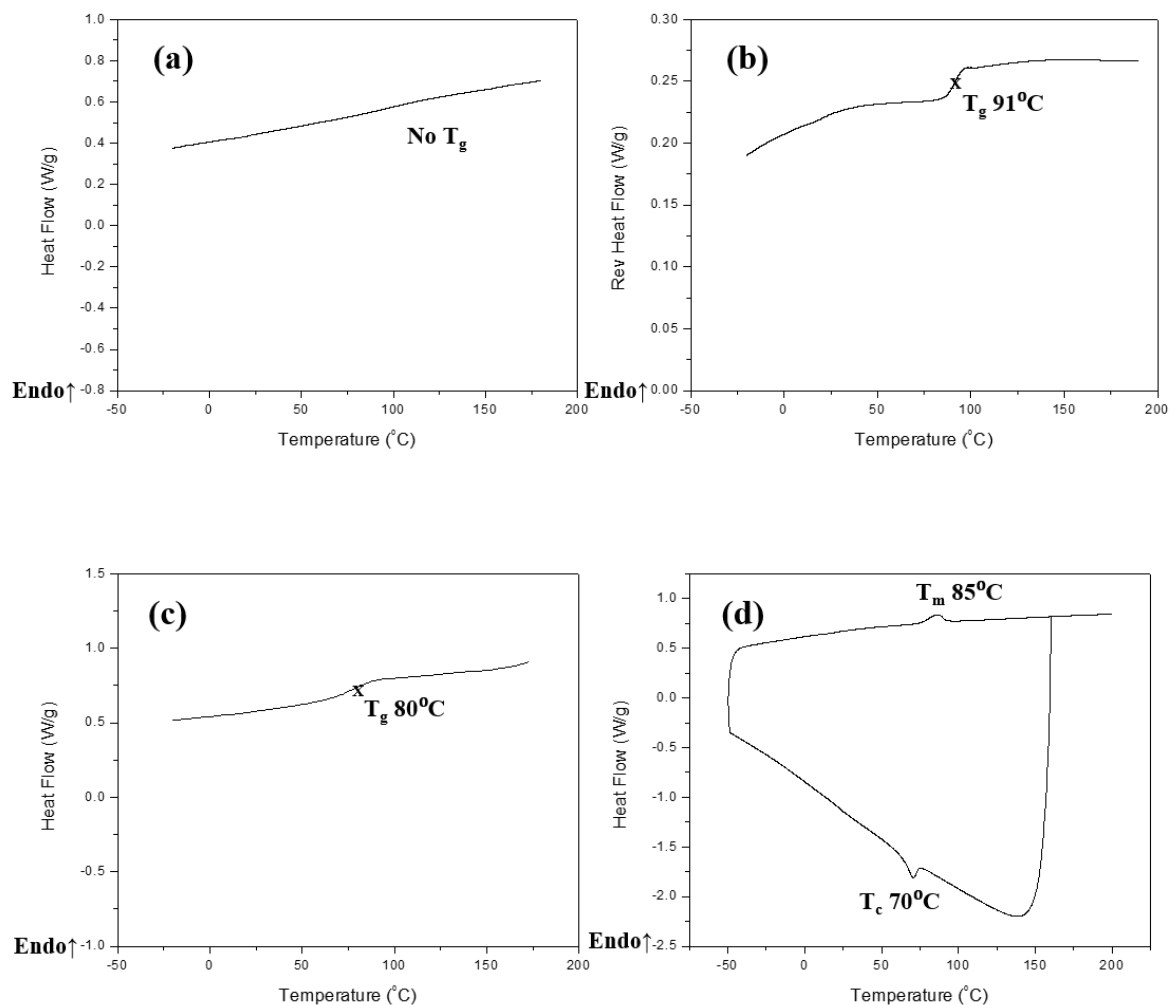


**Figure 7.4** DSC thermograms of C1, C3 and C4 and modulated DSC thermogram of C2

The physiochemical properties of cellulose trioxadecanoates and perpropionylated products are listed in **Table 7.2**. In selecting polymeric materials for amorphous solid dispersion application, a rule of thumb is that re-crystallization of the amorphous drug during transportation and storage is best prevented by using a polymer whose  $T_g$  is 50 °C or greater above ambient temperature, thereby accounting for the plasticizing effects of water (humidity), the drug, and temperature excursions above ambient.<sup>11</sup> This generally requires that the polymer possess a  $T_g$  of 100 °C or higher, and of course the polymer must not crystallize itself. From this perspective, low

DS cellulose trioxadecanoates and their esters, together with some of the high DS cellulose trioxadecanoates are expected to be potential ASD matrix candidates.

**Table 7.2** Physiochemical properties of cellulose trioxadecanoates and perpropionylated products

Cellulose trioxadecanoate (Before propionylation)				Cellulose trioxadecanoate propionate (After propionylation)			
No.	DS <sup>a</sup>	Precipitation behavior	T <sub>g</sub> (°C)	No.	T <sub>g</sub> (°C)	T <sub>m</sub> (°C)	T <sub>c</sub> (°C)
A1	0.47	No	/	A3	90	/	/
A2	2.04	Yes	/	A4	22	92	74
B1	0.39	No	/	B3	93	/	/
B2	1.40	No	/	B4	51	97	/
C1	0.48	No	/	C3	80	/	/
C2	2.02	Yes	91	C4	21	85	70
D1	0.58	No	/	C5	71	/	/
D2	1.86	Yes	126	C6	/	84	67

<sup>a</sup> Determined by <sup>1</sup>H NMR after perpropionylation; / could not be detected.

The results of solubility tests of cellulose trioxadecanoates are summarized in Table 7.3. All the cellulose trioxadecanoates synthesized, DS ranging from 0.39 to 2.04, are soluble in water and DMSO. The derivatives with higher DS (A2, C2, D2), not only exhibit a phase transition behavior in aqueous solution, but also possess significant amphiphilic nature; they are soluble in a wide range of organic solvents including acetone, acetic acid and hot ethanol. This indicates that solution processing of high DS cellulose trioxadecanoates (e.g., for spray-drying) is possible. Low DS trioxadecanoates can be rendered soluble by adding hydrophobic groups such as propionate esters, or functional groups such as ionizable moieties.

**Table 7.3** Solubility range of cellulose trioxadecanoates

Cellulose trioxadecanoate (Before propionylation)								
No.	Method		DS <sup>a</sup>	Solubility				
				H <sub>2</sub> O	Acetone	Acetic acid	Ethanol	DMSO
A1	Acid chloride	1-1	0.47	+	-	-	-	+
A2	Acid chloride	1-3	2.04	+	+	+	*	+
B1	CDI	1-1	0.39	+	-	-	-	+
B2	CDI	1-3	1.40	+	-	-	-	+
C1	TosCl	1-1	0.48	+	-	-	-	+
C2	TosCl	1-3	2.02	+	+	+	*	+
D1	Iminium chloride	1-1	0.58	+	-	-	-	+
D2	Iminium chloride	1-3	1.86	+	+	+	*	+

+ Soluble; - Insoluble; \* Soluble with some heat, precipitate out upon cooling; <sup>a</sup> Determined by <sup>1</sup>H NMR after perpropionylation.

### 7.3.4 pH-Sensitive materials derived from cellulose trioxadecanoate

As described, a general problem when using water-soluble polymers as ASD matrices is early burst release in the gastric environment. Instead of adding hydrophobic alkanoyl groups, we

also attempted to substitute some of the free hydroxyls from cellulose trioxadecanoate with  $\omega$ -carboxyester moieties to impart pH sensitivity, some hydrophobicity from the poly(methylene) chains, and the potential for specific interactions between the pendent carboxyl groups and H-bond acceptors on the drug. Cellulosic polymers with good water dispersibility might also serve as rheology modifiers for waterborne coating application.<sup>41</sup>

In this set of experiments, two cellulose trioxadecanoates were chosen (A1 and A2) with DS(TOD) of ca. 0.5 and 2.0, respectively. Reactions were carried out in polar aprotic, non-derivatizing solvent DMI, by using pyridine as a base catalyst. The only exception was the reactions with adipic anhydride; since weak base is known to initiate homopolymerization of adipic anhydride,<sup>42</sup> no catalyst was used. Ring-opening esterifications with A2 were ineffective. DS values achieved were 0.10 (phthalate) and 0.02 (succinate), by reacting with cyclic anhydrides (3 mol/mol of modified AGU). DS of succinate was unexpectedly low, largely due to the autohydrolysis during the dialysis step. The products after freeze-drying all remained soluble in water. Reaction of A1 with anhydrides (1 mol/mol of modified AGU), provided DS values of  $\omega$ -carboxyester groups of 0.17 (phthalate) and 0.46 (succinate); the products are still soluble in water. However, when 3 equiv. anhydride was used, the isolated products lost aqueous solubility and formed cloudy dispersions in water. The  $\omega$ -carboxyester DS values increased to 0.75 for phthalate and 1.02 for succinate, according to <sup>1</sup>H NMR analysis (**Fig. 7.5**) However, the reaction of A1 with 3 equivalents of adipic anhydride led to crosslinking by the formation of a transparent gel, which was observed and rationalized in our previous studies.<sup>31</sup> In the other 2 cases, the reactions of A1 with adipic anhydride (1 mol/mol of modified AGU) and A2 with adipic anhydride (3 mol/mol of modified AGU) provided organic soluble products with DS (adipate) of 0.20 and 0.49, respectively. However, these values might be artificially higher because the anhydride homopolymerization still existed, the poly(adipic anhydride) formed could not be easily removed through dialysis and its resonance peaks could not be distinguished from those of adipate ester group in the <sup>1</sup>H NMR spectrum. Poly(adipic anhydride) peaks were still distinctive in NMR spectrum after a second wash with non-polar solvent hexanes.

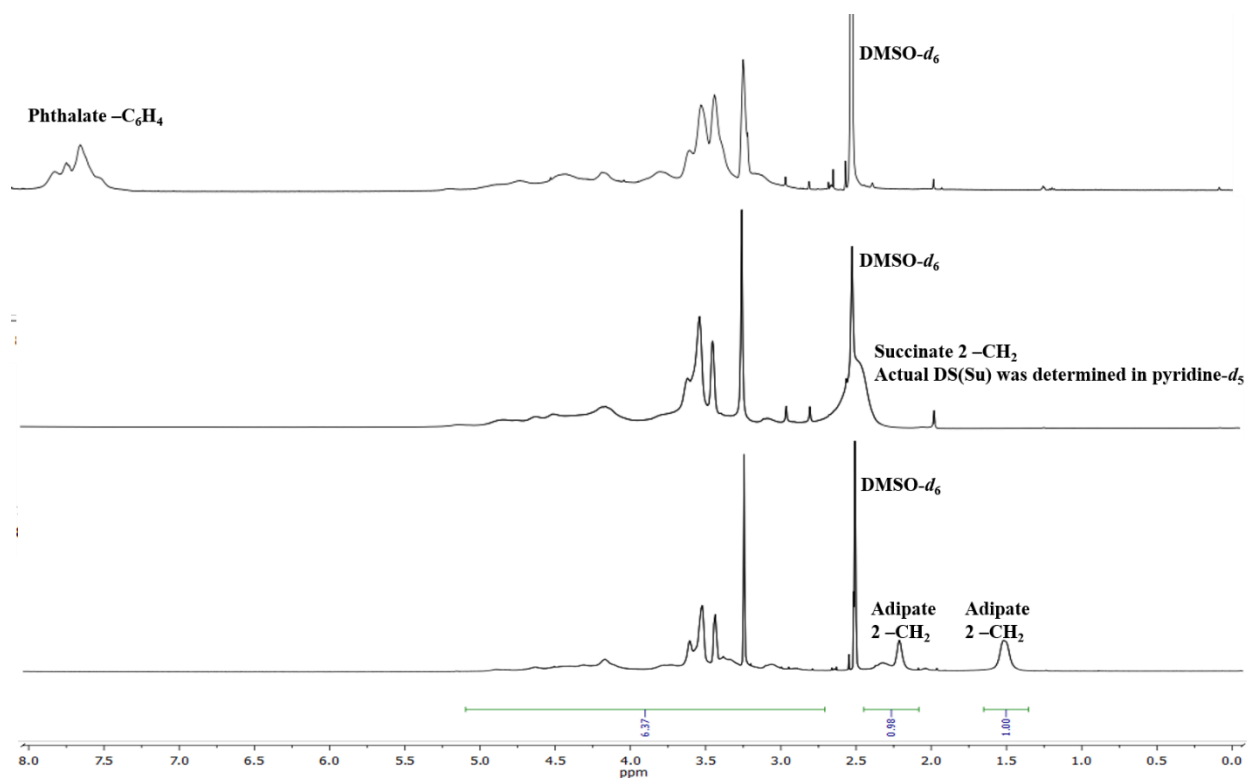


**Figure 7.5**  $^1\text{H}$  NMR of cellulose trioxadecanoate phthalate/succinate/adipate, derived from cellulose trioxadecanoate A1

## 7.5 Conclusion

A family of water-soluble, non-ionic cellulose trioxadecanoates with DS ranging from 0.39 – 2.04 was prepared by the reaction of microcrystalline cellulose (DP 260) through conventional esterification and three *in situ* carboxylic acid activation approaches. NMR spectroscopy after perpropionylation, saponification followed by back-titration and elemental analysis were used to determine the DS values, and the methods and limitations were described. Good solubility in water and polar aprotic solvents allows the further processing of cellulose trioxadecanoates for various applications. Although some highly substituted cellulose trioxadecanoate esters exhibit some tendency for cooperative motion of the side chains, these materials along with their derivatives demonstrate great potential as ASD polymers for enhanced oral drug delivery. Formulation with lipophilic drugs, impact upon creation of supersaturated drug solutions, and stability of amorphous drug in both solid and solution phases will be described in forthcoming reports.

## 7.6 Supplementary Material

Supplementary information available for this chapter includes  $^{13}\text{C}$  NMR of cellulose trioxadecanoate C1 (**Fig. S7.1**),  $^1\text{H}$  NMR of cellulose trioxadecanoate propionate C4 (**Fig. S7.2**), potentiometric and conductometric measurements of cellulose trioxadecanoate C1 after complete saponification (**Fig. S7.3**) and the graphical solution for the DS determination from the carbon and hydrogen contents (**Fig. S7.4**).

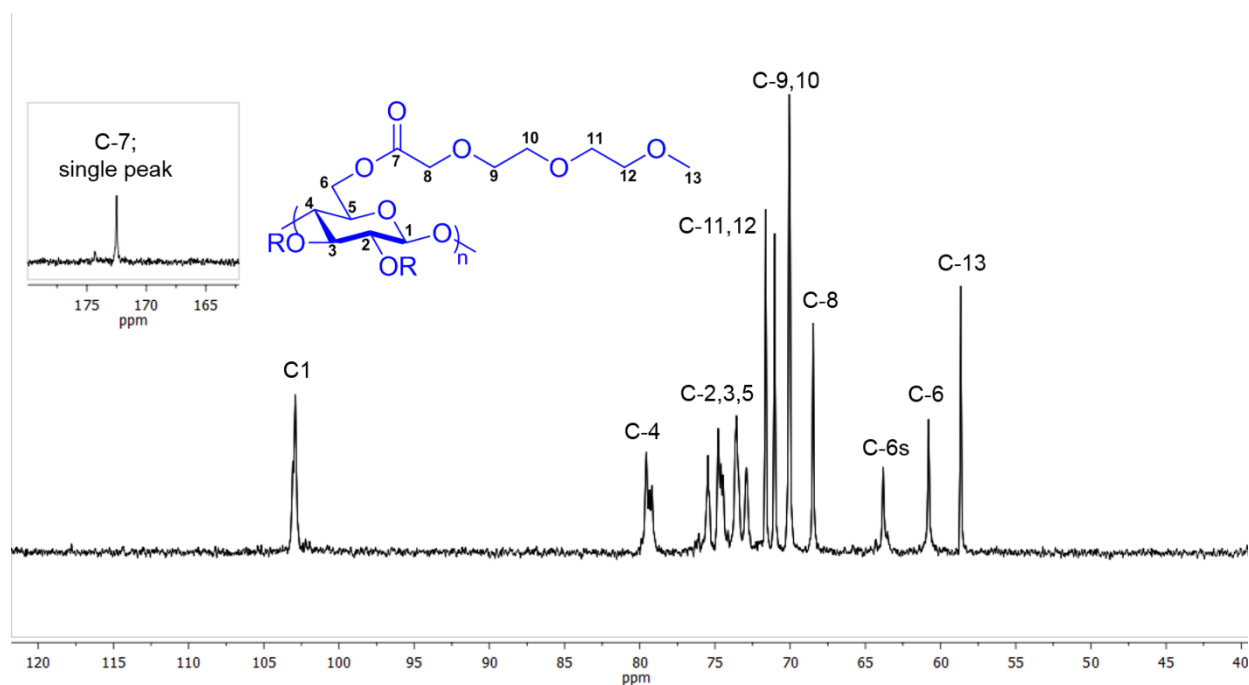


**Figure S7.1**  $^{13}\text{C}$  NMR of cellulose trioxadecanoate C1 in  $\text{D}_2\text{O}$  at  $70\text{ }^\circ\text{C}$  (DS 0.48 via TosCl activation)

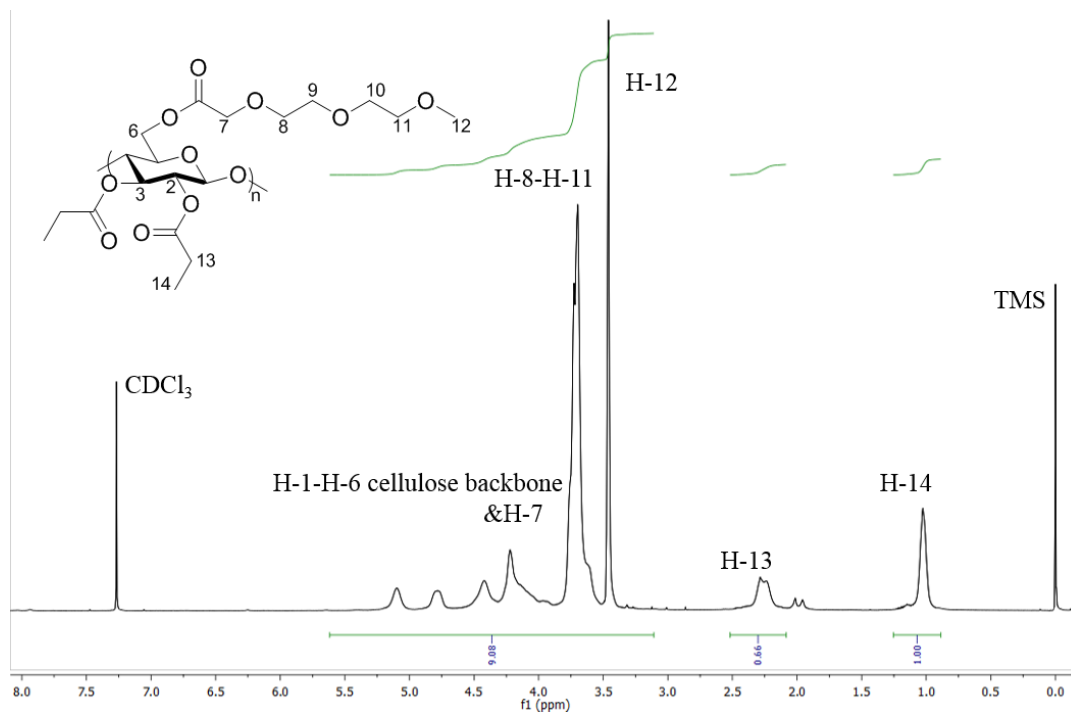


**Figure S7.2**  $^1\text{H}$  NMR of cellulose trioxadecanoate propionate C4 in  $\text{CDCl}_3$  (DS 2.02 via TosCl activation, derived from C2)

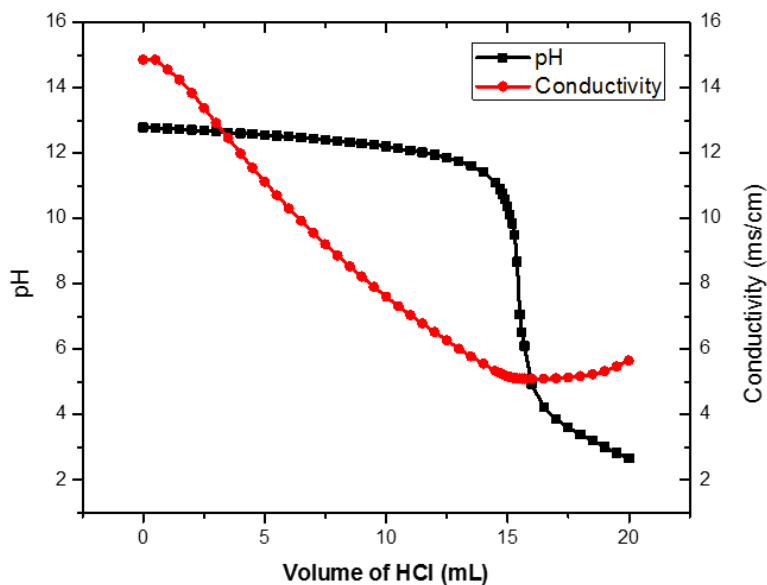


**Figure S7.3** Potentiometric (square dots) and conductometric (diamond dots) measurements of cellulose trioxadecanoate (C1, TosCl activation) after complete saponification. The inflection point for pH measurements is at 15.5 mL and the inflexion point for conductivity measurements is at 15.6 mL



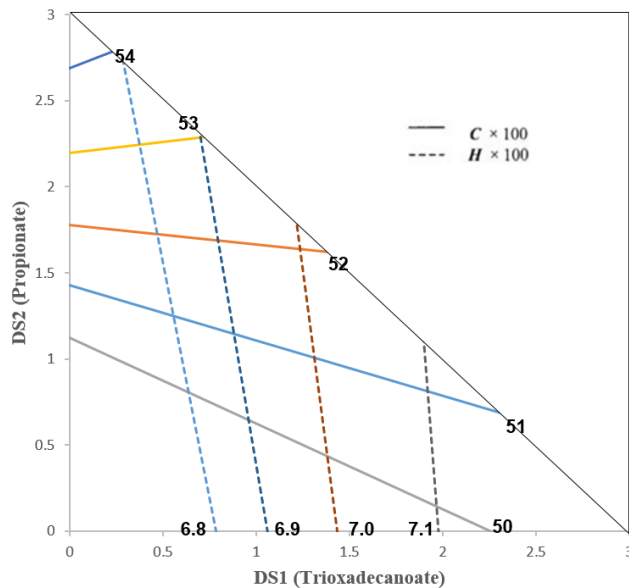


**Figure S7.4** Graphical solution for the DS determination from the carbon and hydrogen contents (C and H). Carbon and hydrogen iso-content lines were shown for the analysis of cellulose trioxadecanoate propionates

## 7.7 Acknowledgement

This project was supported by grants from the U.S. Department of Agriculture (USDA, grant number 2011-67009-20090) and the National Science Foundation (NSF, grant number DMR 1308276). We thank the Department of Sustainable Biomaterials, the Macromolecules and Interfaces Institute and the Institute for Critical Technologies and Applied Science at Virginia Tech for their financial, facilities, and educational support.

## 7.8 References

1. Curatolo, W. J.; Herbig, S. M.; Nightingale, J. A. S. Solid pharmaceutical dispersions with enhanced bioavailability. 1998-305960 901786, 19980727., 1999.
2. Shelton, M. C.; Posey-Dowty, J. D.; Lingerfelt, L. R.; Kirk, S. K.; Klein, S.; Edgar, K. J., Enhanced

dissolution of poorly soluble drugs from solid dispersions in carboxymethylcellulose acetate butyrate matrices. In *Polysaccharide Materials: Performance by Design*, Edgar, K. J.; Heinze, T.; Liebert, T., Eds. American Chemical Society: Washington, D.C., 2009.

3. Friesen, D. T.; Shanker, R.; Crew, M.; Smithey, D. T.; Curatolo, W. J.; Nightingale, J. A., Hydroxypropyl methylcellulose acetate succinate-based spray-dried dispersions: an overview. *Mol Pharm* **2008**, 5, (6), 1003-19.
4. DiNunzio, J. C.; Miller, D. A.; Yang, W.; McGinity, J. W.; Williams, R. O., Amorphous Compositions Using Concentration Enhancing Polymers for Improved Bioavailability of Itraconazole. *Mol. Pharmaceutics* **2008**, 5, (6), 968-980.
5. Kushida, I.; Ichikawa, M.; Asakawa, N., Improvement of dissolution and oral absorption of ER-34122, a poorly water-soluble dual 5-lipoxygenase/cyclooxygenase inhibitor with anti-inflammatory activity by preparing solid dispersion. *J. Pharm. Sci.* **2002**, 91, (1), 258-266.
6. Kai, T.; Akiyama, Y.; Nomura, S.; Sato, M., Oral absorption improvement of poorly soluble drug using solid dispersion technique. *Chem. Pharm. Bull.* **1996**, 44, (3), 568-71.
7. Miller, J. M.; Beig, A.; Carr, R. A.; Spence, J. K.; Dahan, A., A Win-Win Solution in Oral Delivery of Lipophilic Drugs: Supersaturation via Amorphous Solid Dispersions Increases Apparent Solubility without Sacrifice of Intestinal Membrane Permeability. *Mol. Pharmaceutics* **2012**, 9, (7), 2009-2016.
8. Alonzo, D. E.; Gao, Y.; Zhou, D.; Mo, H.; Zhang, G. G. Z.; Taylor, L. S., Dissolution and precipitation behavior of amorphous solid dispersions. *J. Pharm. Sci.* **2011**, 100, (8), 3316-3331.
9. Miller, J. M.; Beig, A.; Carr, R. A.; Webster, G. K.; Dahan, A., The Solubility-Permeability Interplay When Using Cosolvents for Solubilization: Revising the Way We Use Solubility-Enabling Formulations. *Mol. Pharmaceutics* **2012**, 9, (3), 581-590.
10. Miller, J. M.; Beig, A.; Krieg, B. J.; Carr, R. A.; Borchardt, T. B.; Amidon, G. E.; Amidon, G. L.; Dahan, A., The solubility-permeability interplay: Mechanistic modeling and predictive application of the impact of micellar solubilization on intestinal permeation. *Mol. Pharmaceutics* **2011**, 8, (5), 1848-1856.
11. Newman, A.; Knipp, G.; Zografi, G., Assessing the performance of amorphous solid dispersions. *J. Pharm. Sci.* **2012**, 101, (4), 1355-1377.
12. Kennedy, M.; Hu, J.; Gao, P.; Li, L.; Ali-Reynolds, A.; Chal, B.; Gupta, V.; Ma, C.; Mahajan, N.; Akrami, A.; Surapaneni, S., Enhanced Bioavailability of a Poorly Soluble VR1 Antagonist Using an Amorphous Solid Dispersion Approach: A Case Study. *Mol. Pharmaceutics* **2008**, 5, (6), 981-993.
13. Wegiel, L. A.; Mauer, L. J.; Edgar, K. J.; Taylor, L. S., Crystallization of amorphous solid dispersions of resveratrol during preparation and storage-Impact of different polymers. *J. Pharm. Sci.* **2013**, 102, (1), 171-184.
14. Alonzo, D. E.; Zhang, G. G.; Zhou, D.; Gao, Y.; Taylor, L. S., Understanding the behavior of amorphous pharmaceutical systems during dissolution. *Pharm Res* **2010**, 27, (4), 608-18.
15. Ilevbare, G. A.; Liu, H.; Edgar, K. J.; Taylor, L. S., Understanding Polymer Properties Important for Crystal Growth Inhibition-Impact of Chemically Diverse Polymers on Solution Crystal Growth of Ritonavir. *Cryst. Growth Des.* **2012**, 12, (6), 3133-3143.
16. Ilevbare, G. A.; Liu, H.; Edgar, K. J.; Taylor, L. S., Impact of Polymers on Crystal Growth Rate of Structurally Diverse Compounds from Aqueous Solution. *Mol. Pharmaceutics* **2013**, 10, (6), 2381-2393.
17. Ilevbare, G. A.; Liu, H.; Edgar, K. J.; Taylor, L. S., Maintaining Supersaturation in Aqueous Drug Solutions: Impact of Different Polymers on Induction Times. *Cryst. Growth Des.* **2013**, 13, (2), 740-751.
18. Ueda, K.; Higashi, K.; Yamamoto, K.; Moribe, K., Inhibitory Effect of Hydroxypropyl Methylcellulose Acetate Succinate on Drug Recrystallization from a Supersaturated Solution Assessed Using Nuclear Magnetic Resonance Measurements. *Mol. Pharmaceutics* **2013**, 10, (10), 3801-3811.
19. Kar, N.; Liu, H.; Edgar, K. J., Synthesis of Cellulose Adipate Derivatives. *Biomacromolecules* **2011**, 12, (4), 1106-1115.
20. Liu, H.; Ilevbare, G. A.; Cherniawski, B. P.; Ritchie, E. T.; Taylor, L. S.; Edgar, K. J., Synthesis and

structure-property evaluation of cellulose  $\omega$ -carboxyesters for amorphous solid dispersions. *Carbohydr. Polym.*, Ahead of Print.

21. Li, B.; Harich, K.; Wegiel, L.; Taylor, L. S.; Edgar, K. J., Stability and solubility enhancement of ellagic acid in cellulose ester solid dispersions. *Carbohydr. Polym.* **2013**, 92, (2), 1443-1450.
22. Li, B.; Konecke, S.; Harich, K.; Wegiel, L.; Taylor, L. S.; Edgar, K. J., Solid dispersion of quercetin in cellulose derivative matrices influences both solubility and stability. *Carbohydr. Polym.* **2013**, 92, (2), 2033-2040.
23. Li, B.; Liu, H.; Amin, M.; Wegiel, L. A.; Taylor, L. S.; Edgar, K. J., Enhancement of naringenin solution concentration by solid dispersion in cellulose derivative matrices. *Cellulose (Dordrecht, Neth.)* **2013**, 20, (4), 2137-2149.
24. Li, B.; Wegiel, L. A.; Taylor, L. S.; Edgar, K. J., Stability and solution concentration enhancement of resveratrol by solid dispersion in cellulose derivative matrices. *Cellulose (Dordrecht, Neth.)* **2013**, 20, (3), 1249-1260.
25. Liebert, T.; Wotschadlo, J.; Laudeley, P.; Heinze, T., Meltable Dextran Esters As Biocompatible and Functional Coating Materials. *Biomacromolecules* **2011**, 12, (8), 3107-3113.
26. Graebner, D.; Liebert, T.; Heinze, T., Synthesis of novel adamantoyl cellulose using differently activated carboxylic acid derivatives. *Cellulose (Dordrecht, Neth.)* **2002**, 9, (2), 193-201.
27. Zhou, Q.; Zhang, L.; Okamura, H.; Minoda, M.; Miyamoto, T., Synthesis and properties of O-2-[2-(2-methoxyethoxy)ethoxy]acetyl cellulose. *J. Polym. Sci., Part A Polym. Chem.* **2001**, 39, (3), 376-382.
28. Heinze, T.; Schaller, J., New water soluble cellulose esters synthesized by an effective acylation procedure. *Macromol. Chem. Phys.* **2000**, 201, (12), 1214-1218.
29. Dorn, S.; Pfeifer, A.; Schlufner, K.; Heinze, T., Synthesis of water-soluble cellulose esters applying carboxylic acid imidazolides. *Polym. Bull. (Heidelberg, Ger.)* **2010**, 64, (9), 845-854.
30. Alonzo, D. E.; Raina, S.; Zhou, D.; Gao, Y.; Zhang, G. G. Z.; Taylor, L. S., Characterizing the Impact of Hydroxypropylmethyl Cellulose on the Growth and Nucleation Kinetics of Felodipine from Supersaturated Solutions. *Cryst. Growth Des.* **2012**, 12, (3), 1538-1547.
31. Liu, H.; Kar, N.; Edgar, K. J., Direct synthesis of cellulose adipate derivatives using adipic anhydride. *Cellulose (Dordrecht, Neth.)* **2012**, 19, (4), 1279-1293.
32. Edgar, K. J.; Arnold, K. M.; Blount, W. W.; Lawniczak, J. E.; Lowman, D. W., Synthesis and Properties of Cellulose Acetoacetates. *Macromolecules* **1995**, 28, (12), 4122-4128.
33. Bamford, C. H.; Middleton, I. P.; Al-Lamee, K. G., Studies of the esterification of dextran: routes to bioactive polymers and graft copolymers. *Polymer* **1986**, 27, (12), 1981-5.
34. Heinze, T.; Liebert, T.; Koschella, A., New Paths for the Introduction of Organic Ester Moieties. In *Esterification of Polysaccharides*, Springer Berlin Heidelberg: 2006; pp 53-116.
35. Samaranayake, G.; Glasser, W. G., Cellulose derivatives with low DS. II. Analysis of alkanoates. *Carbohydr. Polym.* **1993**, 22, (2), 79-86.
36. Vaca-Garcia, C.; Borredon, M. E.; Gaseto, A., Determination of the degree of substitution (DS) of mixed cellulose esters by elemental analysis. *Cellulose (Dordrecht, Neth.)* **2001**, 8, (3), 225-231.
37. Freire, C. S. R.; Silvestre, A. J. D.; Pascoal Neto, C.; Rocha, R. M. A., An Efficient Method for Determination of the Degree of Substitution of Cellulose Esters of Long Chain Aliphatic Acids. *Cellulose (Dordrecht, Neth.)* **2005**, 12, (5), 449-458.
38. Peydecastaing, J.; Vaca-Garcia, C.; Borredon, E., Accurate determination of the degree of substitution of long chain cellulose esters. *Cellulose (Dordrecht, Neth.)* **2009**, 16, (2), 289-297.
39. Tezuka, Y.; Tsuchiya, Y., Determination of substituent distribution in cellulose acetate by means of a carbon-13 NMR study on its propanoated derivative. *Carbohydr. Res.* **1995**, 273, (1), 83-91.
40. Sealey, J. E.; Samaranayake, G.; Todd, J. G.; Glasser, W. G., Novel cellulose derivatives .4. Preparation and thermal analysis of waxy esters of cellulose. *Journal of Polymer Science Part B-Polymer Physics* **1996**, 34, (9), 1613-1620.

41. Edgar, K. J., Cellulose esters in waterborne coatings. *Polymer Paint and Colour Journal* **1993**, 183, 564-571.
42. Albertsson, A. C.; Carlfors, J.; Stureson, C., Preparation and characterisation of Poly(adipic anhydride) Microspheres for Ocular Drug Delivery. *Journal of Applied Polymer Science* **1996**, 62, 695-705.

## CHAPTER 8 SUMMARY AND FUTURE WORK

Oral drug delivery is a focal point of research on polymeric biomaterials, since it is always preferred by patients and one of the greenest means of drug delivery. Recently there has been an intense interest in ASD formulations with lipophilic pharmaceutical ingredients in which polymeric additives can enhance the drug aqueous solubility, suppress crystallization in the solid phase, and stabilize the drug against recrystallization after forming a supersaturated solution post release.

My doctoral research highlights the development of novel cellulosic polymers designed with a variety of chemical functions in the use of amorphous solid dispersion systems for oral drug delivery. We described extensive studies on chemical modifications on cellulose derivatives, characterization of structure-property relationships and evaluation on the performance of those cellulosic polymers associated with selected poorly water soluble drugs.

### 8.1 Direct Synthesis of Cellulose Adipate Derivatives

One approach is using adipic anhydride (AA) to yield desired products directly. However reaction of cellulose esters in organic solution with in house synthesized AA (**Fig. 8.1**) led to a crosslinked mixture. The gelation is attributed to the fact that AA is extremely prone to homopolymerization by ring-opening polymerization at room temperature even without base initiator, and the crosslinking is induced by reaction of multiple cellulosic chains with poly(AA) impurity.

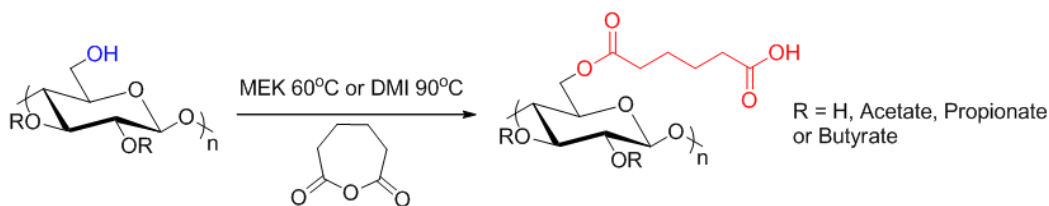


**Figure 8.1** Direct preparation of cellulose adipate esters using adipic anhydride

An improved synthetic procedure has been devised to avoid this problem; fresh, completely pure AA was made after double distillation, free of poly(adipic anhydride) was confirmed by  $^1\text{H}$  NMR and dilution of pure AA with reaction solvent before addition decreased homopolymerization. These modifications enabled esterification to be dominant and prevent subsequent crosslinking. Kinetic studies were also performed. Organic-soluble products with degree of substitution (DS) of adipate up to 0.53 obtained after one-pot synthesis are very valuable drug delivery polymers.

## 8.2 Two-step Synthesis of Cellulose $\omega$ -Carboxyesters (adipates/suberates/sebacates) by Protecting Group.

To avoid crosslinking and achieve higher degree of substitution, a two-step process for the synthesis of cellulose adipate mixed esters was developed, by the reaction of commercially available cellulose esters in homogeneous solution with a carefully designed benzyl-protected long-chain acyl chloride, followed by mild deprotection using Pd-catalyzed hydrogenation under atmospheric pressure (**Fig. 8.2**)

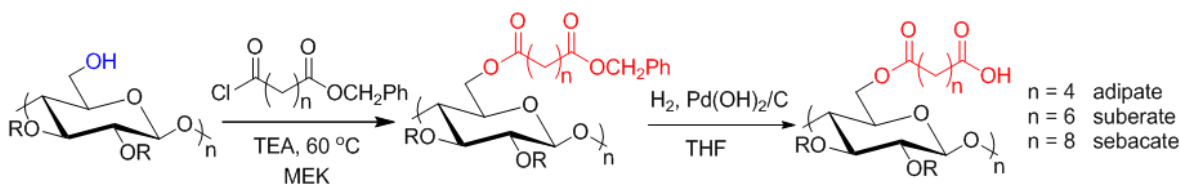


**Figure 8.2** Synthetic route of cellulose adipate/suberate/sebacate mixed esters

This process circumvents the cross-linking problems observed when using adipic anhydride or during the further esterification of carboxylated cellulose (e.g. CMCAB), and it leads to organic-solvent soluble, pH-responsive cellulose mixed esters. No limitation was observed on the type of alkanooate group that may be present. Nearly fully substituted cellulose esters have been synthesized using excess amount of acid chloride, so there is no apparent limitation on achievable  $\omega$ -carboxyester DS. Solubility range, thermal properties and molecular weights of these cellulose

derivatives were extensively studied. Bulk production of amorphous solid dispersions was carried out by co-precipitation or spray-drying techniques and *in vitro* drug release studies were conducted with sample analysis by UV or HPLC, confirming cellulose  $\omega$ -carboxyesters are miscible with lipophilic drugs and corresponding ASD systems enhanced and sustained the apparent solubility of ritonavir.

### **8.3 Mechanistic Understanding of Polymer Impact on Drug Solubilization and Stabilization.**

We worked with Prof. Lynne Taylor's pharmaceutical/physical chemistry group at Purdue University, to design and evaluate superior cellulosic materials for polymer-drug amorphous matrices. The ability of cellulose  $\omega$ -carboxyesters to inhibit the recrystallization (nucleation and crystal growth, respectively) of drugs in supersaturated solution was evaluated in comparison with a mixed group of generally accepted ASD polymers. Polymer-solute interactions were shown to be crucial in disrupting the reorganization of solute molecules into an ordered crystal and further blocking the crystal growth site. Some of the cellulose  $\omega$ -carboxyesters with moderate hydrophobicity were highly effective nucleation and crystal growth inhibitors by providing strong specific interactions (e.g. hydrogen bonding) and non-specific interactions (e.g. hydrophobic-hydrophobic interaction). Our result will support the complete mechanistic understanding of polymer impact on drug solubilization and stabilization.

### **8.4 Further Development of Cellulose-based Polymers: Cellulose Trioxadecanoate**

Cellulose  $\omega$ -carboxyesters were derived from highly substituted cellulose esters, therefore, the hydrophobicity of some of these polymers does result in inadequate release of the drug. Pairwise polymer blend formulation is one solution, or we can develop a versatile cellulose polymer that meet all the needs. A water-soluble cellulose ester with a hydrophilic oligo(ethylene oxide)-containing side chain was developed using a conventional approach and various *in situ* carboxylic acid activation methods. The degree of substitution values of those cellulose esters were

determined by different analytical techniques. Above a certain substitution, the water-soluble products show a LCST, precipitating out of aqueous solution at elevated temperature. This type cellulose polymer can be further modified with hydrophobic or ionic moieties for potential pharmaceutical use.

## 8.5 Proposed Future Work

Novel cellulose  $\omega$ -carboxyesters with valuable properties as described above are targeted as a powerful drug delivery vehicles for commercial use. Still, many issues have to be addressed in order for these polymers to be widely accepted as potent polymer excipients. The production of cellulose  $\omega$ -carboxyester is limited to lab scale (less than 2 grams at a time) due to the inefficiency in the deprotection step. Hydrogenolysis of protecting groups proceeds quite sluggishly at atmospheric temperature and pressure supplied from a H<sub>2</sub>-filled balloon. Higher pressure hydrogenation using a recently-acquired Parr reactor is anticipated in future research to promote rapid hydrogenation. Meanwhile, studies on optimum operating pressure, required time and palladium-based catalyst loading will be performed.

Hydroxypropyl methyl cellulose (HPMC) is a hydrophilic cellulose ether which has been widely used as an excipient for controlled drug delivery. It is also used as a precursor for manufacturing widely-used ASD polymer HPMCAS (acetate succinate). One problem with HPMC is that the hydroxypropyl moiety has ability to chain extend, complicating the manufacturing control and analysis. Dealing with propylene oxide under high pressure also represents a safety issue. The synthesis of the new type of water soluble cellulose derivatives in this dissertation, together with exploring some existing water-soluble polysaccharides (pullulan, alginate salt) open interesting new possibilities for the development of other orally compatible polymer amphiphile candidates. Both hydrophobic ether/esters (methyl, ethyl, propyl, acetate, propionate, butyrate) and pH-responsive carboxyl groups (phthalate, succinate, adipate) can be added to fine-tune the properties of the polymer to accommodate drug compounds having a wide range of physiochemical properties. Similarly, drug release rate and precipitation inhibition of ASDs will be evaluated in detailed fashion as a function of polymer properties.



Meanwhile, an accurate *in vitro-in vivo* correlation will need to be established after animal experiments. Stabilization against recrystallization in buffer solution demonstrated the superiority of designed cellulose  $\omega$ -carboxyester; hydrophobicity and the number of ionizable groups play an important role based on our *in vitro* study. But how well those polymer parameters predict *in vivo* performance is still unresolved. With the generation of data from animal experiments, and its use to refine our understanding of *in vivo* behavior, the development of more reliable *in vitro-in vivo* relationships is expected.

Other than drug delivery application, we will also be looking for using cellulose  $\omega$ -carboxyesters in water-borne coating systems. The amphiphilic nature of those polymers by the introduction of carboxylic acid functionality should enable the aqueous dispersion. A good example is CMCAB, which is easily soluble in organic solvents (e.g. ethylene glycol monobutylether) and dispersible in water when neutralized by a base (e.g. *N,N*-dimethylethanolamine). Attachment of carboxymethyl groups to the cellulose backbone provides cellulose acetate butyrate with sufficient hydrophilicity to maximize flow and levelling without sacrificing re-dissolve resistance. Studies on rheological behavior, solvent, humidity and scratch resistance, metallic appearance and other features present in coating application will be conducted using cellulose  $\omega$ -carboxyesters in comparison with a series of parallel cellulosic polymers with use or promise in coatings, including CMCAB, CAB-SU, direct-carboxylated CAP/CAB (Oxidation of residual free 6-OH groups of a partially esterified cellulose acetate butyrate/propionate to carboxyls) and cellulose acetoacetate esters.